
THE UNIVERSITY
*of* EDINBURGH

# Nitrogen fluxes in forests from atmospheric deposition to soil: use of water flux monitoring and stable isotopes to close gaps in nitrogen transfers


**Daniele Ferraretto**

Thesis submitted for the degree of Doctor of Philosophy

The University of Edinburgh

2020

*When half way through the journey of our life*

*I found that I was in a gloomy wood,*

*because the path which led aright was lost.*

*Dante Alighieri, Inferno, Canto I*

# Abstract

Temperate forest ecosystems are significant sinks for atmospheric nitrogen (N) deposition ($N_{dep}$) yielding benefits such as protection of waterbodies from eutrophication and enhanced sequestration of atmospheric $CO_2$. Many uncertainties remain about the fate of $N_{dep}$ due to the different input fluxes and their spatial and temporal variation, the transformation between different N forms, the complexity of interactions between N and different forest ecosystem components, and the different methods used to quantify N stores and fluxes.

Previously, many studies on the interaction between $N_{dep}$ and forests have focused on $N_{dep}$ at the soil level, assuming that the interaction between $N_{dep}$ and the tree canopy is negligible. However, in the last 20 years an increasing number of studies showed how canopy uptake, calculated as the difference between the $N_{dep}$ input and the fluxes below the canopy (throughfall and stemflow), accounted for a significant fraction of the total input. This could lead to an underestimation of the effects of $N_{dep}$ on forest carbon sequestration. Moreover, transformations of N passing through the canopy might occur which can change the N dynamics and N availability in soil. Previous studies have shown evidence of biological nitrification and $N_{dep}$ processing and retention at the canopy level. However, this was reported only at sites where $N_{dep}$ levels were high or where low background levels were experimentally raised (up to 18 kg N $ha^{-1}$ $y^{-1}$).

The aim of this research was to resolve in a low $N_{dep}$ area, some uncertainties related to $N_{dep}$ processing by forest canopies. The case study area was Griffin Forest (Perthshire, Scotland), a typical Sitka spruce plantation of the UK uplands, characterised by a generally low $N_{dep}$ (5-9 kg $ha^{-1}$ $year^{-1}$). Field monitoring was conducted for 5 years of N fluxes in water onto and below the canopy, litter transfer from the canopy to the soil, and nitrous oxide ($N_2O$) fluxes from forest soils.

Comparison of rainfall (RF, or bulk precipitation) and cloudwater (CW) with throughfall (TF) and stemflow (SF) measured below the canopy suggests strong transformation and uptake of $N_{dep}$ in the forest canopy. The annual mean canopy uptake (CU) of N (calculated as a balance of RF + CW – TF – SF) at Griffin Forest was 70%, and varied between 60% in 2014 and almost 80% in 2012. The data showed a significant long term decreasing trend in bulk deposition of $NO_3^-$ with peaks during the growing season and a significant strong positive correlation between bulk deposition and CU for $NO_3$-N, $NH_4$-N and total N.

These results and a seasonal difference in results were confirmed through a labelled simulated $N_{dep}$ experiment, where the top of the canopy of three selected trees was sprayed with a $^{15}NH_4{}^{15}NO_3$ (98%) - $NH_4NO_3$ solution on two occasions, one during the growing season and one in winter. Background RF and TF and SF below the trees were collected and analysed for $^{15}NH_4$ and $^{15}NO_3$. The N CU in summer (N% = 78±4.5; $^{15}$N% = 85.7±2.9) is much higher than the amount recovered in winter (N% = 51.3±11.9; $^{15}$N% = 43.7±14.2) suggesting at least a partial retention by the plant, together with possible transformations from inorganic to organic N and N gaseous losses. To assess actual plant retention more effectively direct application of a $^{15}$N solution to target branches in situ showed that ~14% of the applied N was recovered in needles and twigs after a period of 24 hours. The short time scale in which this recovery occurred and the particularly dry conditions during the experiment could lead to an underestimation of the actual potential N retention by the canopy as foliar uptake depends on leaf wetness, as literature suggests.

The fate of organic N transfer to forest soils through litter was addressed through $^{15}$N-labelled litter plots sampled 2 and 4 years after the litter replacement. Results show that the different soil features typical of a forest plantation (ridge, undisturbed soil, and furrow) had different $\delta^{15}N$ and estimated $^{15}$N recovery over time. The estimated maximum recovery was ≃52% in 2017 of which ~16% was found in roots. $N_2O$-N losses from soil measured on a 3-year period showed a significant increase in time and they were positively correlate to reduced N bulk deposition. Their order of magnitude was similar to N losses through streamwater and represented a small portion of the atmospheric inputs.

This research has shown that the effects of forest canopies on N deposition occurs at two levels. Firstly, at the canopy level there is consistent uptake of the N input, with only 30% or less directly reaching the soil as inorganic N. A second indirect effect is that the uptaken N, either directly by the plant or through bacterial/fungi sequestration at the phyllosphere level, is likely to be transferred to the soil as organic N via litter and here rapidly used by the plants. The water and gas flux monitoring showed that no major leaching occurs, indicating that the forest acts as a N sink.

The research results confirm the highest figures in the literature of nitrogen canopy uptake. At the relatively low deposition rates present in the UK uplands, $N_{dep}$ represents an important extra source of N to the forest N cycle. Lower N fluxes measured under the canopy, excluding the canopy effect and those taken under high $^{15}$N-N tracer additions, could underestimate the extra carbon sequestration induced

by the $N_{dep}$. The research results and findings are relevant to understanding and modelling N cycling and its impacts on forest growth and carbon storage in similar forest systems in the UK uplands and at a broader scale under similar $N_{dep}$ conditions.

# Acknowledgements

This work would not have been possible without the invaluable help of Prof. Kate Heal. She provided continuous support, ideas, motivation and help in every possible way. This journey would have not been the same without her. Or it would not be at all.

Thanks to my wife Silvia, to believe in this adventure by following me and bearing my ups and downs these 5 years.

Thanks to the Elizabeth Sinclair Irvine Trust of the School of GeoSciences and the Forest Research for funding this project.

Thanks to Richard Nair, who has helped me in many ways, even before my PhD even commenced by setting one of the featured experiments: you have been a marvellous guest in Jena and your suggestions have changed my project in better.

Thanks to Dave Reay and Dr. Nadeem Shah for their extra help as co-supervisors, as well as Dr. Sirwan Yamulki for sharing the information gathered from the Forest Research project on greenhouse gases in Griffin.

Thanks to Maurizio Mencuccini for his precious feedbacks on the project and to give me the opportunity to meet Rossella and Josep who were source of further ideas.

Thanks to the guys from the technical and lab team at the University of Edinburgh for their help in the labs and in field: I owe them more than the few cakes we shared. Many thanks also to people from the NERC LSMSF at Lancaster and Max Plank Institute at Jena for the work on the $^{15}N$ samples, even if we did not meet in person they are part of this work.

Thanks to Mike Spencer for the tutoring in the field and unveiling the secrets of R: I would have not even considered using R without his guidance and help on the creation of the original dataset.

Thanks to Dr. Massimo Vieno for the data he provided me and enlightening information on how to compare our data on wet and dry deposition.

A special thanks goes to Margaret Jarvis: her kindness and logistical support at Griffin made my days there much more pleasurable.

And thanks to all those I haven't mentioned but have participated in making these 5 years a memorable journey.

# Table of contents

# Chapter 1. Introduction

Nitrogen (N) is the most abundant element in the Earth's atmosphere, accounting for 78% of the volume of dry air. It occurs in all living organisms, primarily in amino acids. At standard temperature and pressure two atoms of the element bind with a strong covalent triple bond to form dinitrogen gas ($N_2$). The stability of the $N_2$ molecule makes it virtually unavailable to most living organisms, including plants.

Reactive nitrogen ($N_r$) is defined as all forms of inorganic nitrogen (IN) that are biologically, photochemically and radiatively active, and hence includes all the N forms available to plants. It comes from biological nitrogen fixation as well as from anthropogenic sources. This latter source has increased significantly in the last 100 years since the discovery of the Haber-Bosch process by Fritz Haber at the beginning of the $20^{th}$ century. This has enabled the production of fertilisers that have underpinned the massive increase in food production from agriculture to feed the growing human population so that now about 100 Tg of fertiliser N is used worldwide per year (Erisman et al. 2008). From the mid-1970s, human production of $N_r$ has exceeded the natural production (Ciais et al. 2013).

The $N_r$ released to the atmosphere consists predominantly of three components: $NH_3$, $NO_x$, and $N_2O$, with smaller contributions from organic compounds such as amines (Hertel et al. 2011). Nitrous oxide ($N_2O$) is a form of IN mainly produced from fertilised agricultural soils (Xu et al. 2019) with significant consequences for global warming. More details on the effects of $N_2O$ as a greenhouse gas (GHG) are given in section 1.3.2. The first two components can ultimately be deposited on the biosphere in an aqueous form in precipitation and also as dry deposition (gases and particulates). Collectively these inputs of N from the atmosphere to the earth's surface are called nitrogen deposition ($N_{dep}$).

$N_{dep}$ from anthropogenic sources has increased dramatically since the discovery of the Haber-Bosch process, coupled with the increase of atmospheric $CO_2$ due to the growing use of fossil fuels (Reay et al. 2008), N fertilisation and N-fixing plant cultivation (Zhu et al. 2015). Atmospheric nitrate is mainly derived from fossil fuel burning (Zak et al. 2004) whilst the ammonia form is predominantly from livestock farming and its wastes (Misselbrook et al. 2000). Although a small portion of the N produced through the Haber-Bosch process, $N_r$ coming from anthropogenic N represents a significant proportion of $N_{dep}$, varying widely in quantity and composition. In Western Europe reduced N species, originating from farming and animal husbandry, dominate the total budget of $N_{dep}$ (Holland et al. 2005).

The aim of this PhD research is to improve understanding of the interaction of $N_{dep}$ from the atmosphere with forests and explore the magnitude of these interactions on the forest N cycle. The importance of $N_{dep}$ and its effects on forest growth have been extensively studied. However, the different approaches, different ecological conditions, the heterogeneity of the intensity of $N_{dep}$ and the variety of forms in which $N_r$ is found in the N cycle in forests mean there remains considerable uncertainty about how much of this N is effectively taken up by plants and consequently its effects on plant growth and carbon (C) storage in forest ecosystems. A deeper knowledge of the N cycle in forests is required to inform policies relating not only specifically to forest management, but more widely relating to atmospheric N emissions, forest landscapes and their role in C management and biodiversity.

In this chapter, firstly, $N_{dep}$ in forests will be introduced in the context of forest N cycling and previous relevant studies will be briefly described. Secondly, the main features of the canopy N cycle and a description of the key processes involving reactive $N_r$ will be discussed. Finally, the research objectives and hypotheses will be presented, followed by an outline of the thesis structure.

## 1.1 Nitrogen deposition

$N_{dep}$ may occur as dry or wet deposition. Dry deposition refers to the deposition from the atmosphere of gases and particles originating from natural and anthropogenic sources and consisting mainly of ammonia, nitrogen dioxide and nitric acid (Sparks et al. 2008). Wet deposition refers to N contained in precipitation (snow, rain, cloudwater). The chemical composition of $N_{dep}$ reflects the main source of N and comprises three main forms of N. The first is nitrogen oxides ($NO_x$, the sum of nitrogen monoxide (NO) and nitrogen dioxide ($NO_2$)) released into the atmosphere predominantly from fossil fuel burning (Liu et al. 2013). $NO_2$ may be deposited directly in the dry form as a gas to vegetation, but it is mainly scavenged in the atmosphere by reaction with the OH radical to form nitric acid ($HNO_3$). Nitric acid has a very short lifetime in the atmosphere and quickly reacts with alkaline compounds such as ammonia, leading to aerosol bound nitrate ($NO_3^-$) (Hertel et al. 2011). A second major form of $N_{dep}$ is reduced N of which 80-90% is generated from agricultural sources, mostly from livestock and use of synthetic fertilisers (Bouwman et al. 1997). It occurs as ammonia ($NH_3$) in dry deposition, and the cation ammonium ($NH_4^+$) in wet deposition (Hertel et al. 2011). Other chemical forms of $N_{dep}$ occur in smaller amounts, such as peroxyacetyl nitrate (PAN), a photochemical product of the reaction between volatile organic compounds and nitrogen dioxide ($NO_2$). Long term measurements of PAN are rare, but from the longest continuous measurements in the UK conducted

from 1994 to 1998 at Bush, south-eastern Scotland, PAN has been estimated to account for a small fraction of the overall $N_{dep}$ (McFadyen and Cape 2005). At the global scale $N_{dep}$ varies spatially by one order of magnitude (see Figure 1-1), from about 1 kg N $ha^{-1}$ $y^{-1}$ at low pollution sites (Fenn et al. 2013) to over 50 kg $ha^{-1}$ $y^{-1}$ in areas with severe air pollution (Ackerman et al. 2019; Dentener et al. 2006).

Figure 1-1. Mean annual IN deposition (wet + dry) as simulated for the 2010s. Source: Ackerman et al. (2019)

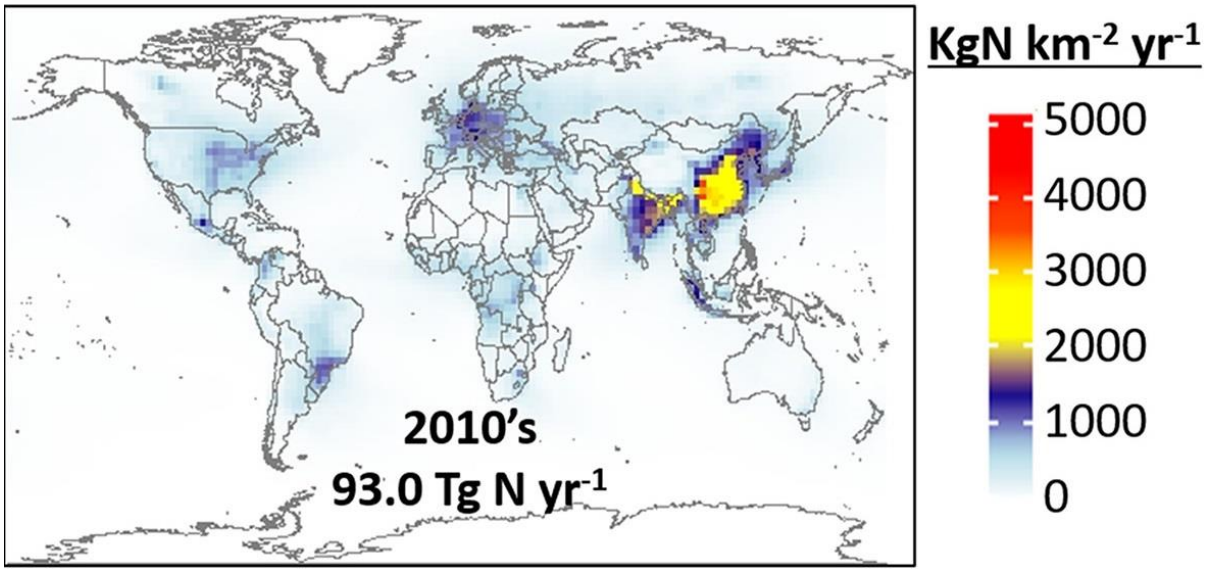


$N_{dep}$ trends in the last 30 years differ between regions of the world, as shown in Figure 1-2. $N_{dep}$ has increased slightly in North America, except on the Atlantic Coast of the USA (Gilliam et al. 2019), and particularly dramatically in China and India. In contrast, $N_{dep}$ has decreased across the tropics and in Europe (-50% in $NO_x$ and -30% in $NH_3$), and this decreasing trend is expected to continue (Dirnböck et al. 2018). On a global scale, N deposition increased by 8 % in the period 1984-2016; oxidised forms have been decreasing steadily, whilst the reduced molecules have increased by 30-35% (Ackerman et al. 2019).

Figure 1-2. Mean annual rate of change in simulated total IN deposition between 1984 and 2016. Source: Ackerman et al. (2019)

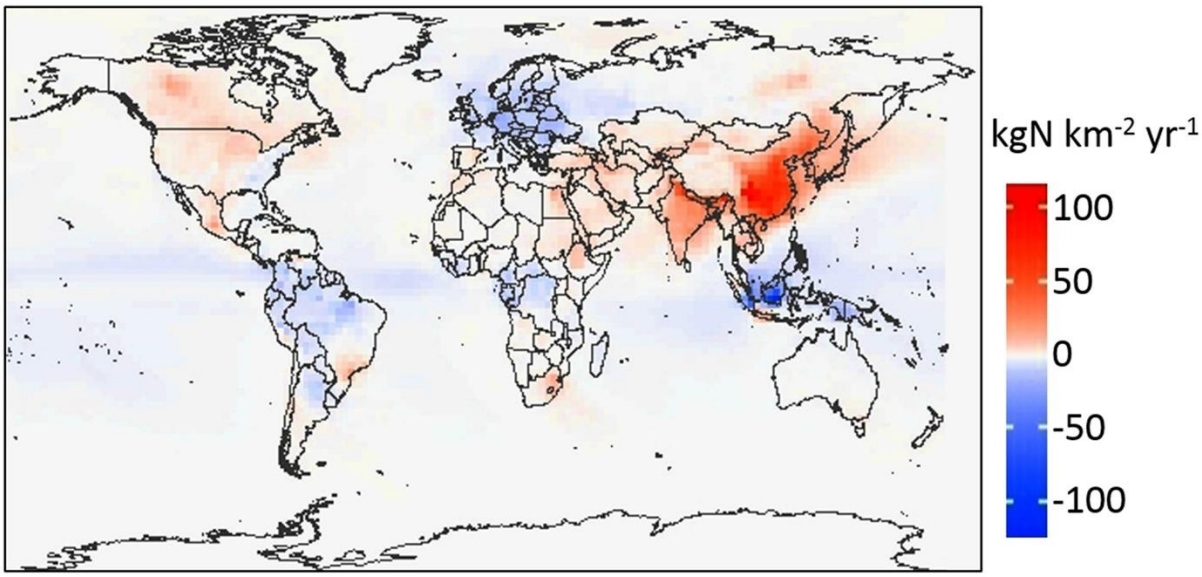


### 1.1.1 Dry deposition

Because of its physical state, dry $N_{dep}$ is more difficult to measure than wet $N_{dep}$. Methodologies for the accurate quantification of dry $N_{dep}$ are expensive and technologically challenging to maintain (Sparks et al. 2008). Therefore models have been created to estimate dry deposition from short-term eddy flux and concentration measurements and annual regional concentration estimates (Sparks et al. 2008). The European Monitoring and Evaluation Programme Unified Model for the UK (EMEP4UK) combines emissions data and measurements of air and precipitation quality to model atmospheric transport and deposition of air pollutants at a grid scale of 5 km x 5 km (Simpson et al. 2012).

### 1.1.2 Bulk deposition

Bulk deposition, i.e. $N_{dep}$ from rainfall and dry sedimenting particles, is the most widely used measure of $N_{dep}$ because of the cheaper and simpler methodology to collect and analyse samples compared to assessing separately wet deposition and dry deposition of aerosols and gases (Dammgen et al. 2005). The ratio between dry and wet $N_{dep}$ varies widely according to site location, and is affected by the proximity to N sources, rainfall regime and air mass movement. For example, de Vries et al. (2008) calculated dry $N_{dep}$ to be 2-7 times greater than wet deposition at the forest sites in Europe reported in Magnani et al. (2007), whilst in a mixed hardwood forest in Michigan (USA) total $NO_3^-$ in dry deposition over a 3-month period was about 30% higher than in wet deposition (Hill et al. 2005). In contrast, Gagkas et al. (2011) estimated that dry deposition on birchwood in the southern Scottish Highlands under two different deposition scenarios accounted for only 13% of total $N_{dep}$. Since the amount and

composition of $N_{dep}$ varies between sites due to the wide range of types of emission and climatic and atmospheric conditions, determination of $N_{dep}$ through either bulk deposition measurement or as the sum of separately assessed wet and dry deposition can lead to different results.

### 1.1.3 Cloudwater deposition

Nitrogen deposition in cloudwater cannot be neglected at locations frequently enshrouded in cloud (such as at high elevation or experiencing coastal fog), since much higher concentrations of N and other atmospheric pollutants have been observed in cloudwater compared to rainwater (e.g. Choularton et al. 1988). Although the total flux of water to a surface may be smaller than rainfall, the frequent cloud cover in these locations can lead to a significant contribution of N in cloudwater to the total annual N deposition, especially over a forest canopy due to its particularly rough surface and greater canopy surface area (Gallagher et al. 1992). For instance, Weathers et al. (2000) showed that IN in cloudwater doubled the IN in wet deposition on forests in Chile, and cloudwater deposition was estimated to represent 10-28% of the total $N_{dep}$ at a high-elevation site in France (Herckes et al. 2002) and up to 18% of the total $N_{dep}$ in the Austrian Alps (Kalina et al. 2002).

### 1.1.4 Effects of nitrogen deposition on forest ecosystems and forest N and C cycles

The impacts of $N_{dep}$ on biodiversity and ecosystem function have been widely studied. In the next paragraphs some of the major effects reported in the literature and particularly relevant for the present study will be briefly described.

*Effects on soil N cycling*. $N_{dep}$ can potentially influence soil N mineralisation, gaseous N emissions and the microbial, fungal and nematode soil communities. Cheng et al. (2019) found that more than 97% of published papers evaluating the effects of $N_{dep}$ on the soil N cycle in forests reported a net increase in rates of N mineralisation (24.9%) and nitrification (153.9%). However it should be noted that many manipulative experiments use very high rates of $N_{dep}$ so the results may not be completely relevant to all locations throughout the world. Furthermore, the effects of $N_{dep}$ on soil N and C cycles may be affected by interactions with climate change. For example, manipulative experiments applying soil warming and N additions at rates predicted over the next 100 years for a subalpine coniferous forest in the Tibetan plateau in China (2-3 $^{o}$C warming, 50 kg N $ha^{-1}$ $y^{-1}$) found that $N_{dep}$ alone increased soil respiration by increasing the soil C and N pools as well as the bacterial community, and soil warming alone increased the protozoa community, and soil warming alone

increased the protozoa community. However, the interaction of $N_{dep}$ and soil warming was antagonistic, leading to a lower protozoa concentration. Dissolved organic carbon (DOC) increased when either warming N addition were applied but significantly decreased (~40%) when both warming and N addition occurred. Dissolved ON in soil increased when N was applied and also when warming and N addition were applied together (Sun et al. 2019). $N_{dep}$ has some known effects on soil C and N dynamics, such as enhancing fine-root production and turnover (Nadelhoffer 2000). Laboratory experiments have shown that litter with higher internal N content has a higher decomposition rate, with further addition of N increasing the decomposition rate, although external N addition did not compensate for a lower internal N content (Vestgarden, 2001). However, long term experimental $NO_3^-$ deposition resulted in greater forest floor biomass compared to ambient $N_{dep}$ despite no increase in detritus production (Zak et al. 2008). This is due to the inhibition of decomposition by $NO_3$ deposition which is consistent with a previously reported decrease in lignin decomposition activity by the microbial community. Significantly higher soil $N_2O$ emissions due to increased $N_{dep}$ were reported in a 10-year manipulative study on a N saturated subtropical forest by Xie et al. (2018). Emissions up to 6 times greater than those from non-treated plots were measured under N additions slightly lower than natural deposition. When enhanced $N_{dep}$ was stopped, $N_2O$ emissions declined to those from the control plots.

*Effects on forest growth, carbon sequestration and cycling*. A number of studies show that $N_{dep}$ influences forest growth and the function of forest ecosystems as a carbon sink. However, there is still much debate on the magnitude of this effect due to the complexity of the N cycle in forests and its variability. The debate was largely initiated by the paper by Magnani et al. (2007), suggesting that temperate and boreal forest receiving total N deposition of up to 15 kg N $ha^{-1}$ $y^{-1}$ would be able to sequester up to 470 kg C $ha^{-1}$ $y^{-1}$ per kg of $N_{dep}$. The results were questioned, for example by de Vries et al. (2008), on the basis of underestimation of the N input, overestimation of C:N ratios within the forest aboveground and belowground pools and other factors co-varying with wet N deposition. They ultimately suggested that the total net ecosystem production (NEP) would be 30-70 kg C per kg $N_{dep}$. In their response, Magnani et al. (2008) questioned the assumptions of de Vries et al. (2008), particularly that they had underestimated the canopy N uptake, that may account for up to 70% of $N_{dep}$ and provide more than a third of tree N requirements. Quantification of canopy N uptake from $N_{dep}$ and its relationship with tree C storage therefore emerged as a vital research topic for understanding and predicting the C sequestration potential of forests. Some of the later research on this topic is described next.

A meta-analysis at global scale (Schulte-Uebbing and de Vries 2017) of N fertilisation studies conducted in tropical, temperate and boreal forests estimated that temperate and boreal forests responded strongly to N addition and sequestered 13 and 14 kg C per kg of $N_{dep}$, respectively, in aboveground woody biomass, accounting for about 12% of the global forest biomass sink for C. Tropical forests, however, did not respond significantly to N addition. Across the EU, Etzold et al. (2020) estimated, based on data from 442 even-aged single species forest stands, that $N_{dep}$ is the most important driver of forest growth together with forest density and age. In the same study $N_{dep}$ was shown to be at least as important as climate in modulating forest growth, with a potential negative effect at high deposition rates. This negative effect of $N_{dep}$ was also reported by Flechard et al. (2020) in a study of the interaction between C and N on forests in the EU. They estimated an overall response of 40-50 kg C $kg^{-1}$ $N_{dep}$ but no growth response for deposition rates above 25-30 kg $ha^{-1}$ $y^{-1}$. High $N_{dep}$ can lead to lower effects of N addition on the increase of aboveground C accumulation, as Gentilesca et al. (2013) demonstrated for experimental plots of *Picea sitchensis*. Elevated $N_{dep}$ has also been shown to result in lower belowground C allocation to mycorrhiza (Rotter et al. 2020).

*Other impacts on the forest ecosystem*. $N_{dep}$ has been recognised as one of the most important threats to global biodiversity (Steffen et al. 2015; Sala et al. 2000). Decrease in biodiversity due to $N_{dep}$ to the detriment of slow growing species has been reported even in N limited environments (Meunier et al. 2016). Here, $N_{dep}$ released primary producers from N limitation, resulting in increased N content in plants which benefitted herbivores with high N requirements, but diminished belowground production due to mechanisms that reduced microbial biomass. Salemaa et al. (2019) found that in low $N_{dep}$ boreal forest sites $N_2$ fixation by bryophytes was suppressed. At the EU scale, models predict that both wet and dry $N_{dep}$ will continue the declining trend of the past 2 decades. However, European forest ecosystems have not yet shown large scale responses in understory vegetation, tree growth or vitality to decreasing $N_{dep}$ (Dirnböck et al. 2018).

$N_{dep}$ also contributes to the N saturation of forest soils, resulting in negative impacts on soil acidification, water quality and biodiversity (De Schrijver et al. 2008). For example, Dise and Wright (1995) reported that for European forests, N leaching occurred when $N_{dep}$ in throughfall exceeded 25 kg N $ha^{-1}$ $y^{-1}$.

Other studies reveal further interactions between $N_{dep}$ and forest canopies. For example, there seems to be a considerable effect generated in forest ecosystems by

combined N and sulfur (S) deposition. In a long-term study of the effects of repeated aerial application of N and S in mist to a Sitka spruce application in southern Scotland and then cessation to mimic recovery from N and S deposition, different effects were found of N and S deposition applied separately and together (Guerrieri et al. 2011). Where N only was applied, it acted as a fertiliser and enhanced $CO_2$ assimilation. However, in sites where both N+S had been deposited in significant quantities, S had a negative effect on tree water use efficiency (WUE), maybe caused by both reduced assimilation at the leaf level and reduced stomatal activity (Guerrieri et al. 2011). A meta-analysis conducted as part of the same study, showed a greater increase in WUE when N was applied onto tree canopies compared to soil applications. Therefore, the effect of $N_{dep}$ on forest canopies appears to be not solely controlled by the amount and form of N deposited, but by the way in which application occurs and by other constituents of canopy atmospheric deposition also influencing canopy processes and forest function.

## 1.2 The canopy nitrogen cycle

Figure 1-3 gives a schematic overview of the nitrogen pools, fluxes and transformations in forest ecosystems. $N_r$ is present in a variety of chemical forms in each pool and flux. In the atmosphere nitrate ($NO_3^-$) and ammonium ($NH_4^+$) form part of the wet $N_{dep}$. Dry deposition comprises nitrogen dioxide ($NO_2$), nitric acid ($HNO_3$) and $NH_3$, with the reduced form of N accounting for most dry deposition (Vieno et al. 2014). When $N_{dep}$ reaches the forest canopy and passes to the forest soil via throughfall (TF) and stemflow a number of transformations can occur. Ammonia can be processed through nitrification to nitrite ($NO_2^-$) and nitrate ($NO_3^-$). From nitrate it can be reduced and fixed as organic nitrogen (ON). In the forest soil, N can also be fixed by bacteria and algae from the molecular form to ammonia.

Litter is a substantial flux of N from the canopy to the soil. The rate of depolymerisation and mineralisation of litter varies between different pools from hours to decades. In a temperate beech forest in southern Germany, a rapid transfer of $^{15}N$-labelled litter N was measured, with microbial biomass being the main sink (Guo et al. 2013b). Over time, soil non-extractable N increased, becoming the dominant $^{15}N$ sink, with plant biomass accounting for a minimal proportion of added $^{15}N$ after ~2.5 years.

Among the potential N losses from the forest ecosystem, leaching can occur especially under high (>25 kg N $ha^{-1}$ $y^{-1}$ TF $N_{dep}$) $N_{dep}$ levels (Dise and Wright 1995). Whilst ammonium is quite immobile in the soil profile due to the soil cation exchange capacity, nitrate is highly mobile and nitrate leaching can occur when TF $N_{dep}$ exceeds

8-10 kg N $ha^{-1}$ $y^{-1}$. Between 8-25 kg N $ha^{-1}$ $y^{-1}$ TF $N_{dep}$, both full retention and no retention of N can occur in forests depending on the 'N status' of the system: N poor systems have a high retention and N rich systems have a low retention (Butterbach-Bahl et al. 2011). *Picea sitchensis*, the most commercially important species grown in Scottish forests, is a relatively demanding species both in terms of moisture and nutrients (Klinka et al. 2000), so there is a need to investigate if enhanced N leaching occurs as the result of soil N saturation at low and average levels of $N_{dep}$.

The final process closing the N biochemical cycle in forests is denitrification under anoxic conditions (to NO, $N_2O$ and ultimately $N_2$). This is the most poorly understood process in the terrestrial N cycle (Wexler et al. 2014), but it is important for assessing if N from $N_{dep}$ is still accumulating in the forest. The next sections will describe in more detail some of the processes mentioned above.

Figure 1-3: Fluxes and pools of nitrogen in forest ecosystems. Blue arrows indicate aqueous fluxes, grey arrows show N transformations in soil (see Fig. 1-4 for more detail on some of these processes), black arrows indicate N uptake from roots.

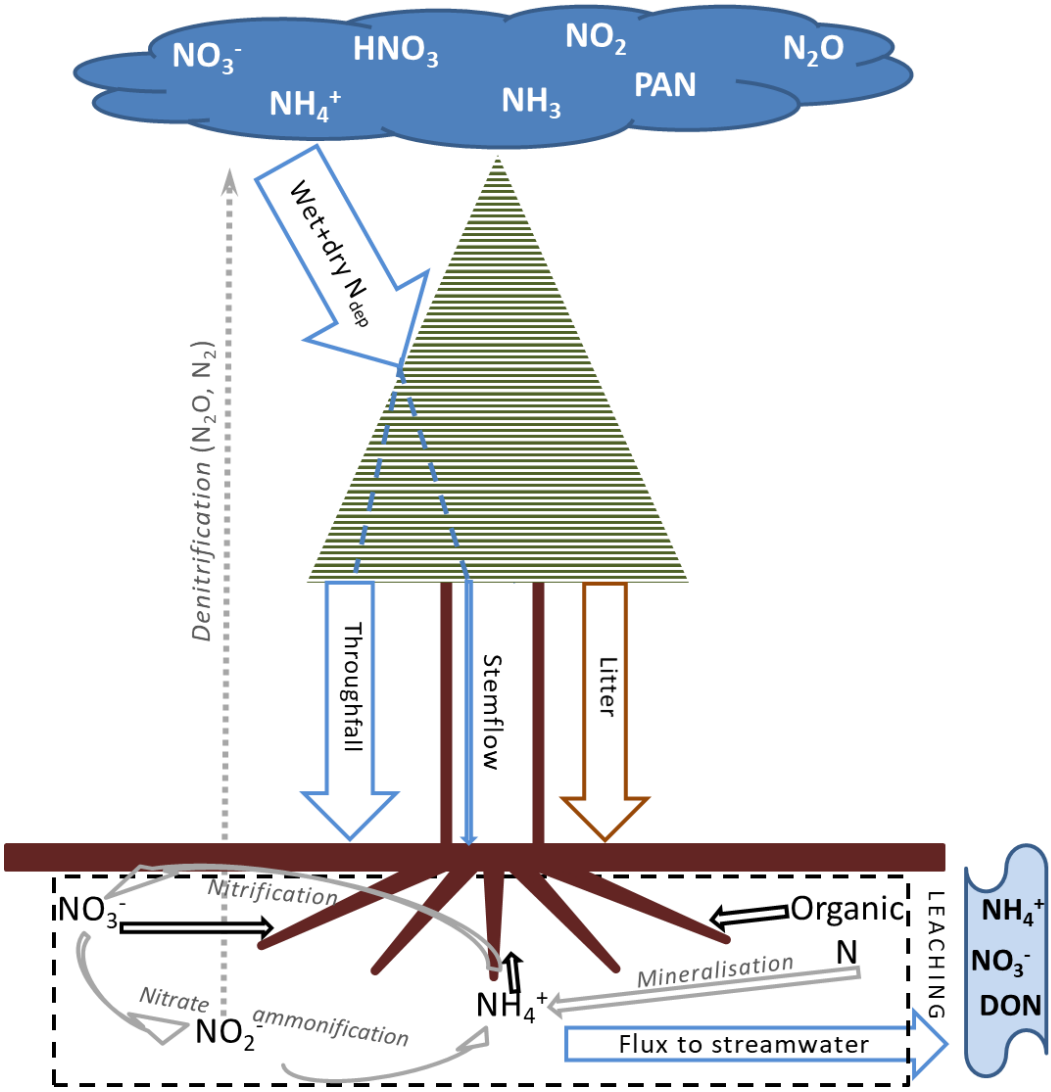


### 1.2.1 Nitrogen transformation by forest canopies

#### 1.2.1.1 Nitrification in forests

Nitrification is a key microbial process in the N cycle that links the oxidation of ammonia or ammonium produced from the degradation of soil organic matter (Ward 2013) or from $N_{dep}$ from the atmosphere (Guerrieri et al. 2020) to the loss of fixed nitrogen in the form of $N_2$. The process follows two steps: ammonia or ammonium are reduced to nitrite via hydroxylamine, followed by the oxidation of nitrite to nitrate, as summarised for ammonia in Equation 1-1:

$$NH_3 \rightarrow NH_2OH \rightarrow NO_2^- \rightarrow NO_3^- \quad \text{(Eq.1-1)}$$

Nitrification is the only natural pathway whereby nitrate is produced within an ecosystem. Because the process can operate at low rates even with relatively low ammonium concentrations, it occurs in many environments (Dodds et al. 2017). Until recently, nitrification was considered a two-step process, where ammonia-oxidising bacteria and archaea oxidise ammonia to nitrite which is then converted to nitrate by nitrite-oxidising bacteria (Maier 2009). However, in 2015, bacteria of class *Nitrospira* were found capable of converting ammonia to nitrate (so-called Comammox – COMplete AMMonia OXidiser), challenging the century-long perception of the two-step process (Shi et al. 2018). To date, commamox *Nitrospira* have been identified and studied predominantly in natural aquifers or engineered ecosystems, with only one study investigating commamox *Nitrospira* in forest soil (Shi et al. 2018) identified during the present literature review. It is expected that further investigations of commamox *Nitrospira* in forest soils could lead to new perspectives on nitrification in forest ecosystems.

Nitrification rates are influenced by several environmental factors including light, soil temperature, $O_2$ (since nitrifying organisms are obligate aerobes), ammonium availability, pH, organic carbon availability (Hawkes et al. 2007), and C:N ratio in soil (Zhang et al. 2019). However, in soil the availability of substrate is thought to be the primary limiting factor (Hawkes et al. 2007).

Nitrification in forests has traditionally been viewed as a process occurring only in the soil, but recent studies indicate that it occurs also in the forest canopy, where $N_{dep}$ is processed and transformed. For example, in a study by Watanabe et al. (2016) increased nitrate concentrations were measured in unfiltered TF from Japanese cedar after 4 weeks incubation compared to filtered TF samples. In addition, archaeal ammonia monooxygenase subunit A (amoA) genes were found in filters used for TF samples and on leaf surfaces, indicating the presence of bacteria able to oxidise ammonia. These results were interpreted as evidence for the potential for microbial denitrification in tree canopies. Guerrieri et al. (2015) quantified canopy nitrification of 27% and 34% of $N_{dep}$ transformed by nitrification in a Scots pine and a beech forest, respectively, in the UK under medium-high levels of $N_{dep}$ (13-19 kg $ha^{-1}$ $y^{-1}$) using a double stable isotope approach $\delta^{18}O$ and $\Delta^{17}O$. A recent study by Guerrieri et al. (2020) showed similar results (up to 20% of $NO_3$- $N_{dep}$ in TF derived from canopy nitrification) in a Mediterranean holm oak (*Quercus ilex*) in Spain. In this study microbial communities and the abundance of nitrifiers on foliage and in rainfall and TF were characterised through metabarcoding and quantitative polymerase chain

reaction analyses. This study is a first step towards relating the magnitude of nitrification in the canopy to aboveground microbial mass and composition.

#### 1.2.1.2 Changes from inorganic to organic nitrogen from Ndep to throughfall

An increase in ON in TF compared to ON in $N_{dep}$ has been measured in several studies at natural abundance or in manipulative studies. Hill et al. (2005) observed an 81% increase in dissolved organic nitrogen (DON) in collectors under the canopy of a forest dominated by aspen in Michigan (USA). Gaige et al. (2007) applied a labelled solution of IN over the canopy of a mature coniferous forest and found that both $^{15}NH_4$ and $^{15}NO_3$ were converted to DON within days from the application, suggesting that canopy DON formation was a rapid process related to recent N inputs from the atmosphere. Cape et al. (2010) reported results from two studies in Scotland, one on mature Scots pine exposed to ammonia gas and the other in which additional IN wet deposition was applied to the canopy of Sitka spruce. In both cases ON in TF increased, but only represented about 10% of the additional IN supplied, suggesting a limited capacity for net ON production in forest canopies under Scottish summertime conditions.

### 1.2.2 Methods to probe canopy nitrogen uptake

The majority of $N_{dep}$ manipulation experiments in forests have applied N to the forest floor rather than to the canopy. This method is obviously cheaper and easier to implement and is based on the assumption that the canopy does not interact substantially with $N_{dep}$. However, this assumption has been demonstrated to be invalid by many studies using a variety of methodologies and conducted at different scales. These studies include: (1) canopy applications of $NH_4NO_3$ mist treatments (Chiwa et al. 2004) or $^{15}N$-labelled IN solution (Dail et al. 2009) *in situ* in forests or to potted seedlings (Nair et al 2015); (2) forest canopy N budgets constructed by measuring N fluxes in precipitation and TF (Sievering, 2007); (3) and mixed methods (e.g. Zhang et al. 2015, comparing canopy addition of N and understory addition). As already mentioned, using a double labelled isotopes approach Guerrieri et al. (2015) showed that nitrification occurred in tree canopies under medium-high $N_{dep}$ (13-19 kg N $ha^{-1}$ $y^{-1}$), with up to 60% of $NO_3^-$ in TF derived from nitrification occurring in tree canopies. However, the combined isotopic approach was effective only at high deposition sites, whereas only the $\Delta^{17}O$ isotopic approach was successful in showing biological processing of $NH_4^+$ at the low deposition site (9 kg N $ha^{-1}$ $y^{-1}$).

A recent study (Liu et al. 2020) demonstrated that the forest canopy acts like a buffer to $N_{dep}$ for the below canopy ecosystem by maintaining the soil nematode community composition and fine root biomass under elevated $N_{dep}$. By comparing a N application under the canopy (UAN) with a wet application over the canopy (CAN) the study showed that more than half of the N added to the forest canopy was retained by the forest canopy, but in the UAN treatment the soil nematode community decreased significantly more than in the canopy application. The study concluded that experiments to investigate the effect of $N_{dep}$ on forest ecosystems in which $N_{dep}$ is applied to the forest floor might result in an incomplete and potentially misleading understanding of the effects of $N_{dep}$ on forest ecosystems by overestimating the negative effects.

The experiments mentioned above were conducted in different ecological conditions on different types of forests. They indicate that understanding of canopy N uptake cannot be neglected and that $N_{dep}$ should be considered for understanding of forest N cycling and forest growth. However, the quantification of the phenomena is usually restricted to a relatively small-scale scenario, such as seedlings or individual trees. Investigating it in a widespread forest type/plantation type typical of the UK uplands could help to address this scale gap.

## 1.3 Nitrogen in soil

The soil pool represents nearly 90% of total N storage in forest ecosystems (Zhu et al. 2014), mainly concentrated as organic N in the superficial layers of the forest floor. As weathering of geological parent material contributes only marginally to mineral N (Eickenscheidt and Brumme 2013), most of the soil N comes from N transfer from the plants to the forest floor and the turnover of fine roots. $N_{dep}$ may represent another important source of N input since it is readily available to soil bacteria, mycorrhizae and plants.

Many manipulation studies reported in the literature aimed to measure the effects of extra IN input to soil on the dynamics of C and N pools by applying mineral N in relatively high loads for short time periods (see the meta-analysis by Knorr et al. (2005)) or occasionally over longer time periods (Frey et al. 2014). Whilst these studies address the effects of inorganic $N_{dep}$ reaching the forest soil after passing through the canopy, they implicitly assume that the interaction of the atmospheric reactive N with the canopy is negligible. Moreover, unrealistic N addition rates of mineral N are frequently required to provide sufficient isotopic signal in soil and plants for detection of changes, potentially altering nutrient cycling and microbial

communities. For these reasons labelled mineral additions to soil are less effective in understanding the internal cycling of the N derived from litter and roots in forests.

Labelled litter experiments have focused on internal N from leaf litter (Eickenscheidt and Brumme, 2013; Nair et al. 2017; Zeller et al. 2001; Zeller et al. 2000) or root litter (Guo et al. 2013a; Guo et al. 2013b). Such studies are not abundant in the literature, mainly due to the budgetary and time constraints for the preparation of the labelled substrate. For example, Guo et al. (2013b) obtained labelled litter by direct foliar application of labelled N to trees *in situ* using the methodology described by Zeller et al. (1998) and collecting leaves just before abscission, whilst Nair et al. (2014) generated labelled litter by injecting a $^{15}NH_4{}^{15}NO_3$ solution into the stem of Sitka spruce trees and harvesting whole branches after 4.5 months, from which the needles were stripped. The use of labelled litter allows the transformations and translocation of organic N to be followed in the forest floor whilst acting as a source of nutrients through processing and breakdown of structural organic compounds by soil biota (Zeller et al. 2001).

All the labelled litter experiments cited above were conducted on broadleaf species, with the exception of the experiment by Nair et al. (2017) which was conducted in 40-year Sitka spruce plantation in Southern Scotland. In the experiment the fate of $^{15}N$ in plots with and without $^{15}N$ labelled litter addition was investigated in soil, roots, soil microbial biomass and leachate for 18 months after labelled litter addition. No longer term data are available on how mineralisation of Sitka spruce litter develops in forest soils over time. Whilst the research conducted for this PhD thesis did not explicitly analyse the effect of $N_{dep}$ and litter N on C stored in the soil and trees, a clearer picture of N fluxes and pools can help in modelling the effects of $N_{dep}$ over temperate forests under medium-low $N_{dep}$ regimes which represent 16% of forests worldwide (Hansen et al. 2010).

### 1.3.1 Nitrification in soil

The process of nitrification has already been briefly described in section 1.2.1.1 above in relation to nitrification in the forest canopy. Nitrification in soil is a central process for the formation of several N forms (Butterbach-Bahl et al. 2011) as illustrated in Figure 1-4. Nitrification is mostly an aerobic process, and it is optimal when soil aeration porosity is 50%–60% of the total porosity (Jalota et al. 2018). In general, the nitrification rate in soil increases with increasing soil moisture content as long as the soil is not saturated (Stark and Firestone 1995). Nitrification is carried out by three microbial groups: (1) autotrophic ammonia oxidizers, (2) autotrophic nitrite oxidizers,

and (3) heterotrophic nitrifiers (Prosser 2005). The first step of nitrification is the oxidation of ammonia into nitrite and is performed by ammonia-oxidising bacteria (AOB) and ammonia oxiising archaeea (AOA) (Beeckman et al. 2018). The second step in which nitrite is oxidised into nitrate involves several genus bacteria among which Nitrobacter and Nitrospira. Autotrophic nitrification is a process where nitrifiers use reduced nitrogen as an energy source for carbon dioxide fixation. Autotrophic nitrification in soil is thought to be primarily limited by the availability of substrate ($NH_3$ – $NH_4^+$) (Hawkes et al. 2007). Plants may indirectly influence soil autotrophic nitrification via consumption of ammonium, hence removing the substrate for the process, or directly affect the process via toxic compunds in root exudates (Castaldi et al. 2009). Heterotrophic nitrifiers use organic $N_r$ both as an energy source and C source and can oxidise both ammonium and organic N compounds (Butterbach-Bahl et al. 2011). Nitrification increases the probability of N loss through leaching or further reduction to gaseous N forms as a precursor of denitrification.

Figure 1-4. Nitrification in soil and processes related to the intermediate and end-products of nitrification. Source: Butterbach-Bahl et al. 2011.

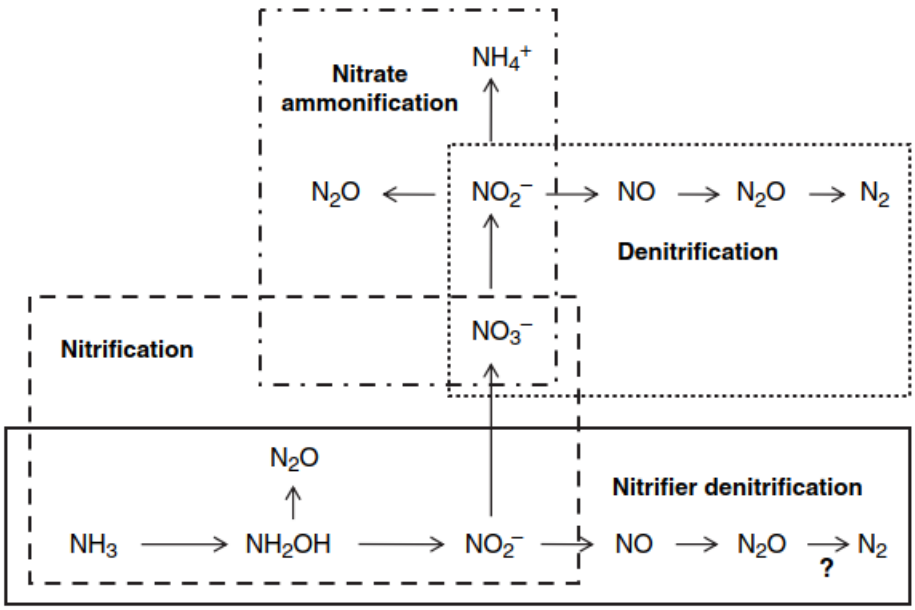


### 1.3.2 Denitrification in soils

Denitrification is a microbial process in which a large range of microorganisms use nitrate ($NO_3^-$) or nitrite ($NO_2^-$) as electron acceptors when $O_2$ is limited.

$$NO_3^- \rightarrow NO_2^- \rightarrow NO + N_2O \rightarrow N_2 \quad \text{(Eq 1-1)}$$

This process occurs in tropical, temperate and boreal soils, in natural and intensely managed ecosystems and in aquifers (Skiba 2008). Approximately 80% of $N_2O$ anthropogenic emissions in atmosphere are likely to come from land use for food production by agriculture (Ciais et al. 2013).

Although the N loss from denitrification is small compared to the biosphere N-store, this process has been extensively studied. Initially the focus was on agricultural systems, where since the discovery of the process at the end of the 19$^{th}$ century by Gayon and Dupetit it was evident that a substantial proportion of fertiliser applied could be lost through this process (Focht 1986). More recently, denitrification has been more widely studied in other ecosystems for two opposing reasons, relating to environmental improvement and degradation, respectively. The first reason is the potential of denitrification to alleviate environmental impacts of nitrates in surface and groundwaters (Ambus and Zechmeister-Boltenstern 2007). The second reason is that denitrification is a source of nitric oxide (NO) and nitrous oxide ($N_2O$) contributing to climate change. $N_2O$ is a potent greenhouse gas, with 298 times the global warming potential of $CO_2$ (Myhre et al. 2014). In the stratosphere, $N_2O$ is oxidised to form NO and $NO_2$ which catalyse the destruction of ozone, making $N_2O$ the single most important cause of stratospheric depletion emission in the 21$^{st}$ century.

Covering approximately 20% of the Earth's land area, forest ecosystems are a major but poorly quantified source of $N_2O$ and NO, with tropical forests estimated to account for ~18% of all atmospheric $N_2O$ sources (Butterbach-Bahl and Kiese 2005). The fraction of $N_2O$ of the total gaseous products of anaerobic denitrification that is emitted to the atmosphere as $N_2O$ from forests is highly dependent on the structure and wetness of the soil (Smith et al. 2003). If a $N_2O$ molecule can readily diffuse from the site of production into an oxygenated pore it is highly probably that it will be emitted to the atmosphere. On the other hand, $N_2O$ produced in deeper, water-saturated soil layers is often reduced to $N_2$. This variable ratio of $N_2O/N_2$ produced during denitrification affects the accuracy of estimation of N loss through denitrification. For example, for different hardwood forest sites in the USA Kulkarni et al. (2015) estimated growing season $N_2O$ and $N_2$ emissions of 0.005 and 3-4 kg $ha^{-1}$, respectively. These figures indicate that methods that measure $N_2O$ only account for a minor portion of the total N output and therefore accurate estimation of total N losses through denitrification requires estimation of $N_2$ emissions, which is challenging. $N_2$ estimation is possible, either with methods replacing $N_2$ from the portion of soil undergoing the measurement (see Butterbach-Bahl et al. 2002) or using $^{15}N$ tracers (e.g. Morse and Bernhardt 2013). Cheaper and widespread methods can only

measure $N_2O$ as small changes in $N_2$ concentration due to denitrification are impossible to detect due to the high natural abundance of $N_2$ in air.

#### 1.3.2.1 Potential effects of nitrogen deposition on denitrification in forests

Forests exposed to enhanced $N_{dep}$ may generate increased N outputs (Ambus and Zechmeister-Boltenstern 2007). Effluxes of NO, $N_2O$ and ultimately $N_2$ may increase because of increased nitrification and denitrification processes. Field experiments, such as the EU-project NOFRETETE, showed that temperate forests could be a more important source of nitrous oxides than previously expected, leading to underestimations of $N_2O$ emissions. This could depend on the high temporal (hot moments) and spatial (hotspots) variability typical of the denitrification process (Groffman et al. 2009). The NOFRETETE project compared 13 forest sites from across Europe and found a significant positive correlation between NO soil emissions and $N_{dep}$, but not for $N_2O$. Fang et al. (2015) also reported that at six temperate forest sites in China, $NO_3^-$ leaching and denitrification rates significantly increased with increasing $N_{dep}$. With the global trend of increasing $N_{dep}$, increased rates of N loss through leaching and denitrification are to be expected.

#### 1.3.2.2 Methods to probe soil denitrification

As mentioned above, depending on the specific interaction of soil and climatic variables at the microscale the process of denitrification releases $N_2O$, NO and $N_2$ at different ratios. There are several sampling methods and analytical techniques which measure one or more of these bio-products, each one with advantages and disadvantages. This section aims to provide an overview of the different approaches to estimate soil denitrification as background to the measurement of $N_2O$ emissions conducted as part of this research and reported in Chapter 5.

*Chamber methods*. This is the most common approach to measuring gas fluxes from the soil surface. The chamber is placed over the soil surface for a period of time during which samples are taken for analysis to determine the change in concentration of $N_2O$. Chambers can be either manual or automated. Manual static chambers need to be manually sealed and sampled at fixed time intervals controlled by the operator. Their main advantage is that they are easily deployed and do not require extremely accurate or rapid analytical techniques. On the other hand they are highly labour intensive and allow only a limited number of readings (Rapson and Dacres 2014). Automated static chamber setup, sampling frequency and duration are electronically controlled. The chamber lids are mechanically closed at regular intervals and gas from

the chamber headspace is drawn into a gas analyser and circulated back to the chamber (Fassbinder et al. 2013). Automatic chambers allow a higher number of readings over a longer period of time but due to their cost they are suited for smaller study areas (1-25 $m^2$).

*Micrometeorological methods*. They measure gas fluxes above forest canopies over large areas (1-10 $km^2$). Sensors are placed on towers that measure wind, temperature and gas concentrations over time. Eddy covariance is the most direct and preferred method for measuring a flux over a surface. The instantaneous vertical flux density at a point in the atmosphere is the product of the vertical wind speed (measured with a 3D anemometer) and gas concentration at the same point (determined with a gas analyser). However, the need of fast and sensitive gas analysers and access to power to run equipment limits the use of this technique.

The methods presented above do not allow measurements of $N_2$ fluxes that represent the major N gaseous loss from soils and the most difficult flux to determine. The methods below have been used to help determine $N_2$ fluxes.

*Soil core method in a $N_2$-free atmosphere* (Chen et al. 2019, Kulkarni et al. 2015). In this method soil cores are sampled, refrigerated and enclosed in a direct flux gas-flow soil core system where existing soil gases are substituted by a mixture of helium and oxygen and analysed for $N_2O$ and $N_2$.

*$\delta^{15}N_{NO3}$ and $\delta^{18}O_{NO3}$ stable isotopes approach to indirectly measure denitrification* (Wexler et al. 2014). This indirect approach is especially suited to the determination of gaseous loss from soil respiration at a catchment scale by analysing shallow groundwater, avoiding the problem of directly measuring $N_2$ fluxes and the high spatiotemporal variability of denitrification processes. $NO_3^-$ isotopic composition reflects both sources and processes leading to its fractionation.

In the absence of methods to estimate $N_2$ emission, measuring $N_2O$ flux alone represents a tool to compare forest soil fluxes to other similar studies in the literature, but the uncertainty due to the high variability of $N_2O$/ $N_2$ ratio must be taken into account.

## 1.4 Thesis objectives and hypotheses

The aim of this thesis is to analyse the interaction between $N_{dep}$ and forest N cycling by separating the direct interaction of $N_{dep}$ with the forest canopy from the indirect

effects on the soil pool. The aim will be achieved through the following objectives, each with alternative hypotheses (H1-H3).

Objective 1: To quantify the active role of the forest canopy at the field plot scale in the uptake of $N_{dep}$ under medium-low $N_{dep}$ conditions by measuring the N water fluxes above and below the canopy for 5 years to determine canopy nitrogen uptake (CNU).

H1: It is expected that less N will be found under the canopy in TF and stemflow compared to the canopy bulk $N_{dep}$ (N in rainfall and cloudwater samplers, collecting wet deposition and a fraction of dry deposition) and that this proportion will vary seasonally. It is also expected that the N outputs in streamwater will represent a small loss within the forest N cycle, indicating that the forest has not reached N saturation and N is still a limiting factor in forest growth.

Objective 2: To determine whether canopy nitrogen uptake is varies between field plot and individual tree scales and over seasons and also to investigate canopy N uptake processes by applying a $^{15}N$ labelled solution to individual trees.

H2: It is expected that CNU rates and seasonal patterns will be similar in the field plot monitoring and at individual tree scales and N absorption by the canopy will happen predominantly soon after the application, as found by Adriaenssens et al. (2012).

Objective 3: To follow the fate of the organic N transferred from the canopy in litter to the soil on a 4-year timescale and analyse the N losses from soil as $N_2O$ to close the forest N cycle.

H3: A minor fraction of the labelled organic N will be recovered after 4 years. A part of the N recovery is also expected to be found in roots as ON is reallocated to the plant.

H4: $N_2O$ emissions are positively correlated to $N_{dep}$ and represents a minor loss of N for the forest N cycle.

## 1.5 Thesis structure

The thesis is organised into six chapters.

This introductory chapter is followed by a methodology chapter (chapter 2) that introduces the case study area and the reasons behind its choice and also provides an overview of the field sampling strategy and frequency and the laboratory analysis of samples. An explanation of data quality and identification of outliers will be given,

whilst the detailed methodology for each experiment will be provided in the following chapters.

Chapter 3 addresses Objective 1. It describes the results of 5 years of monthly monitoring of IN fluxes in water in Griffin Forest, including precipitation above the canopy, fluxes below the canopy and in streamwater. These values were scaled to estimate the N balance at the forest sub-catchment scale.

Chapter 4 addresses Objective 2, presenting the results of different experiments using $^{15}N$ labelled solutions. In the first experiment, simulated labelled $N_{dep}$ was applied to three individual trees at higher rates than natural deposition on two occasions in summer and winter to estimate the magnitude of CNU magnitude outcomes and identify any seasonal pattern. A second experiment targeted branches on mature Sitka spruce trees in situ with a pure $^{15}N$-labelled solution.

Chapter 5 focuses on the biggest N pool in forests, the soil and the major transfer of N from the canopy to the soil via litter deposition and $N_2O$ losses from denitrification. Objective 3 is addressed through a $^{15}N$-labelled litter experiment in which the rates of organic N decomposition were measured after 4 years. The results are used to estimate the reallocation of transferred N in soil and roots and to comment on the time scale and mechanisms of decomposition.

Chapter 6 brings together the main results of Chapter 3, 4 and 5 in the context of the latest understanding of canopy nitrogen uptake in forest worldwide. Particular attention will be given to the significance of the results in the wider national and global context of forest restoration as a goal to achieve multiple objectives as addressed by the recent National Forestry Strategy.

# Chapter 2. Site description and methodology for the long-term water and litter sample collection

This chapter will give a general overview of the reasons behind the choice of the site, a Sitka spruce plantation in the Scottish Highlands. After an introduction to the history of plantations in UK and to some of the specific features of plantations that need to be taken into account in the research design, the chapter will describe the general methodology followed in the field and laboratories for the collection and analysis of the water samples in the period 2011-2017. Field data and lab data will be described in their main features – numerosity, missing data, outliers – and it will be described how the data collected by different researchers were managed and merged. The experiments that used $^{15}N$ labelled litter and $^{15}N$ labelled applications to the crown and branches will be described in their specific Chapters 4 and 5.

Finally, this chapter will explain how the sampling results have been scaled to values per hectare and report the data quality check and corrections. This includes the removal of the outliers and the use of regressions, where possible, to get a thorough 5 years dataset for the nitrogen (N) deposition ($N_{dep}$).

## 2.1 Site description

The research site is located in Griffin Forest, Perthshire, Scotland, UK (56° 36'23.59" N, 3° 47' 48.55" W, median elevation 350 m, see Fig. 2-1), on the north facing slope of the Tay River valley, ~4 km from the town of Aberfeldy (56° 37' 18.307" N 3° 52' 1.088" W, 87 m a.s.l.). The main land use of the area is also shown in Fig. 2-1.

Figure 2-1. Land use map of the study area (1:50000). Source: Edina digimap. The location of the study area in the UK is shown in the inset map (source: library *map*; black diamond shows the latitude and longitude of Griffin Forest).

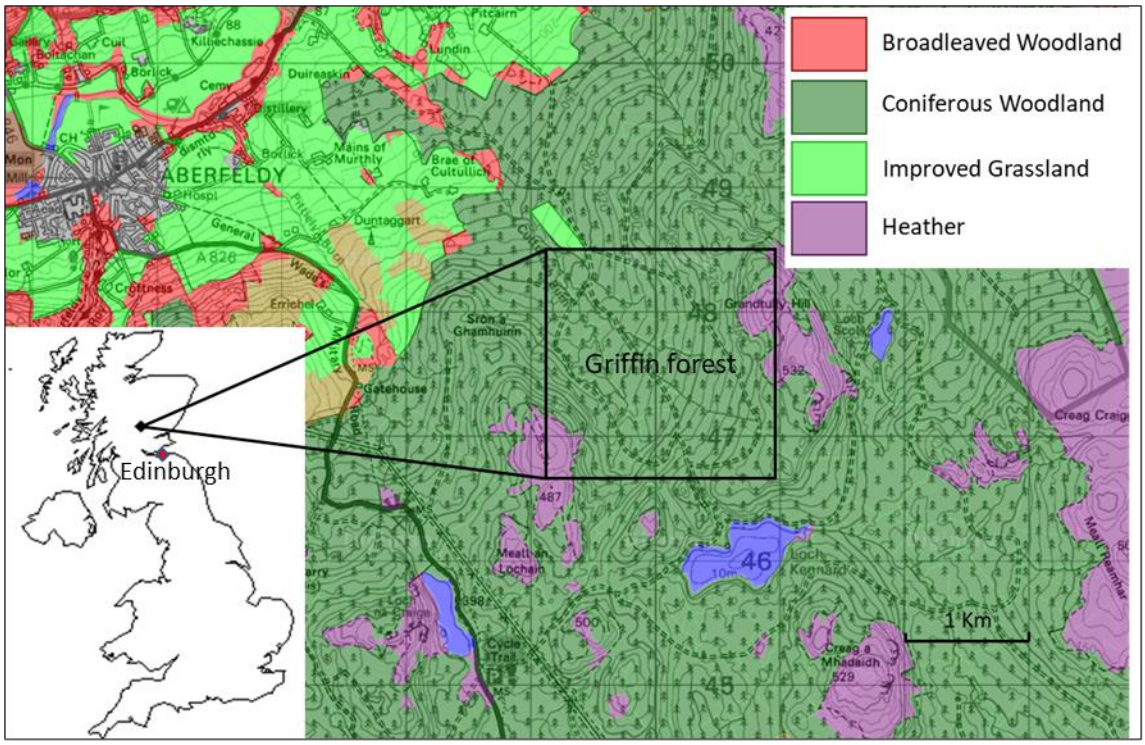


This area is characterised by relatively cool winters and warm summers, compared to Scotland as a whole. Fig. 2-2 shows the monthly minimum and maximum mean temperature and rainfall for Aberfeldy.

Figure 2-2. Summary of monthly air temperature (a) minimum and (b) maximum, and (c) rainfall at Tummel Bridge. The black middle bar shows the average monthly value, the upper and lower green bars indicates the temperature reached by the 20% and 80% of the measurements. Data period: 1981-2010. Data source: Met Office UK. url: https://www.metoffice.gov.uk/research/climate/maps-and-data/uk-climate-averages/gfj4sg07z

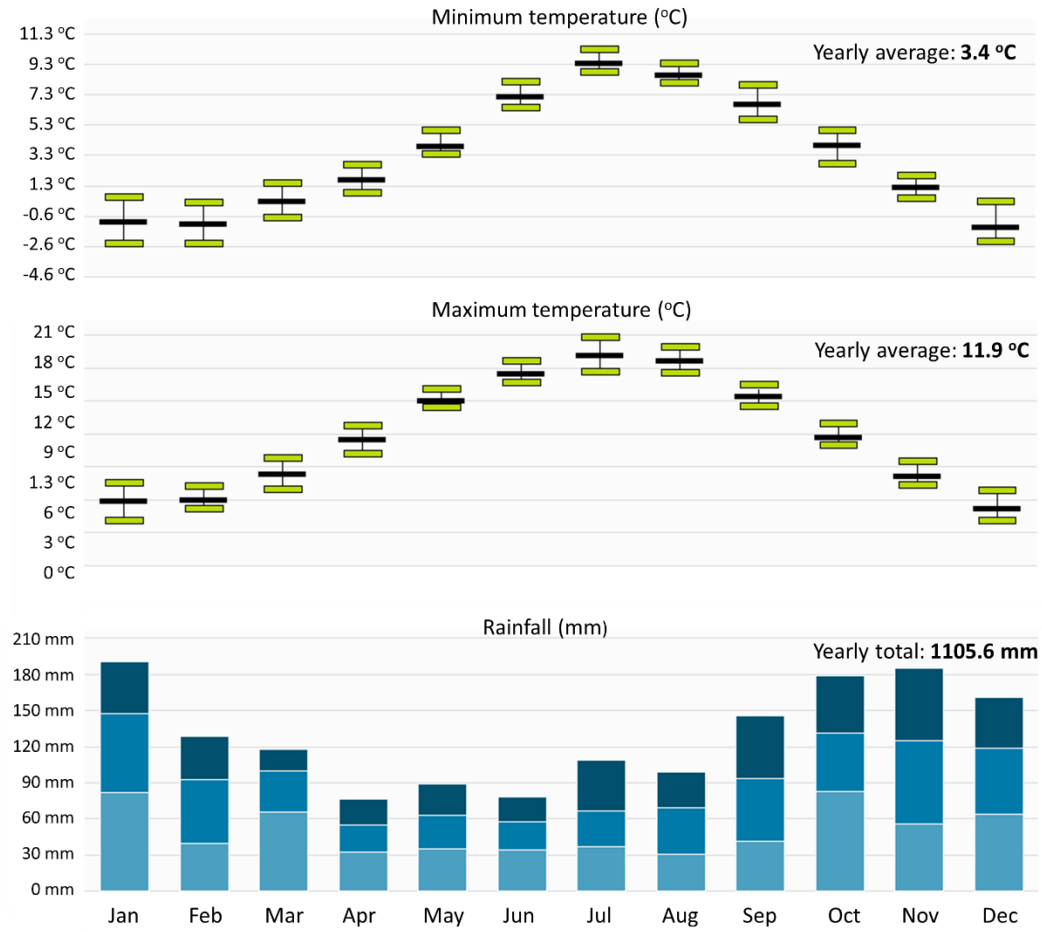


Rocks in the Aberfeldy area belong to the Dalradian supergroup, metamorphosed marine sediments of late-Precambrian and Lower Palaeozoic age (Craig 1925). The bedrock underlying the forest is characterised by psammite and semipelite with minor inclusions of metalava and metatuff, covered by Devensian till deposits. The soils have been classified as a stagno-humic gley of the Strichen soil association (Clement et al. 2012).

### 2.1.1 Forests in the UK, from past to the present

The present status of Scottish forest cover reflects a recent afforestation process started in the second decade of the 20$^{th}$ century. At the start of the past century, less than 5% of the UK was covered by forest. In contrast, after the last Ice Age different types of forests covered the Highlands, mainly pine and oak, apart from the extreme northern portion and the islands where the forest cover mainly consisted of birch and

hazel. The forest extent reached its maximum about 6,000 years ago, when investigations of pollen distribution suggest that at least 60% of Scotland was covered by some sort of vegetation. Soon afterwards there is evidence of massive utilisation and deforestation by early farming communities dating from 4000 years ago (Oosthoek 2013). In north-west Scotland the pine forests were largely replaced by blanket bog before any large impact by man, whilst in the eastern Highlands human activity was the main destructive agent, stretching over a period from about 1700 BC to about 1000 AD.

During the First World War about 182,000 ha of mostly broadleaved woodland were felled in the UK, mainly to provide timber for trench warfare. This created the need for a strategic policy to create and maintain woodland stock bringing about what can be considered the foundations of today's forestry policy and practices in the UK: the Forestry Act of 1919. The Forestry Commission (FC) was created and a target was set to create 0.75 million ha of new forest, so that the UK no longer had to rely on timber imports. Due to the Second World War, and the consequent need for more timber, in 1943 the FC set a new ambitious target of 1.2 million ha to be afforested and a further 0.8 million ha of "effective" forest to be created by restocking existing woodlands. Afforestation continued from the 1940s, despite the loss of strategic interest related to warfare, and at the end of the 1970s the 1943 target was reached. In December 1980 a ministerial statement announced a forestry policy that no longer mentioned a total area of plantations but envisaged an afforestation rate of 20,000-25,000 ha per year, later increased to 30,000 ha in March 1986. Blanket afforestation consisting of even-aged conifer monocultures that are harvested and replanted was common. The rapid expansion of coniferous plantations occurred on land where tree growth is least satisfactory, in the uplands, in order to avoid competition with agriculture and to reduce unit costs. As of 1986, 34% of hill, moor and rough grazing in Scotland had been afforested (Tompkins 1989).

The area of woodland in the UK at 31 March 2017 exceeded 3 million ha, 1.4 million of which is located in Scotland, representing over 18% tree cover in Scotland. Conifers account for 51% of the overall forest cover in the UK, almost three quarters of which are located in Scotland. Sitka spruce accounts for around half of the conifer area in the UK and is even higher in Scotland (58% according to the Forestry Commission (2017)).

Since the creation of the Forestry Commission in 1919 much has changed in the approach to forestry in the UK. The last decades have witnessed a strong

development of the concept of sustainable development and multiple benefits from ecosystem services, and thus forestry has increasingly broadened its objectives towards a sustainable forest management, in which the economic aspects need to meet the environmental and social functions of the forest (Forestry Commission 2017).

Nevertheless, at the time Griffin Forest was established forestry practices remained intensive and focused on ground cultivation and drainage, planting of conifer monocultures, and fertilising. The industry had become steadily more dependent on a single species, Sitka spruce, with lodgepole pine used where the ground was poorest. In 1995, Sitka spruce represented about 45% of all conifers in Tayside, over one third of the forest cover of the region.

### 2.1.2 Background to the Griffin Forest plantation

The main factors determining the maximum height at which trees can grow are altitude, climate (especially wind exposure) and soil quality. The potential maximum height of the tree line in Scotland is about 610 m at Creag Fhiaclach in the Cairngorms (Pears 1967), north of the study area, which is significantly lower than in Northern America and Scandinavia at similar latitudes. This is due to the combination of the cool and wet oceanic climate and the wind exposure. Soil type also indirectly reflects these two factors as they influence rainfall pattern and amount, a key factor in the genesis of soil together with topography. The formation of blanket peat in the Scottish uplands, starting after the last glaciation, is another limiting factor on the growth of trees that has been changed with the use of drainage in plantations to make the growth of tree roots possible (Oosthoek 2013).

The Griffin Forest plantation was established in 1980-1981 on an area classified as heather moorland, on altitudes comprised between 278 and 531 m asl. Before planting the trees, heather (*Calluna vulgaris* (L.) Hull) was burnt and the ground was ploughed to improve drainage and bring subsurface soil nutrients to the surface, creating a surface characterised by 3 different features: ridge, furrow and undisturbed soil, with ridges 1.9 m apart. Trees were planted at a spacing of 1.9 m on the ridges, so that the total number of trees was 2770 trees $ha^{-1}$ (Clement et al. 2012).

The area of ~4,000 ha was planted predominantly (80%) with Sitka spruce (*Picea sitchensis* (Bongard) Carriere 1855) and additional species such as Douglas fir (*Pseudotsuga menziesii* (Mirb.) Franco), Japanese larch (*Larix kaempferi* (Lamb.) Carr.), Scots pine (*Pinus sylvestris* L.) and downy birch (*Betula pubescens* Ehrh.).

The measured species in the experimental plots (T and C as shown in Fig. 2-3) are Sitka spruce (97.3%) and *Pseutotsuga menziesii* (2.1%) with rare presence of willow and birch at the edges of the plots.

From 1989 to 1996 a series of fertilisations with nitrogen, phosphorus and potassium by helicopter was carried out to improve the competition of the spruce against heather and other surface vegetation. The total application of fertiliser was approximately 350 kg $ha^{-1}$ of urea (163 kg N $ha^{-1}$), although some areas where heather was believed to be more competitive received up to 1400 kg $ha^{-1}$ of urea (653 kg N $ha^{-1}$).

Thinning was conducted in 2003/4 in the eastern part of the forest and in 2005 in the western part by removing every fifth row and cutting every third tree on the row either side of the thinned row. Overall one third of trees were removed, reducing the density to ~1750 trees $ha^{-1}$. At the time of the present study, the average height of the Sitka spruce exceeded 20 meters.

This forest has hosted a number of research projects mainly led by the University of Edinburgh and was one of the case study areas of the EU-supported Euroflux project (Clement et al. 2012), which aimed to assess the role of European forests as carbon sinks over their life time. During the years 1997-2001 Clement et al. (2012) calculated that Griffin forest sequestered about 6000 kg C $ha^{-1}$ $y^{-1}$. One eddy covariance tower (in plot T) from this experiment remained and was used during part of this study. Other MSc and BSc dissertations conducted at the University of Edinburgh (School of GeoSciences from 2002, Institute of Ecology & Resource Management before 2002) provided useful information for the development of the methodology of this study.

## 2.2 Forest plot monitoring

The current project design was informed by the NERC funded project “Impacts of nitrogen deposition on the forest carbon cycle: from ecosystem manipulations to national scale predictions” (NERC Reference: NE/G00725X/1, 2010-2014). The project measured $CO_2$ fluxes through a flux mast and two triangular lattice masts that had been installed in 1997; microclimatic data were also collected until summer 2014. Rainfall collectors, throughfall and stemflow samplers and the streamflow gauges were installed during the NERC project and were subsequently used for this study. In 2013, 18 gas sampling chambers were also installed (see Fig. 2-3) by Forest Research to measure greenhouse gas emissions from the forest soil (more details are given in Chapter 5.2.2). The NERC project also involved stem injection (of off-site saplings) of $^{15}N\text{-}NH_4NO_3$ to produce labelled litter (Nair et al. 2014) which was then

applied to $^{15}N$-labelled litter plots established in Griffin Forest in July 2013. This past labelling event was made use of in the current study (detailed on Chapter 5.2.1) with the aim of using the stable isotope approach to improve understanding the N dynamics in soil and close the N budget in a forest plantation. Collection and analysis of the water samples and gas chamber sampling was made by the author alone from April 2015 to the end of the study (April 2017) after a period of shadowing the former research assistant who had conducted all the collections and gas chambers sampling from mid-2013. In the period 2011-2013 other PhD candidates, undergraduate students or researchers conducted the monitoring under the supervision of Prof. Kate Heal. The data collected by others were available partly as Excel files and partly in paper format; they were brought together and analysed by the author.

The location of the sampling points is shown in Fig. 2-3. The two rainfall collectors are located downhill and uphill of the forested study plots. The black arrow indicates the northern access point to the study area, located about 2 km from the lower rainfall gauge. Initially the NERC project aimed to compare two plots of ~30 ha size within Griffin Forest with similar altitude and orientation, one of them designated as a control plot (C) and one as a treatment plot (T) where a solution containing $^{15}N$-labelled $NH_4NO_3$ was to be sprayed over the canopy by helicopter, similar to the Gaige et al. (2007) experiment. The T plot is located at 56°36'22'' N, 3°47'41'' W, elevation c.360 m and the C plot is a sub-basin lying slightly downhill at 56°36'38'' N, 3°47'40'' W, elevation c.350 m. Due to logistical constraints, the planned treatment could not be conducted and the two plots were monitored together to provide a representative area of the forest.

Figure 2-3. Location of the study plots and subplots in Griffin Forest. Image source: Edina digimap. SW = streamflow; TF = throughfall; SF = stemflow; RF = rainfall and cloudwater monitoring points. The yellow pin indicates the lower RF collector, the red pin shows upper rainfall and fog collectors location.

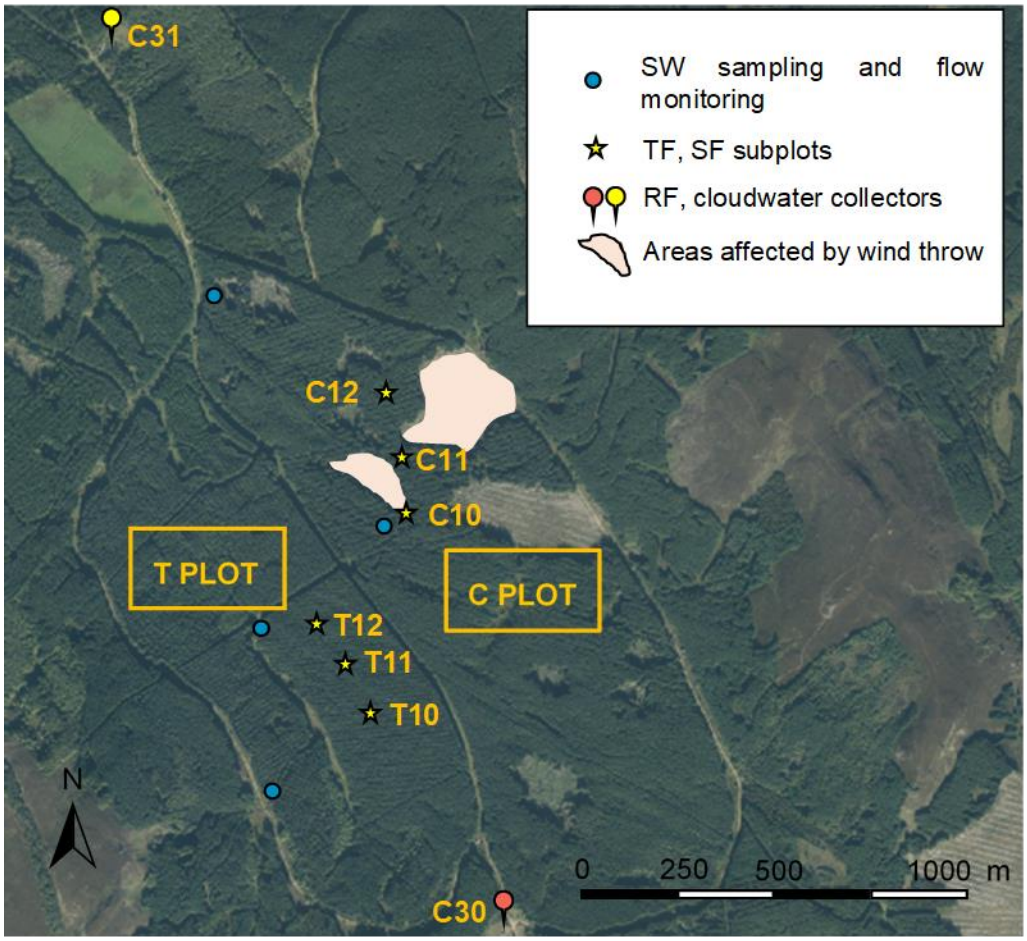


In both C and T plots, three subplots were identified (coded as T10, T11, T12, C10, C11, C12, locations shown in Fig. 2-3), each of these covering similar features of forest cover, soil type, altitude and exposure. Note that a storm in 2014 caused localised tree wind throw in the C plot (the two areas closer to the subplots C10 and C11 are shown in fig. 2-3). As a result, even if the installed throughfall and stemflow collectors were not directly damaged, the C plot forest cover was locally less dense and could show slightly different soil and air temperatures and interception characteristics compared to the T plot, especially in subplots C10 and C11. Due to the locally lighter density of the canopy it is reasonable to expect an increased variability in air and soil temperatures, as well as a lower interception. Although air and soil temperatures were not part of the present study, some data have been collected during a side project aiming to measure the greenhouse gases loss from soil (see Chapter 5.2.2). The information on soil and air temperature in the two plots

can be found in Appendix A, whilst an analysis of differences in interception/TF depths rate between the two areas can be found in Chapter 3.2.

The main objectives of the long-term experiment were addressed to analyse the interaction of the forest canopy with the $N_{dep}$ by comparing the nitrogen input from the atmosphere to the nitrogen recovered below the canopy. Two bulk rainfall collectors, one “harp-wire” fog collector, 18 throughfall/litter and 22 stemflow collectors and 4 streamflow flux and sample collection points were established. Sampling started in October 2011 and ended in May 2017. Sampling was conducted monthly, varying according to the precipitation to reduce the risk of losing part of the samples due to bottles/barrels overflowing.

### 2.2.1 Rainfall collectors

wo rainfall collectors were installed, one uphill of the T plot (56°35'59.8"N 3°47'21.5"W, elevation: 440 m) and a second downhill from the C plot (56°37'11.0"N 3°48'21.6"W, elevation: 286 m), both in the scarce open areas available at the site, sufficiently far from the plantation in order to minimise any turbulence due to the presence of tall obstacles. Their position was chosen to take account of altitude effects in Griffin; due to their location respect to the T and C site they should not be considered specifically representative of a single site. At the upper station a “harp-wire” collector to measure the cloudwater (Fig. 2-4) was also installed at a short distance from the rainfall collector, sufficient not to cause interferences between the two collectors.

Figure 2-4. Rainfall (left) and harp-wire cloud/fog collector at Griffin upper site. Photo: Kate Heal

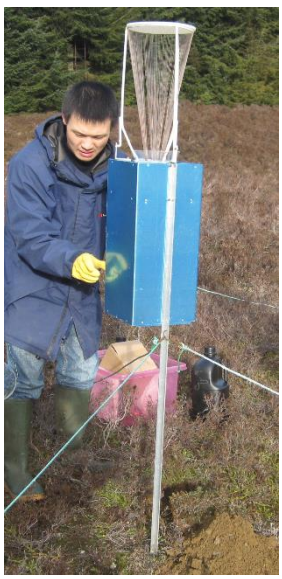

Rainfall and cloudwater were collected using borosilicate glass funnels (r = 7.5 cm) into black HDPE bottles, chosen to minimise light for biofilm growth (as recommended in Dammgen et al. (2005)). The maximum (measured) volume of the bottles is 2.7 L for the rainfall and 5.7 L for the cloudwater collectors, respectively. These volumes were chosen to ensure the collection of 1 month of precipitation, based on previous rainfall measurements situate the site. Glass wool was placed in the mouth of each funnel as a filter for debris and other macro particles (e.g. pollen, dust, insects and bird droppings). Concentrated orthophosphoric acid was added as a biocide agent to the collection bottles before exposure: 2.5 mL to each of the rainfall bottles and 5 mL in the cloudwater collection bottle due to its bigger capacity. No biocide agent was used in the throughfall and stemflow collectors due to the high volumes of sample collected and the need to dispose of most of the sample on site, potentially causing a local increase of soil acidity. Also, some biocides can interfere with the colorimetric analysis of the samples. For instance, Cape et al. (2001) showed that thymol in samples led to an overestimation of $NH_4^+$, whilst the use of sodium azide in this study in field tests before the $^{15}N$ application to the canopy led to undetectable $NO_3^-$ concentrations in throughfall samples. Cloudwater deposition was calculated as the difference between the cloudwater volume and the rainfall volume measured at the nearby rainfall collector, divided by the capture efficiency of the harp-wire collector (0.29) and multiplied by the average capture efficiency of Sitka spruce (0.06) (Heal et al. 2004).

### 2.2.2 Throughfall collection

Three replicate sub-plots were established in the NERC project in 2011 within each plot (see Fig. 2-3), and three throughfall (TF) collectors were installed in each subplot, each one representing different positions below the forest canopy: one TF was installed below thinning lines (they represented about 20% of the plantation surface), one under full density and one under partially thinned rows (categories covering 40% of the surface); they also considered the northerly-southerly aspect on either side of the thinned rows as it was expected that there might be more canopy evaporation and thus lower TF from the southern side of the thinned trees. this choice over-represents the thinned area of the forest and could lead to slight overestimate the TF. Throughfall was collected through two inclined gutters of a fixed length (4.02 m) and width (0.234 m) which drained to a 120 L HDPE barrel (see Fig. 2-6). The gutter angle ranged from 12° to 17°, with a median value of 16°, so as to maximise the surface area of collection without causing any ponding and ensuring ready drainage to the collectors to minimise evaporative loss. The barrel was covered but allowed the throughfall to drain

through a central metal colander (r = 12.25 cm) which acted as a filter, retaining litter or other undesired objects and preventing the entry of animals into the barrel. Each barrel was placed on a concrete slab next to a dug channel to allow drainage of water when the sampler was emptied. The depth of the water collected was measured with a plastic metre rule as close as possible to the centre of the barrel and converted into a volume through the calibration relationships described in Appendix B. For all the TF 120 L barrels the depth was recorded at the closest centimetre. Any relevant observation on the samplers (i.e. drainers partially out of the colander, presence of debris, bird droppings on drainers or colander, slugs, worms or insects in the barrels, foam or anomalous turbidity) was recorded together with the TF depth measurement. Disposable nitrile gloves were used at all times during measurements and sample collection. Each sample bottle was rinsed three times with the matching barrel, then filled to the brim and placed in the cool box.

Mean throughfall depth (TF, mm) was calculated by dividing each water volume by the total surface projection of the gutters and the colander, as follows:

$$TF_{mean}\,(mm) = \left( \frac{\sum_{i=1}^{n} \frac{V_i}{x_i}}{n} \right) \qquad \text{(Eq. 2.1)}$$

Where, n = number of TF collectors

Vi = volume of throughfall (L) in the $i^{th}$ barrel calculated through the relevant calibration formula,

$x_i$ = total available surface for TF collection, calculated as:

$x_i \cong w * l * \cos\alpha * 2 + \pi r^2$, (Eq. 2.2)

w = throughfall gutter width (m)

l = throughfall gutter length (m)

α = gutter angle from horizontal (rad)

r = colander radius (m)

Figure 2-5. Throughfall sampler at subplot T12. May 2017

### 2.2.3 Stemflow collection

Each stemflow sampler comprises a c.30 L covered barrel, placed on a concrete slab which was dug into the ground in order to maintain as cool a sample temperature as possible and so minimise sample degradation. A length of cut-away 5 cm diameter vinylflex tubing was wrapped around the trunk of each selected tree and attached with sealant and small nails to collect stemflow running down the tree trunk and direct it into the sampler through a hole in the sampler lid.

The rationale for the stemflow sampler distribution was similar to that used by Heal et al. (2004) for water balance investigation of Sitka spruce in south-west Scotland. Information on the diameter breast height (DBH) structure of the plots was gathered through a DBH survey conducted by Amy Harbinson (BSc dissertation student) in 2010 in both plots, comprising 3859 stems. The surveyed trees were divided into 8 DBH categories with equal number of trees in each and the median DBH of each category (ranging in value from 7.0 to 29.0 cm) was targeted for the stemflow samplers and replicated three times. Seventeen samplers were located in unthinned rows; five more samplers were deployed with the aim of assessing the effect of thinning. The target stem diameters and locations for trees to host stemflow samplers were selected to be close to the throughfall sampler plots. Table 2-1 shows the target DBHs and the number of SF samplers selected per each DBH division.

A two-way ANOVA was conducted on the Tukey-transformed SF data to test the significance of thinning on the SF collectors. Two groups of 6 SF collectors were selected, one with the collectors on the thinned lines and one of equal numerosity

with collectors with the closest DBH to the first group. Normality and presence of extreme outliers was checked before proceeding; no significance variance was found between the groups (pr (> F) = 0.68).

Table 2-1 – range of DBH classes, median DBH and number of samples selected per each category.

| Division | DBH min (cm) | DBH max (cm) | Median DBH (cm) | Number of SF samplers |
|---|---|---|---|---|
| 1 | 0.5 | 10.0 | 7.0 | 2 |
| 2 | 10.0 | 14.5 | 12.5 | 2 |
| 3 | 14.5 | 17.5 | 16.0 | 3 |
| 4 | 17.5 | 20.0 | 18.5 | 5 |
| 5 | 20.0 | 22.0 | 21.0 | 3 |
| 6 | 22.0 | 24.0 | 23.0 | 2 |
| 7 | 24.0 | 27.0 | 25.5 | 3 |
| 8 | 27.0 | 45.5 | 29.0 | 2 |

The target stem diameters and locations for trees to host stemflow samplers were selected to be close to the throughfall sampler plots. The calculation of the stemflow volume collected is similar to that of throughfall. Similar to throughfall, stemflow volume was calculated by converting the water depth in the collection to a volume (see equations in Appendix B). Since there was no apparent effect of thinning, to estimate the mean stemflow volume across the study area, the mean volume of the samplers of each of the 8 classes was calculated, and the mean value of the 8 classes was scaled to a hectare by multiplying it by the tree density (1750 $ha^{-1}$).

### 2.2.4 Throughfall and stemflow depth to volume conversion

The volumes of the HDPE barrels used to collect TF and SF were chosen based on the mean monthly volumes measured at the site by Xiangqing Ma (2000, data not published). Barrels, with a capacity of 30 L, were used for most of the stemflow samplers and also for the multiple throughfall collectors set up in the short-term experiment involving application of $^{15}N$-labelled $N_{dep}$ to the canopy (see Chapter 4.2.1.1). The square and round barrels with a volume of over 120 L were used for the throughfall collectors.

Calibration of each type of barrel was conducted in the laboratory by Ian Smith in March 2011 as part of the NERC project by repeatedly adding a litre of water and measuring the water depth in the centre of the barrel. The linear regression relationship obtained for each barrel type ($R^2 \geq 0.999$) was used to convert the water depth measured in the centre of each barrel in the field to the nearest cm into a volume. The attribution to the nearest cm gives uncertainties in the volume

estimations of ~0.4 L for the small 30 L barrels, 0.6 L for the 120 L square barrels and 1 L for the round 120 L barrels; these volumes represent ~ 1% of the maximum capacity of each barrel type.
For water depths in the barrels less than 1 cm, the volume was estimated in the field by using 250 mL Nalgene bottles.

To scale up SF from individual trees to the whole study site the relationship between SF volume and stem diameter at breast height (DBH) was investigated which, if found, could be applied to the measured distribution of DBHs from measurements of 3859 trees in the whole study site. In Fig. 2-6 the results of the survey by Harbinson (2010) are shown; trees were measured. Relationships were examined by individual sampling dates, but none were significant, in contrast to the study on a Sitka spruce forest in south-west Scotland by Heal et al. (2004), where significant positive relationships were shown between stemflow volume and $(DBH)^2$.

Figure 2-6 Distribution of the surveyed trees in Griffin by classes of 0.5 cm. The x-axis shows the thresholds dividing the 3859 trees into 8 categories containing equal numbers of trees to select trees for SF sampling (see also Table 2-1 and surrounding text).

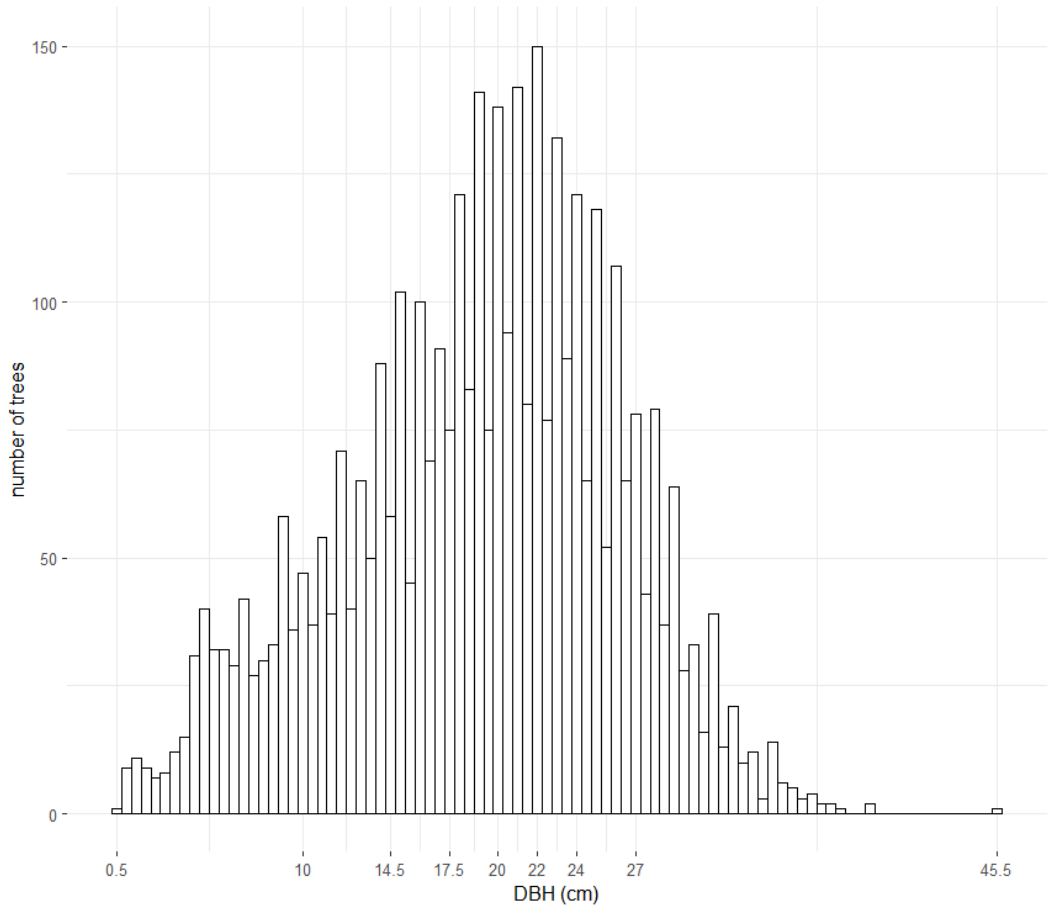

Therefore, it was examined instead whether the expected stemflow volume-DBH2 relationship was affected by rainfall intensity, based on the hypothesis that relative interception decreases with the magnitude of the event and this relationship is not linear (Llorens et al. 1997). For this analysis the 2012-2016 rainfall (RF) dates were divided into three groups: (1) the wettest rainfall collection dates (mean RF>4.2 mm d-1during the collection period; (2) intermediate rainfall collection dates (mean RF depth between 2.1 and 4.2 mm d-1) (3) the driest rainfall collection dates (mean rainfall RF<2.1 mm d-1). The thresholds were chosen after a visual inspection of different density plots obtained by dividing the RF events in 3 groups based on the overall distribution of rainfall intensity (see Fig. 2-7 for the density plot obtained with the chosen thresholds).

Figure 2-7 Density plot for the RF events sub-groups. Thresholds were set at 2.1 and 4.2 mm $d^{-1}$.

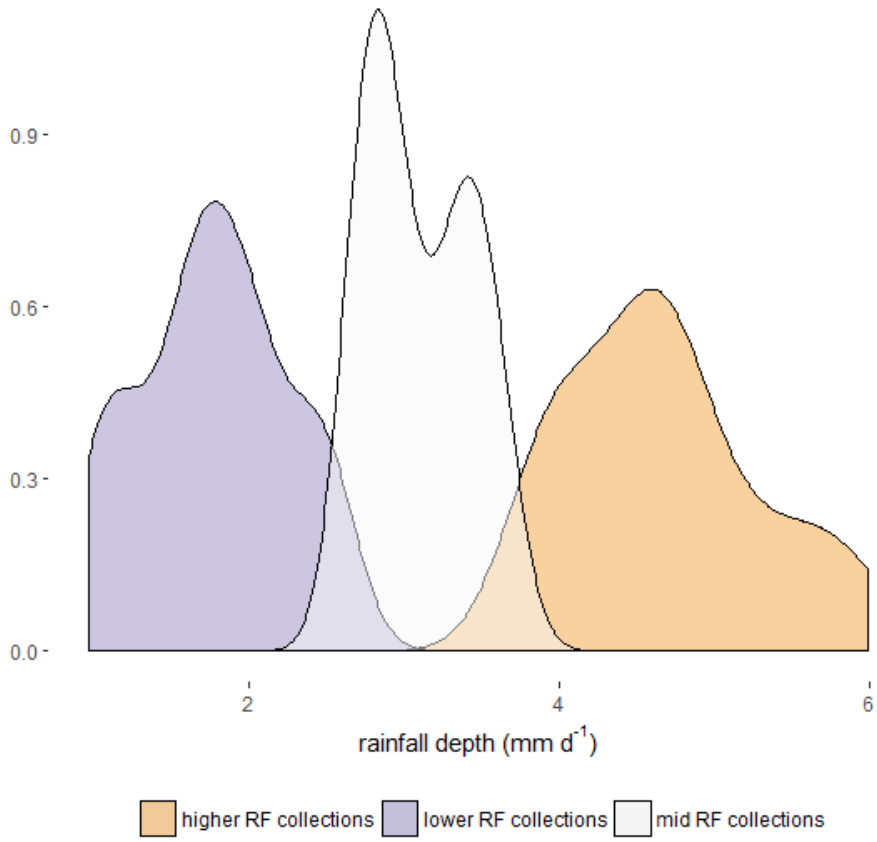


Mean daily RF was normally distributed within each of the three RF groups. A multiple regression was calculated for each group (by date and $DBH^2$) using the following linear model in R:

$SF_{vol} \sim DBH^2 + date$ (Eq. 2-3)

The regression model for each rainfall category gave a fitted model for all dates and for each individual sampling date. The results are show in Table 2-1.

Table 2-2. Results of multiple regressions on SFvol ~ $DBH^2$ by date for different rainfall intensity groups.

| Rainfall intensity group | Number of collection dates | Mean [median] RF in mm $d^{-1}$ | Adjusted $R^2$ | F | p-value |
|---|---|---|---|---|---|
| High RF | 20 | 4.67 [4.61] | 0.14 | 3.859 | p<0.001 |
| Intermediate RF | 17 | 3.10 [2.99] | 0.23 | 5.713 | p<0.001 |
| Low RF | 28 | 1.77 [1.75] | 0.38 | 11.03 | p<0.001 |

The highest $R^2$ value was found for the driest dates, with values decreasing as rainfall intensity increased. Regression analyses were conducted first with all dates included, and then with possibly suspect data excluded aside of those mentioned in Table 2.2, for example dates when SF collectors were overflowing or where other issues, such as under-estimation of SF due to displacement of the pipe from the collector that have been otherwise kept in the database for the calculations shown in Chapter 3. However, removal of suspect data points from the analysis did not increase the $R^2$ values shown in Table 3-1.

Alternative linear models including RF were better fitting than other more complex linear models where RF depth was added as an independent variable and the interaction between rainfall depth and DBH was added, but they did not show better fitting relationships between the variables. Therefore SF measurements were scaled up across the study area by using the 8 classes set as described above. Each of the SF sampling trees was assigned to the relevant DBH class and a mean SF volume was calculated for the sample trees in each DBH class for each date and the obtained value was multiplied by 1750, the estimated number of trees per hectare after the thinning.

The apparent absence of any relationship between DBH and SF at the study site can be explained by the characteristics of the canopy in a mature plantation. The strong interconnection of the tree crowns due to the large size of mature trees and the small distances between them means that SF volume was affected by the whole forest canopy, rather than by the canopy of individual trees. In addition, trees in the same DBH class were unevenly distributed within and between each site (Harbinson 2010)

which meant that trees of the same DBH could either dominate the surrounding trees or be dominated by bigger trees around it. Consequently, SF fluxes varied widely among trees of the same DBH class.

### 2.2.5 Litter collection.

When $N_{dep}$ from the atmosphere is low and in the absence of fertilisation, the reallocation of N through litter is central to soil nutrient supply in forest ecosystems (Aber et al. 1998). Litter was included in the sample collection with the aim to provide a more comprehensive picture of the N transfer from the canopy to the soil. This organic source of N, together with the inorganic N measured through the water fluxes under the canopy, were used in the experiment with labelled litter (Chapter 5) to estimate the N reallocated to the plant.

On each sampling occasion all the litter was collected from the gutters and colander of the 18 TF samplers. Each individual sample was oven dried at 70°C until no changes in weight were observed and then weighed and stored separately in sealed bags. The litter mass deposited per ha was calculated by dividing each sample litter mass by the projection of the surface of the corresponding gutter and the area of the colander (similarly to what was shown for TF in Eq. 2.1 and 2.2 above). Values for the litter N concentration were measured as part of an undergraduate dissertation in litter collected in each of the TF samplers in January, May and September 2012 (Mitchell 2013). These data were used to estimate N flux in litter from the forest canopy to the soil.

### 2.2.6 Streamflow: discharge and leached nitrogen

Four 90° V-notch thin-plate weirs (British Standard 1981) were installed in Griffin Forest, two in each plot. In the T plot one weir is located upstream of the plot and the other downstream to calculate a net balance of the N leached from the plot (see Fig. 2-8, T21 and T20 sampling points).

The stream flow data used in the present study are instantaneous discharge as measured monthly by recording the height of the water head of each V-notch when streamwater samples were collected near the weirs for measurement of N concentration. This allows at least approximations to be made of N leaching from the forest at different times of the year. Discharge was estimated by measuring the water depth above the centre of the V notch and converting to discharge using British Standard tables (British Standard 1981). When possible, a second estimate of the

instantaneous discharge was made with the volumetric method, using a 10 L bucket and stopwatch and calculating the mean flow from at least three consecutive measurements. Comparison of discharge values measured by the two methods (see Appendix D) showed that the V notch measurement method was reliable within the range of the bucket flow gaugings.

Leaching of inorganic N from the forest into stream runoff was calculated separately for the sub-catchments of Plot C and for those in plot T through Equation 3-2 and 3-3 shown in Chapter 3. For both equations sub-catchments areas are needed to scale the N loss over time to the area so to compare it to the other N fluxes assessed in this study. The areas of the Griffin Forest sub-catchments were calculated from Ordnance Survey Land-Form PROFILE DTM 1:10000 data (tiles NN84NW and NN94NW), provided by Ordnance Survey/Edina. Catchment areas were delineated from the catchment outlet coordinates using the fill, flow direction and flow accumulation tools in ArcGIS 10.3 by Leo Peskett.

Figure 2-8. Griffin watersheds and location of V-notch weirs for streamflow measurement and nearby streamwater sampling

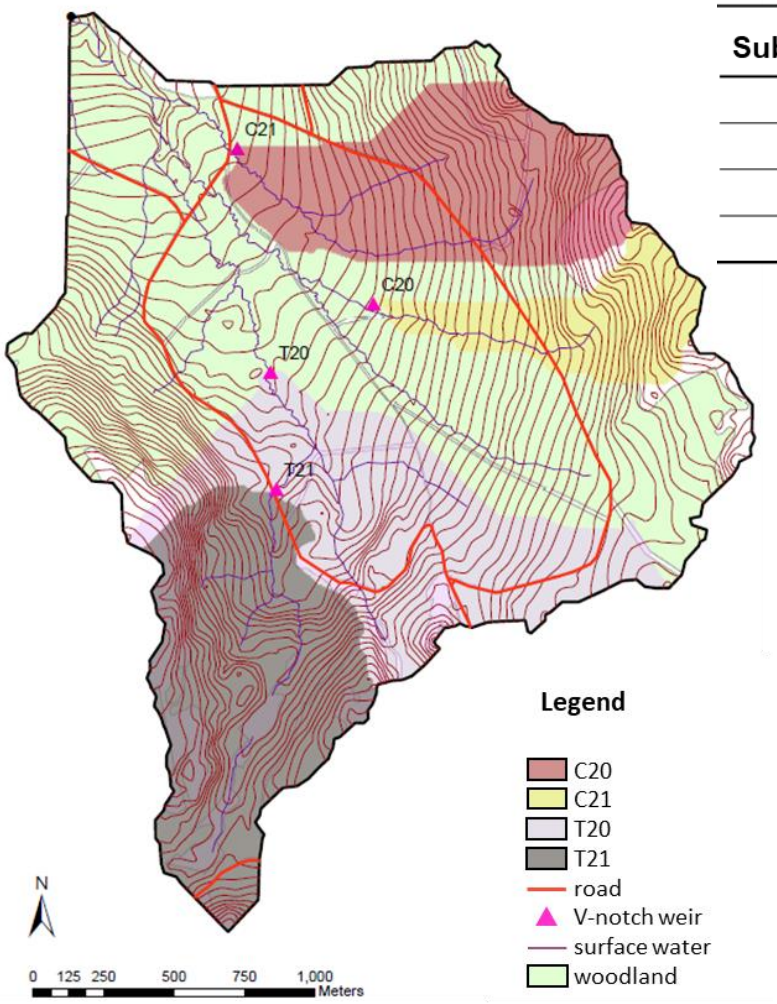


| Sub-catchment | Area (ha) |
|---|---|
| C20 | 30 |
| C21 | 67 |
| T20 | 158 |
| T21 | 80 |

### 2.2.7 Water sample preparation and analysis

Before field sampling, all the Nalgene HDPE sampling bottles (250 mL, 1 L for the streamwater) were washed with N free detergent, then rinsed six times with tap water and left to dry. The black HDPE bottles for rainfall and cloudwater sampling were also rinsed three times with deionised water and left to dry before adding the biocide. To act as field and equipment controls for sample contamination, two Nalgene bottles were rinsed three times with deionised water and filled with it just before leaving for the field, and brought along with the empty bottles and subsequently processed in the same manner as the samples. The resulting mean concentrations from the control bottles were subtracted from the sample concentrations.

In the field, all TF, SF and streamwater bottles were rinsed three times with the sample before the collection. All water samples were stored in a coolbox in the field after collection and then at 4°C on return to the laboratory until filtration, normally conducted within 24 hours of collection. A 60 mL syringe was flushed out three times with at least 30 mL of sample, then the same amount was taken from the Nalgene bottles and filtered through EMD Millipore Millex™ sterile syringe filters (0.45 µm pore size) into a biotite container after discarding the first 5-10 mL, and stored at 4°C until analysis, performed within a week of filtration. Automated colorimetric analysis was performed in the School of GeoSciences laboratories at the University of Edinburgh to determine $NH_4^+$ and $NO_3^-$ concentrations. Two separate Bran&Luebbe Autoanalysers AA3 were used for $NH_4^+$ and $NO_3^-$ analysis. To determine the $NH_4^+$ concentration, the sample was reacted with salicylate and dichloroisocyanuric acid to produce a blue compound with absorbance measured at 660 nm, using nitroprusside as a catalyst. To determine the $NO_3^-$ concentration, nitrate in the sample was reduced to nitrite by hydrazine in alkaline solution and then reacted with sulphanilamide and N-(1-Naphthyl) ethylenediamine to form a pink compound with absorbance measured at 550 nm. Five different standards (0.5, 1, 2, 4 and 8 mg $L^{-1}$ $NO_3/NH_4$) were used to calibrate the instruments. For quality control, one of the standards was analysed as a sample to verify the calibration at the beginning, middle (after about 20-25 samples) and the end of each run.

The remainder of the water samples were stored at 4°C until the analysis results were available and rerun when outliers did not have a clear explanation (e.g. contamination due to known causes).

## 2.3 Data Analysis

Data analysis was carried out using R and several packages in the RStudio™ development environment. All field and laboratory data from 2011 to 2014 were available either in electronic format (.xls files) or paper format and were compiled into a database by the author. The field and laboratory results were saved into separate monthly Windows Excel datasheets and then imported and saved into a RSQL database after some basic calculations were conducted. These included converting water depth in the barrels into water volumes (TF and SF) and TF depth (mm), rainfall and cloudwater (as mass of sample net of the bottle and biocide mass) into precipitation depth (mm), V-notch head measurement (cm) into water flow (L $s^{-1}$), converting the $NO_3^-$ and $NH_4^+$ concentrations to N and subtracting the mean values of the two blanks from the N concentration results. Table 2-3 summarises the number of

samples/concentrations measurements in the overall dataset and missing and outlier values.

Table 2-3. Number of samples and N concentration measurements in the Griffin Forest monitoring programme overall in 2011-2017 and for the period 2012-2016 when complete annual datasets were collected. In the 2012-2016 period 1304 samples were collected and analysed by the author, and 1347 were collected by others. The numbers of missing and outlier samples/values are also stated and explained in more detail below.

| | **Rainfall and cloudwater samples** | | **TF samples** | | **SF samples** | | **SW samples** | | **Litter *** | **total** | |
|---|---|---|---|---|---|---|---|---|---|---|---|
| FIELD VOLUME / DEPTH / FLOW MEASUREMENTS | | | | | | | | | | | |
| Samples 2011-2017 | 198 | | 1113 | | 1311 | | 233 | | | 2950[a] | |
| **Samples 2012-2016[b]** | 185 | | 1068 | | 1262 | | 221 | | | 2736 | |
| ***of which missing samples[c]*** | *0* | | *4* | | *52* | | *1[d]* | | | *65* | |
| ***of which overflowing*** | *20* | | *110* | | *277* | | *Not applicable* | | | *457* | |
| ***outliers*** | *0* | | *0* | | *0* | | *0* | | | *0* | |
| DETERMINATION OF $NH_4^+$ AND $NO_3^-$ CONCENTRATIONS IN THE LABORATORY | | | | | | | | | | | |
| | $NH_4^+$ | $NO_3^-$ | $NH_4^+$ | $NO_3^-$ | $NH_4^+$ | $NO_3^-$ | $NH_4^+$ | $NO_3^-$ | weight | $NH_4^+$ | $NO_3^-$ |
| **Samples 2012-2016[e]** | 174 | 174 | 1044 | 1044 | 1276 | 1276 | 200 | 200 | 540 | 2694 | 2694 |
| ***of which NA*** | *0* | *3[f]* | *16* | *16* | *71[g]* | *71[g]* | *7* | *7* | *0* | *94* | *97* |
| ***outliers*** | *5* | *0* | *3* | *1* | *7* | *1* | *0* | *5* | *0* | *15* | *7* |

[*] number of litter samples for dry mass determination used to estimate litter deposition rate reported in Chapter 3.
[a] includes 97 measurements of stream discharge using the volumetric method as described in the text above and reported in Appendix D.
[b] the sampling date 15 December 2011 and 5 January 2017 are included as the values have been used to produce the mean daily fluxes for December 2016.
[c] TF and SF missing samples were mainly due to empty barrels caused by either barrels that had fallen over or the SF vinylflex tubing found out of the hole in the barrel lid. On one sampling occasion (15 December 2014) a fallen tree damaged one of the TF gutters (C10T3) that was repaired on the following occasion (05 February 2015). Consequently, two TF samples were lost from C10T3.
[d] bottle broke on during transport from the field to the laboratory.
[e] the total number of samples do not include the 2 blanks analysed on each sampling occasion for both $NH_4^+$ and $NO_3^-$ (59 dates including 5 January 2017).
[f] on one occasion (24 September 2015) due to possible contamination all precipitation $NO_3^-$ analysis results were discounted.
[g] some of the SF samples were not analysed due to the negligible amount of sample (<0.25 L) or due to sample leaking or broken bottles/caps during transport from the field to the laboratory).

### 2.3.1 Overflowing samplers

The database contains a code for rainfall, throughfall and stemflow samplers affected by overflowing (OF), as well as a quality check code for other sources of sample loss

(e.g. broken or fallen collectors, pipe not connected to the SF barrels, funnels frozen in the rainfall collectors). Table 2-4 shows the details of OF samples in the period 2011-2017 for the rainfall samplers. For rainfall samplers a precautionary approach was taken. As overflows mainly affected the rainfall collectors, it was preferred to retain the data collected without adjustment, to avoid artificial overestimations of N input or low ratios of above: below canopy N.

Table 2-4 Dates of rainfall collector overflows

| Date | OF samplers | Field notes |
|---|---|---|
| **24/01/2014** | Lower; upper NA | Upper site not accessible due to high snow |
| **27/02/2014** | both | Upper site was two months cumulative precipitation |
| **31/10/2014** | upper | Funnel in lower site not in the bottle |
| **27/11/2014** | both | |
| **21/07/2015** | both | |
| **20/11/2015** | both | |
| **17/12/2015** | both | |
| **19/01/2016** | upper | Funnels pushed out probably due to freezing |
| **20/02/2016** | lower | At upper site only partial sample as funnel out |
| **22/06/2016** | upper | |
| **22/11/2016** | upper | |

Due to the volume of the collectors, OF occurred less frequently in TF than in SF, and when it did occur, a small percentage of collectors was affected. On 8 sampling dates more than 50% of TF and SF collectors overflowed, together representing about the 50% of the OF samplers. These dates were mostly during November-January, when precipitation were usually higher and/or freezing or snow occurred. Full details of the TF and SF OF are provided in Appendix C. Overflowing TF and SF data were used in the analysis without adjustment, similarly to overflowing data from the rainfall collectors.

Pearson correlation coefficients between rainfall, cloudwater, TF depth and stemflow (SF) volumes show high values (>0.85) between similar collectors types (rainfall and

cloudwater bottles, TF and SF barrels) and generally lower values between fluxes over and under the canopy (Fig. 2-9). The strong positive correlations between monthly mean values of different samplers provide further confidence in the quality of field volume measurements.

Figure 2-9 Pearson correlation coefficients between sampler mean monthly depths (mm $day^{-1}$) of rainfall (RF), throughfall (TF), cloudwater (fog collector) and stemflow (SF)

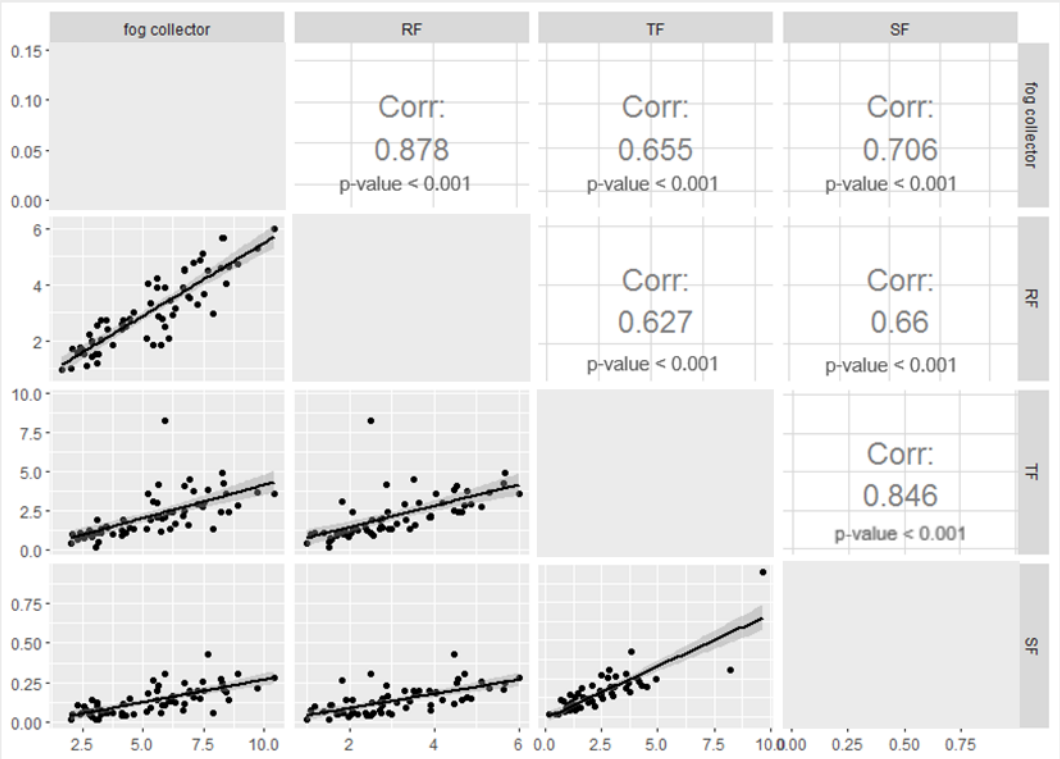


## 2.3.2 Corrections to the database

Before any further analysis, all datasets were analysed for outliers through the Tukey method which uses the interquartile range (IQR) approach by considering outliers as values above and below 1.5 x IQR. Any outliers identified by this method were deleted from the database. No outliers were found in the TF, SF, RF and cloudwater water volumes datasets.

When applied to the N concentration data, the Tukey method identified a very high number of potential outliers, attributed to several reasons:

a) high levels of $NH_4^+$ and $NO_3^-$ concentrations were measured in rainfall samples in March-April 2013 and April 2014, resulting in high calculated $N_{dep}$. This high

$N_{dep}$ values were also found in external measurements (see Fig. 3-8); in these cases no data have been rejected;

b) data from several TF and SF samplers showed higher N flux values compared to the inputs, This occurred in months with low precipitation or relatively low N mass flux values, hence with greater variability of [$N_x$] and N mass flux calculated;

c) variability between samplers that can be the result of different factors: variable collected water volume, contamination in the barrels from various (seasonal) sources – the most common being pollen, insects, slugs in spring, summer and autumn.

Streamwater N concentration data were checked for outliers through the same procedure adopted for the above and below canopy fluxes. Using this approach 5 outlying values were removed; dates, N form and sampling point are shown in Table 2-5. Two more potential outliers were considered but not removed as they occurred in both streams at the C site on the same date (24 July 2014), hence indicating that they are likely to be genuine high values rather than due to contamination. A precautionary approach was adopted aimed at minimising the number of rejected data. Table 2-5 shows the outliers removed from the database as either one order of magnitude higher than mean natural abundance or one order of magnitude higher than comparable samples taken on the same date:

Table 2-5. Outliers removed from the database

| Date | Sampler code | Sampler type | N form |
|---|---|---|---|
| 26/04/2012 | T10S2 | SF | $NH_4$-N |
| 20/07/2012 | C21 | SW | $NH_4$-N |
| 28/07/2013 | C20 | SW | $NO_3$-N |
| 28/07/2013 | T10S2 | SF | $NH_4$-N |
| 22/08/2013 | C10S1 | SF | $NH_4$-N |
| 22/08/2013 | T11T2 | TF | $NH_4$-N |
| 03/10/2013 | C31D1 | RF | $NH_4$-N |
| 03/10/2013 | C20 | SW | $NO_3$-N |
| 24/04/2014 | T12T1 | TF | $NH_4$-N |
| 20/06/2014 | T12S2 | SF | $NH_4$-N |
| 24/07/2014 | T10S2 | SF | $NO_3$-N |
| 24/07/2014 | T10S2 | SF | $NH_4$-N |
| 27/11/2014 | T21 | SW | $NH_4$-N |

| | | | |
|---|---|---|---|
| 23/02/2015 | T10S1 | SF | $NH_4$-N |
| 23/02/2015 | T10S2 | SF | $NH_4$-N |
| 21/04/2015 | T12T1 | TF | $NH_4$-N |
| 17/06/2015 | C31D1 | RF | $NH_4$-N |
| 21/07/2015 | C31D1 | RF | $NH_4$-N |
| 24/09/2015 | C20 | SW | $NO_3$-N |
| 19/10/2015 | T11T2 | TF | $NO_3$-N |
| 22/06/2016 | C31D1 | RF | $NH_4$-N |
| 25/07/2016 | C30D1 | RF | $NH_4$-N |

### 2.3.3 Cloudwater data substituted by regression relationships with rainfall data

Regression relationships and interpolations were used only for the input data (RF and cloudwater) to get a complete picture of the N input over 5 years of monitoring 2012-2016 inclusive. The remaining data (below canopy fluxes and streamwater) were not corrected, apart from the removal of the outliers shown in Table 2-5.

A regression relationship between water depths measured in the cloudwater collector and the rainfall collector nearby was calculated to correct otherwise negative values generated by anomalous lower volumes in the harp-wire cloudwater collector. The linear model was obtained excluding any dates when the nearby precipitation collector was either OF (see Table 2.5) or labelled QC (quality control check) and nine sampling dates where cloudwater depth was lower than the rainfall depth measured in the nearby rainfall collector (Table 2-6). The regression relationship for the remaining 25 sampling dates, with all units as mm $d^{-1}$ is:

$$cloudwater\ collector = 1.505 * RF + 0.352 \quad \text{(Eq. 2.4)}$$

Where $R^2 = 0.845$, $p = 5.8e^{-10}$ and there was a good linear distribution of the residuals. The excluded cloudwater collector depths were predicted using Eq. 2.4 with a confidence interval of 95% and the lower values of the interval were used to substitute for the measured cloudwater depth values. As higher water volumes lead to higher estimation of $N_{dep}$, when possible lower values of the interval were preferred to avoid overinflating N input estimates, thereby obtaining higher CNU values. This principle was also applied to the data shown in Table 2-7.

Table 2-6. Sample collection dates when cloudwater depths (mm $d^{-1}$) < RF depth (mm $d^{-1}$) and predicted value calculated using Eq. 2.4

| Sample collection date | Cloudwater (mm $d^{-1}$) | RF (mm $d^{-1}$) | Δ (mm $d^{-1}$) | Predicted cloudwater (mm $d^{-1}$) |
|---|---|---|---|---|
| 25/05/2012 | 2.75 | 4.64 | -1.89 | 6.70 |
| 21/06/2012 | 2.00 | 4.07 | -2.07 | 5.94 |
| 20/11/2015 | 1.36 | 4.77 | -3.42 | 6.88 |
| 19/01/2016 | 3.60 | 3.70 | -0.10 | 5.43 |
| 20/02/2016 | 1.77 | 3.39 | -1.62 | 4.98 |
| 24/05/2016 | 0.64 | 2.71 | -2.06 | 3.92 |
| 25/07/2016 | 2.54 | 3.00 | -0.47 | 4.39 |

Assuming that the N concentration in the cloudwater should always be equal to or greater than those measured in RF, similar linear regression relationships between cloudwater and rainfall were calculated for each of the $NO_3$-N and $NH_4$-N concentration datasets. The linear models have a $R^2 = 0.891$, p-value $=2.2e^{-16}$ on 64 sampling dates for the $NO_3$-N concentrations and $R^2 = 0.888$, p-value $= 2.2e^{-16}$ on 64 sampling dates for the $NH_4$-N concentrations. Tables 2-6 and 2-7 show the $NO_3$-N and $NH_4$-N concentrations in cloudwater that were substituted for by those calculated through the relevant linear models.

Most of those values that need to be determined through regression are either extremely low N concentrations or the relative difference in measured concentrations between cloudwater and RF are small (percentages are shown in Tables 2-6 and 2-7). All of the substitutions have made using the lower value of the 95% confidence interval of the regression, apart from three values in Tables 2-7 and 2-8 indicated by [a], where the mean interval value was chosen as the prediction confidence interval since the lower value was still lower than the RF value.

Table 2-7. Sampling dates showing cloudwater [$NO_3$-N] < RF [$NO_3$-N] that were substituted by regression. All predicted values are the lowest value of the 95% prediction confidence interval, except those marked with a, where the fit value was used.

| Sample collection date | (1) RF $NO_3$-N (mg $L^{-1}$) | (2) Cloud $NO_3$-N (mg $L^{-1}$) | (3) (2)-(1) (mg $L^{-1}$) | Δ as % of cloudwater $NO_3$-N | Predicted cloudwater $NO_3$-N (mg $L^{-1}$) |
|---|---|---|---|---|---|
| **21/08/2014** | 0.09 | 0.09 | 0 | 4% | 0.14 |
| **31/10/2014** | 0.13 | 0.11 | -0.02 | 13% | 0.24 |
| **27/11/2014** | 0.24 | 0.24 | 0 | 2% | 0.52 |
| **25/03/2015** | 0.32 | 0.13 | -0.19 | 60% | 0.72 |
| **21/07/2015** | 0.18 | 0.14 | -0.04 | 21% | 0.36 |
| **19/10/2015** | 0.31 | 0.26 | -0.05 | 17% | 0.7 |
| **17/12/2015** | 0.03 | 0.01 | -0.03 | 80% | 0.07[a] |
| **19/01/2016** | 0.13 | 0.04 | -0.08 | 67% | 0.23 |
| **24/04/2016** | 0.29 | 0.19 | -0.1 | 34% | 0.65 |
| **20/09/2016** | 0.32 | 0.17 | -0.14 | 46% | 0.71 |

Table 2-8. Sampling dates showing cloudwater [$NH_4$-N] < RF [$NH_4$-N] to be substituted by regression using RF [$NH_4$-N]. All predicted values are the lowest value of the 95% prediction confidence interval, except those marked with [a], where the mean interval value was used.

| date | (1) RF $NH_4$-N (mg $L^{-1}$) | (2) cloud $NH_4$-N (mg $L^{-1}$) | (3) (2)-(1) (mg $L^{-1}$) | (3)/(1) | Predicted cloudwater $NO_3$-N (mg $L^{-1}$) |
|---|---|---|---|---|---|
| 15/11/2012 | 0.08 | 0.04 | -0.04 | 54% | 0.11 |
| 10/12/2012 | 0.11 | 0.05 | -0.05 | 50% | 0.16 |
| 24/01/2014 | 0.1 | 0.06 | -0.05 | 43% | 0.16 |
| 27/02/2014 | 0.23 | 0.2 | -0.03 | 13% | 0.41 |
| 27/03/2014 | 0.1 | 0.09 | -0.02 | 16% | 0.15 |
| 20/06/2014 | 0.35 | 0.33 | -0.02 | 6% | 0.66 |
| 24/07/2014 | 0.96 | 0.7 | -0.26 | 27% | 1.77 |
| 21/08/2014 | 0.5 | 0.16 | -0.35 | 69% | 0.95 |
| 23/09/2014 | 0.29 | 0.29 | 0 | 1% | 0.54 |
| 27/11/2014 | 0.2 | 0.19 | 0 | 1% | 0.35 |
| 21/07/2015 | 0.2 | 0.12 | -0.08 | 40% | 0.35 |
| 23/08/2015 | 0.35 | 0.25 | -0.1 | 29% | 0.66 |
| 20/11/2015 | 0.29 | 0.21 | -0.08 | 28% | 0.54 |
| 17/12/2015 | 0.01 | <LOD | -0.01 | 100% | 0.02[a] |
| 24/04/2016 | 0.3 | 0.26 | -0.04 | 14% | 0.56 |
| 24/05/2016 | 0.5 | 0.47 | -0.03 | 5% | 0.94 |
| 19/08/2016 | 0.05 | 0.04 | -0.02 | 30% | 0.12[a] |
| 20/09/2016 | 0.68 | 0.62 | -0.06 | 9% | 1.28 |
| 12/10/2016 | 0.12 | 0.1 | -0.01 | 11% | 0.18 |

Finally, regression was used to calculate the rainfall $NH_4$-N concentration in the upper RF collector from the nearby cloudwater collector for July 2016, where the value for the RF collector was removed as an outlier, possibly due to contamination. This linear model has a $R^2 = 0.86$, p-value $2.2e^{-16}$ for 65 sampling dates. Similarly to what was explained above for cloudwater and rainfall samples. the lower value of the 95% interval was chosen as predicted value.

### 2.3.4 Data reconstructed by interpolation

In September 2015 contamination from an unknown source caused elevated $NO_3$-N concentrations in all three rainfall and cloudwater samples. In order to conduct N flux calculations, these data were predicted using linear interpolation of the concentrations

measured in the month immediately before and afterwards weighted by the number of days between the collections.

### 2.3.5 The daily values database for water volume and fluxes

The database was amended for cloudwater depths and $NO_3$-N and $NH_4$-N concentrations and with outlier $NO_3$-N and $NH_4$-N measured in water samples removed as described above. The amended database was then saved into a second RSQL database as a daily value, calculated as the value of a sampling collection (volume for SF, depth for TF and rainfall, instantaneous discharge in L $s^{-1}$ for streamwater) divided by the days since the previous sampling collection. All the results as tables, plots and statistics were created in R, importing data from the RSQL database, unless stated otherwise.

## 2.4 Conclusions

This chapter has provided a description of the main features of the study site and the methodologies used in the field and laboratory, describing the tools deployed for the long-term data collection.

Checks of the extensive 5-year database identified data quality issues for a small number of datapoints. A few outliers were identified, mainly in measured sample $NH_4$-N concentrations. All corrections followed a precautionary approach to avoid inflating recovery values and artificially strengthening the core hypothesis, i.e. that the canopy might uptake a fraction of $N_{dep}$. This principle was at the base of the choice not to correct the OF events for RF samples, as the correction to the volume would also add the uncertainty of the [N] which could be either diluted or increased by the lost sample. As to the under-canopy fluxes OF was mainly limited to SF collectors and affected 22% of the stemflow depth values.

Having only one cloudwater sampler shows the limits of a single measurement point as very small differences between measured N concentrations in cloudwater and RF samples can lead to negative flux estimates. However, significant regression relationships proved to be useful for estimating cloudwater N concentrations that do not inflate the input N fluxes. These limitations of these data will be taken into account in the presentation and discussion of the results in Chapter 3.

# Chapter 3. Results from the long-term plot monitoring

## 3.1 Introduction

Nitrogen (N) deposition ($N_{dep}$) is a worldwide phenomenon that threatens ecosystem function and biodiversity (Stevens et al. 2018). It varies widely in amount and chemical composition depending on the sources of emissions (Sutton et al. 2008). However, whilst in some forest ecosystems $N_{dep}$ exceeds critical loads (10-12 kg N $ha^{-1}$ $y^{-1}$ in Levy et al. 2020) and could lead to adverse impacts, such as increased susceptibility to diseases and pests (Wortman et al. 2012) or eutrophication of aquatic systems (Paerl 1993) and soil and water acidification (Aber et al. 1989), several studies (e.g. Magnani et al. 2007) have shown that $N_{dep}$ is beneficial to forest growth and, therefore, increased carbon sequestration. There has been a rapid increase in the last two decades of studies investigating the effects of $N_{dep}$ on forest ecosystems (Zhang et al. 2015). Many of these studies have involved N application to forests mainly through either application of different forms of N to the forest floor or by applying a N solution to the top of the canopy (or on a smaller scale by direct application to tree branches). Results from this second approach have demonstrated interaction of $N_{dep}$ with the forest canopy through direct uptake (e.g. Avila 2017; Houle et al. 2015) and a change of stoichiometry in N forms (oxidised and reduced inorganic N (IN) and organic N (ON)) between $N_{dep}$ and throughfall and stemflow below the canopy.

Whilst these effects of the forest canopy on $N_{dep}$ are now widely recognised and described, the variety of methodological approaches that have been used in different forest types and ecological conditions has resulted in a wide range of reported canopy N uptake (CNU) figures.

The aim of Chapter 3 is to determine the importance of CNU within the N cycle of a Sitka spruce plantation, as well as to form the basis for a comparison of different approaches for determining CNU in the field (in Chapter 4). This will be achieved through the following objectives:

1) Determine the CNU of a Sitka spruce upland plantation under natural low $N_{dep}$ conditions by measuring IN fluxes over and under the canopy.

2) Estimate the transfer of ON to the soil and the N losses from the forest in streamwater, closing the main gaps in the N cycle of the forest soil.

The objectives will be met by estimating the N fluxes from data collected during the long-term monitoring programme at Griffin Forest from October 2011 to May 2017. Only complete calendar years of collection - 2012 to 2016 - will be analysed in order to make seasonal comparisons between years.

The first three sections of this chapter present water quantity fluxes, comparing rainfall (RF) and precipitation (cloudwater and rainfall), throughfall (TF), stemflow (SF) and streamflow (SW). The uncertainties highlighted in Chapter 2 due to overflowing of RF collectors are addressed by comparing the data of this study to external data. The chapter then focuses on N concentrations and estimates of N mass fluxes in water onto and beneath the canopy. Finally, canopy to forest floor litter N fluxes and other minor fluxes are discussed to give an overall estimation of the N fluxes in aquatic pathways and litter in Griffin Forest.

## 3.2 Precipitation, throughfall and stemflow amounts

The mean measured annual RF in Griffin for the period 2012-2016 was 1073 mm $y^{-1}$, with a minimum of 874 mm in 2013 and a maximum of 1176 mm in 2012. The monthly RF values are the mean of the two rainfall collectors and are shown in Fig. 3-1 together with the cloudwater values, calculated as explained in Chapter 2.2.1.

Figure 3-1. Monthly values of mean RF depth and cloudwater depth at Griffin Forest by year for 2012-2016. Months in which at least one RF sampler overflowed are labelled with a star (✡)

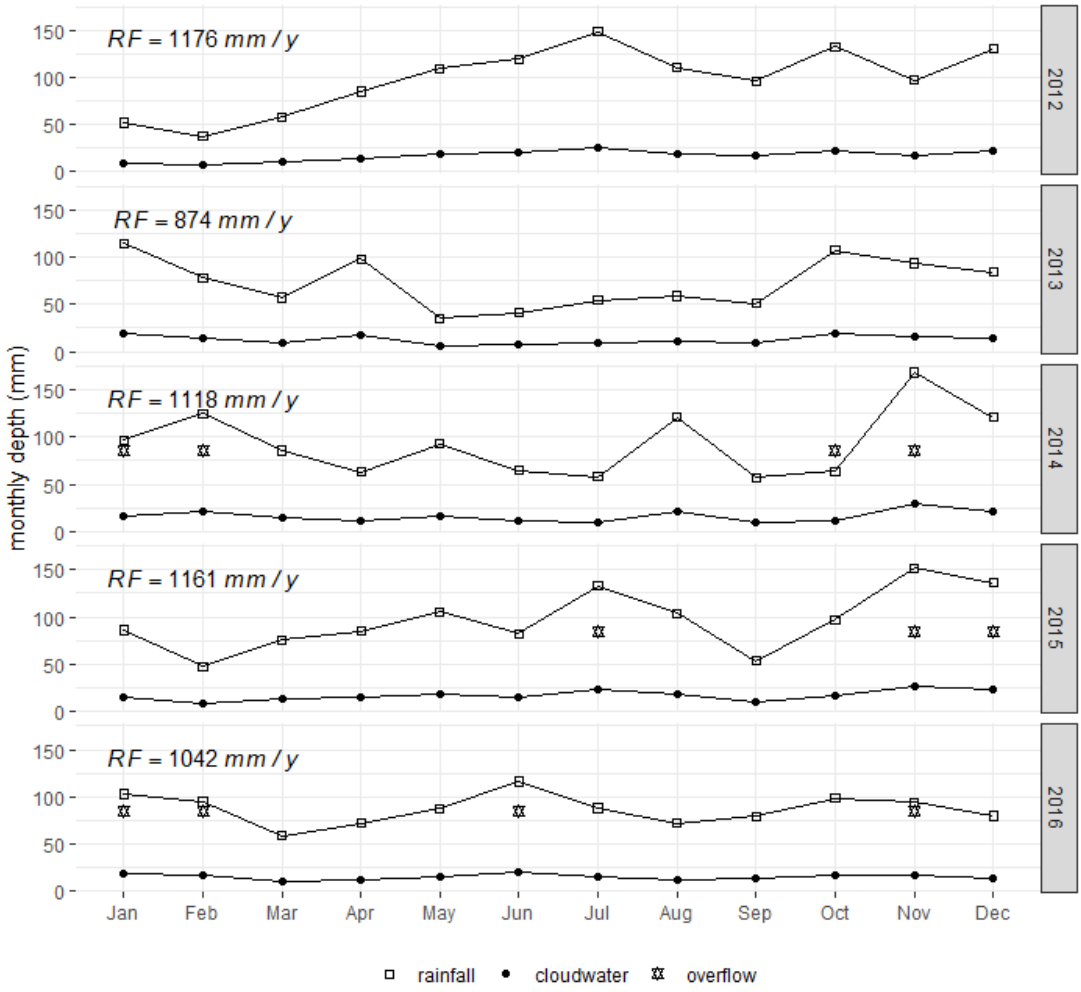


The measured rainfall data were compared to those measured at the Aberfeldy Dull rain gauge for the same time period, obtained from the Met Office Integrated Data Archive System (MIDAS) UK Daily Rainfall dataset. The total rainfall measured in the 5 year period at Aberfeldy Dull (56°37'15.6"N 3°55'30.0"W, height 100 m asl, 8 km from the case study area) was 9% higher than the rainfall measured in this study. One reason for this could be underestimation of rainfall at Griffin due to the occurrence of some rain gauge overflows which were not corrected for, as already discussed in Chapter 2.3.1 (details in Table 2-4). Since most of the rain gauge overflows occurred during the winter months, this explanation is consistent with the comparison of monthly rainfall data between Griffin and Aberfeldy shown in Figure 3-2, in which Aberfeldy rainfall exceeds Griffin rainfall predominantly in the winter months. Excluding rainfall for the dates on which rain gauge overflows occurred, 9% more

rainfall occurred at Griffin during the 5-year period compared to Aberfeldy. This is what might be expected due to the higher elevation of the rain gauges at Griffin Forest (286 m and 440 m) compared to the Aberfeldy Dull gauge since rainfall is usually expected to increase with elevation (Duckstein et al. 1973). A further reason for differences in the rainfall datasets between Griffin and Aberfeldy is the difference in the data collection. The monthly data at Aberfeldy are the sum of daily rainfall measurements, whereas the monthly data at Griffin are a weighted mean of sequential cumulative rainfall measurements.

Figure 3-2. Comparison between monthly measured mean rainfall at Griffin Forest and Aberfeldy (Dull) 2012-2016 (source: Met Office). The stars (✡) show the months where overflows in RF samplers affected the RF depth estimation at Griffin Forest.

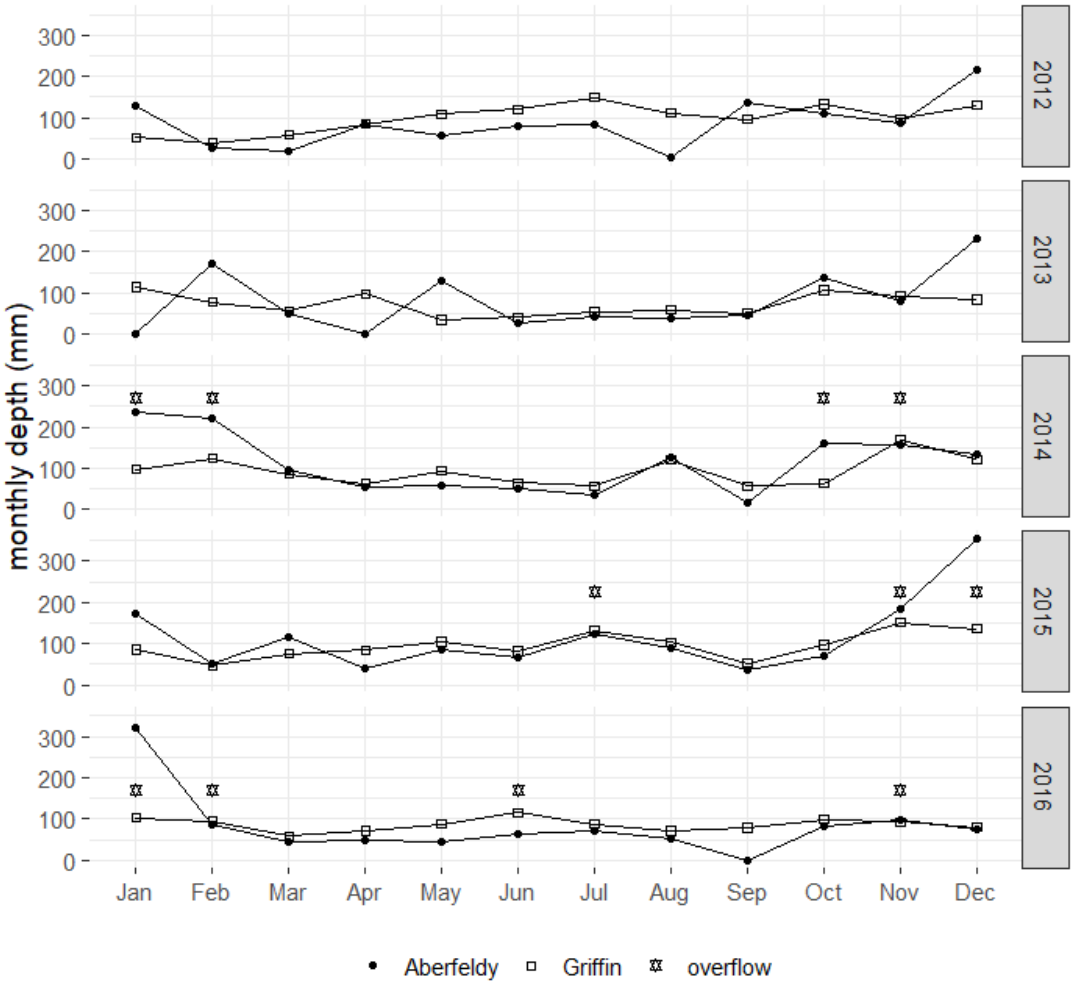


The discrepancies in Figure 3-2 which are principally attributed to overflowing rain gauges at Griffin Forest are consistent with the higher ratios of monthly precipitation/TF depth shown in Figure 3-3, where in October 2014 and January 2016

TF appears to equal the precipitation. The forest interception (calculated as the difference between precipitation onto the canopy and the sum of TF and SF below the canopy) was 47% of the measured precipitation on average in the 5-year monitoring period. This value is similar to other studies conducted on Sitka spruce plantations. For example, interception of 52% of precipitation was reported for a 37-year-old Sitka spruce forest in south-west Scotland (Heal et al. 2004).

Figure 3-3. Monthly precipitation (mean of two rain gauges + cloudwater) and mean throughfall at Griffin Forest by year for 2012-2016. The stars (✡) show the months where overflows in RF samplers affected the RF depth estimation at Griffin Forest.

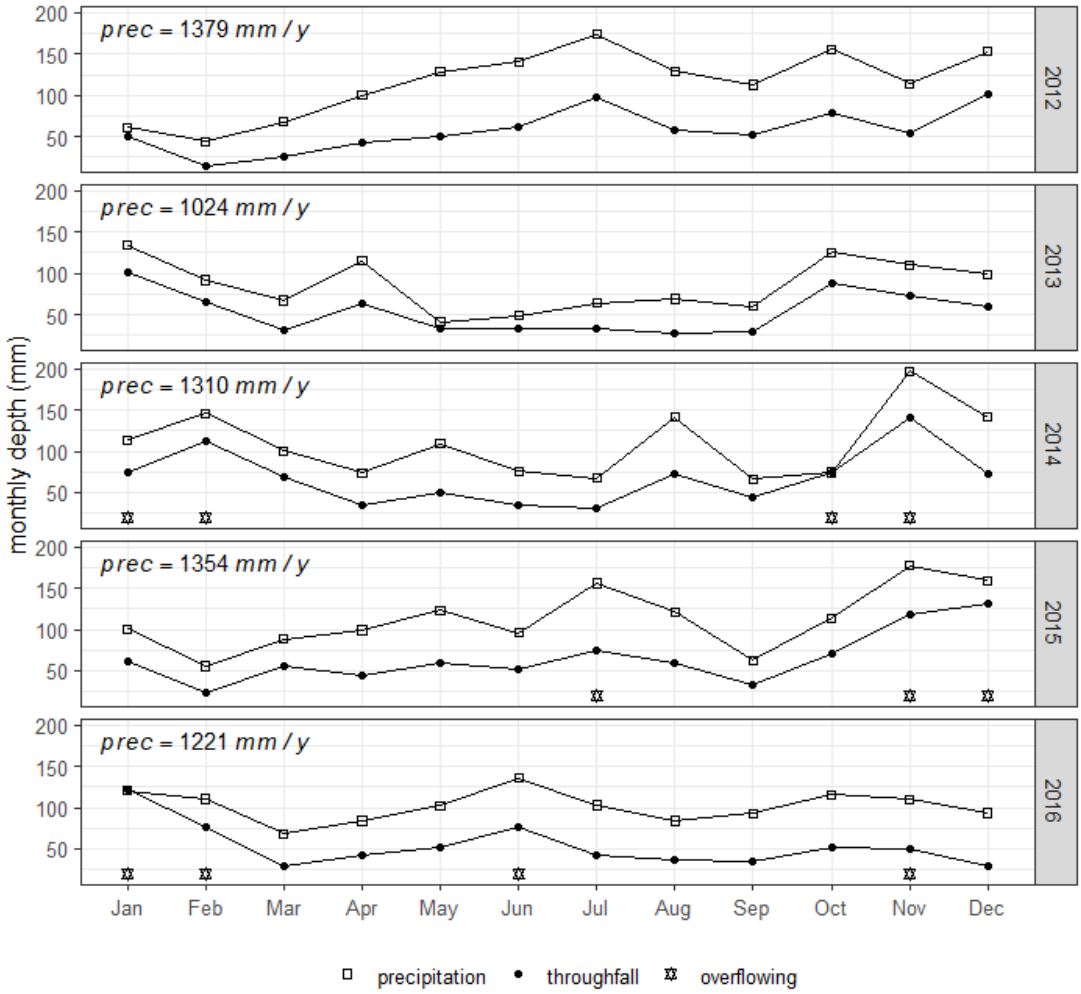


Fig. 3-4 shows the monthly TF depth by plot. Some differences in TF depths between the two plots are visible. TF in the T plot was 3.4% higher overall for the 5-year period and higher than TF in the C plot for 42 months. On one occasion only, January 2012, TF depth in the C plot was notably higher than in the T plot (22.3%). These results are rather unexpected, as it was anticipated that canopy interception would be lower

in the C plot (and thus TF would be higher) due to the wind throw in 2014. It therefore appears that the disturbances did not affect the water fluxes under the canopy and that the differences between the two plots are a natural consequence of the heterogeneity of canopy closure that can occur in even aged plantations.

Figure 3-4 Mean monthly TF depth in the T and C plots at Griffin Forest by year for 2012-2016. The time series for the C plot does not show any data for December 2016 as only the T plot was sampled in January 2017.

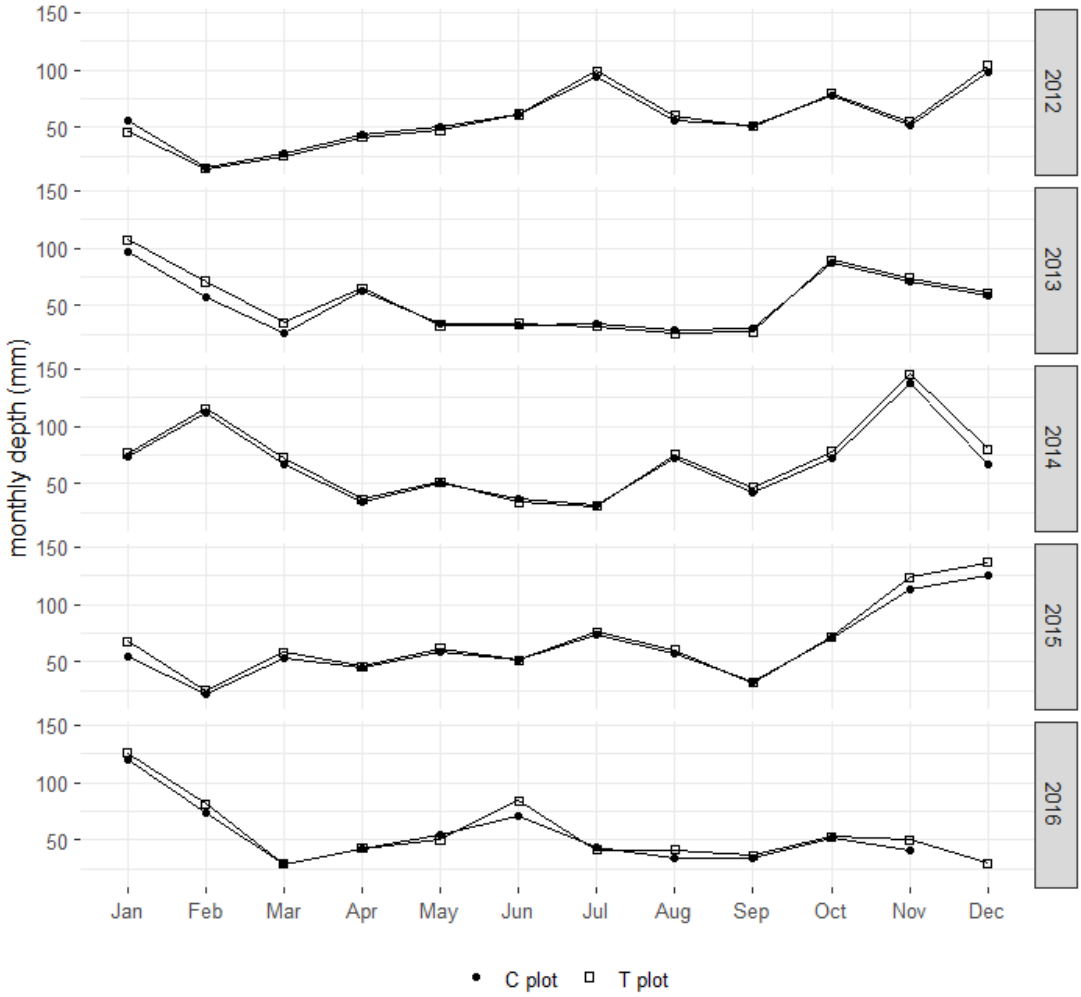


Stemflow represented a minimal part of the hydrological balance by volume, c.1% of the mean annual precipitation over the study period, accounting for an annual maximum of 3% in 2016. Details of the SF volumes measured in individual samplers are given in Appendix E together with TF depths by sampler.

## 3.3 Atmospheric nitrogen deposition

Inorganic $N_{dep}$ has a strong gradient across the EU, ranging from 2 to 44 kg N $ha^{-1}$ $y^{-1}$ (Stevens et al. 2010). Within this deposition gradient the measured bulk deposition (as the sum of wet-only deposition and dry deposition in the RF collector) and cloudwater N fluxes confirm Griffin Forest as a low N deposition site. Figure 3-5 shows the monthly $N_{dep}$ fluxes for $NO_3^-$-N and $NH_4^+$-N. For each rainfall flux data point the error shown is calculated through standard methodologies of error propagation from the SE of the field measurement of rainfall depth and N concentration determination. The propagation of error on the $n^{th}$ data point was calculated as:

$$\frac{\delta n}{N} = \sqrt[2]{\left(\frac{\partial a}{a}\right)^2 + \left(\frac{\partial b}{b}\right)^2} \qquad \text{(Eq. 3-1)}$$

where *N* is the mean value of monthly N flux, *a* is the mean precipitation depth value, *b* is the mean N concentration value, and *δn*, *δa* and *δb* are the associated standard errors. Similarly, the equation shown above was applied to combine data from two consecutive sampling dates to obtain the monthly propagated error of each N flux.

As there was only one cloudwater collector, the error for N in cloudwater was assumed to be equal to the RF SE of the mean. This assumption is conservative as N mass in cloudwater is usually lower than in RF, hence its propagated error should be lower.

In the monitoring period 2012-2016 cloudwater contributed a mean of 2.6 kg N $ha^{-1}$ $y^{-1}$, about 60% of the N input from rainfall. This value shows how the exclusive use of bulk rainfall data to estimate $N_{dep}$ usually leads to considerable underestimations, as highlighted by Balestrini et al. (2007) at five different temperate forest sites.

The contribution of reduced and oxidised N to the overall $N_{dep}$ in Griffin varied during the monitoring period. $NH_4$-$N_{dep}$ was generally lower than $NO_3$-$N_{dep}$ in 2012 both in RF and cloudwater, and higher in the years 2014-2016. In these latter three years, the contribution of $NH_4$-$N_{dep}$ appeared to be higher in the summer season (May-September), as expected due to the higher contribution of the agricultural sector to emissions of reduced N. However, assessment of the seasonality of N bulk deposition data with the seasonal Mann-Kendall Trend Test using the R-package *trend* (Polert 2018), showed no seasonal trends in $NH_4$-N. The test did identify seasonality of bulk

$NO_3^-$ deposition ($p = 0.02$), with highest deposition occurring in summer, and a negative trend during the study period (Figure 3-6). The estimated Sen's slope ($p = 0.03$) is -0.1 kg $NO_3$-N $ha^{-1}$ $y^{-1}$.

One of the peak $N_{dep}$ events shown in Figure 3-5 coincides with an event detected all over the UK. At the end of March-early April 2014 the UK received a strong southerly airflow, increasing the airborne particulate matter (PM) values. Vieno et al. (2016) showed that a substantial contribution of secondary inorganic ammonium nitrate PM in this episode came from agricultural ammonia emissions from continental Europe. The measured high $N_{dep}$ values of $NO_3$-N and $NH_4$-N at Griffin Forest in April 2014 are further supported by relatively high modelled reduced and oxidised $N_{dep}$ values (see Fig. 3.7, discussed later).

Figure 3-5 Monthly $N_{dep}$ as $NO_3$-N and $NH_4$-N in rainfall (RF) and cloudwater (fog) at Griffin Forest for 2012-2016. Error bars were calculated by propagating RF SE of the mean as explained in Eq. (Eq. 3-1)

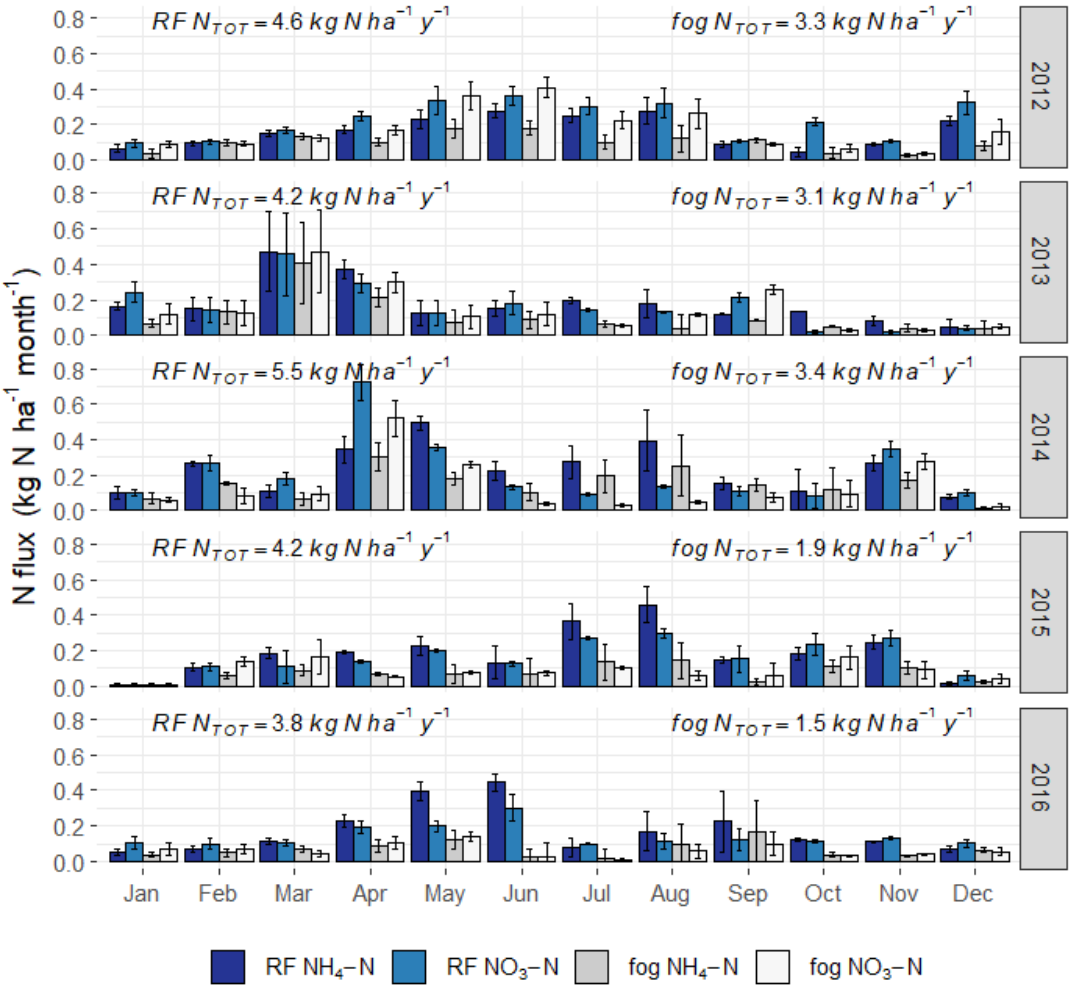

Figure 3-6 Trends in bulk $NO_3$-N deposition (kg $ha^{-1}y^{-1}$) during the study period at Griffin Forest. The observed data are decomposed (R package *trend*) showing the decreasing trend during the study period, the summer seasonal peaks and the random factor.

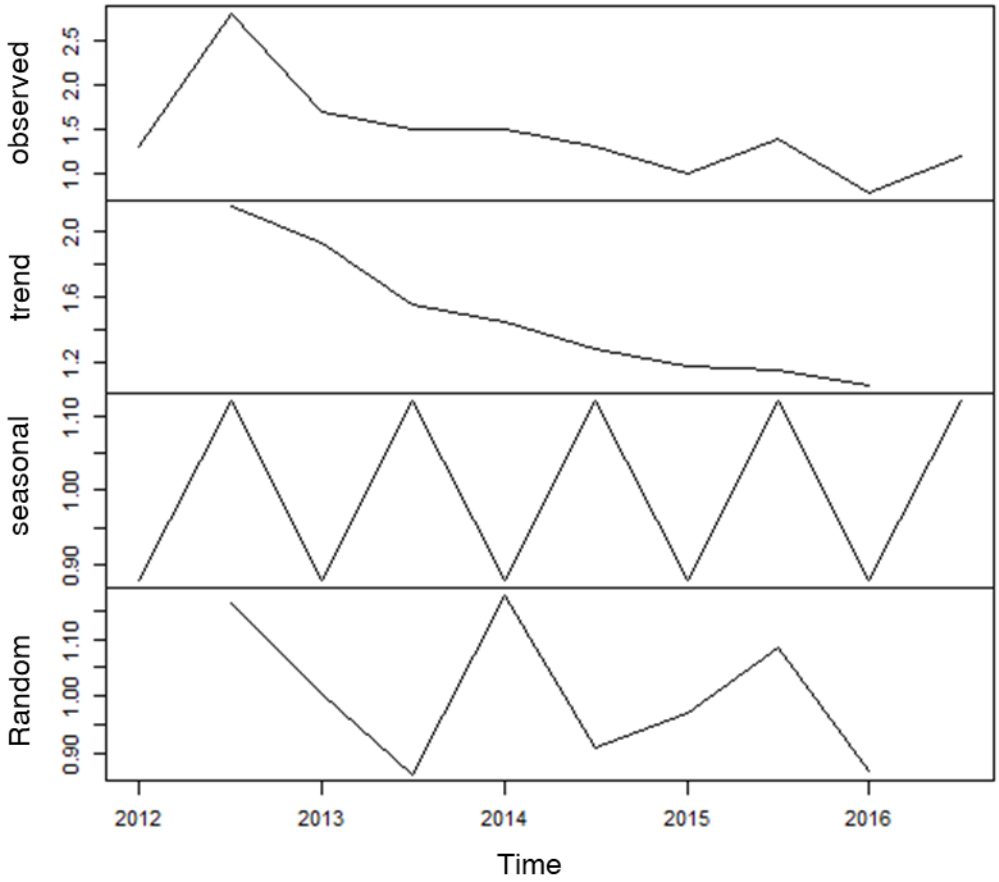


As a quality control check on the field measurements, measured total $N_{dep}$ ($NO_3$-N and $NH_4$-N in rainfall and cloudwater) was compared with those extracted from the EMEP4UK version rv4.3 atmospheric chemistry transport model (Levy et al. 2020) for the relevant 5 km x 5 km UK grid square for the monitoring time period. Total modelled $N_{dep}$ in EMEP takes into account all oxidised ($NO_x$) and reduced forms ($NH_x$) of N in wet and dry deposition.

Comparison of the measured and EMEP datasets (Figure 3-7) shows similar trends and orders of magnitude for most of the monitoring period, although EMEP $N_{dep}$ values were generally lower than $N_{dep}$ measured in the field. However it is known that the EMEP model tends to underestimate wet deposition when compared to field measurements (Dore et al. 2008)

Figure 3-7 Monthly measured $NO_3$-N and $NH_4$-N $N_{dep}$ in Griffin Forest compared to EMEP model outputs for the grid square including the study area. Annual total $N_{dep}$ values are also shown. EMEP date were not available for December 2016

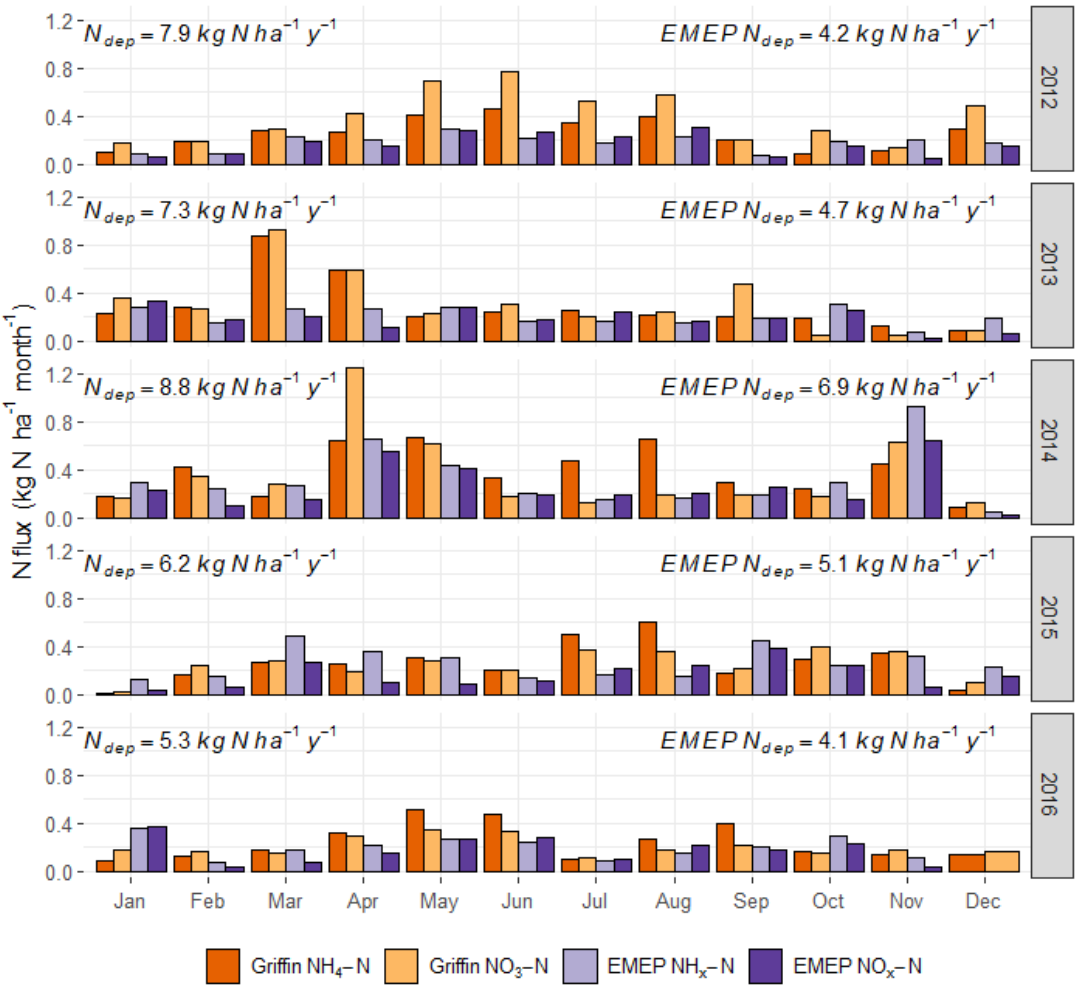


The monthly total $N_{dep}$ for the measured and modelled datasets for the whole study period 2012-2016 were significantly positively correlated (Pearson correlation coefficient = 0.53, $p<0.001$), but the significance of the correlation varied between years (see Table 3-1). For 2016 the correlation between the two datasets for the period January-November (December data were not available for EMEP) was not significant. However, if the January monthly data are excluded the correlation coefficient increases to 0.725 and becomes significant ($p = 0.018$), without a substantial change in the measured Griffin yearly total $N_{dep}$. This difference involving a single month could be explained by the different scales which the two datasets represent and applies to the whole time series. The Griffin data represent point measurements, whilst the EMEP data represent a 25 km$^2$ (5 km x 5 km) grid square which may have included some plumes of N deposition coming from the area of

Aberdeen, as shown in 2014 data on annual wet deposition of oxidised N in the British Isles (Figure 3-8).

Figure 3-8 Annual wet deposition of ONX (mg $m^{-2}$) on UK. Source: http://www.emep4uk.ceh.ac.uk/wetdepOXN

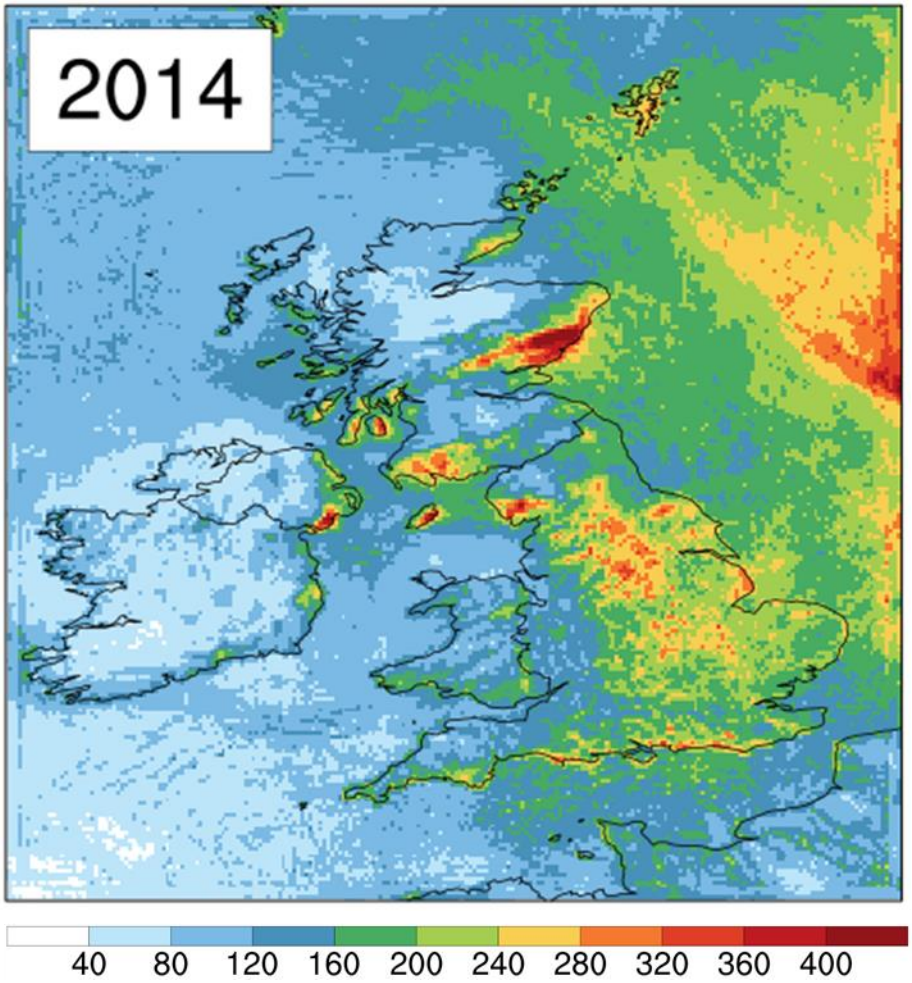


Measured $N_{dep}$ in January 2016 was also affected by overflowing gauges, as shown in Fig. 3.3 where TF depth almost equals the precipitation depth. However, overflowing gauges alone do not explain the low correlation in 2016 with January 2016 included. Even though a similar situation occurred in October 2014, there was still a high correlation coefficient between the two datasets with p-value<0.01 in 2014.

Table 3-1 Correlation coefficients and p-values between Griffin Forest measured and EMEP modelled monthly $N_{dep}$ data by year.

| Year | Pearson correlation coefficient | p-value |
|---|---|---|
| 2012 | 0.859 | <0.001 |
| 2013 | 0.255 | 0.424 |
| 2014 | 0.749 | 0.005 |
| 2015 | 0.181 | 0.574 |
| 2016[a] | 0.725[b][0.367] | 0.018[b][0.266] |

[a]December 2016 EMEP data not available; [b]January 2016 was excluded, in square brackets are the results with January 2016 included.

## 3.4 Below canopy N fluxes in TF and SF

Figure 3-9 and Figure 3-10 show the N concentrations measured in TF and SF samplers over the 5-year monitoring period after removal of a few outliers noted in Table 2-5. Nevertheless, the black dots in the figures show that a number of outliers identified using the Tukey method were retained as a conservative approach in order not to lower the overall calculated recovered N unless specific contamination risks were noted in the field or laboratory. Dates were divided into seasonal subgroups and a seasonal median of all concentrations measured in each 3-month period was calculated to show any possible seasonal trends (blue horizontal lines in Figures 3-9 and 3-10), though no clear patterns were apparent.

In general, the mean total inorganic N concentration by sampling date was higher in SF than in TF. $NH_4$-N and $NO_3$-N concentrations show a different pattern between TF and SF depending on the N form. The mean $NH_4$-N concentration was generally lower in the TF than in SF on the same date (42 out of 59 sampling dates). This could be a consequence of the different volumes of TF and SF water fluxes that dilute the IN from dry deposition differently: SF represented on average about 1% of the water fluxes under the canopy, hence the dilution factor is two orders of magnitude lower than in TF. There was a less clear-cut pattern in relative $NO_3$-N concentrations

between TF and SF samplers, although the mean TF concentration was higher than SF in 35 sampling dates out of 59. Compared to TF, N concentrations in SF were more variable between samplers within sampling dates. Even though some SF concentrations were rejected from the dataset the SF values still contain a higher no of outliers compared to TF as explained in Chapter 2.3.2

To investigate any associations in measured IN concentrations between TF and SF, Pearson correlation coefficients were calculated (using R package *ltm*) between mean N form concentration by date and the results are shown in Table 3-2. $NH_4$-N concentrations in TF and SF are more highly positively correlated than $NO_3$-N concentrations. Notably, the second and third highest correlation coefficients are between $NO_3$-N and $NH_4$-N concentrations in SF and between $NH_4$-N and $NO_3$-N in TF. The correlation coefficients are higher within each flux than between fluxes and this could be explained by the different transit times of TF and SF. Due to the expected longer transit time of SF water flux compared to TF flux the chance for both the IN forms in SF to undergo biological or cation exchange processing would increase. Correlation coefficients were also calculated between $NO_3$-N and $NH_4$-N concentrations in TF and SF and in RF and cloudwater. None of the correlations between the concentrations of the different N forms in SF and RF or cloudwater were significant, but those between TF and RF/cloudwater were ($p<0.001$). The highest correlation coefficient was between TF and RF $NO_3$-N concentrations ($R = 0.845$), whilst for $NH_4$-N concentrations the correlation coefficient was higher (0.569) than between TF and cloudwater (0.453). The correlations results show that TF IN concentration is related to $N_{dep}$ whilst SF is not.

Table 3-2. Pearson correlation coefficients calculated between mean RF, cloudwater, TF and SF IN concentrations by sampling date (n=59). The figures above the diagonal are the correlation coefficients, and those below the diagonal are the corresponding p-values

| | TF $NH_4$-N | TF $NO_3$-N | SF $NH_4$-N | SF $NO_3$-N | RF $NH_4$-N | RF $NO_3$-N | cloudwater $NH_4$-N | cloudwater $NO_3$-N |
|---|---|---|---|---|---|---|---|---|
| TF $NH_4$-N | ***** | 0.533 | 0.78 | 0.409 | 0.569 | 0.435 | 0.453 | 0.308 |
| TF $NO_3$-N | <0.001 | ***** | 0.336 | 0.559 | 0.571 | 0.845 | 0.704 | 0.683 |
| SF $NH_4$-N | <0.001 | 0.01 | ***** | 0.639 | 0.328 | 0.097 | 0.09 | -0.071 |
| SF $NO_3$-N | 0.001 | <0.001 | <0.001 | ***** | 0.248 | 0.267 | 0.159 | 0.065 |
| RF $NH_4$-N | <0.001 | <0.001 | 0.012 | 0.061 | ***** | 0.713 | 0.816 | 0.652 |
| RF $NO_3$-N | 0.001 | <0.001 | 0.469 | 0.043 | <0.001 | ***** | 0.848 | 0.894 |
| cloudwater $NH_4$-N | <0.001 | <0.001 | 0.502 | 0.234 | <0.001 | <0.001 | ***** | 0.891 |
| cloudwater $NO_3$-N | 0.019 | <0.001 | 0.597 | 0.626 | <0.001 | <0.001 | <0.001 | ***** |

Significant negative Pearson correlations were found between RF depth and $[N_x]$ for both TF and SF (TF $NH_4$-N: -0.43, $p = 0.001$; TF $NO_3$-N: -0.322, $p = 0.013$; SF $NH_4$-N: -0.409, $p = 0.001$; SF $NO_3$-N: -0.303; $p = 0.020$). These results indicate that dilution plays a role in determining the N concentrations in understory fluxes.

Figure 3-9 Boxplots of monthly $NO_3$-N and $NH_4$-N concentrations in 18 TF samplers at Griffin Forest, January 2012-November 2016, shown by season. Not all months were sampled as sampling frequency was adapted to precipitation amount (see Appendix E). The last sampling date used to build up the 5 years dataset, 5 January 2017, has not been included. The horizontal line inside each box represents the median and the lower and upper hinges correspond to the first and third quartiles. The upper and lower whiskers depict the largest and smallest values respectively within 1.5 * the interquartile range (IQR). Dots represents outliers. The blue horizontal line in each season represents the seasonal median, calculated as the median of all concentrations measured in all samplers in that season.

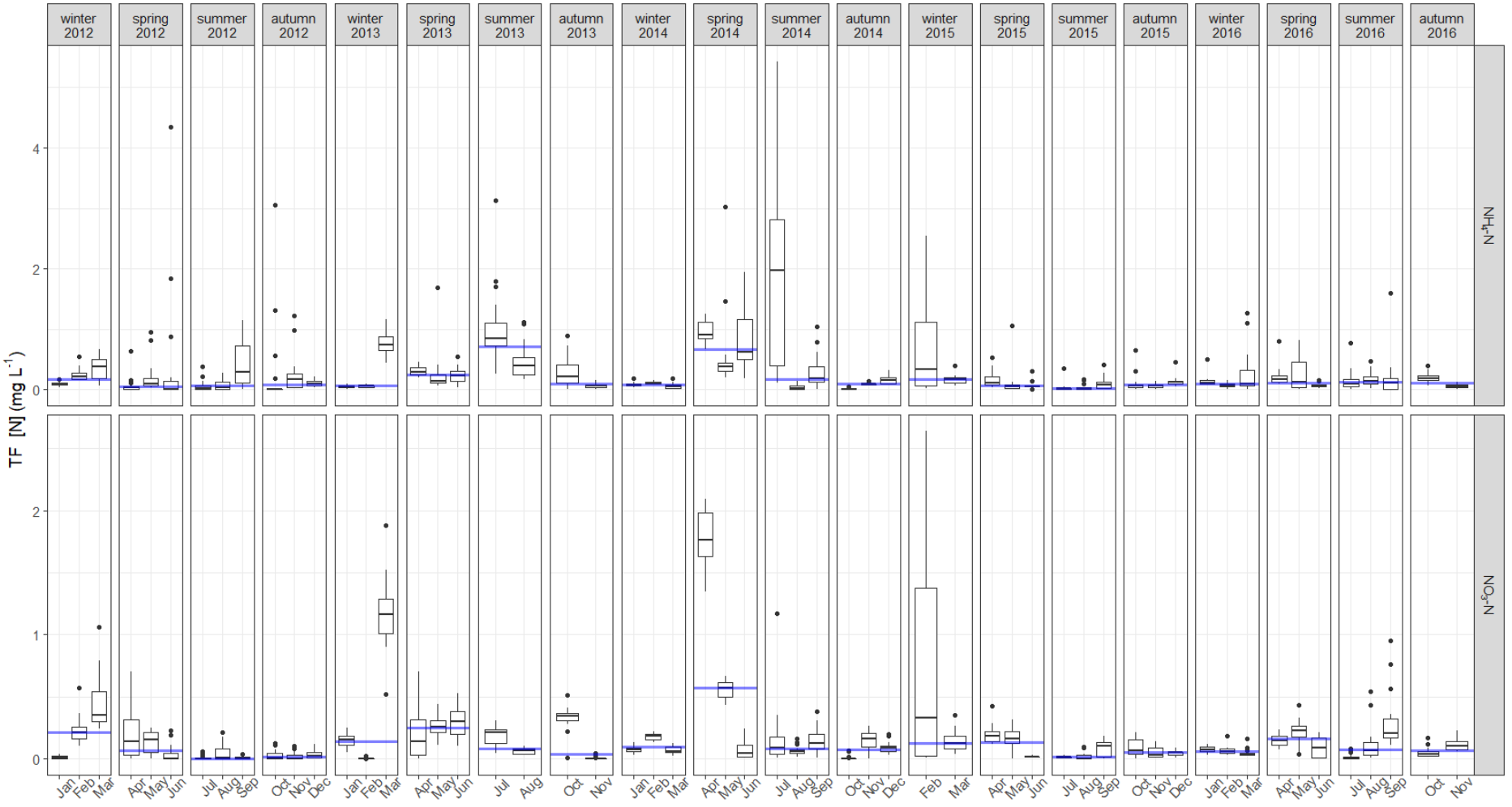

Figure 3-10 Boxplots of monthly $NO_3$-N and $NH_4$-N concentrations in 22 SF samplers at Griffin Forest, January 2012-November 2016, shown by season. Not all months were sampled as sampling frequency was adapted to precipitation amount (see Appendix E). The last sampling date used to build up the 5 years dataset, 5 January 2017, has not been included. The horizontal line inside each box represents the median and the lower and upper hinges correspond to the first and third quartiles. The upper and lower whiskers depict the largest and smallest values respectively within 1.5 * the interquartile range (IQR). Dots represents outliers. The blue horizontal line in each season represents the seasonal median, calculated as the median of all concentrations measured in all samplers in that season.

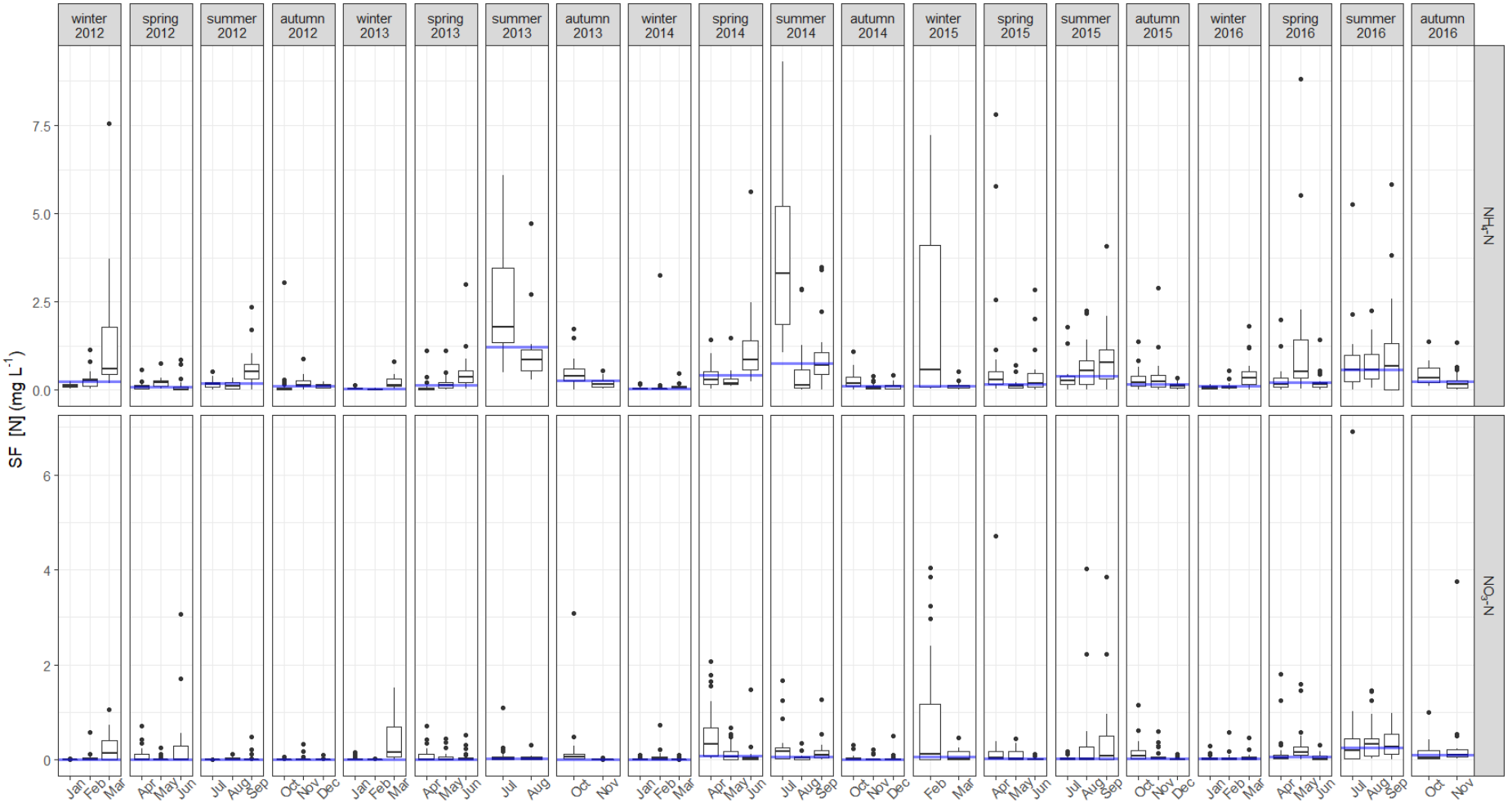

Figure 3-11 compares monthly and annual N fluxes in TF and SF. SF represents a limited below canopy N flux; the total annual N SF flux in the years 2012-2016 was 0.10-0.14 kg N $ha^{-1}$. In the 5-year monitoring period, the total N flux in SF represented only 6% of the N flux in TF. Furthermore, on all dates the monthly N fluxes in SF were lower than the values of the 95% confidence interval for the mean monthly N TF flux. The reduced N form always contributed more than the oxidised form to N fluxes in SF, and a higher proportion compared to TF N fluxes. When compared to the N fluxes in TF, $NH_4$-N in SF was 8% of the TF $NH_4$-N flux, whilst $NO_3$-N in SF accounted for 3% of the TF $NO_3$-N flux. Similar to the bulk N deposition data, assessment of the seasonality of the monthly TF and SF IN fluxes was conducted using the seasonal Mann-Kendall Trend Test. Significant seasonality was identified only for monthly $NO_3$-N flux in SF ($p = 0.002$), with a peak in spring, but no longer-term trend over the monitoring period 2012-2016. Annual N fluxes in SF were very consistent throughout the monitoring period, but there was greater inter-annual variability in the TF fluxes, with fluxes in 2013 and 2014 approximately double those measured in the other years. However, this variability seems due to random effects more than seasonal variations.

The occurrence of the highest TF and SF N fluxes in the months of high N input appeared to indicate a relationship between N fluxes in TF, SF and $N_{dep}$. The effect of $N_{dep}$ fluxes on TF and SF was thus investigated by calculating Pearson correlation coefficients, similarly as for IN concentrations. Significant positive correlations were found between $NO_3$-N fluxes in RF and TF (0.699, $p < 0.001$) RF and SF (0.494, $p < 0.001$), and TF and SF (0.577, $p < 0.001$), indicating that TF and SF $NO_3$-N fluxes are strongly related to the N input. In contrast, $NH_4$-N fluxes under the canopy were not significantly correlated with the $NH_4$-$N_{dep}$, although $NH_4$-N fluxes in TF and SF were significantly correlated (0.408, $p = 0.001$). This shows that TF and SF $NH_4$-N fluxes are more strongly correlated with each other than to atmospheric input, indicating that other processes, such as cation exchange or biological transformations (e.g. nitrification) are influencing the below canopy $NH_4$-N fluxes.

Figure 3-11 Mean monthly $NO_3$-N and $NH_4$-N flux in TF and SF (± propagated SE of the mean of field and laboratory measurements) 2012-2016 for 18 TF samplers and 22 SF samplers at Griffin Forest.

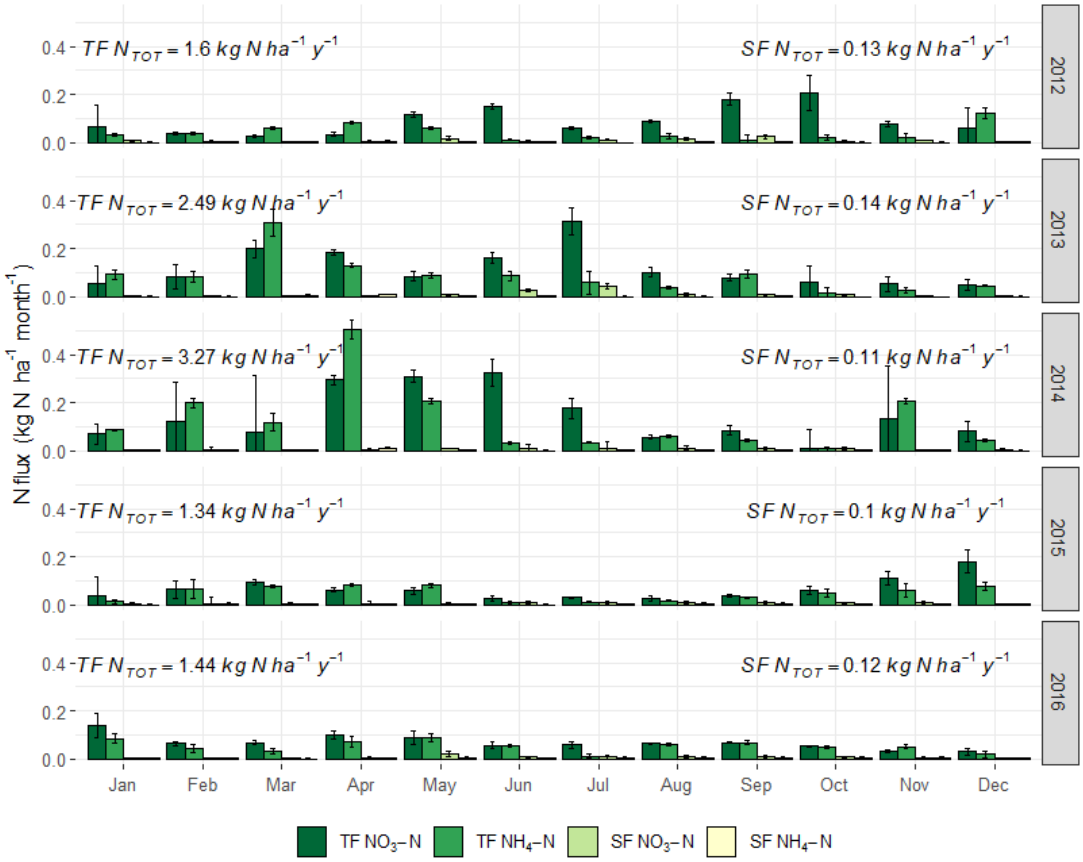


## 3.5 Below canopy organic N transfer in Sitka spruce litter

Annual values of litter mass deposition to the forest floor at Griffin Forest were calculated as follows. Firstly, the dry mass of each litter sample collected in the TF samplers was transformed into a dry mass per surface area in the same way as for TF depth. Next the mean of all samples collected in a month was calculated and the results are shown in Figure 3-12.

Figure 3-12 Mean monthly litter dry mass (DM) collected in the 18 TF samplers at Griffin Forest for 2012-2016. The error bars are the SE of the collected samples. Samples from winter months in 2014-2016 were not collected due to snow or ice in the collectors. The May 2015 sample was collected but mislaid before weighing. Older data were not available or the stored litter samples were not found.

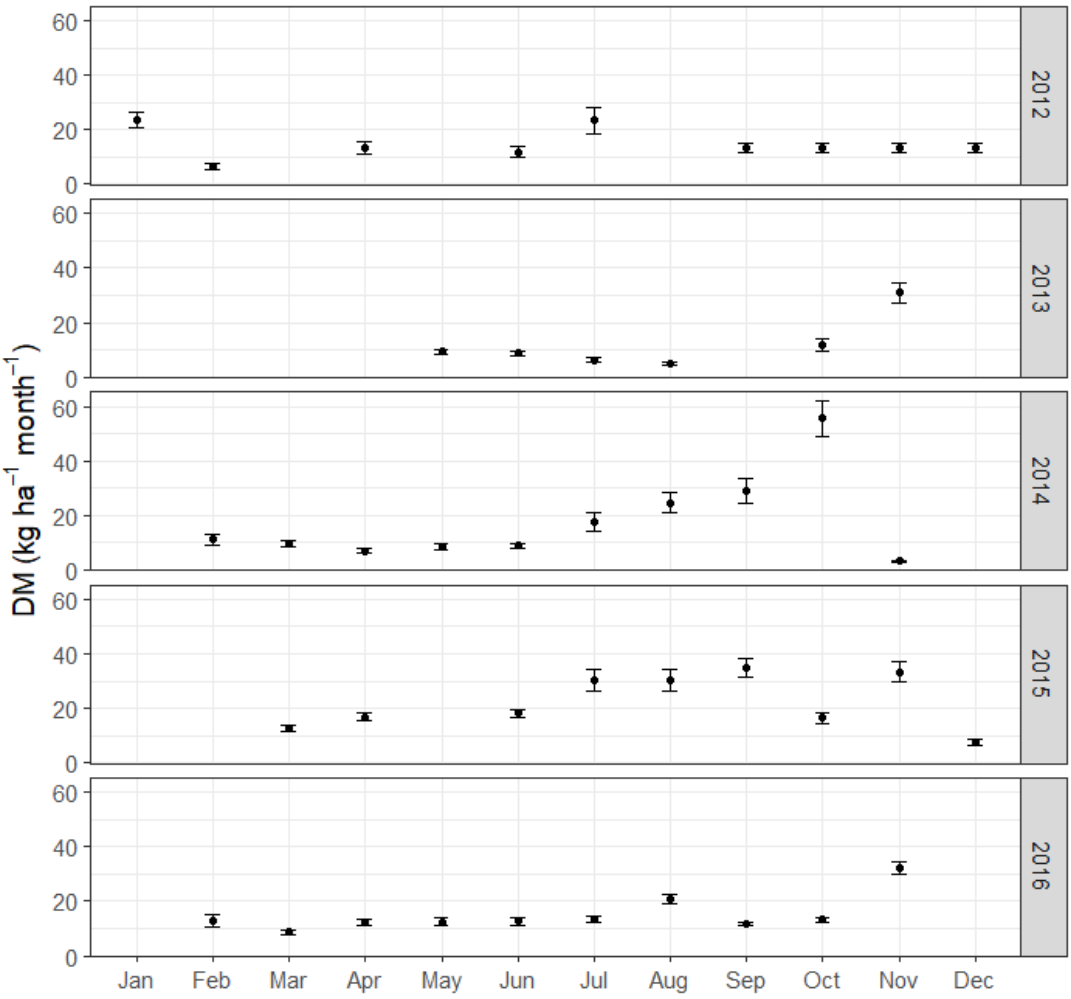


The monthly mean values were then summed per year of collection, divided by the number of days of collection and multiplied by the days of the year. The results for each available collection per date were then aggregated by year as a mean daily value and multiplied by 365. This calculation takes account of those periods when no data were available, mostly winter months when ice and snow on the collectors made litter collection impossible. The litter % N content of 0.31 used to estimate the N mass flux in litter is the mean value determined in 54 litter samples collected in January, May and September 2013 in the same TF collectors used in this project (Mitchell, J. 2013). From this the mean annual N mass transferred from the canopy to the forest floor in the period 2012-2016 was 4.4±1.4 kg N ha$^{-1}$ y$^{-1}$. Fig. 3-13 shows the estimated litter N fluxes by year in Griffin. The wide yearly variation of litter DM transferred to

the soil N entails a proportional variation in ON transfer to the soil which ranges from 2 to over 6 kg N $ha^{-1}$ $y^{-1}$. These transfers almost double the figures of IN transfer through TF and SF.

Figure 3-13 Annual N fluxes in litter from the canopy to the forest floor at Griffin Forest during the study period. Error bars are 95% CI of the mean.

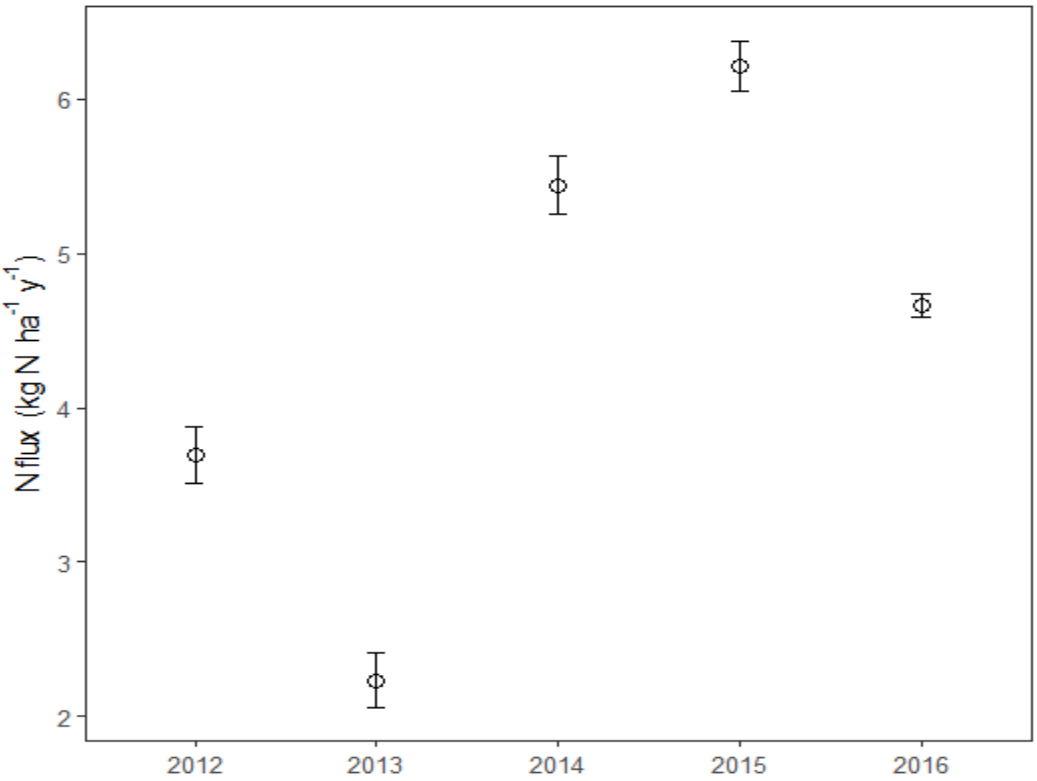


## 3.6 The forest canopy inorganic N balance in Griffin Forest

Figure 3-14 shows the bulk $N_{dep}$ (as rainfall and cloudwater deposition) compared with the below canopy inorganic N fluxes in water (TF+SF) at Griffin Forest on a monthly basis during the 5-year monitoring period. All errors are calculated as explained in Chapter 3.3 and 3.4.

Figure 3-14 Monthly N fluxes in water above (denoted as $N_{dep}$, the sum of N in RF and cloudwater) and below the forest canopy at Griffin (as sum of N in TF and SF) (± propagated SE of the mean of field and laboratory measurements). Annual values for $N_{dep}$ mass deposition and % of $N_{dep}$ mass recovered below the canopy are also shown.

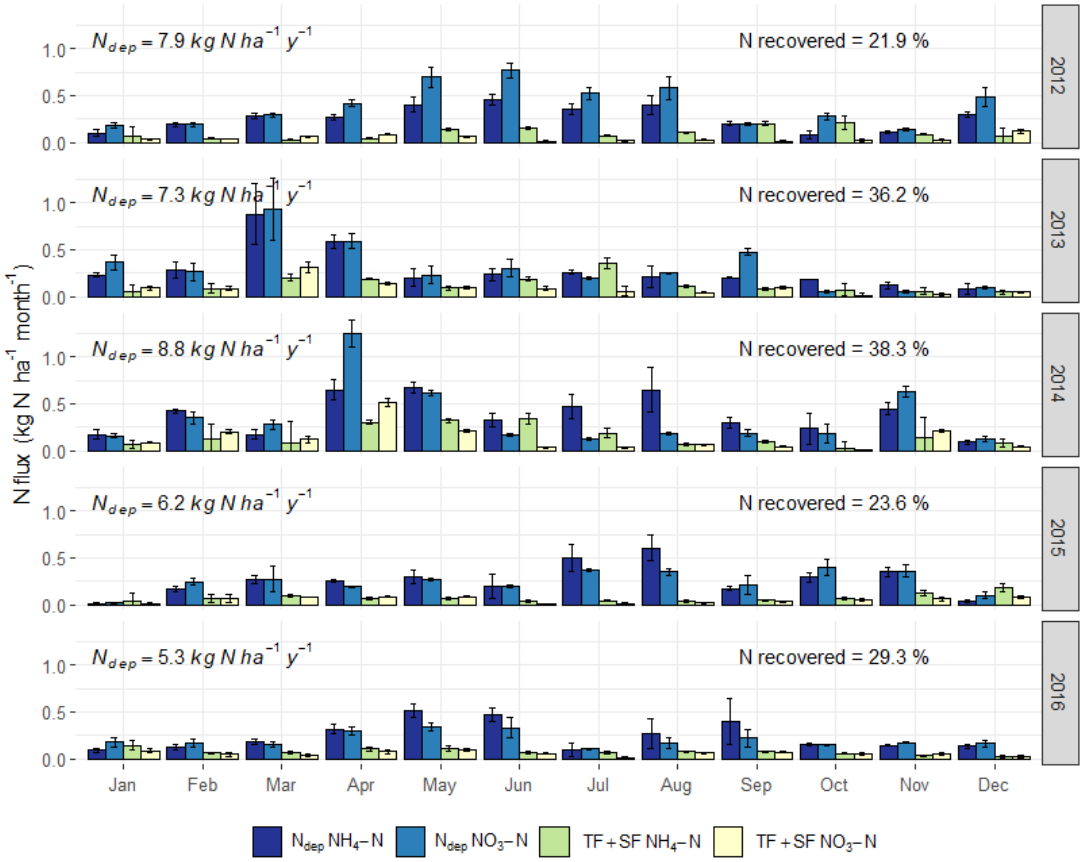


The mean annual canopy N uptake (CNU) at Griffin Forest for the period 2012-2016 was consistent across the 5-year monitoring period at c.70%.

Similar values have been reported in other studies conducted in comparable environmental conditions and/or tree species. Sievering (2007)) calculated a CNU of 80% by measuring the N fluxes over and under the canopy of a temperate mountain spruce-fir forest under very low total N deposition. Similar figures were also reported in Gaige et al. (2007). In their experiment they applied 19.8 kg N ha$^{-1}$ y$^{-1}$ over the canopy; 70-80% of the applied N were not found in TF and SF. Nair et al. (2016) reported that 60% of simulated $^{15}N_{dep}$ directly applied to branches and needles of 3 year-old Sitka spruce seedlings was recovered in aboveground tissues and this pathway was much more effective than plant uptake when N was applied to the soil (only 21% uptake by the seedlings).

Lower figures were reported by Houle et al. (2015) from a 12-year experiment in a eastern Canadian boreal forest. They estimated a mean CNU of 52-59%, higher for $NH_4^+$ (60-67%) than for $NO_3^-$ (45-54%), in contrast to the Griffin Forest annual CNU estimates which were 56-73% for $NH_4^+$ and 63-89% for $NO_3^-$ in the period 2012-2016. From a model constructed to predict DIN leaching from forests based on long-term monitoring data from 57 forest sites in Europe, van der Salm et al. (2007) determined that for a median $N_{dep}$ of ~21 kg $ha^{-1}$ $y^{-1}$ around 6.5 kg $ha^{-1}$ $y^{-1}$ was not recovered in TF (i.e. ~30% of the $N_{dep}$). Furthermore, nearly all N was retained in the forest canopy when $N_{dep}$ was less than 14 kg $ha^{-1}$ $y^{-1}$.

Several studies in very low N deposition sites where $NO_3$-N deposition is much greater than $NH_4$-N deposition report very high figures for CNU. In a 2-year study, Fenn et al. (2013) reported that in three mixed conifer forests in Washington State (USA) $NO_3$-N flux in TF ranged from 77% to 91% of the wet deposition, whilst $NH_4$-N flux was increased by passage through canopy by up to 153%-276% of the atmospheric input, where $NO_3$-N wet deposition was about 4 times greater than $NH_4$-N wet deposition. The same study reports similar results from Edmonds et al. (1995), Johnson and Lindberg (1992) and Klopatek et al. (2006). The latter study, which investigated old growth stands of Douglas fir, showed seasonal differences in CNU for both total N and different N forms. The percentage of $N_{dep}$ recovered in TF in winter was lower than in summer. In particular, the interception of $NH_4$-N during the winter months was negligible, whilst in the same season the input levels of $NO_3$-N were reduced by about 80% in the first 5 m of the canopy to reach about 90% of $N_{dep}$ at the forest floor level. In contrast, in summer CNU was higher for $NH_4$-N (86-90%) than for $NO_3$-N (67-79%).

To investigate whether there was also a seasonal pattern in CNU in Griffin Forest, CNU percentages for total N and $NH_4$-N and $NO_3$-N were compared for the warmest months (May-September) and coldest months (November-March) (Table 3-3). This division of months was based on air temperatures measured in 2013-2016 during the static chamber sampling (described in Chapter 5) and aimed to create two seasonal groups with distinct differences in air temperature (November-March 3.0±1.2 °C; May-September 11.1±0.6 °C), as temperatures in April (5.7±0.8 °C) and October (9.3±1.2 °C) were intermediate between the two groups. Clear differences in CNU between seasons were not evident, due to overlapping errors, especially for total N and $NH_4$-N, although there was potentially a seasonal difference in $NO_3$-N CNU, with higher

values in summer than in winter. Hence there might be space for a seasonal variation in $NO_3$-N canopy uptake that is worth to be explored further.

Mean CNU of $NO_3$-N and $NH_4$-N across the monitoring period are both higher in warmer months than colder months, but the seasonal difference is greater for $NO_3$-N than $NH_4$-N (12% and 4% difference, respectively). However, CNU values vary between years, particularly for $NH_4$-N which had lower mean values in the warm season than in the colder season in 2012, 2013 and 2014 although the overlap in errors could mask an opposite trend. In 2015 and 2016 $NH_4$-N retention is higher in the warmest months and this difference greatly exceeds the error estimates.

CNU of $NO_3$-N at Griffin Forest was very high during the warmest months (mean of 83% in May-September 2012-2016) and always higher than in the colder months. Canopy uptake of $NO_3$-N in both summer and winter has also been reported in other studies, although both Klopatek et al. (2006) and Fenn et al. (2013) showed a higher retention during winter. In both of these studies winter was also the wettest period and whilst a greater $N_{dep}$ was associated with greater precipitation, no relationships between precipitation amount and CNU were mentioned.

Possible mechanisms of canopy N retention include foliar uptake, a well-known phenomenon (Sparks 2008) widely observed in herbaceous plants (Bourgeois et al. 2019) and trees (Adriaensenss et al. 2011) and absorption by bark (up to 45% of applied $^{15}NO_3^-$ was recovered in this pool by Dail et al. (2009)). The second experiment presented in Chapter 4 was conducted to help shed light on these potential mechanisms.

The results in Dail et al. (2009) led to the conclusion that physico-chemical interactions with plant surfaces are likely to be the predominant mechanisms of canopy N retention. However, this could be an oversimplification. Guerrieri et al. (2015) demonstrated that biological nitrification occurs in the forest canopy. The quantification of these mechanisms is still at an early stage but other studies have demonstrated their occurrence, for example in TF below Japanese cedar (Watanabe et al. 2016) and in a recent paper by (Guerrieri et al. 2020), where 20% of $^{15}NO_3^-$ in TF in a Mediterranean oak forest was shown to derive from canopy nitrification. If we make the reasonable assumption that similar processes can occur in Sitka spruce (Guerrieri et al. (2015) demonstrated that biological nitrification occurs in Scots pine forest in the UK) this could mean that part of the $NH_4$-N that is accounted as CNU is

transformed to $NO_3^-$ and then retained by the canopy through either foliar uptake or physico-chemical interactions mainly occurring on the surface of bark and branches.

Table 3-3. "Seasonal" $N_{dep}$ (± propagated SE) and N retention (% ± propagated SE) at Griffin Forest in each year of the monitoring period. Figures and propagated errors are calculated from the mean values of monthly retention for the specified months.

| Year | May-Sep $N_{dep}$ | Nov-Mar $N_{dep}$ | May-September N retention | | | November-March N retention | | |
|---|---|---|---|---|---|---|---|---|
| | kg N $ha^{-1}$ $y^{-1}$ | kg N $ha^{-1}$ $y^{-1}$ | $NH_4$-N % | $NO_3$-N % | N total % | $NH_4$-N % | $NO_3$-N % | N total % |
| 2012 | 4.6±0.1 | 2.3±0.1 | 63±14 | 95±10 | 83±9 | 70±23 | 78±13 | 75±12 |
| 2013 | 2.6±0.2 | 3.3±0.3 | 25±64 | 74±17 | 31±19 | 72±32 | 67±38 | 69±27 |
| 2014 | 3.7±0.3 | 2.8±0.1 | 58±22 | 70±7 | 63±16 | 62±55 | 57±15 | 59±24 |
| 2015 | 3.2±0.3 | 1.8±0.1 | 87±16 | 89±12 | 88±13 | 39±23 | 70±28 | 56±20 |
| 2016 | 2.9±0.3 | 1.5±0.1 | 78±23 | 74±23 | 76±20 | 49±8 | 71±26 | 61±12 |
| **Mean** | **3.4±0.1** | **1.8±0.1** | **65±16** | **83±7** | **74±8** | **61±13** | **71±11** | **67±9** |

## 3.7 N flux in streamwater from the forest

Streamwater samples normally contained the lowest $NO_3$-N and $NH_4$-N concentrations compared to the RF, TF and SF samples, often below the limit of detection (LOD) for the colorimetric analysis (0.003 mg $L^{-1}$ for $NO_3^-$, 0.01 mg $L^{-1}$ for $NH_4^+$). Figure 3-15 shows the time series of streamwater N concentrations at each of the four sampling points near the V-notch weirs in the study area (see Figure 2-8). Gaps in $NO_3$-N concentration data for the sampling points in the C plot are due to the removal of outliers, as explained in Chapter 2.3.2. The two streams in the C plot are characterised by a greater variation in $NO_3$-N concentrations than the stream in the T plot. All three streams have very low $NH_4$-N concentrations and the few peaks in concentration (e.g. summer 2013 and winter 2014, corresponding with higher discharges) were measured simultaneously at all of the sampling points.

There is a clear difference of mean [N] between the two N forms in streamwater, with $NO_3$-N concentrations being generally higher and more variable than $NH_4$-N, even after the removal of outliers. No clear seasonal trends are apparent for either of the N forms or at the different sampling points, although some of the minima for $NO_3$-N are found in spring and autumn. These minima occur during the periods of most intense biological demand for nutrients in river channels as explained by Mulholland and Hill (1997). In spring this is likely due to the effect of higher in-stream N demand from blooms of algae (autotrophs) linked to higher light levels in spring in forest streams before leaf growth. In contrast, in autumn an increased demand for nutrients from streamwater is associated with fungi and bacteria (heterotrophs) that colonise and decompose the instream leaf litter with a low N/C ratio (Mulholland and Hill, 1997). Due to the different forest composition, however, this second scenario does not apply to Griffin Forest as the autumn pulse of organic matter is typical of hardwood forests. Another control on streamwater $NO_3$-N concentrations suggested by Mulholland and Hill (1997) is seasonal variation in the dominant catchment hydrological pathways, with greater contribution of more nitrate-enriched groundwater in summer, resulting in lower winter and higher summer concentrations. However, given the generally low $NO_3$-N concentrations and their lack of seasonal variability in streamwater at Griffin Forest, it is unlikely that this control is important here.

Figure 3-15 Instantaneous discharge (L $s^{-1}$, blue lines) and streamwater $NH_4$-N and $NO_3$-N concentrations (mg $L^{-1}$) on each sampling occasion at Griffin Forest for 2012-2016. C20/T20 = solid line; C21/T21 = dashed line.

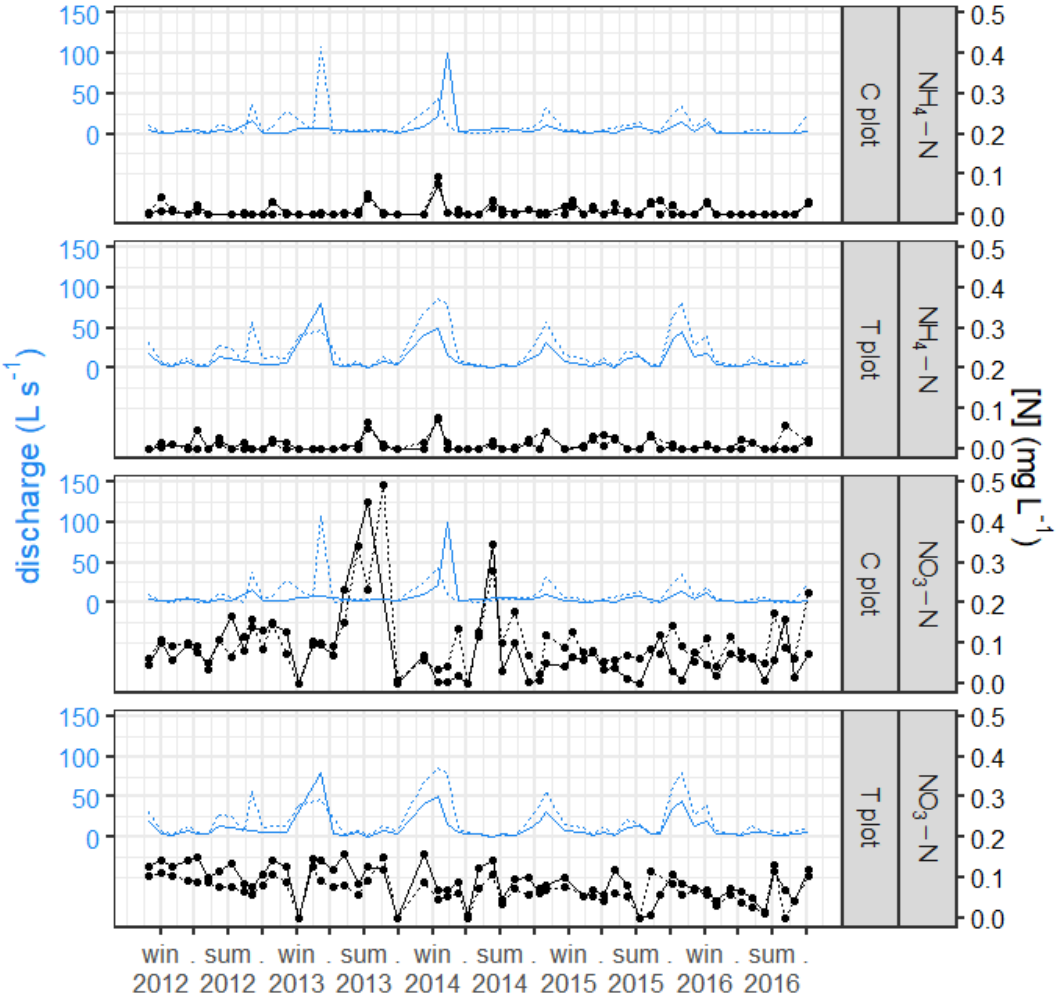


Spot measurements of discharge ($Q_n$, L $s^{-1}$) at each of the four streamwater sampling points (sub-basins, $SW_n$) were normally made during each sampling visit as explained in Chapter 2.2.6. A daily discharge volume (L) was then calculated and multiplied by the measured [N] to give a daily N mass flux. It was assumed that the measured $Q_n$ and [N] was constant between each sampling occasion. Hence the daily N flux was multiplied by the number of days in the month (*dpm*) to obtain the monthly N mass flux at each streamwater sampling point. This was then divided by each sub-basin area ($area_n$, ha, calculated as explained in Chapter 2.2.6) to obtain the N mass loss in streamwater per hectare. At the C plot, the streamwater samples and flow measurements are made on two separate sub-basins, so the N flux shown for completion in Appendix F was calculated as the mean of the two values of the sub-basins, each obtained as follows:

$$SW_n = \frac{Q_n * 24 * 3600 * [N_n] * dpm}{area_n} \quad \text{(Eq. 3-2)}$$

For the T plot, since the streamwater sampling and flow measurements were conducted at two different locations on the same stream, the streamwater N fluxes per hectare from the intervening area of forest were calculated as the difference in the N mass flux between the two sampling points, divided by the difference in the two sub-basin areas as follows:

$$SW_T = \frac{((Q_d * 24 * 3600 * [N_d]) - (Q_u * 24 * 3600 * [N_u])) * dpm}{area_d - area_u} \quad \text{(Eq. 3-3)}$$

Where *d* and *u* represent the downstream (T20) and upstream (T21) water sampling points, respectively.

Figure 3-16 shows the monthly difference in N fluxes between the downstream and upstream sampling points in the T plot. Throughout the monitoring period, the reduced N flux in streamwater was almost zero. The $NO_3$-N flux was also low, although a few peaks occurred, mostly in the streams draining the C plot (reported in Appendix F) and generally one order of magnitude lower than the monthly $N_{dep}$ value. Streamwater $NO_3$-N flux is generally higher than $NH_4$-N in both plots, apart from January and February 2014 in which the only peaks of $NH_4$-N flux occur during the time series and in the C plot only. Negative values of N flux from the T plot (clearly apparent in February - April 2013 for $NO_3$-N) occur when the calculated N mass flux at the downstream sampling point was lower than at the upstream sampling point. A likely explanation for these negative values is uptake of N in the stream channel (Peterson et al. 2001).

Assessment of the seasonality of the monthly $NH_4$-N and $NO_3$-N fluxes in streamwater at all sampling locations was conducted using the seasonal Mann-Kendall Trend Test (package *trend*). Significant seasonality was detected only in the $NH_4$-N flux of the T plot (as difference of fluxes between T20 and T21; $p = 0.01$), with minimum values at the end of the winter and maximum values in early spring. However, these values are highly affected by a single low value in February 2014 that constitutes a random effect in an otherwise flat trend.

The low values of N flux in streamwater suggest that Griffin Forest acts as a sink for N as no significant losses occur as leaching. In Chapter 5 the dynamics of N in soil at Griffin Forest will be examined, including consideration of soil extractable N and a further potential output N flux via soil denitrification.

Figure 3-16 Monthly N leaching of $NH_4$-N and $NO_3$-N to streamwater for the T plot, calculated as the difference in flux between the downstream and upstream sampling points, for 2012-2016. The N flux per year is also shown above every series .

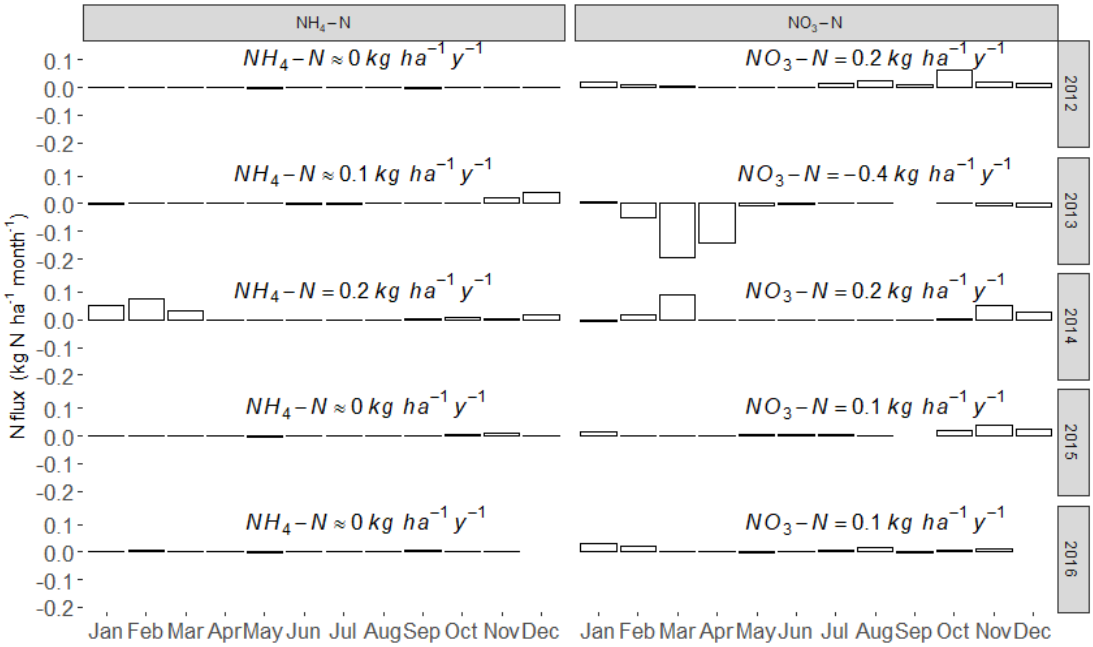


In conclusion, acknowledging the limitations due to the monthly streamwater sampling frequency, the data shown above suggest that the amount of N leaching from Griffin Forest through streamwater is relatively small, according to the thresholds suggested by Dise and Wright (1995) and well below the 10% of the N in rainfall reported in Magnani et al. (2007) as the lower range of leaching in low deposition conditions.

## 3.8 Conclusions

Figure 3-17 summarises the N fluxes at Griffin Forest reported in the different sections of this chapter and those that will be addressed in Chapters 4 and 5. The mean annual N fluxes in bulk deposition and cloudwater indicate that Griffin is a relatively low N deposition site (as defined by Cape et al. (2010) for a study in southern Scotland).

The inorganic N fluxes under the canopy at Griffin occur predominantly as TF and they are about the half of the organic N transfer via litter.

The proportion of inorganic N/organic N input to the soil may affect soil dynamics. Nadelhoffer (2000) described a likely scenario of fine-root turnover and production increasing with N availability as well as a decline in fine-root production as a proportion of total above- plus belowground production. Manipulative studies assessing the effects of inorganic N addition from simulated $N_{dep}$ to forest soils found that nitrogen-induced soil carbon accumulation is of equal or greater magnitude to carbon stored in trees due to suppression of organic matter decomposition (Tonitto et al. 2014). However, this effect was found to be dependent on levels of N addition which were one to almost two orders of magnitude higher than the inorganic N flux that reaches the forest floor at Griffin.

The flux of dissolved organic nitrogen (DON) in TF and SF was not measured in this study. This flux could be the result of biological processing at the canopy level of part of the inorganic N from bulk deposition and cloudwater which is not found under the canopy. However, Cape et al. (2010) reported that in a Sitka spruce plantation in southern Scotland the organic N flux in TF was less than 10% of the above canopy N input. Assuming that these figures may reasonably apply to Griffin Forest, the plantation still has a substantial mean CNU of 56% if compared to $N_{dep}$ in rainfall only, > 70% including the $N_{dep}$ in cloudwater and > 60% even after correcting for the potential extra DON below canopy flux.

ON in $N_{dep}$ was not measured at Griffin. Although ON is estimated to be up to 25% of the total $N_{dep}$ worldwide (Jickells et al. 2013) and other studies confirm such high figures (Neff et al. 2002), the missing potential input does not undermine the main objective of this chapter, i.e. measuring the magnitude of CNU based on the IN input, the main source of reactive N from the atmosphere.

Streamwater N flux estimates for Griffin Forest indicate that the forest plantation is not leaching N. Indeed, in some periods the forest appears to act as a N sink. N leaching from streamwater is one of the key indicators for N saturation and therefore Griffin Forest does not appear to be N saturated.

Figure 3-17 Summary of mean annual N fluxes measured in Griffin in the period 2012-2016. Propagated SE are shown for fluxes under the canopy. The boxes outlined in red indicate the fluxes that will be investigated in the following Chapters 4 and 5.

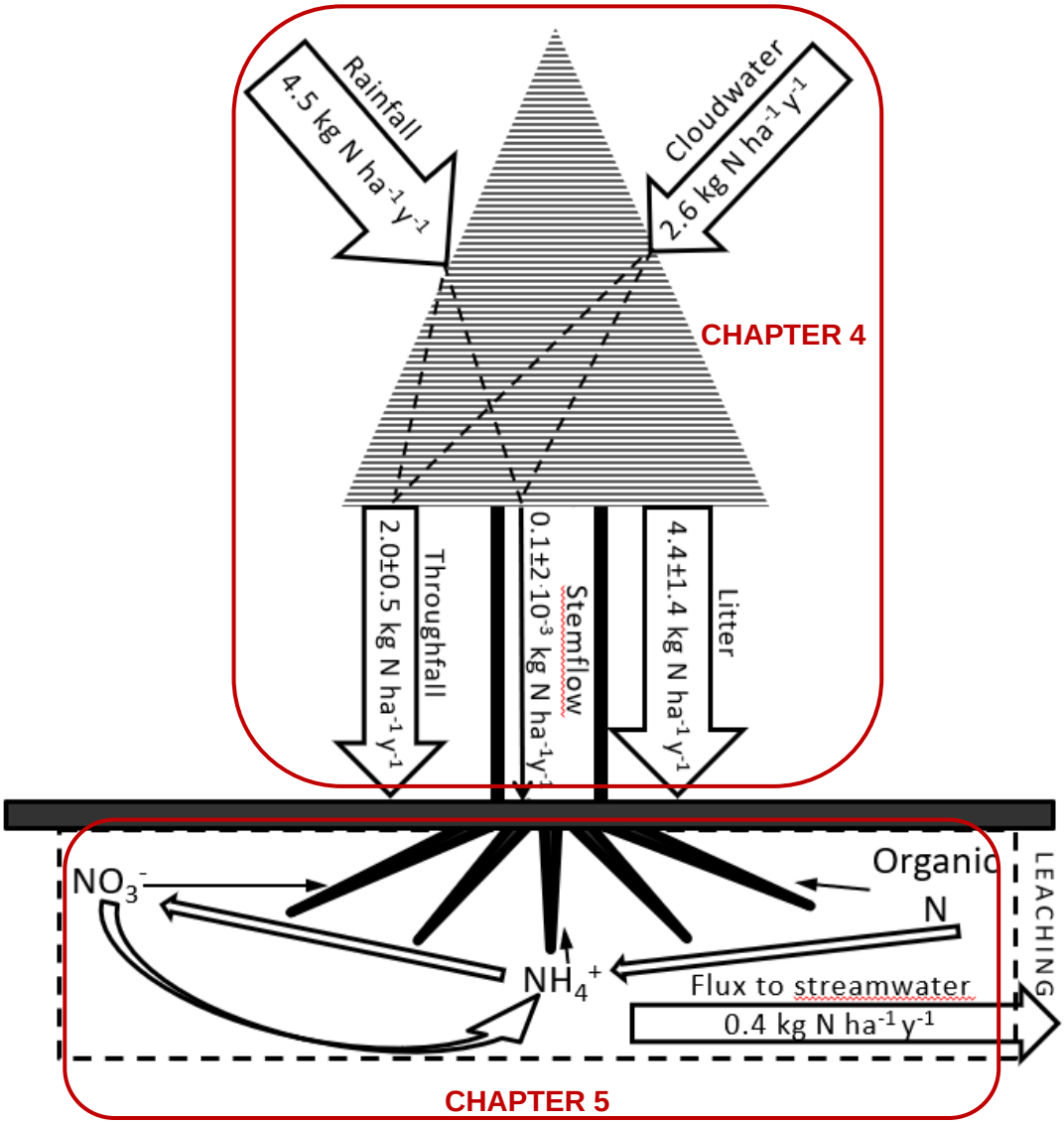

# Chapter 4. Alternative approaches for estimating canopy nitrogen uptake using stable isotopes

## 4.1 Introduction

This chapter follows on from the results of the long-term monitoring of nitrogen (N) fluxes in water in Griffin Forest, where a consistent N loss was measured in the water fluxes under the canopy compared to the measured N deposition fluxes from the atmosphere ($N_{dep}$). The 5 years monitoring programme demonstrated uptake of a substantial proportion of N deposition by the forest canopy, whereby 70% of the $N_{dep}$ was not recovered in the throughfall (TF) and stemflow (SF) fluxes below the canopy. Results in Chapter 3 failed to show clear seasonal patterns in canopy retention between N forms, although potential differences were noted for $NO_3$-N uptake.

Relatively high CNU values (45-67%) reported in beech and spruce forests in Central Europe (Schwartz et al. 2013) and in oak forests at agricultural sites in the Mediterranean area (60-65% in Avila et al. (2017)) confirm that CNU is a widespread phenomenon potentially occurring at high rates across many different forest systems. Nevertheless, Zhang et al. (2015a) in an overview of the state of the art on CNU studies with additions over and under the canopy, showed that results may depend on variables such as application technique, forest type, $N_{dep}$ and environmental conditions. They conclude that an improved understanding is needed of the effects of these variables on CNU.

The long-term field monitoring in this research followed the natural abundance approach to assessing the N canopy budget that has been widely used in the literature (e.g. Houle et al. 2014; Fenn et al. 2013; Schwarz et al. 2014; Wortman et al. 2012) and showed comparable results to studies at other low $N_{dep}$ sites. However, no other known papers have used alternative methods to confirm the results of a comparison between N fluxes above and below the canopy. Over the last two decades, the majority of alternative approaches applied different forms of N fertiliser to the forest floor, either in solid form or solution. Among these studies, Fowler et al. (2015) examined the effects of a 13 year-long application of ammonium sulphate to whole-tree harvested plots, whilst Gentilesca et al. (2013) used 46% urea prills soil N additions alone or in combination with P and/or K to assess the effects of $N_{dep}$ and N supply on carbon (C) accumulation. Talhelm et al. (2013) studied changes in understory vegetation through multiple applications of 30 kg $ha^{-1}$ $y^{-1}$ of N in the form of $NaNO_3$ pellets during the growing season. A smaller number of studies applied N

to the forest canopy increasing the natural deposition with or without use of stable N isotopes. Gaige et al. (2007) represents one of the few examples of large-scale application of N over the canopy. By using a mixed application of N, $^{15}NO_3^-$ and $^{15}NH_4^+$ their study suggested a high retention by the canopy after comparing the TF N fluxes with the application levels, and also implies the absence of nitrification at the canopy level. Cape et al. (2010) exposed a Scots pine plantation to $NH_3$-N fumigation to measure the formation of organic N from dry IN atmospheric sources and estimated that about 10% of the likely retained $NH_3$ was transformed into ON. In the same paper, a study from Chiwa et al. (2004) is also reported where organic N formation from $NO_3^-$ and $NH_4^+$ wet deposition was measured to be up to 24% of the applied IN.

From the examples given above it emerges that there is some variation in terms of the scale of the application, the application technique utilised and N forms used (organic N applications will be described in Chapter 5). Also, the objectives of the experiments varied and, in some cases, did not address N retention. A comparison of different approaches within the same study would help to compare N retention estimates obtained in different experimental conditions.

This chapter aims to:

1) determine the CNU under an increased $N_{dep}$ scenario by comparing different approaches at a tree scale with those presented in Chapter 3 at a multiplot scale;
2) verify possible seasonal differences in the total N uptake and between different IN forms that were only partly addressed in Chapter 3; in particular the use of $^{15}N$ aims to verify if nitrification or a preferential uptake of ammonium or nitrate happens after a deposition event on the canopy.
3) give more insight on the possible mechanism through which $N_{dep}$ is retained by the canopy.

In the present study, the effects of scale and seasonality on CNU were investigated and compared with the long-term plot-scale monitoring results. This was done by stable isotope addition of a $^{15}NH_4{}^{15}NO_3$ double-labelled solution to the canopies of selected Sitka spruce trees *in situ* on two occasions, once in summer and then in winter (representing the growing and dormant seasons, respectively), simulating the highest $N_{dep}$ event values measured in the 5 years monitoring. A second experiment aimed to measure whether at least a part of the $N_{dep}$ not recovered in TF is taken up by some of the tree components, namely twigs and needles. A double-labelled $^{15}NH_4{}^{15}NO_3$ solution was applied directly to individual branches, similarly to Boyce

(1996) and Nair et al. (2016). The results provide new insights into the fate of $N_{dep}$ at the canopy level adding potentially important new information on seasonal variations and N dynamics at the canopy level. Consequently, these experiments should help to improve understanding of the interactions between $N_{dep}$ and N cycling in forests.

The two experiments described in this chapter will be presented separately, each with a separate methodology, results and discussion, before an overall conclusions section at the end of the chapter.

## 4.2 Experiment 1 - N retention by individual trees

### 4.2.1 Methodology

#### 4.2.1.1 Experimental set-up

To validate and better understand data from the 5 years monitoring of N interception by the canopy at Griffin Forest, simulated $N_{dep}$ was applied to three Sitka spruce trees *in situ* using $^{15}N$ to label the applied solution and calculate the total recovery of the applied $^{15}N$ in throughfall and stemflow. The trees selected for the experiment (T1, T2 and T3) were located close to the existing eddy covariance tower in the T plot so that the canopy was accessible for applying the solution by hand with a sprayer fitted with an extension lance. They were part of the even aged Griffin Forest plantation (~4,000 ha planted between 1980 and 1981), had similar diameter at breast height (DBH, T1: Ø = 28 cm, T2: Ø = 30 cm, T3: Ø = 26.5 cm) and their heights were 1.5-2 m above that of the tower (20 m).

The maximum reachable distance with the extension lance from the tower was 5.4 m so the selected trees needed to be located within this distance from the tower. Fig. 4-1 shows the distances measured on the ground between the tower and the selected trees (T1, T2 and T3) and between T1, T2 and T3 and the surrounding trees. Numbers in brackets are the main branch lengths as estimated from the ground. The tower and the hut housing equipment were located in one of the thinned rows, where tree branches had more space to grow. In all other directions the canopy was closed, and the branches of surrounding trees intersected those of T1, T2 and T3.

Figure 4-1. Schematic of the location of the target trees around the eddy covariance tower in the T plot at Griffin Forest. Numbers in brackets are the main branch lengths as estimated from the ground. The starred tree adjacent to T1 and T2 is the same tree. T2 was ~4.5 m from the nearest corner of the tower.

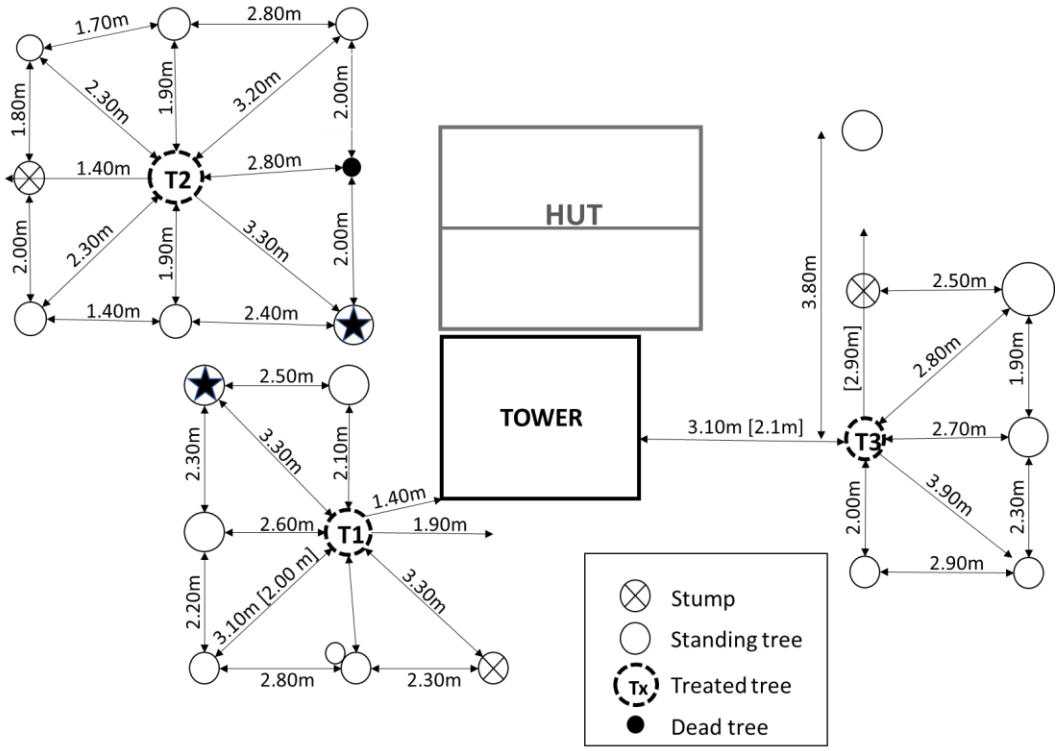


Under each tree, 1 stemflow and 4 throughfall collectors were set up in the same manner as the long-term monitoring collectors (see Figure 4-2).

Figure 4-2. TF collectors and SF collector under T2, April 2017

The throughfall collectors were designed to cover a surface area of approximately 20% of the theoretical crown projection, i.e. 1/1750 of a hectare (5.7 $m^2$) since there are 1750 stems $ha^{-1}$. The actual crown projection was estimated from the ground by measuring all distances from the sample tree stem to the surrounding stems and estimating the maximum extent of the branches. This value was used to scale the collected TF to the expected total TF from each tree, as the collectors only covered a fraction of the area under each crown.

A third rainfall collector of the same design as the other 2 RF collectors (see Chapter 2) was installed in the proximity of the upper RF and fog samplers. This enabled RF collection associated with the sampling occasions for the canopy application experiment to be conducted separately from the monthly RF collection for the 5-year monitoring programme. The RF collector dedicated to the canopy application experiment was used for the first 3 TF and SF sampling dates after the first application in August 2016 to measure rainfall depth only. However, following damage by wind, the RF depths after September 2016 reported in this chapter are the mean value of the two existing RF samplers.

#### 4.2.1.2 N application and collection

The crown of each of the three target trees was sprayed on two occasions (5 August 2016 and 28 February 2017) with 3.5 L of a 98% atom $^{15}N$ double-labelled enriched $NH_4NO_3$ solution ($\delta^{15}N$ = +1000) applied from the top of the tower. The mass of total applied N (~7.6 g $NH_4NO_3$/ tree crown, representing an input of 4.66 kg N $ha^{-1}$) was chosen to be of the same order of magnitude as the highest $N_{dep}$ event in the previous 4 years (April-May 2014, 3.2 kg N $ha^{-1}$) and not exceeding the minimum annual deposition (5.3 kg N $ha^{-1}$ in 2016). The two application dates (August and February, hereafter referred to as "summer" and "winter", respectively) were chosen to be representative of the growing season and the dormant season respectively. The timing of the application was also constrained by the weather as calm and dry conditions were required. The volume of solution applied to each tree (3.5 L) was chosen to ensure full wetting of the canopy, but with throughfall minimised. This volume was estimated through a test conducted in February 2016, in calm but partly wet conditions with intermittent light drizzle, when ~5 L deionised water was applied to the crown of each tree whilst the ground below each tree was covered with a 5 m x 5 m PVC sheet. Less than 250 mL was collected under each tree in the wetter conditions of the test than those chosen for the two labelled applications.

The quantities of $NH_4NO_3$ and $^{15}N$-enriched $NH_4NO_3$ applied in the field to each target tree are shown in Table 4-1, calculated from the mass of N dissolved in 3.5 L of deionised water (DIW) after deducting the mass of the solution remaining in the sprayer at the end of the application. $\delta^{15}N$ per each tree is calculated from the mass of $NH_4NO_3$ and $^{15}NH_4{}^{15}NO_3$ as follows:

$$\delta^{15}\mathrm{N}\ (‰) = \left[\left(\frac{mass^{15}N(^{15}NH_4{}^{15}NO_3) + mass^{15}N(NH_4NO_3)}{mass\,N(NH_4NO_3)}}{R_{std}}\right) - 1\right] \times 1000 \qquad \text{(Eq 4-1)}$$

where $R_{std}$ = 0.0036764 (Mariotti, 1983).

Table 4-1. Labelled and unlabelled $NH_4NO_3$ applied to the target trees.

| Tree code | $NH_4NO_3$ (g) | | $^{15}NH_4{}^{15}NO_3$ (mg) | | $\delta^{15}N$ per mil | |
|---|---|---|---|---|---|---|
| | Summer | Winter | Summer | Winter | Summer | Winter |
| T1 | 7.594 | 7.602 | 25.176 | 25.290 | +999 | +1002 |
| T2 | 7.982 | 7.980 | 26.546 | 26.513 | +1002 | +1001 |
| T3 | 7.083 | 7.084 | 23.622 | 23.542 | +1004 | +1001 |

After the $^{15}N$-labelled solution application to the crowns, the TF and SF sampling was timed to collect the samples as soon as possible after significant rainfall events and to minimise storage time in the collection barrels and any potential artefacts introduced due to microbiological activity. The volumes of TF and SF were measured in the same way as for the long-term monitoring collectors. Samples of at least 5 L (when available) of TF and SF were collected for analysis. This volume of water was required to ensure that at least 50-150 µg N was collected in the acidified filters for mass spectrometry analysis and also to provide spare sample as a backup, in case any problems were encountered with the preparation of samples for mass spectrometry analysis. The entire water in the four TF collectors below each tree on each sampling occasion was transferred into a 10 L Nalgene bottle in the field to create a composite TF sample for each tree. When the volume of the TF in the collectors below each tree exceeded the maximum volume of the 10 L Nalgene bottles, a representative composite sample of 5-10 L was obtained for each tree by blending the water collected in the four throughfall samplers in proportion to the water depth in each barrel. After each collection, any remaining water in the TF and SF barrels was emptied. Control (no N and labelled N application) TF and SF samples were taken at subplot T12 (see Figure 2-3), about 100 m from the tower used for the $^{15}N$ application, and consisted of one TF sample and one SF sample obtained by mixing a 0.5 L sample from each of the three TF/SF samplers in T12. An additional rainfall (RF) sampler was installed in the proximity of the upper RF and fog samplers. As explained above, it was used for the first 3 summer sampling dates but was discontinued from the fourth sampling date (4 September 2016) after it was damaged by wind.

TF and SF collection after each application continued until enhanced N concentrations were no longer measured in TF and SF samples below the target trees. Collection after the August 2016 application ended about 4 months later in December 2016, whilst collection after the winter application ended in April 2017, 5

weeks after the application. Table 4-2 lists the application and TF and SF collection dates. Air temperature and hours of daylight complete the information provided to describe the environmental conditions in which the samples were collected.

Table 4-2. Timeline for applications and TF and SF collections and environmental conditions for the $^{15}N$-labelled simulated $N_{dep}$ experiment. Air temperatures are the mean value of 2 measurements made in the area of the experimental plot mid-morning and mid-afternoon on each sampling date. Rainfall depth on 13 March 2017 is the total cumulative value from the date of the winter application (28 February). Hours of daylight were calculated as the time between sunrise and sunset using R package *suncalc* and inputting the site latitude (56.6079°N) and longitude (-3.7959°E)

| Date | Action | Hours of daylight (hh:mm) | Temperature (°C) | Rainfall since previous collection (mm) |
|---|---|---|---|---|
| 05-08-2016 | summer application | 15:53 | -- | -- |
| 10-08-2016 | collection 1 | 15:32 | 13.7 | 14.9 |
| 12-08-2016 | collection 2 | 15:23 | 12.5 | 12.5 |
| 20-08-2016 | collection 3 | 14:48 | 12.2 | 10.1 |
| 04-09-2016 | collection 4 | 13:39 | 9.1 | NA |
| 28-10-2016 | collection 5 | 09:26 | 4.5 | 156.7 |
| 19-12-2016 | collection 6 | 06:49 | 2.0 | 59.9 |
| 28-02-2017 | winter application | 10:35 | -- | -- |
| 06-03-2017 | collection 1 | 11:04 | 2.3 | NA |
| 13-03-2017 | collection 2 | 11:38 | 3.1 | 84.91 |
| 06-04-2017 | collection 3 | 13:32 | 6.0 | 30.8 |

#### 4.2.1.3 Preparation and analysis of throughfall and stemflow samples for $\delta^{15}N$

Concentrations of $NH_4^+$ and $NO_3^-$ were determined in a 20 mL filtered subsample of each sample as described already in Section 2.2.7. All TF and SF samples were stored at room temperature for less than 24 hours after collection, before refrigeration at 4°C until the N concentration results were available. Then, based on the concentration determined, sufficient sample volume was processed to obtain 50-150 µg of $NH_4$-N through the ammonia diffusion method described below.

The ammonia diffusion method described by Sebilo et al. (2004) is particularly suitable for this experiment as it has been demonstrated to generate accurate and reproducible values of $\delta^{15}N$ for very small quantities of $NH_4^+$ and $NO_3^-$ in aqueous samples. The method involves conversion of $NH_4^+$ and $NO_3^-$ in the water sample into $NH_3$ (gas) through two subsequent extractions from each sample, by means of pH

adjustment (to volatilise $NH_4$ to $NH_3$) and reduction ($NO_3^-$ to $NH_4^+$), respectively, which is entrapped in an acidified glass filter wrapped in hydrophobic, gas permeable PTFE tape (Sebilo et al. 2004). A volumetric adjustment of the procedure described in Sebilo et al. (2004) was necessary to process up to 1 L of sample, due to the usually low concentration of dissolved N in the throughfall and stemflow at natural abundance.

For the technique, incubation bottles were prepared by filling with a 0.5 M HCl solution, shaking for about 10 seconds, then left to stand for 5 minutes, followed by rinsing three times with DIW and finally drying in a furnace at 400°C for 1 hour. The preparation of the filter packages (Whatman™ Binder-Free Glass Microfibre Filters, Fisher Scientific, UK) was conducted on a sheet of clean aluminium foil wearing disposable gloves and using scissors, tweezers and spatulas that had been previously cleaned with ethanol. The microfibre filters were cut into 0.5 cm x 1.5 cm rectangles which were ashed in the furnace at 400°C for 1 hour. 30 µL of 8 N $H_2SO_4$ was pipetted onto each filter, then the filter was wrapped and enclosed in 19 mm width PTFE hydrophobic tape by firmly pressing all sides with a spatula. A first set of filters was placed into the incubation bottles with a variable amount of sample, calculated from the N concentrations measured through colorimetric analysis (as described in section 2.2.7) to contain between 50 and 150 µg of $NH_4^+$-N. NaOH (5 M, 2 mL 150 $mL^{-1}$ of solution) was pipetted into each incubation bottle and the bottle was immediately sealed with sealing parafilm, left for 1 week at room temperature and moved gently daily to remove any drops of condensation from the walls or film. The first filter package was then removed. After $NH_4$ had been removed from the solution, the $NO_3^-$ contained in the sample was captured by placing a new filter package into the bottle addition of 300 mg of Devarda's alloy to each bottle. The bottle was resealed and incubated for one more week in the same manner as the first step, before removal of the second filter pack.

After 1 week of incubation - 2 weeks in total - the wrapped filters were retrieved from the bottles, frozen, then freeze-dried in the School of GeoSciences, University of Edinburgh, and sent to the NERC Life Sciences Mass Spectrometry Facility (LSMSF, Lancaster, UK) for $\delta^{15}N$ analysis. Differing known masses of the freeze-dried filters were weighed, enough to yield 100 µg N, or else the whole filter if this was not possible, using a high precision micro-balance (Sartorius Ltd.) and then sealed into a 6 mm x 4 mm tin capsule (Elemental Microanalysis Ltd., Okehampton, UK). Samples were then combusted in an automated Carlo Erba NA1500 elemental analyser coupled to a Dennis Leigh Technologies Isotope Ratio Mass-Spectrometer. In-house working standards of either natural abundance or $^{15}N$-enriched flour were analysed

after every twelfth sample resulting in analytical precision of 0.24‰ for the natural abundance standard. These standards have been calibrated against the certified reference material IAEA-N1 (NIST number 8547, National Institute of Standards and Technology, Gaithersburg, USA). All $\delta^{15}N$ results are expressed relative to the international standard of atmospheric air.

The high osmotic pressure of the acidified filters, floating on an alkaline solution, may have caused partial infiltration of alkaline solution that could have neutralised the acidified filters before all $NH_3$ was captured. A partial N recovery could result in lower $\delta^{15}N$ values (Sebilo et al. 2004). Due to the narrow width of the PTFE hydrophobic sealing tape (10 mm) used in the first batch of samples prepared (TF and SF collected on 10 August 2016), some of the filters appeared swollen after 7 days of incubation perhaps due to infiltration of NaOH. To test whether NaOH infiltration had affected uptake of $NH_3$ by the filters and therefore the analysis results, duplicates of the first batch of samples were prepared changing the shape of the acidified filters (same area, smaller width and greater length) to increase the area sealed by the PTFE tape. In these the swelling was absent or minimal and the analysis did not show major differences in $\delta^{15}N$. Furthermore, the high amount of N collected on the filters indicates that if any neutralisation occurred, it happened at an advanced state of N absorption by the filters. Therefore, it was concluded that possible initial methodological problems with the ammonia diffusion technique did not affect the mass recovery of $^{15}N$ in the summer application experiment.

#### 4.2.1.4 Calculation of the $^{15}N$ recovery in throughfall and stemflow

The amount of $^{15}N$ on each sampling occasion was calculated, assuming that $^{15}N_0$ = 0 since the barrels had been emptied on the previous sampling. Control samples were not used for the calculations showed below. Their purpose was to determine when N concentration and $\delta^{15}N$ in the TF and SF samples below the treatment trees decreased to the background levels, and therefore they identify the time period for the recovery calculations.

The $^{15}N$ input for each tree was calculated adding the mass of $^{15}NH_4{}^{15}NO_3$ (98%) to the mass contained in the $NH_4NO_3$ applied to each tree. To calculate the $^{15}N$ found in TF and SF, the $^{15}N$ atom percent was calculated from the $\delta^{15}N$ analysis result ($\delta$) as:

$$atom\ percent = \frac{\delta + 1000}{\delta + 1000 + \frac{1000}{Rstd}} \times 100 \qquad \text{(Eq. 4-2)}$$

where $R_{std}$ = 0.0036764 (Mariotti, 1983). Then the $^{15}N$ mass flux on each sampling date for each of TF or SF was calculated as:

$$_{flux}^{15}N_x = flux_{vol} \times mass\ N_x \times \alpha \times \sigma \times atom\%_{flux\ x} \quad \text{(Eq. 4-3)}$$

where $\alpha$ = 15/19 ($NH_4$) | 15/63 ($NO_3$); $\sigma$ = scaling factor, i.e. the ratio between the surface area of the TF collectors and the projection of the crown on the ground. After calculating separately the $^{15}N$ mass flux in TF and SF for each tree, the recovery of each N form was calculated for each tree as:

$$N_{recovery}\ (\%) = \frac{TF^{15}N + SF^{15}N}{^{15}N_{applied}} \times 100 \quad \text{(Eq. 4-4)}$$

For both seasons the recovery calculations and their corresponding propagated errors were based on the first three collection dates (10, 12 and 20 August 2016; 6 March, 13 March and 6 April 2017, respectively).

### 4.2.2 Results

The TF and SF fluxes in the individual tree and of rainfall during the experiment are shown in Table 4-3. As expected, TF was always lower than RF on all sampling dates. TF volumes follow similar temporal trends under sample trees, whilst there was more variability in SF among trees. The tower was located in a thinned area, so that the growth of the crowns of trees T1 and T3 were less restricted compared to T2. T2 had the largest DBH (30 cm) but was surrounded by trees in all directions, restricting crown growth. The crown shape, however, seems less relevant than the diameter in explaining the differences in SF volumes, as supported by the SF volumes below T3 (SF3), i.e. the tree with the smallest DBH but widest crown. On three sampling dates SF3 volumes were lower than both S1 and S2, whilst and on three other occasions it was higher than at least one of the other two SF samplers. The lack of consistent proportionality between the SF volumes between the three experiment trees suggests that other factors, e.g. the wind direction, could influence SF volume collected.

Table 4-3. RF depth (new collector for the first 3 sampling dates; mean of upper and lower gauges after August 2016), TF mean depth (as mean depth of the 3 trees), TF depth and SF volumes (codes follow the tree numbering) collected following the summer 2016 and winter 2017 $^{15}N$-labelled simulated $N_{dep}$ applications to the 3 target trees in Griffin Forest. The final collection after the summer 2016 application was on 19-12-2016.

| Date | RF depth (mm) | TF depth (mm) | TF volume (L) | | | SF volume (L) | | |
|---|---|---|---|---|---|---|---|---|
| | | | TF1 | TF2 | TF3 | SF1 | SF2 | SF3 |
| 10-08-2016 | 14.9 | 4.0 | 4.08 | 3.48 | 3.70 | 0.96 | 0.46 | 0.62 |
| 12-08-2016 | 12.5 | 7.8 | 8.00 | 6.00 | 8.00 | 7.00 | 5.00 | 3.75 |
| 20-08-2016 | 10.1 | 7.1 | 7.00 | 6.25 | 6.75 | 4.75 | 4.70 | 2.00 |
| 04-09-2016 | NA[1] | 21.4 | 22.46 | 17.01 | 21.00 | 15.55 | 17.01 | 3.19 |
| 28-10-2016 | 156.7 | 84.8 | 82.92 | 74.56 | 82.56 | 9.74 | 28.64 | 17.01 |
| 19-12-2016 | 59.9 | 41.0 | 46.21 | 32.40 | 37.49 | 4.00 | 26.46 | 8.00 |
| 06-03-2017 | --[1] | 45.4 | 41.12 | 41.12 | 46.21 | 27.18 | 16.27 | 9.73 |
| 13-03-2017 | 84.9[2] | 7.9 | 7.50 | 7.00 | 7.80 | 5.00 | 7.00 | 5.00 |
| 06-04-2017 | 30.8 | 25.3 | 24.40 | 22.22 | 25.13 | 11.19 | 22.09 | 4.65 |

[1] no sample as rainfall collector destroyed by wind (see section 4.2.1.1). [2] RF depth is the cumulative value for 06-03-2017 and 13-03-2017 sampling dates.

Table 4-4 shows the N concentrations [N] in TF and SF measured after the summer and winter applications and also in the control samplers, where available. On the first two sampling dates [N] in TF and SF samples collected under the crowns of the experimental trees after the summer application were much higher than $N_{dep}$ during the long-term monitoring programme at Griffin. The TF and SF concentration values measured in the controls on 20/08/2016 are lower than in TF and SF collected below the treatment trees T1-T3 for both the reduced and the oxidised N form. However, the mean TF concentrations measured at both T and C plots on that date (20/08/2016) were 0.116 mg $L^{-1}$ for $NO_3$-N and 0.172 mg $L^{-1}$ for $NH_4$-N, so that the [N] of the blended control TF and SF samples from the T12 subplot shown in Table 4-4 represents the minimum value measured at Griffin on that occasion.

Control TF and SF samples were not taken in the week after the application when they were expected to be markedly lower than the treated samples, and they were not required for the calculations of N recovery. [N] in TF and SF below treatment trees T1-T3 were elevated on the second sampling (2 days after the first sampling), whilst on subsequent sampling dates [N] were the same order of magnitude as those measured in the control samples.

Similar [N] to the TF and SF samples below the experimental trees were measured in the bulk RF samples on 19/08/2016 ($NO_3$-N = 0.131 mg $L^{-1}$; $NH_4$-N = 0.036 mg $L^{-1}$), suggesting that the canopy retention of the applied N had mostly occurred by that date. This is supported by Figure 4-3 which shows how the cumulative N retention after the first two collections in August was substantial for both oxidised and reduced N (~78%). For both the N forms the gap between cumulative input and cumulative recovery in TF and SF increases over time, suggesting that the uptake of the N application pulse is rapid. It also suggests that either retention is higher at lower N inputs or nitrification and other uptake processes are faster during warmer temperatures.

Table 4-4. N concentrations in TF and SF under the sampled trees at each sampling date after the summer 2016 and winter 2017 $^{15}$N-labelled simulated $N_{dep}$ applications to the 3 target trees in Griffin Forest. Where available, values from control SF and TF samples (CSF and CTF) are shown.

| Date | CSF | SF1 | SF2 | SF3 | CTF | TF1 | TF2 | TF3 |
|---|---|---|---|---|---|---|---|---|
| | | | | $NH_4$-N (mg $L^{-1}$) | | | | |
| 10/08/2016 | | 0.001 | 0.007 | 0.498 | | 2.983 | 4.205 | 3.837 |
| 12/08/2016 | | 0.077 | 0.139 | 0.152 | | 3.008 | 0.481 | 0.122 |
| 20/08/2016 | 0.140 | 0.186 | 0.154 | 0.878 | 0.001 | 0.282 | 0.128 | 0.359 |
| 04/09/2016 | 0.465 | 0.108 | 0.376 | 0.656 | 0.350 | 0.225 | 0.137 | 0.362 |
| 28/10/2016 | | 0.306 | 0.104 | 0.341 | | 0.291 | 0.330 | 0.395 |
| 19/12/2016 | | 0.653 | 0.138 | 0.142 | 0.065 | 0.387 | 0.103 | 0.401 |
| 06/03/2017 | | 0.093 | 0.093 | 0.100 | | 0.901 | 0.859 | 0.996 |
| 13/03/2017 | 0.072 | 0.103 | 0.072 | 0.110 | 0.100 | 0.130 | 0.137 | 0.142 |
| 06/04/2017 | 0.019 | 0.065 | 0.033 | 0.114 | 0.026 | 0.138 | 0.323 | 0.194 |
| | | | | $NO_3$-N (mg $L^{-1}$) | | | | |
| 10/08/2016 | | 0.016 | 0.000 | 0.009 | | 2.712 | 3.686 | 3.911 |
| 12/08/2016 | | 0.034 | 0.001 | <LOD | | 2.732 | 1.054 | 0.030 |
| 20/08/2016 | 0.330 | 0.023 | 0.014 | 0.064 | 0.080 | 0.354 | 0.853 | 0.635 |
| 04/09/2016 | 0.003 | 0.043 | 0.059 | <LOD | <LOD | 0.043 | 0.042 | 0.052 |
| 28/10/2016 | | 0.019 | 0.019 | 0.019 | | 0.040 | 0.044 | 0.051 |
| 19/12/2016 | | 0.010 | 0.002 | 0.009 | 0.170 | 0.067 | 0.024 | 0.044 |
| 06/03/2017 | | 2.696 | 5.223 | 0.463 | | 1.416 | 1.585 | 1.545 |
| 13/03/2017 | 0.006 | 0.055 | 0.013 | 0.019 | 0.050 | 0.060 | 0.056 | 0.065 |
| 06/04/2017 | 0.030 | -0.007 | 0.009 | -0.003 | 0.054 | 0.034 | 0.040 | 0.057 |

Figure 4-3. Cumulative N mass by N form recovered under the crowns (as TF+SF, dot-dash line, mean value for the 3 experimental trees ± 0.95 CI of the mean) after the summer 2016 application and compared to the cumulative N input ($N_{input}$, solid line ± 0.95 CI of the mean). The N input curve is the mean of the sum of the N applied to each tree on 5 August 2016 and the cumulative natural $N_{dep}$ sampled at the upper and lower RF gauges scaled to each tree canopy area. All collection dates are shown on the x axis as labels except the first date, 10 August, to improve the readability. Recovered N masses below each experimental tree on each sampling occasion are indicated by the empty circles.

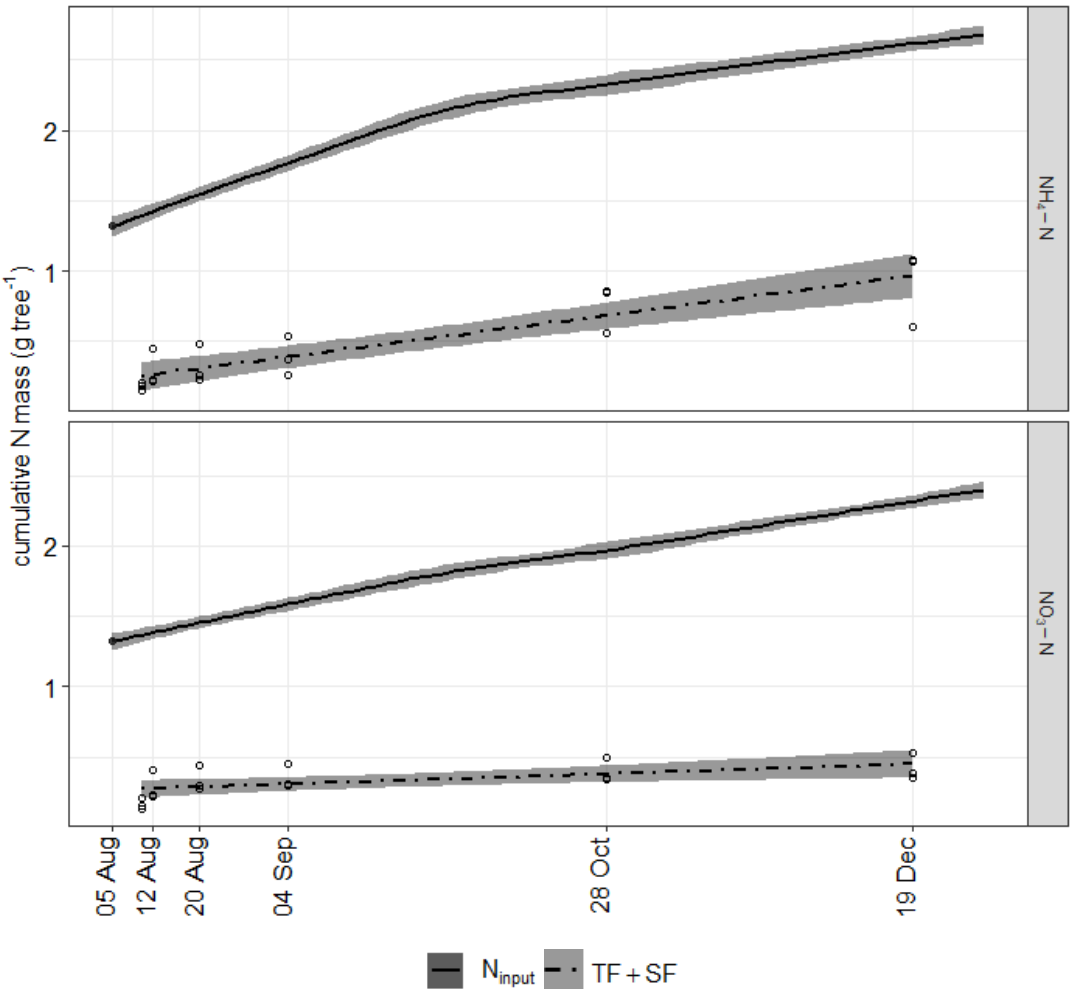


In TF collected after the summer application, $\delta^{15}N$ values showed a similar temporal pattern for both the N forms (Figure 4-4). The signal was markedly high on the first two sampling dates, and then declined rapidly from the third sampling onwards to reach values close to the natural abundance. However, on the first date $\delta\,^{15}NH_4$ was 2 orders of magnitude higher than the natural abundance, whilst $\delta\,^{15}NO_3$ had much lower values (ranging from +30‰ to +50‰). In contrast, $\delta^{15}N$ values in SF were low on all collection occasions.

Similar to the recovery in [N] in TF after the summer application, on the third sampling date (20 August, Figure 4-4) $\delta^{15}N$ values in TF reached values close to the natural

abundance ($\delta^{15}N$ values in the TF control samples were low and relatively constant, varying from -5‰ to -2‰ for $NH_4$-N and from -16‰ to -9‰ for $NO_3$-N), i.e. within two weeks after the treatment and encompassing two rainfall events. The $\delta^{15}$ $NO_3$-N signal for both TF and SF showed a relative peak on the 28th of October, almost 2 months after the previous sampling. On that date the $NO_3$-N concentrations in TF for all of the treated trees were extremely low, so that the contribution to the overall $^{15}N$ recovery was estimated to be negligible. These data suggest that small amounts of N from a 3 months deposition event are still exchanged from the tree canopy to the forest floor.

Figure 4-4. Cumulative N mass recovered below the tree canopy (black line, mean value for the 3 experimental trees ± 0.95 CI of the mean shown by the grey area) and the $\delta^{15}N$ signal measured for TF and SF on each sampling occasion (boxplots summarising results for the 3 experimental trees) after the summer 2016 application. The 2nd sampling date (12 August) is not shown as a label on the x axis to improve the readability. Recovered N masses below each experimental tree on each sampling occasion are indicated by the empty circles. The main and secondary y axis are square root transformed to enhance the readability of the $\delta^{15}N$ boxplots.

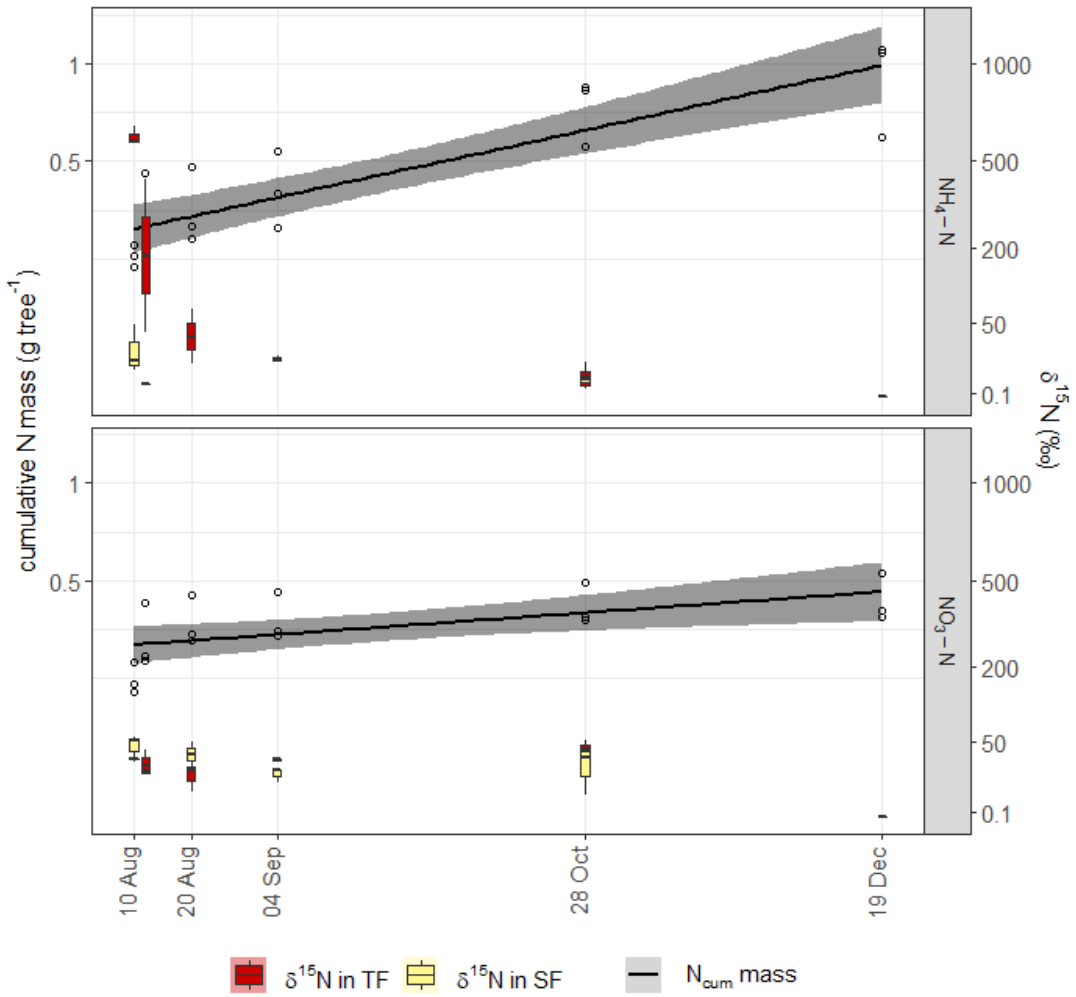


Due to unusually dry conditions in March 2017, the timings of the TF and SF collections after the winter application differed from those following the summer

application. The first rainfall event occurred a week after the winter application, and another week passed before a second rainfall event, whilst in a similar time frame three collections had been completed following the August 2016 application. This was reflected in the different temporal evolution of [N] measured in the TF and SF samples after the summer and winter applications. [N] measured in TF and SF under the experimental trees were markedly higher than in the environmental $N_{dep}$ on the first sampling date after the winter application, as expected, and similar to after the summer application (see Table 4-4). However, the [N] of both forms in TF and SF on the second sampling date (13 March) were of the same order of magnitude as normally measured under mean natural $N_{dep}$ conditions. This is reflected in Figure 4-5 which shows that most N in TF and SF was recovered under the crowns after the first collection, as the cumulative curve is almost horizontal. No peaks of natural $N_{dep}$ were detected during the collection period and this condition helps in the interpretation of the trend of the fluxes under the canopy.

Figure 4-5. Cumulative N mass by N form recovered under the crowns (as TF+SF, dot-dash line, mean value for the 3 experimental trees ± 0.95 CI of the mean) after the winter 2017 application and compared to the cumulative N input ($N_{input}$, solid line). The N input curve is the mean of the sum of the N applied to each tree on 5 August 2016 and the cumulative natural $N_{dep}$ sampled at the upper and lower RF gauges scaled to each tree canopy area. Recovered N masses below each experimental tree on each sampling occasion are indicated by the empty circles.

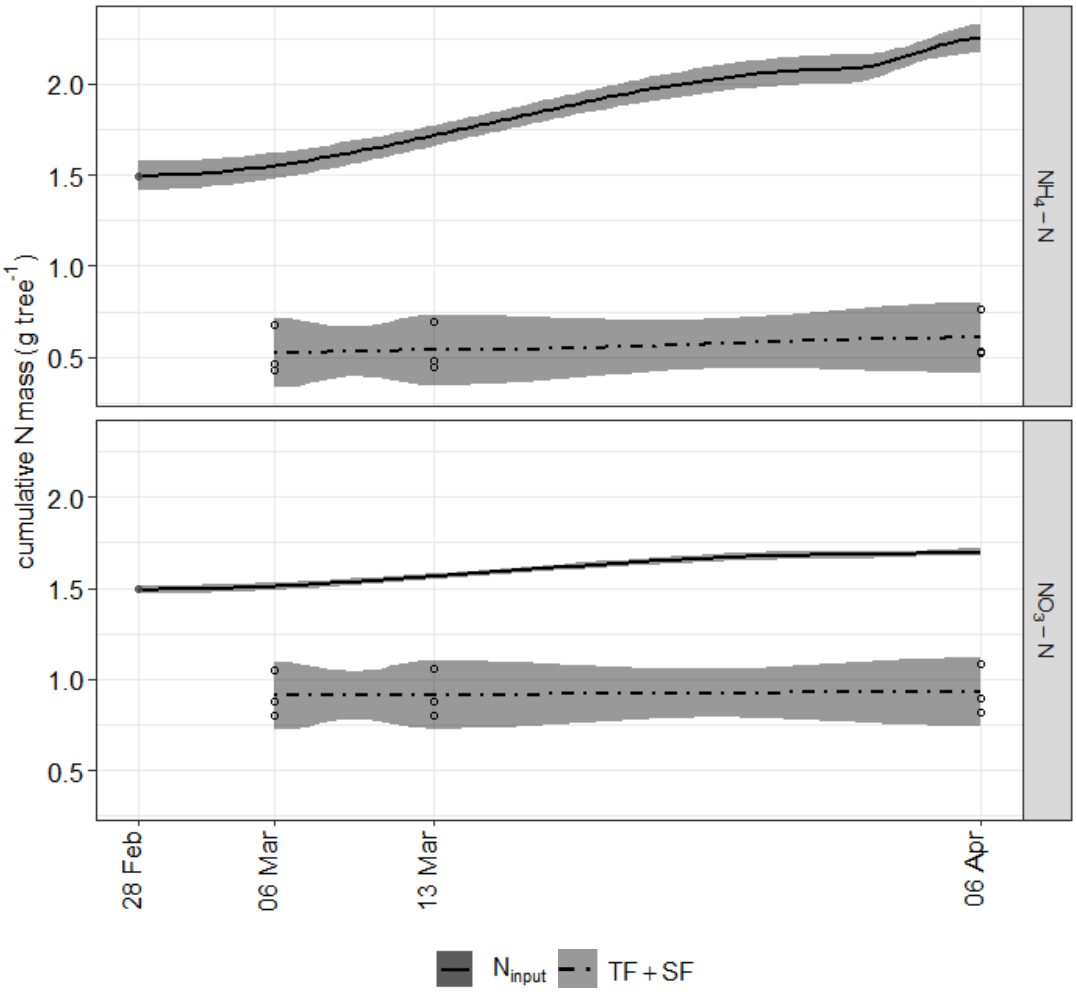


Following the winter application $\delta^{15}NH_4$-N values in SF were close to natural abundance ($\delta^{15}N$ for control SF = +3.56‰; $\delta^{15}N$ for control TF = -3.96‰) after the first collection on 6 March (Figure 4-6), whilst $\delta^{15}NO_3$-N values in TF and SF remained two orders of magnitude higher than natural abundance ($\delta^{15}N$ for control SF = +5.85‰; $\delta^{15}N$ for control TF = -9.84‰) on the second collection date (13 March), albeit lower than on the first collection. $\delta^{15}N$ values of both N forms were similar to natural abundance and close to 0 on the third and final collection on 6 April 2017.

Figure 4-6. Cumulative N mass recovered below the tree canopy (black line, mean value for the 3 experimental trees ± 0.95 CI of the mean shown by the grey area) and the $\delta^{15}N$ signal measured for TF and SF on each sampling occasion (boxplots summarising results for the 3 experimental trees) after the winter 2017 application. Recovered N masses below each experimental tree on each sampling occasion are indicated by the empty circles. The main and secondary y axis are log transformed to enhance the readability of the $\delta^{15}N$ boxplots.

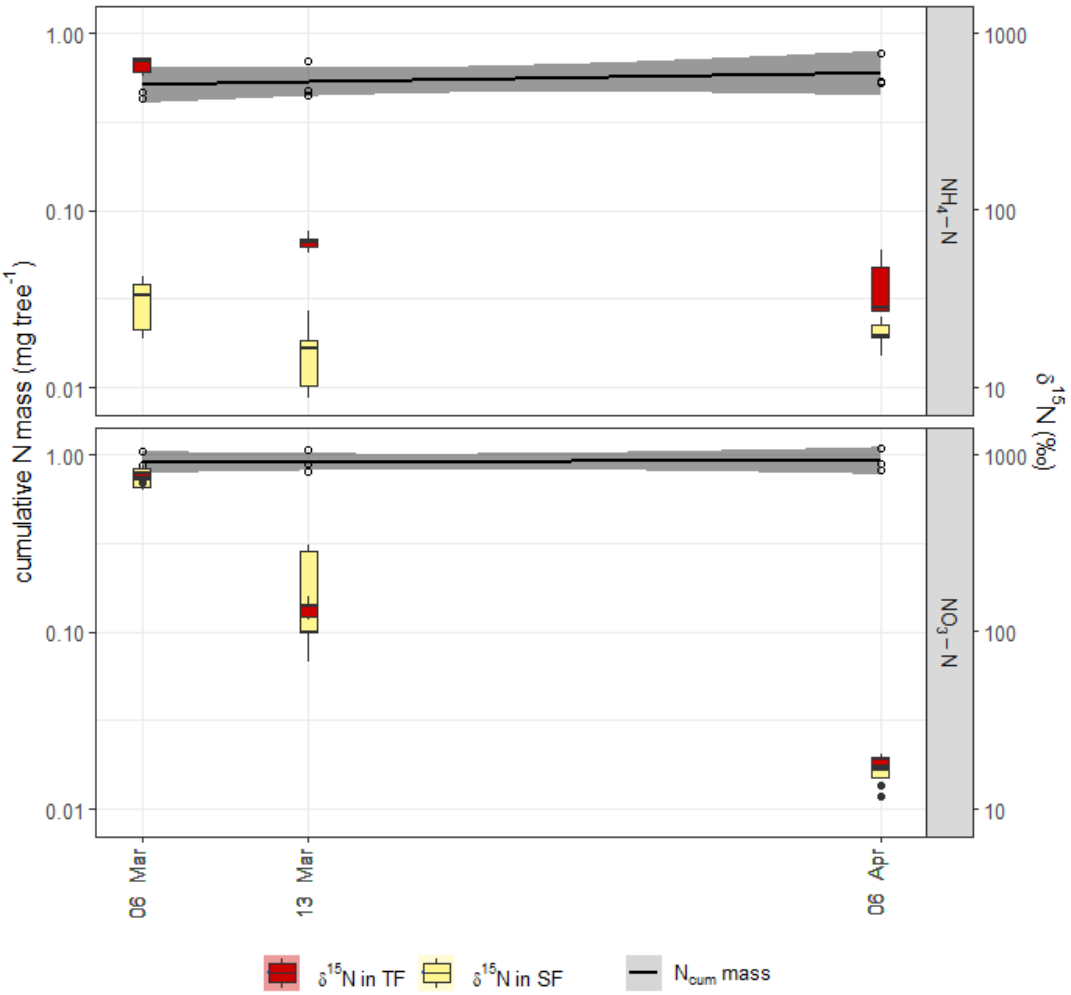


Table 4-5 shows the % recovery for each N form in the summer and winter application experiments. The errors have been based on an error of ±10 cm on the measure of the crown projection on the floor (as radius of a circumference centred on the tree stem) and an error of ±0.25 L on the water volumes (estimated using 10 L Nalgene bottles). These errors were propagated through the collection dates. The error from the atom % variance (n =3) was added to the propagation function but discarded later due to its proportionally small value (3 or more orders of magnitude smaller than the error of the crown projection estimation).

Canopy retention of both forms of N was lower after the winter application compared to after the summer application, particularly for $NO_3$-N. In winter, canopy retention was less than 40% of the applied $NO_3$-N for both the N concentration and stable

isotope approaches, with a lower retention (23%) estimated using $^{15}N$ than by N mass (39%). This result is the opposite of what was measured in the summer application, where the stable isotope approach showed higher retentions than the estimations made with the N concentrations only. In the winter application, the retained $NH_4$-N was higher than the $NO_3$-N, differing from the seasonal recovery for the period November-March 2016 (Table 3-3), where the calculated retention for $NH_4$-N was 49 ± 8% compared to the much higher 71 ± 26% retention for $NO_3$-N.

The total $^{15}N$ retention was estimated to be higher than the N retention in summer and in line with both the N forms. In winter the total $^{15}N$ recovered was lower than the estimated retention through the unlabelled N. In winter, however, the amount of $^{15}NH_4$-N was equal to the $NH_4$-N % recovery, whilst the $^{15}NO_3$-N recovery was markedly lower than the $NO_3$-N recovery.

Table 4-5. Percentage of N and $^{15}N$ retained by the canopy by N form and season of application. The propagated error is based on the error propagation of crown area estimation and water volume measurements. $\delta^{15}N$ variation between replicates was assumed ≈0 as it was 3 or more orders of magnitude smaller than the error of the crown projection estimation.

| | **$NH_4$-N** | **$NO_3$-N** | **Total N** |
|---|---|---|---|
| **Summer N retention** | 77.7 ± 4.6% | 78.4 ± 4.4% | 78.0 ± 4.5% |
| **Summer $^{15}N$ retention** | 83.5 ± 3.3% | 87.8 ± 2.5% | 85.7 ± 2.9% |
| **Winter N retention** | 64.0 ± 8.5% | 38.6 ± 14.6% | 51.3 ±11.9% |
| **Winter $^{15}N$ retention** | 64.1 ± 8.7% | 23.4 ± 10.5% | 43.7 ±14.2% |

### 4.2.3 Discussion

The results of the canopy application experiment confirm the high mean canopy nitrogen uptake, i.e. the difference between inorganic N (DIN) in bulk deposition + cloudwater deposition and throughfall (similar to the definition in Houle et al. 2015), in the 5-year monitoring programme in Griffin Forest described in Chapter 3. The summer % total N retention figures estimated from both the $^{15}N$ recovery and the N concentration approaches in the experiment are very similar to the total N retention annual figure estimated at the plot scale for 2016 (71%, see Chapter 3, Figure 3-14 and Table 3-3) and are even closer to those measured during the 2016 summer period (76%). These similarities were not necessarily expected due to the different scale of the experiment. Also, the N input in the canopy experiment was relatively high compared to the N deposition measured in 2016, the lowest value of the 5 years monitored.

Lower values of canopy N retention have been reported in the literature under a wide range of environmental and experimental conditions, including variations in mean annual $N_{dep}$, precipitation amount, mean annual temperature, tree species, and measurements under natural $N_{dep}$ abundance or high/low $N_{dep}$ additions. A comparison of the main results from studies in temperate or boreal forests cited in this thesis is given in Table 4-6. A further factor in the experimental conduct that might affect reported canopy N retention is that fewer studies have been conducted involving N additions to the canopy compared to those using additions to the ground (Zhang et al. 2015a).

Table 4-6. Overview of studies on tree canopy N uptake (CNU) cited in Chapters 3 and 4, showing key site and method details and CNU results. NA = not available.

| Site name/location | Tree species | Mean annual $N_{dep}$ (kg $ha^{-1}$ $y^{-1}$) | Mean annual precipitation (mm $y^{-1}$) | Mean annual air temperature (°C) | Methodology | $N_{dep}$ applied (kg $ha^{-1}$ $y^{-1}$) | $NO_3$-N canopy uptake (%) | $NH_4$-N canopy uptake (%) | Reference |
|---|---|---|---|---|---|---|---|---|---|
| Griffin Forest, Scotland UK | Sitka spruce | 7.1 | 1218 | 7.8 | 5-year monitoring 2012-2016 | Natural abundance | 76% | 63% | This thesis |
| Griffin Forest, Scotland UK | Sitka spruce | -- | -- | -- | Canopy application in growing season and dormant season | 9.2 + $^{15}N$ | 88% (summer)<br>23% (winter) | 84% (summer)<br>64% (winter) | This thesis |
| Deepskye, Scotland UK | Sitka spruce (16 y) | NA | NA | NA | Canopy mist treatments in growing season 1996-2000 | 44.8 | 34% | 31% | Chiwa et al. 2004 |
| Novaggio Forest, Switzerland | Beech and Norway spruce | 19-37 | 1281 | NA | Method missing | Natural abundance | 20-25% | 20-25% (75% of the total CNU) | Wortman et al. 2012 |

| | | | | | | | | | |
|---|---|---|---|---|---|---|---|---|---|
| Howland Integrated Forest Study, Maine USA | Red spruce and balsam fir | <5 | NA | NA | Above canopy wet application | 18 | 29% | 61% | Gaige et. al. 2007 |
| Lac Laflamme (L); Tirasse, Quebec Canada (T) | Balsam fir (L); Black spruce (T) | 1.3-1.4 | 1170; 860 | 0.6; 1.1 | 13-year monitoring | Natural abundance | 45-54% | 60-67% | Houle et al. 2014 |
| Olympic, Mount Rainier, and North Cascades National Parks, Washington State USA | Western hemlock, Douglas fir | 1.2-2.2 | 2321-3148 | NA | 2–year-monitoring | Natural abundance | 87-93% | Increased by 60-117% at 2 sites, -16% at 3rd site | Fenn et al 2013 |
| Deepskye, Scotland UK | Scots Pine | 8-10 | 334 (May-August, period | NA | 1-year gaseous (g) and wet treatment (w) | 21.5 (g); 7.3 (w) | Total IN 20%. +24% ON found in TF+SF | | Cape et al. 2010 |
| Washington, USA | Douglas fir (~25 y) | ~6 | 1900-2200 | 8.7 | 3-year monitoring | Natural abundance | <80% (winter) 40-50%* (summer) | 0 (winter) ~95% (summer) | Klopatek et al. 2006 |

| | | | | | | | | |
|---|---|---|---|---|---|---|---|---|
| 27 forests in Germany | Beech, Norwegian spruce; oak spp. | 10.1-11.8 | 500-1000 | 6-8.5 | N budget | Natural abundance | Total IN: Up to 45% in spruce forests; up to 67% in beech forests | Schwartz et al. 2013 |

*Atmospheric $NO_3^-$ decreased to ~ 0% of the input in the first 5 m from the top of the tree, then increased to about 60% of the atmospheric input in the following 20 m and decreased again in the last 5 m from the forest soil, suggesting an internal source of N within the canopy

Klopatek et al. (2006) followed IN retention through a 25-year-old stand of Douglas fir for 3 years, measuring the CNU at 5-m height intervals from the top of the trees. The CNU was positive throughout the year but with significant seasonal differences between the two N forms. In summer the CNU of $NH_4$-N increased initially at 0-5 m from the top of the trees, indicating a source or generation of $NH_4$-N in the forest canopy, and then decreased to reach almost 100% uptake by the forest floor. $NO_3$-N CNU followed a different trend: uptake of $NO_3$-N was greatest in the upper canopy, and then decreased more gradually to almost 50% towards the forest floor. These results can be explained by a significantly higher rate of nitrification in the upper canopy.

Fenn et al. (2013) found that in three coniferous forests on the northern US Pacific coast subjected to a low $N_{dep}$, 90% of $NO_3$-N from wet deposition was retained by the canopy. A possible explanation of the different CNU results at Griffin Forest compared to those reported by Fenn et al. (2013) could be the different annual precipitation amounts, which in Fenn et al. was almost double and in Klopatek et al. (2006) was about 50% higher than the mean annual precipitation in Griffin. Frequent and large rainfall events can dilute the [N] in wet deposition and may have reduced the time in which IN stayed on the canopy in these studies, compared to at Griffin Forest. The clear difference in the trend in $NO_3^-$ reported by Klopatek et al. (2006) could be due to a higher nitrification rate converting some of the $NH_4^+$ into $NO_3^-$. This effect would be more significant during higher temperatures in summer than in winter. Assuming that nitrification occurs also in the canopy at Griffin Forest, although at lower rates, this would explain the lower $NO_3$-N recovery found in summer using the $^{15}N$ approach compared to the N mass balance alone.

The mean summer N retention values for the experiment show similar figures to those shown in Chapter 3. The CNU was slightly higher than the value for total N calculated for the 2016 growing season (76%, Table 3-3) and higher than the mean retention measured in the period 2012-2016 (70%). Comparing the results with the “seasonal” N retention, the cumulative $NH_4$-N and $NO_3$-N recovered on 10 and 12 August 2016 were similar to the mean retention measured in May-September 2016 ($NH_4$-N = 78±23%, $NO_3$-N = 74±23%) although the mean values showed the opposite trend, with $NO_3$-N being the form better retained in this experiment. However, the propagated standard errors of the mean retention of total N and the different N forms for the growing season as shown in Chapter 3 - Table 3-3 (20%) greatly exceed the

difference so it is not possible to confirm whether the seasonal data measured at two different spatial scales show exactly the same trend.

Similar to the summer application in the present experiment, less than 30% of the applied N (20% after correction for N dripping from the canopy during the application) was recovered under the trees after N application during the growing season to a red spruce and hemlock forest under very low total deposition conditions (~3-4 kg $y^{-1}$ $ha^{-1}$) (Gaige et al. 2007). Separate applications of $^{15}NH_4^+$ and $^{15}NO_3^-$ in the same experiment showed that more $NO_3^-$ than $NH_4^+$ was recovered under the canopy in contrast to the long-term monitoring in Griffin which showed that $NO_3^-$ retention was generally similar to or higher than $NH_4^+$, particularly during the dormant seasons in 2015 and 2016. However, the results in Chapter 3 also indicated a decreasing trend in $NO_3$-$N_{dep}$ over time and a seasonality of $NO_3$-$N_{dep}$ with summer peaks, together with a seasonality in retention of $^{15}NO_3$-N, with higher retention in summer. These trends suggest an increased demand of $NO_3$-N by the canopy in summer that could be compensated by a relative increase of retention of the reduced form. The high $^{15}NO_3$ retention measured in summer contrasts with the lower retention following the winter $^{15}N$ labelled application.

In the summer application, N retention by the canopy was higher when estimated using the stable isotope approach relative to the N concentration approach. This might be attributed to the preparation of the TF and SF samples for $\delta^{15}N$ analysis using the ammonia diffusion technique (as explained in section 4.2.1.3).

Although lower than in summer, canopy retention of $NH_4$-N following the winter application was 1.6 to 2.7 times greater than for $NO_3$-N. This result is opposite to the findings of Fenn et al. (2013) who reported from studies deploying ion exchange resins above and below the canopy of north-west Pacific USA forests that most of the $NO_3$-N (80-90%) was retained during the winter months whilst $NH_4$-N flux increased after passage through the canopy. In winter $NO_3$-N retention estimated using the stable isotope approach (23.3±10.5%) was lower than the $NO_3$-N retention estimated by N mass. The result is also opposite to that reported in winter by Klopatek et al. (2006) in winter. As already noted earlier, in their study $NO_3$-N decreased to almost 0% of the input with most of the CNU happening in the upper 5 m of the tree crown. In contrast, $NH_4$-N mass flux increased in the first 5 m of the canopy and then decreased to about 45% of the input by the forest floor, a similar value to that reported

in the present study. The differences could be explained by a lower canopy nitrification rate occurring in Griffin Forest than in the Klopatek et al. (2006) study in both seasons.

The amount of N and $^{15}N$ used in the application experiments at Griffin Forest was such that no significant effects of $^{15}N$ enrichment are expected from other sources in the time period considered for the recovery calculations. In summer, a difference of 9.4% between TF+SF $NO_3$-N and $^{15}NO_3$-N means was measured which exceeded the SE (see Table 4-5). These results are consistent within the samples. Minor differences among samples were expected due to errors coming from the scaling due to the approximation of each canopy projection to the ground, to the possible uneven application of the mist from the platform, and the effect of the interaction of the targeted tree canopy with the branches of the surrounding trees.

In winter, the canopy nitrification rate is expected to be lower than in summer. The apparent differences in winter between mean CNU of $NO_3$-N assessed by the N concentration and $^{15}NO_3$ recovery approaches (see Table 4-5) may be explained solely by the SEs of both the mean figures which exceed the difference in the means. This is also supported by the nearly identical mean values for the CNU of $NH_4$-N in winter assessed by the N concentration and $^{15}NH_4$ approaches, of 64% of the applied N.

After the winter application only about 39% and 23% of $NO_3$-N and $^{15}NO_3$-N respectively were retained by the Griffin Forest canopy. Such low retention is markedly lower than the results of the studies mentioned earlier in this section. However, winter precipitation at Griffin Forest is much lower than at the sites studied by in Fenn et al. (2013) and Klopatek et al. (2006) and this could have a significant effect on CNU through the dilution of IN concentration in bulk deposition (Hambuukers and Remakle 1993). The low retention of $NO_3$-N in the canopy application experiment is also markedly lower than the mean winter retention estimated from the 5-year monitoring programme at Griffin Forest (61%). The difference cannot be explained satisfactorily by biological activity occurring in the TF and SF collectors in the long-term monitoring due to the greater time between collections in the canopy application experiment and either leading to N loss through nitrification or transformation of IN to ON (although this was not measured). Indeed, if such biological activity had occurred, it would have caused lower apparent CNU in summer, when biological activity is expected to be higher and such a difference would be more easily detected.

In both seasons the measured CNU in Klopatek et al. (2006) was negative in the first 5 m below the top of the canopy, which could indicate "hidden" $NH_4$-N possibly from dry deposition washed down by the wet deposition. Accepting this explanation, the Klopatek et al. (2006) results for $NH_4$-N CNU would be very similar to those in this experiment. Similarly, the long period without precipitation at Griffin Forest in March 2017 (mentioned in section 4.2.2) could have led to substantial accumulation of dry deposited N on the canopy, which might account for some of the difference between the mean CNU estimated with the $^{15}N$ approach (23%) compared with the total N approach (38%).

Variations in relative abundance of $NO_3^-$ in N deposition have been associated with different retention patterns for different N forms (Houle et al. 2015). In their 13-year monitoring study of N canopy uptake in Canadian boreal forest, the reduced N form was taken up preferentially in the areas where N deposition was higher. This is consistent with the retention rates after the winter application experiment, as seasonal natural $N_{dep}$ was about 2.7 kg N $ha^{-1}$ $y^{-1}$, a relatively high amount for winter at Griffin Forest and very close to summer values. In addition, reduction of CNU in winter compared to summer was less for $NH_4^+$ than for $NO_3^-$ due to a different response to the increased $N_{dep}$ induced by the experimental application. The mean total CNU recorded in Griffin Forest on March 2017 (water sample data were collected and analysed until March 2017 but are not shown in Chapter 3 where only full years were presented) was 88%, of which 92% for $NH_4$-N (total $NH_4$-N input = 0.47 kg N $ha^{-1}$ $y^{-1}$) and 76% for $NO_3$-N (total $NO_3$-N input = 0.15 kg N $ha^{-1}$ $y^{-1}$). This suggests that the trend at the plot level in Griffin follows the same trend as the present experiment but contrasts with that described in other experiments, where in winter $NO_3$-N was better retained than $NH_4$-N. The excess of N as result of the application has apparently exceeded the system capacity to either retain or transform the extra N input and this is particularly evident for $NO_3^-$ for which relative CNU was lower even with a much lower natural input than the reduced N.

The lower canopy retention of $NO_3$-N in winter compared to $NH_4$-N found in this experiment could also be due to changes in total N input (Avila et al. 2017). The natural $N_{dep}$ in 2016 was the lowest measured in the 5-year monitoring period, especially in the colder months, whilst the application experiment used deposition equivalent to the highest level measured in Griffin. Higher $N_{dep}$ generally resulted in higher % canopy N retention during the long-term monitoring (see Table 3-3). A wide

range of CNU values have been reported for low N deposition sites, ranging from 45-54% (Houle et al. 2015) to values above 90% (as those mentioned above).

Barnes et al. (2008) showed that even in high N deposition sites, forests are not N saturated and retain or reprocess the vast majority of $NO_3^-$ delivered from the atmosphere. This transformation can happen at least partly in the phyllosphere, as demonstrated in red spruce under high atmospheric N input (Papen et al. 2002) or in the apoplastic space inside the needle under similar N input rates (Teuber et al. 2007). Furthermore, the identification of ammonia monooxygenase (amoA) genes in throughfall samples collected under the canopy of Japanese cedar (Watanabe et al. 2016) has been interpreted as indicating that microbial nitrification in incubated TF samples could occur due to microbes washed off the tree canopy by precipitation. Zhang et al. (2015a) reported archeal and bacterial amoA on leaf surfaces suggesting that, based on the estimated amount of bacteria per leaf surface, about one third of the N application over the canopy which is not found in TF could be retained and undergo nitrification in the canopy. This is a very recent field of study with a limited number of studies. These mechanisms could explain the high missing N which could be retained at the canopy level even if not entirely taken up by needles via stomata.

Amongst studies in which N was applied to the forest canopy, Chiwa et al. (2004) applied 6 different simulated mist treatments to a 14-year old Sitka spruce plantation in southern Scotland. The treatments were combinations of ammonium nitrate and sulphate, including ammonium nitrate and sulphate only and 2 controls. The total N applied was ~50 kg $ha^{-1}$ $y^{-1}$ in the high-N treatments, with 30-35% of the applied N retained by the canopy. The cations measured in TF showed an increase of $K^+$, $Mg^{2+}$, $Ca^{2+}$ and $Na^+$ alongside a loss of $H^+$ and this was attributed to a weak organic acid anion exchange mechanism.

One of the assumptions made in the design of this study is that following the fate of IN from the atmosphere to the forest floor would account for most of the N in the fluxes above and below the canopy, as ON represents a negligible fraction of the total N. As a consequence, this study did not take organic N into account. Cape et al. (2010) reported that up to the 10% of the additional DIN supplied to a Sitka spruce canopy located in southern Scotland was found in TF as organic N. As DON was not measured in this study, similar amounts of N in the fluxes through the canopy can be assumed. In addition, evidence of biological nitrification in the canopy on conifer trees

in Scotland has been reported by Guerrieri et al. (2015), although the presence of bacterial activity alone is not sufficient to determine whether a transformation from DIN to DON occurs.

Indeed, in a study of throughfall and bulk deposition where high atmospheric organic N inputs (34% to 72% of the total N deposition) were reflected in DON dominating TF at two of the experimental sites in a study in central-northern Spain on evergreen holm oak forests (Izquieta-Rojano et al. 2016). Due to the differences between this study and at Griffin Forest, particularly in terms of N inputs, temperature and precipitation, however, it is unlikely that organic N represents similar proportions of the total N in TF and SF in Griffin Forest. Nevertheless, it is worth considering organic N when calculating a potential N balance and this could represent an area of further research.

Gaseous N losses were not measured during the N application experiments at Griffin Forest but they could represent part of the DIN not recovered under the canopy. For example, Dail et al. (2009) estimated that gaseous loss accounted for 5-10% of the applied $^{15}N$ in growing season applications. Measurements from Hill et al. (2005) showed that much of the dry deposited N was lost and some of it was likely revolatilised.

The simulated $^{15}N$-labelled $N_{dep}$ double application successfully showed that the targeted trees were able to uptake higher amounts of N at the same CNU rates or higher than the 5-year monitoring during the summer season. The differences in $NO_3$-N and $^{15}NO_3$-N retention in summer may be explained by canopy nitrification, although this process was not quantified. In contrast, in winter CNU rates in the labelled N application experiment were lower than in the 5-year monitoring programme, and differed between N forms, with much lower CNU for $NO_3$-N compared to $NH_4$-N.

## 4.3 Experiment 2 - $^{15}N$ recovery in tree leaves and twigs

### 4.3.1 Introduction

The previous experiment confirmed the high canopy N retention measured in the 5-year monitoring study at Griffin Forest, reported from other studies and also highlighted differences in N retention between seasons and between oxidised and reduced N forms. However, the mechanisms of N canopy uptake require clarification since the overall canopy N uptake figure is much higher than the reactive N retention by leaves that has been reported in other studies to be negligible (Adriaenssens et al. 2011) or accounting for <15% of the $N_{dep}$. For example, 5% of $NH_4$ and 1% of $^{15}N$ applied directly to red spruce branches was assimilated (Boyce et al. 1996), whilst 7-14% of N uptake by saplings was measured at two different sites (low elevation deciduous species and high elevation conifers) with no differentiation in absorption rates between the oxidised and reduced N forms (Garten et al. 1998).

The highest figures of N retention in a $^{15}N$ labelled experiment were measured by Nair et al. (2016). In their experiment six treatments including controls were applied monthly to 3-year old Sitka spruce saplings during a 1-year experiment conducted at Forest Research near Edinburgh which aimed to estimate how much CNU enhanced carbon sequestration. The treatments included a combination of $^{15}N/N$ labelled wet deposition and $^{15}N$ labelled litter. In particular, the highest CNU measured in the experiment occurred in the saplings treated with simulated $N_{dep}$, where ~60% (of which ~20% in needles and ~24% in branches) of $^{15}N$ applied directly to branches on a monthly basis was retained aboveground. This result is quite unique in the literature as it accounts for the highest recovery of $N_{dep}$ and the application is the only one known to Sitka spruce. Experiment 2 in this chapter aims to emulate the experiments by Nair et al. because those experiments also reported high rates of CNU and therefore might be most relevant for explaining the high CNU values reported in this thesis. The difference in tree age between that experiment and the present study has been acknowledged in the design of the experiment at Griffin Forest. In order to be representative of mature trees, branch heights was added as a factor potentially affecting the interaction between vegetation and $N_{dep}$, since differences in available light and direct precipitation (precipitation mediated by the upper branches) could affect the potential uptake of branches at different heights. Such differences would not be expected in ~1 m tall saplings located at a distance from each other to avoid

interaction among treatments. Nevertheless, some aspects of the experimental design, such as examining whether differences in N uptake exist between new and old twigs and needles, have been kept as similar phenological differences are expected.

Branch treatments were also used by Wortman et al. (2012) who applied $NH_4^+$ and $NO_3^-$ ions at concentrations double their mean concentrations in site precipitation to leaves of beech and oak or to 2- and 3 year old spruce shoots at two high N deposition sites (33 kg $ha^{-1}$ $y^{-1}$ total $N_{dep}$ in the period 1997-2007). Although the focus of the research was investigating the effects of high N application on photosynthetic efficiency it provided an estimation of CNU; about 20-25% of the total $N_{dep}$ was taken up by the canopy, over 75% of which resulted from $NH_4^+$ exchange.

In interpreting the results of the first experiment in the current chapter, similarly to Chapter 3 and to Sievering et al. (2007) it was assumed that all the $N_{dep}$ measured over the canopy that is not found under the canopy is potentially retained by using a double approach (N mass and $^{15}N$ recovery). This second experiment focuses on direct N uptake by needles and twigs, which is one of the potential mechanisms to explain the CNU figures calculated in the long-term study and in the experiment described earlier in this chapter. In Section 4.2.3, other CNU mechanisms were described – e.g. uptake by microorganisms in the canopy, transformation of IN to ON, gaseous N emission (this last process will be assessed only for the loss from soil, see Discussion in Chapter 5 for more details) and revolatilisation (Hill et al. 2005). This second experiment aims to close the figures of the N fluxes to the forest floor by giving a minimum figure of the percentage of IN deposition that is effectively taken up by the canopy by using a methodology similar to that described in Adriaenssens et al. (2012), Wortman et al. (2012) and Nair (2016). The hypothesis is that up to the 60% of the applied $^{15}N$ will be found in the treated twigs and needles.

The novelty of this work is that no other known studies have used all of these approaches together to investigate CNU and explain its fate in the same case study area. The results will also help compare CNU figures obtained through different methodological approaches.

### 4.3.2 Methods

#### 4.3.2.1 Field and laboratory methods

Pure (98%) double-labelled $^{15}NH_4{}^{15}NO_3$ solution was applied to branches in situ at Griffin Forest, following the procedure of Nair et al. (2015) who applied this solution to 3 year-old Sitka spruce saplings in a quantity (54 g N $ha^{-1}$ $y^{-1}$) small enough not to increase significantly the total amount of natural $N_{dep}$.

Ten branches were selected from two different trees, 5 on each tree, in the T plot for the labelled N solution application from the eddy covariance tower on two occasions in May 2017. One of the selected trees was also part of the previous $^{15}N$-labelled simulated $N_{dep}$ experiment (tree T1, see Figure 4-1). The branches selected were easily reachable from the tower, to minimise losses of solution during application, and were distributed across three different heights in the crown, from about 17 to 20 m height, corresponding to the upper three levels of the tower.

For each branch 2 sub-branches were selected, one for the application and one as a control, being at least 3 years old to be comparable with previous studies (Nair et al. 2015). The controls were used to determine N % and $\delta^{15}N$ before the treatment and did not undergo any special treatment except for the girdling of five of them as explained next. In order to determine whether any $^{15}N$ is transferred to other compartments of the tree in the 24 hours from application to the removal of the branches, 5 treated branches and 5 controls were girdled to stop the transport of metabolic products through the phloem (Zhang et al. 2015b). In this experiment girdling was conducted 2 hours after the first application on 6 May 2017, as practised in other studies (e.g. Högberg et al. (2001)). A strip of phloem about 1 cm wide was removed from the base of the branch by making two incisions approximately 1 mm deep with the use of pruning shears.

In the previous $^{15}N$-labelled simulated $N_{dep}$ experiment the total amount of $^{15}NH_4{}^{15}NO_3$ applied (23.6-26.5 mg N $ha^{-1}$ $y^{-1}$) was chosen so that the isotopic label could be traced in TF and SF with relatively low [N]. The N pool in trees is several orders of magnitude higher than N inputs from the atmosphere, especially in the branches and needles (Sicard et al. 2006), ranging from 0.5 to slightly over 1% of the total dry mass (Nair et al. 2014) and thus such a small N addition would be very difficult to trace due to dilution and fractionation in different tree compartments. Hence calculations of the

amount of labelled N to use in the branch tracer experiments considered the potential dilution in the needle and branch pools and assumed that only a fraction of label is retained.

Branch lengths were roughly measured in the field to estimate the amount of $^{15}NH_4{}^{15}NO_3$ solution to apply in proportion to the surface area of the branches and twigs. The branch surface area was estimated using a simple model based on the maximum length and width of each branch to calculate the surface of a kite-shaped geometric figure. The total amount of $^{15}N$ used in this experiment was calculated by scaling a $N_{dep}$ mass of 48 g $ha^{-1}$ (9.73 mg applied on an estimated total branch surface area of 2.03 $m^2$), keeping similar figures to those used in the $^{15}N$ application experiment reported by Nair et al. (2016), where a concentration of 54 g $^{15}N$ $ha^{-1}$ $y^{-1}$ was used to assess the $^{15}N$ recovery on Sitka spruce saplings after one year of treatment.

The $^{15}N$ solution was applied by brush in two batches of 500 mL each, one before and one after girdling, in order to identify any potential translocation of $^{15}N$. The first application was carried out on 6 May 2017 at 15:00, and the second at 9:00 am on 7 May 2017, on both occasions in dry, still and sunny conditions. Indeed, late spring 2017 was extraordinarily dry at the study sites, with only 1.15 mm $d^{-1}$ precipitation measured in Griffin in the 2 months prior to the application. In order to create closer conditions to those normally found in situ, after the first application of labelled solution to the branches on the morning of 6 May, the surface of the branches was wetted again on two occasions during the afternoon using DIW.

All branches were removed in the late afternoon of 7 May 2017 with a lopper, wrapped in separate plastic bags and returned to the laboratories in Edinburgh. Similar to Nair et al. (2016), the new twigs and needles (<2 years) were separated from the old twigs and needles (2 or 3 years old) due to the usually higher N content in the young shoots and needles. Therefore N uptake in this experiment was assessed in four "compartments": new twigs, old twigs, new needles, and old needles. A more accurate total length of each branch was measured in the laboratory by measuring all of the twigs that received the $^{15}N$ application and using them to calculate the mean $^{15}N$ applied by length. This was then used to calculate the recovery by component and by age. All of the sampled twigs were then washed and rinsed 3 times with DIW the day after collection in the field, then dried to constant weight in an oven at 70°C. The dry

mass per cm of needles and twigs of each branch and age class (new/old needles and twigs) was calculated. The dried samples were ground to a fine powder in a Retsch MM-200 ball mill. A subsample of this powder (80 samples in total) was sent to the NERC LSMSF (Lancaster, UK) for $\delta^{15}N$ analysis using an elemental analysis isotope radio mass spectrometer (EA-IRMS) as described previously in section 4.2.1.3.

Figure 4-7. Schematic illustrating where the girdling was applied in 50% of the selected branches in the branch experiment. The same rationale was applied to the ungirdled branches.

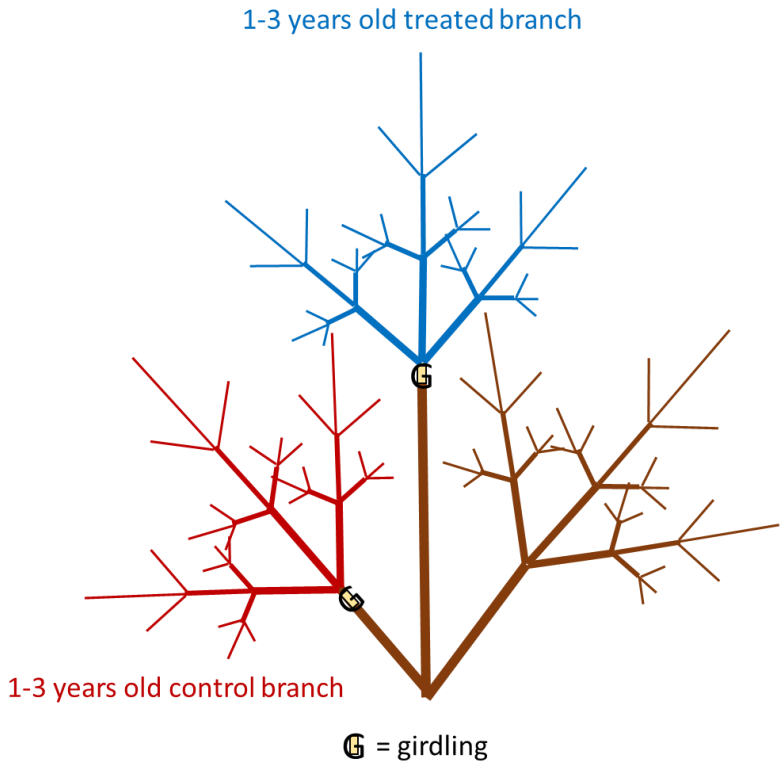


### 4.3.2.2 From $\delta^{15}N$ to $^{15}N$ recovery: calculations, scaling and data analysis

The IRMS results for each branch/twig sample, expressed as $\delta^{15}N$ (‰) were converted to atom percent (atom%) as follows:

$$atom\% = \frac{100 \times \mathrm{RA} \times (\delta^{15}\mathrm{N}/1000 + 1)}{1 + \mathrm{RA} \times (\delta^{15}\mathrm{N}/1000 + 1)} \qquad \text{(Eq. 4-5)}$$

where RA is the absolute ratio of $^{15}N/^{14}N$ in the air, and the international standard value of 0.0036782 (Mariotti, 1983) was used.

Then $^{15}N$ atom excess was calculated as:

$$atom\%_{excess} = atom\%_{labelled} - atom\%_{unlabelled} \quad \text{(Eq. 4-6)}$$

Where $atom\%_{unlabelled}$ is the $\delta^{15}N$ measured in the control twigs and needles of each branch. The N concentration [N] (%) was converted to N content $cm^{-1}$ in each compartment and then the $^{15}N$ excess in each compartment was calculated as:

$$^{15}N_{excess\ content}\ (mg\ cm^{-1}) = \frac{N_{content} \times\ ^{15}N_{excess}}{100} \quad \text{(Eq. 4-7)}$$

These values were divided by the applied $^{15}N\ cm^{-1}$ to calculate the % of $^{15}N$ recovered in each compartment and weighted by the relative length of the compartment to the whole branch length to calculate the total recovery per branch.

### 4.3.3 Results and discussion

The measured N concentrations were low in all compartments in both the treated and control branches (Figure 4-8). Data were not normally distributed even after square root, cubic root, log and Tukey transformation, so the Mann–Whitney U nonparametric test was used to test differences between groups. Needles of different ages did not show notable differences in N% ($p = 0.903$), whilst the difference was significant between new and old (2-3 years) twigs ($p < 0.0001$). No significant differences were found between controls and treated branches ($p = 0.39$). The % N in needles is slightly lower than the range (1.5-2%, with some higher values) reported by Gentilesca et al. (2013) for Sitka spruce plantations of similar age at other sites in Northern and Central Highlands. This could be due to the timing of the sampling of this study in spring, when conifers accumulate N in the younger needles to mobilise later for new shoot growth (Wyka et al. 2016), in contrast to Gentilesca et al. (2013) where sampling was conducted later in summer. At the time of the experiment the new buds were bursting and this could mean that much of the N cumulated in the younger needles was mobilised and partially found in the new twigs, on its way to the buds. Alternatively, it may be an indicator of N deficiency in the sampled trees.

Figure 4-8. Boxplots of % N in twigs and needles by age (n = 10). The red boxes represent the treated branches and the black boxes the controls. The horizontal line inside each box represents the median and the lower and upper hinges correspond to the first and third quartiles. The upper and lower whiskers depict the largest and smallest values respectively within 1.5 * the interquartile range (IQR). Dots represent outliers.

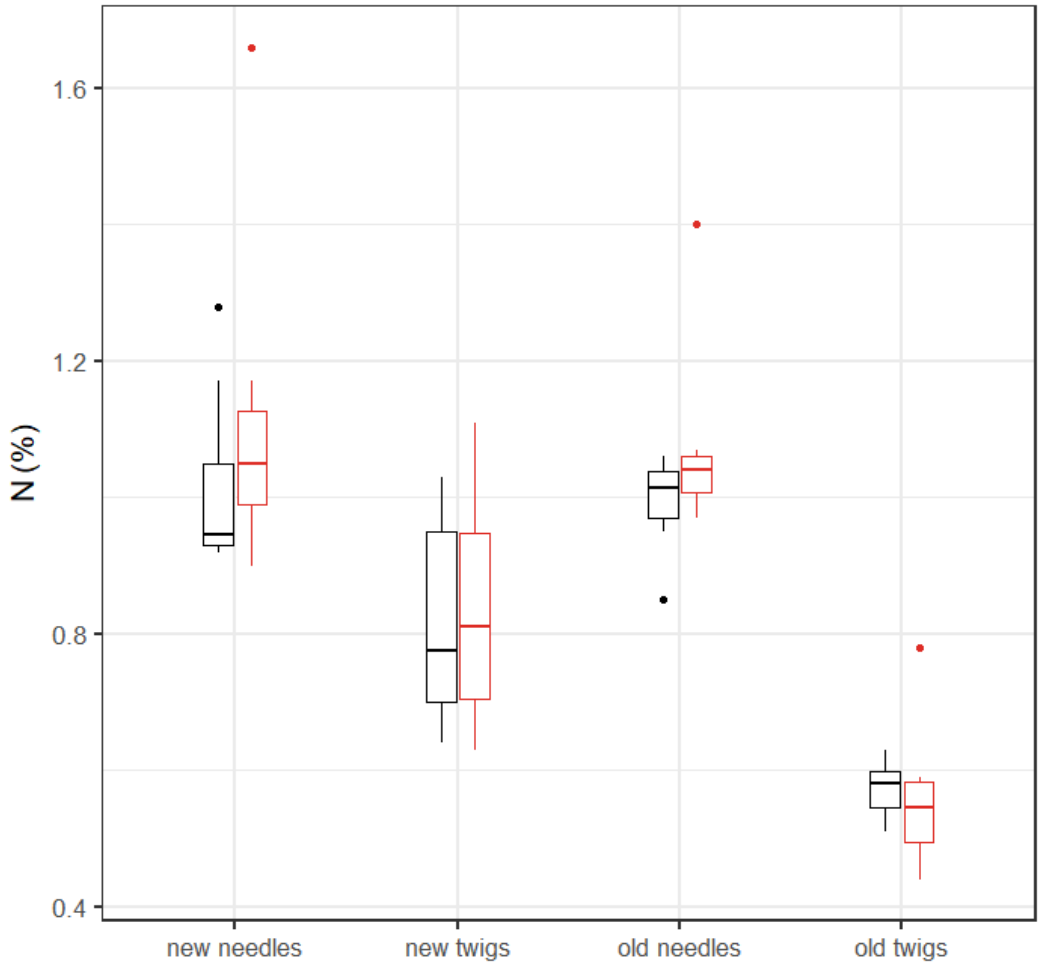


The IRMS results show clear $^{15}N$ enrichment of both twigs and needles in the treated compartments compared to the controls (Figure 4-9), particularly for the twigs. Similarly to the N% values, the Mann–Whitney U nonparametric test was used to test differences in $\delta^{15}N$ between treated branches and controls (p-value <0.001). Among the treated samples, $\delta^{15}N$ differs significantly also between needles and twigs (p-value<0.001) and between old and new twigs (p-value <0.001). Old and new needles did not show significant differences (p-value = 0.93). This confirms the hypothesis that at least some of the applied N has been retained by the canopy.

Figure 4-9. Boxplots of $\delta^{15}N$ by tree component and age of 10 replicates. The red boxes represent the treated branches and the black boxes represent the controls. The horizontal line inside each box represents the median and the lower and upper hinges correspond to the first and third quartiles. The upper and lower whiskers depict the largest and smallest values respectively within 1.5 * the interquartile range (IQR). Dots represent outliers.

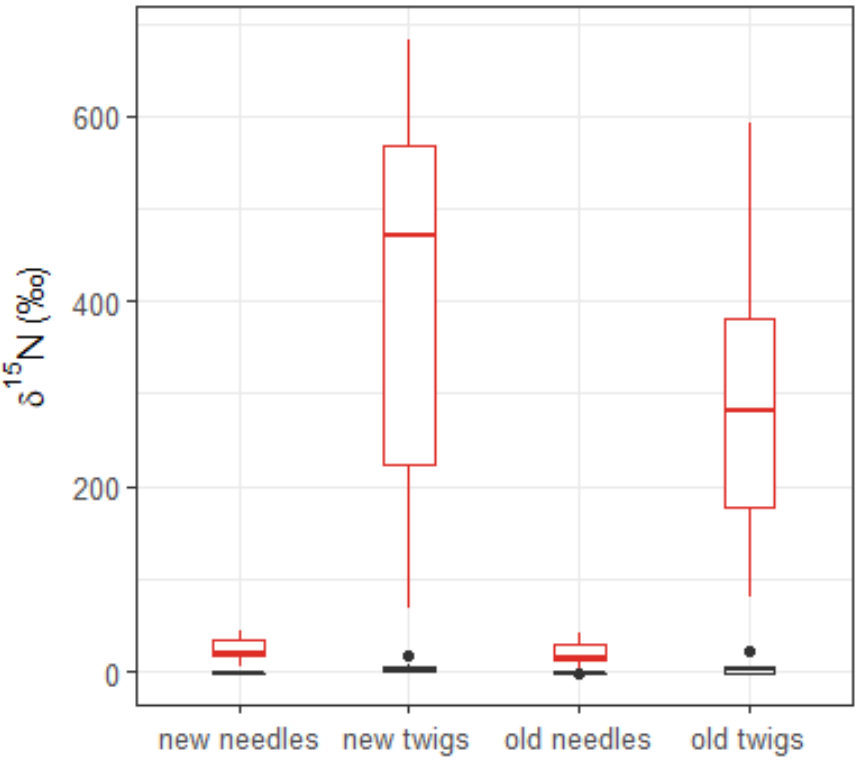


Figure 4-10 shows the same $\delta^{15}N$ results for treated branches only separated into girdled and non-girdled branches. The data suggest higher $\delta^{15}N$ values in the girdled branches compared to the non-girdled branches. The Mann-Whitney U nonparametric test was used to test any significant differences in $\delta^{15}N$ between girdled and non-girdled samples, as the data were not normally distributed even after square root, cubic root, logarithmic and Tukey transformation. Tests were conducted on all girded/non girdled samples (p-value = 0.62) and separately on new needles (p-value = 0.691), old needles (p-value = 0.548), new twigs (p-value = 0.548 and old twigs (p-value = 0.222). In none of the sub-groups did girdling show a significant effect on the $\delta^{15}N$ value.

Figure 4-10. Boxplots of $\delta^{15}N$ by tree component and girdling for the treated branches only (n=5). The orange boxes represent the girdled treated branches and the black boxes represent the non-girdled treated branches. The horizontal line inside each box represents the median and the lower and upper hinges correspond to the first and third quartiles. The upper and lower whiskers depict the largest and smallest values respectively within 1.5 * the interquartile range (IQR). Dots represent outliers.

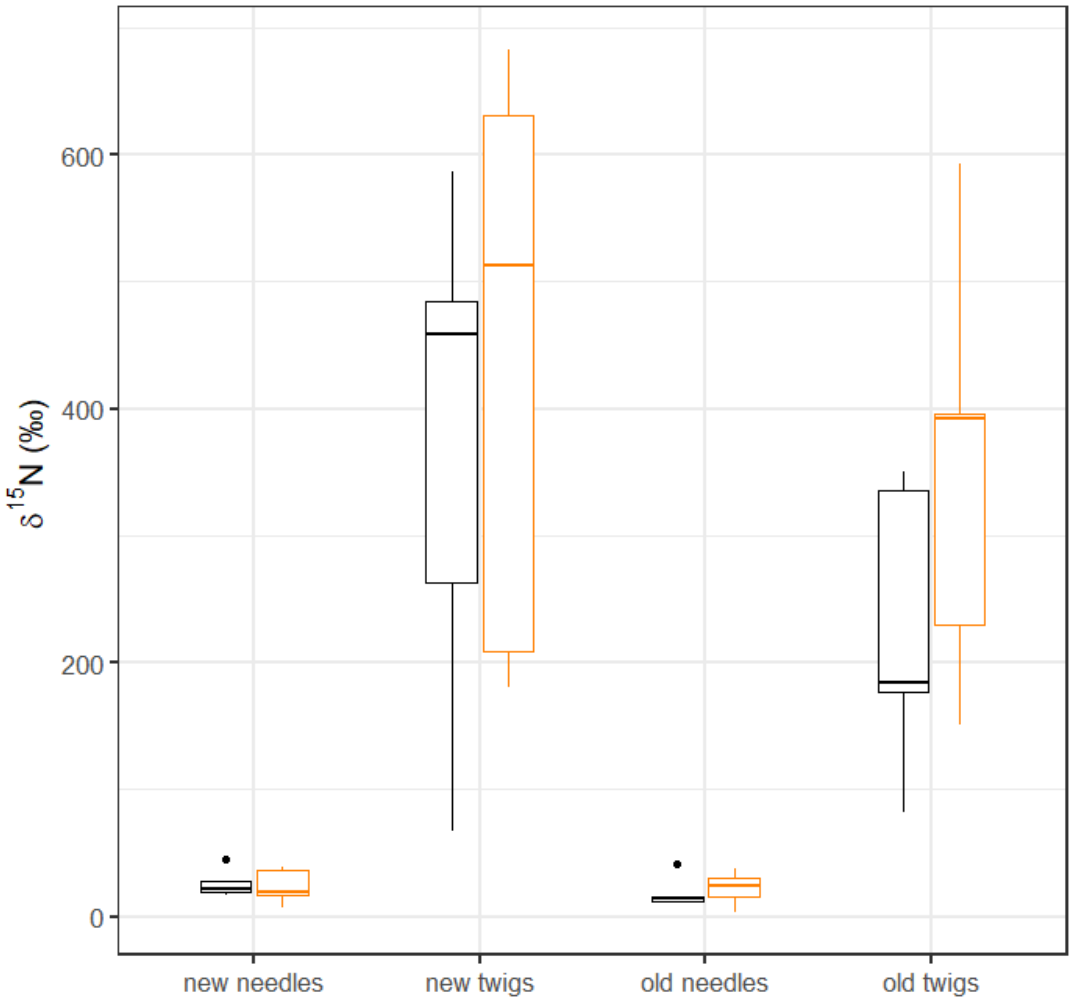


Most of the recovered $^{15}N$ was found in the twigs (Table 4-7), further supporting the big differences in $\delta^{15}N$ between compartments as shown in Figure 4-5. This confirms at least partial allocation of applied $^{15}N$ to plant tissues and suggests that part of the N could be retained in or on bark, as shown in Dail et al. (2009). These uptake figures are likely an under-estimate of branch uptake since the application of the labelled N solution in the experiment did not allow interaction of throughfall with multiple branches which, according to Boyce et al. (1996) could lead to assimilation rates up to 3-6 times larger.

In the analysis of the results, 5 variables were tested for significance in the $^{15}N$ recovery: the compartment type (needles and twigs) and the compartment age (old and new), the tree (two trees, one of which was previously targeted for the $^{15}N$-$N_{dep}$ simulation), branch height on the tree (branches were selected at 3 different levels on the tower) and girdling. ANOVA tests showed that only the variable "compartment", i.e. new and old twigs and needles, had a p value < 0.05 for significant enrichment. The Akaike information criterion (AIC), used to assess which linear model best explained the labelled N recovery, showed that compartment alone was a better explanatory model (AIC = 217.2) than more complex linear models in which combinations of the other variables were added.

Table 4-7. $^{15}N$ recovered per compartment type and age and for the total branch. Values are expressed as mean percentage of the $^{15}N$ applied ± SE (n=10). Column 3 and 4 show mean recovery in girdled and non-girdled branches ± SE (n=5). In the last column Nair et al. (2016) results are shown as a comparison. Their partial total recovery does not show SE as it was not available in the paper.

| Compartment | $^{15}N$ recovered (%) | $^{15}N$ rec. in girdled branches(%) | $^{15}N$ rec. in non-girdled branches(%) | Nair et al. (2016) |
|---|---|---|---|---|
| **New needles** | 1.6 ± 0.1 | 1.4 ± 0.2 | 1.8 ± 0.2 | 7.2 ± 0.4 |
| **New twigs** | 5.7 ± 1.0 | 5.3 ± 0.9 | 6.1 ± 1.8 | 20.8 ± 2.9 |
| **Old needles** | 1.8 ± 0.3 | 1.9 ± 0.5 | 1.7 ± 0.3 | 13. 4 ± 2.4 |
| **Old twigs** | 5.3 ± 0.7 | 5.8 ± 1.4 | 4.7 ± 0.7 | 3.12 ± 0.1 |
| **Total recovery per branch** | 14.4 ± 1.5 | 14.4 ± 2.6 | 14.4 ± 1.8 | *44.5* |

The same test showed no significant difference in $^{15}N$ content in the treated branches between girdled and non-girdled branches. This is also evident from the recovery values shown in Table 4-7 where girdled and non-girdled branches have the same mean total recovery; girdled branches show a lower mean recovery in new twigs and needles and a higher mean recovery in old twigs than non-girdled branches. This suggests that no transfer of N occurred to other tree compartments within 24 hours from the first application before girdling. The second application was made the following day in the morning, about 16 hours after the girdling was completed, and 8 hours before the branch collection. In Nair et al. (2016) higher figures of recovery are found in woody sections (including 15.6% in stem not reported in Table 4-7). Their experiment included 13 applications along one year; assuming that the two

experiments involve similar retention mechanisms this suggests that the reallocation to other compartments of the tree happens over a longer time.

Although it was expected that the Nair et al. (2016) results may represent a maximum value CNU for Sitka spruce, the total uptake measured is Experiment 2 is lower than expected, especially considering the relatively high retention measured at a plot scale in March-April 2017 (>80%). The experimental results could have been affected by the particularly dry conditions before the application experiment which might influence the N uptake due to reduced biological activity of the trees. Mean daily rainfall measured at Griffin Forest between 13 March and 7 May 2017 (date of the branches collection) was 1.15 mm, whilst the two application days were warm and dry. Soil drought reduces leaf specific conductivity (Sterck et al. 2008) and foliage reduces transpiration up to 75% as soil water potential decreases from saturation to -0.5 MPa (Magnani et al. 2002).

A further reason why dry conditions might affect the results is their effect on foliar nutrient uptake mechanisms. Foliar uptake of water has been demonstrated for at least 124 species of plants worldwide (Dawson and Goldsmith 2018), including conifers, in some cases contributing significantly to total leaf water content (Berry et al. 2014). For over 40 years the prevailing paradigm was that stomata are impermeable due to a combination of surface tension, wettability and stomatal morphology (Schönherr & Bukovac 1972) and the possibility of solute uptake through stomatal liquid water transport was not considered. Although Fernandez and Eichert (2009) recognised that stomata might play a role, they still endorsed cuticular solute penetration as the main mechanism of foliar uptake. Burkhardt and Hunsche (2013) demonstrated using scanning electron microscopy to visualise stomatal uptake that a “microscopic leaf wetness”, i.e. a minute amount of persistent liquid water on leaf surfaces which is invisible to the naked eye, can form continuous thin layers on hydrophobic leaf surfaces with potential influence on the foliar exchange of ions. According to Burkhardt and Hunsche (2013), microscopic leaf wetness could occur directly through the needle surfaces of the selected branches and could at least partly explain the measured uptake in both girdled and non-girdled branches, although the dry conditions could have the reduced the foliar uptake by reducing the microscopic water layer.

Dry conditions can also indirectly affect the potential canopy N uptake due to enhanced losses of $NH_3$ arising from the greater importance in these circumstances of dew as a night-time reservoir and a strong morning source of $NH_3$ (Wentworth et al. 2016). This release of $NH_3$ may have led to overestimations of dry and wet N deposition to forest canopies in the literature by assuming that all wet and dry deposition remains at the canopy (leaves, twigs and bark) surface. Wentworth et al. (2016) suggest that this $NH_3$ loss happens through the morning dew evaporation and in dry conditions the process could be magnified, leading to higher losses of $NH_3$.

Finally, several studies have shown that N can partly be lost by desorption from a wetted leaf surface (Wyers and Erisman (1998); Burkhardt et al. (2009)). However, the dry conditions in which the present experiment was conducted suggest that desorption might be negligible in this case. However, the process might have affected the canopy N uptake measured in the long-term monitoring (Chapter 3) as well as in the labelled simulated $N_{dep}$ experiment (Experiment 1 in this chapter).

In section 4.2 the possible effects on canopy N uptake measurements were briefly discussed: some inorganic N could be processed into organic N or lost through nitrification either on the surface of the needle or inside the needle by bacteria. Although macroscopic epiphytes were not visible on the target trees and branches used in experiments 1 and 2, they may play a role in canopy N uptake and dynamics. It is estimated that $10^6$-$10^7$ bacteria $cm^{-2}$ live on leaf surfaces, often forming large aggregates in the depressions formed at the junctions of epidermal cells (Vorholt 2012).

Studies of amoa genes found on leaves and their role in N oxidation are still relatively new and there appear to be no specific studies linking the abundance of amoa genes on tree leaves with the potential volume of ammonia oxidation. However, evidence from both agricultural (Bowatte et al. 2015) and forest systems (Northern spruce under high $N_{dep}$ in Papen et al. (2002)) indicates that nitrification should be considered in high $NH_3$ environments. Bowatte et al. (2015) measured a relatively high emission of $N_2O$ from leaves on grazed pasture (0.001-0.25 mg $N_2O$-N $m^{-2}$ leaf area $h^{-1}$) remarking that the $N_2O$ was not formed on the leaf surfaces but reflected transport of $N_2O$ from the soil. However in this experiment ammonia oxidising bacteria (AoB) on leaves were found to convert 0.12% of the oxidised ammonia into $N_2O$. This value was one order of magnitude higher than the minimum emission and one order of magnitude lower

than the maximum emission attributed to soil AoB in the same field so process should be considered a significant contributor to ecosystem $N_2O$ emissions. The conditions in the Bowatte et al. (2015) study - a high $NH_3$ agricultural environment- greatly differs from those in Griffin Forest. However, recently Guerrieri et al. (2020) showed in a study conducted on a Mediterranean holm oak that about 20% of $NO_3^-$ in TF in August derived from nitrification, after a severe drought. The same study also found that canopies and TF have more diverse microbial communities than RF. Again this is a study where ecological conditions are different from those in the present study, but the quantification of nitrification processes in the canopy indicates that the role of ammonia oxidising archaea and bacteria should not be neglected and might account for at least part of the CNU measured in this experiment.

Finally, in the experiments presented in this chapter the amount of the applied N converted to organic N or lost by gaseous emission was not estimated. However, assuming that any N gaseous losses were of the same order of magnitude as the soil emissions (0.12% of $NH_3$ converted to $N_2O$ was found in Bowatte et al. (2015)), and the transformation from inorganic to organic N is comparable to the figures calculated by Cape et al (2010) (10% of the applied N), it could be assumed that the measured recovery of 14% of the N applied to the branches represents the minimum uptake, particularly considering the dry conditions and potential multiple interaction of other lower branches with the enriched throughfall which would occur outside the experimental set-up.

## 4.4 Conclusions

Chapters 3 and 4 have provided a comprehensive assessment of CNU in a Scottish Sitka spruce plantation through multiple approaches at different spatial and temporal scales. Chapter 3 showed very high values of N retention (70%) by the canopy over 5 years of low-medium $N_{dep}$. The high retention figures were confirmed by the first, tree-scale, experiment in Chapter 4, together with a clear difference between seasons (>80% CNU in summer, <50% in winter) and within N species in the winter season, with $NH_4^+$ still highly retained (64%) whilst <25% of the applied $NO_3^-$ was retained by the canopy. These approaches to CNU calculations through the N balance between fluxes over and under the canopy still lacked evidence of the effective uptake of N by the tree tissues. This was confirmed by the second experiment in Chapter 4 that estimated a minimum of 14% of N uptake by the branches. This indicates that

retention in needles and branches represented 1/5 of the uptake and by comparing it with other experiments these figures could be underestimating the total CNU that might be found aboveground.

This study has shown that a very low amount of $N_{dep}$ is deposited as IN on the forest floor. Most of the N is intercepted by the canopy where it is either lost (possible explanations include gaseous losses, nitrification on leaves) or taken up (including by microorganisms) and later transferred to the soil as organic N via litter or by internal transfer.

The next chapter will focus on the ON cycle in the soil, taking into account the negligible IN transfers from the canopy and the higher litter transfers, with the aim of closing the N cycle in the plantation.

# Chapter 5. Estimating organic N allocation and denitrification losses to close the forest N cycle

## 5.1 Introduction

In relatively low nitrogen (N) deposition ($N_{dep}$) systems the main source of N input is atmospheric reactive N. Chapters 3 and 4 focused on the main inorganic N (IN) inputs from the atmosphere and their transfer to the forest floor through the canopy. However, the reallocation of organic nitrogen (ON) within the system is central to the forest N balance. Nitrogen supply in soils is dominated by amino acids both in N-fertilised and N-limited forest stands (Oyewole et al. 2015). The most relevant source of N for plants in the absence of fertilisation, increased N fixation (Liang et al. 2016) or high N deposition (Corbeels et al. 2003) is represented by N transfer through litter. The fluxes estimated in Chapter 3 show that the ON transfer to the soil as litter is twice that of annual inorganic transfer from the atmosphere as throughfall (TF) and stemflow (SF) in the temperate forest plantation system investigated. These transfers, along with the release of N from litter decomposition, are the main fluxes of N to the soil available for the trees. Findings from Chapter 4 suggested that a fraction of the uptaken $IN_{dep}$ could be chemically bound on the surface of branches or bark. In addition, the small fraction of IN reaching the soil floor can be incorporated into soil organic matter. The incorporation of mineral N into soil organic matter has been verified through $^{15}N$ spectrometry by Aber et al. (1998). Following this, soil organic matter can be seen as the link between both organic and inorganic N fluxes through the canopy and the closure of the N cycle through N translocation from the soil to the plants or N output from the system as leaching or gaseous emissions.

To put these results into the context of N cycling in temperate forest systems, Figure 5-1 has been produced for the present study, in which the N processes and flows analysed in Chapters 3-5 of this thesis are marked in red.

Figure 5-1. Pools (brown and dark green boxes), processes (light boxes) and fluxes (arrows) for N in Griffin Forest (a temperate forest plantation with minimal understory vegetation). Inputs, outputs and internal recycling are separated by dashed lines. Adapted from the flow chart of N cycling for a Scots pine forest in Finland in Korhonen et al. (2013).

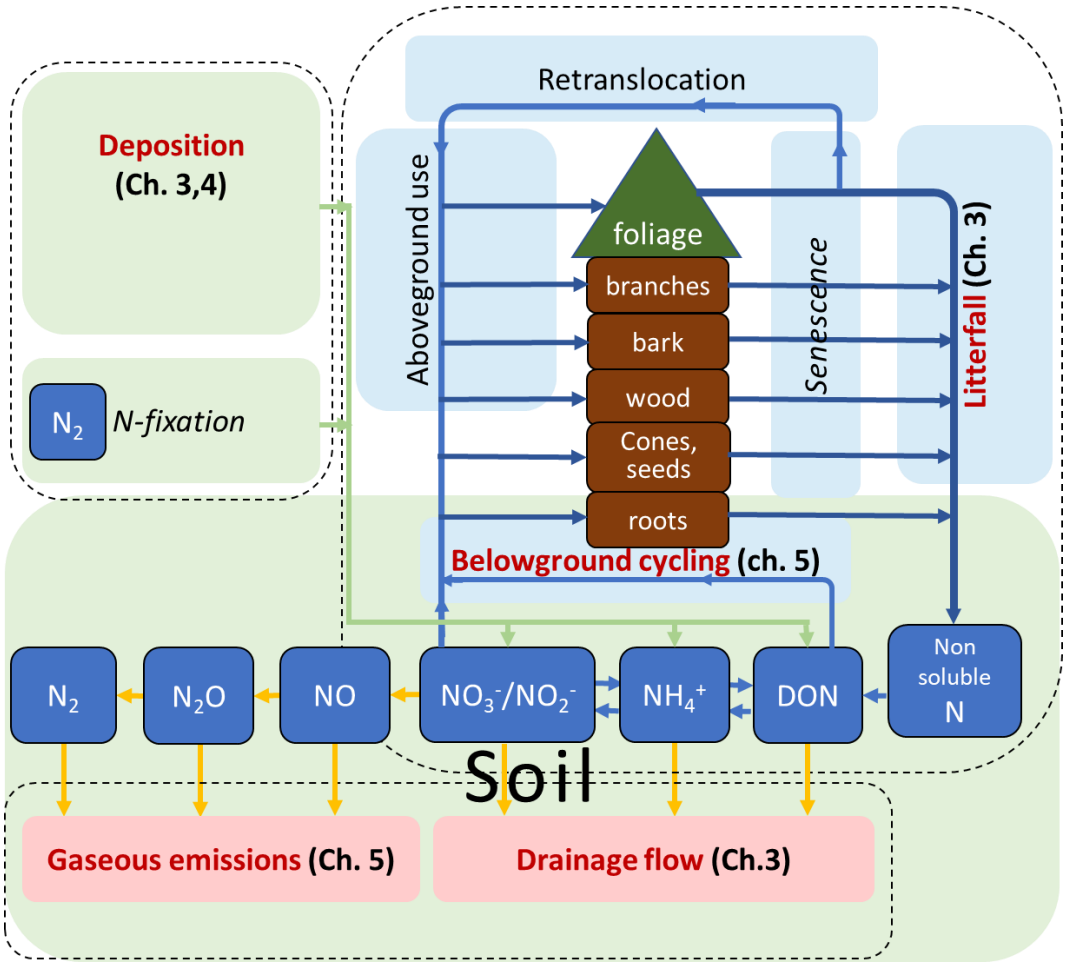


Soil is the largest N pool in boreal and temperate forests amounting to 9-15 Mg N $ha^{-1}$, followed by N stored in trees and understory vegetation (Ambus and Zechmeister-Boltenstern 2007). The soil N store is much bigger than N inputs ($N_{dep}$ and N fixation) and outputs (denitrification, volatilisation and leaching), ranging from 1.1 x $10^4$ kg N $m^{-2}$ in temperate forests to 2.9 x $10^4$ kg N $m^{-2}$ in boreal forests (Averill et al. 2014). Forest soil receives a spatially variable amount of wet and dry $N_{dep}$ (mainly as IN), ranging from less than 1 kg N $ha^{-1}$ $y^{-1}$ in the absence of human inputs up to ~50 kg N $ha^{-1}$ $y^{-1}$ (Dentener et al. 2006). The deposition of oxidised N in Europe peaked in the 1980s and since then has decreased to half of its maximum value (Dirnböck et al. 2018). However, reduced N deposition is twice as high as in 1900 and projected to remain at these levels for the coming decades (Engardt et al. 2017). Nitrogen and carbon dynamics in soil can be influenced by increasing $N_{dep}$ in several

ways and often the responses can be bidirectional. With reference to its interaction with C dynamics in soil and aboveground biomass, increasing $N_{dep}$ may lead to: (1) increased production of greenhouse gases (GHG) including $N_2O$ and NO due to increasing microbial respiration (Liu and Greaver 2010) and leading to N loss; (2) increased growth and biomass of fine roots and stimulation of their turnover and production (Nadelhoffer 2000); (3) increased soil C storage due to reduced activity and abundance of fungi that decompose lignin (Entwistle et al. 2018) and reduced respiratory C loss (Janssens et al. 2010, Maaroufi et al. 2015, Kang et al. 2016). Ultimately $N_{dep}$ can lead to soil N saturation and leaching and increased aboveground biomass production at tree level, but eventually as N saturation is reached an increase of tree mortality can lead to loss of forest net primary production (Aber et al. 1998). Although N saturation has been observed in forest ecosystems subjected to N deposition levels of less than 10 kg $ha^{-1}$ $y^{-1}$ (De Schrijver et al. 2008), it was not observed in the present research. The results presented in Chapter 3 of the small amount of atmospheric IN reaching the soil surface and the very low N concentrations measured in streamwater suggest that there is no significant N leaching from Griffin Forest soil as would be expected if N saturation had occurred (Peterjohn et al. 1996).

In the last decade several studies have shown that ON in soil represents the main N supply for plants. The direct uptake of ON in the field by trees was first demonstrated by Näsholm et al. (1998) in a boreal coniferous forest and has since then been well established (Näsholm et al. 2009, Inselsbacher and Näsholm 2012, Oyewole et al. 2016). The uptake of ON from roots in the form of amino acids (amino-N) can be direct via shuttle mechanisms or be mediated by plant-fungal or plant-bacterial symbioses. Following uptake, the amino-N plays a key role in long distance within plant N transportation, metabolism, N storage and regulation of N uptake in woody plants (Pfautsch et al. 2015). The soil organic N pool is largely composed of amino-N and their oligomers and polymers. In the last decade several laboratory and field studies have shown that plants are able to uptake amino-N and proteins through the mediation of mycorrhizal fungi (Näsholm et al. 2009, Vadeboncoeur et al. 2015) or directly without assistance from other organisms (Paungfoo-Lonhienne et al. 2008). The dominance of N retention from organic sources over IN was measured by Nair et al. (2017) in a controlled experimental study of 3-year-old Sitka spruce saplings, where $^{15}N$ from labelled litter was better retained than simulated $N_{dep}$ from mineral amendments.

Despite the importance of ON as a supply for plants, many manipulative studies investigating N sinks and N dynamics in soils have used inorganic $^{15}N$ as a tracer (Koopmans et al. 1996, Dail et al. 2009, Lovett et al. 2013). Whilst this approach might account satisfactorily for the movements of mineral N among soil sinks (Nadelhoffer et al. 1999, Templer et al. 2012), it yields an incomplete understanding of the actual N dynamics occurring in soil and of N uptake by trees. For example, through an experiment involving addition of $^{15}N$-labelled IN and ON to conifer seedlings Öhlund and Näsholm (2001) showed that ON (in the form of arginine and glycine) was comparable to IN as a source of N for seedling growth. High doses of IN applied directly to the soil surface have often been used to simulate $N_{dep}$ or simply as a fertiliser addition, despite the fact that the assumption that plants preferentially (or exclusively, see for example Haynes 1986 and Cole 1981) uptake IN rather than ON has been gradually abandoned since the late 1980s (Pfautsch et al. 2015). Studies, such as that by Tietema et al. (1998), which involved 0-80 kg N $ha^{-1}$ $yr^{-1}$ application of $^{15}N$-labelled IN in forest throughfall and reported partial N retention by the soil but with an inverse relationship to N input, cast doubt on how far high IN addition experiments might explain plant N uptake mechanisms under field conditions.

Results from more recent studies using new techniques have changed the paradigm of plant IN/ON uptake preferences in soil. The use of non-destructive sampling techniques such as microdialysis have helped to monitor N fluxes in soils with minimal disturbance, making possible data collection in real time on N transformations to determine the fate of N (Cloutier et al. 2019). The change of paradigm – i.e. that most of the soil N available for plants was coming from ON – was instigated by the use of microdialysis methods reported by Inselsbacher et al. (2011). Following that study, Inselsbacher and Näsholm (2012) showed that the amount of ON directly taken up by forest plants could be greatly underestimated and may account for >80% of the soil N supply. Also using microdialysis, Hill et al. (2019) revealed new aspects of N dynamics in soil, in particular the formation of IN and ON hotspots in soil solution in proximity to plant roots at concentrations orders of magnitude higher than normally found in the bulk soil solution. The importance of amino-N as the main N soil supply has been confirmed by several studies. For example, Oyewole et al. (2016) reported that amino-N could represent the main soil N supply in both fertilised and non-fertilised Scots pine forest stands. Other approaches have also shown how ON can be taken up by roots without being previously mineralised. Vadeboncoeur et al. (2015) demonstrated that at least 14% of $^{13}C$-$^{15}N$ double labelled whole cells were taken up

by roots, whilst Hedwall et al. (2018) showed that N addition to boreal forest plots increased tree growth, with no significant difference in growth response between IN and ON additions.

The soil compartment is also the portion of the ecosystem where most N losses occur through processes of leaching and gaseous emissions (see Figure 5.1). Losses of N through leaching in boreal and temperate ecosystems can vary from as low as 1-2 kg N $ha^{-1}$ $y^{-1}$ (Sponseller et al. 2016) and mostly as dissolved ON (DON) (Kortelainen et al. 2006) to >7 kg N $ha^{-1}$ $y^{-1}$ in European temperate forests (Kopacek et al. 2013), whilst the majority of IN inputs are retained even under moderately high levels of $N_{dep}$ (Dise and Wright 1995). In Chapter 3.7 it was shown that IN flux loss through streamwater in Griffin Forest was very low throughout the year, and on some occasions IN fluxes in streamwater downstream were lower than those upstream. Another source of uncertainty relating to N losses comes from estimation of N lost through denitrification in soil, i.e. the reduction of nitrate ($NO_3^-$) and nitrite ($NO_2^-$) to nitric oxide (NO), nitrous oxide ($NO_2$) and dinitrogen ($N_2$) carried out primarily by facultatively anaerobic bacteria. Van Breemen et al. (2002) estimated that denitrification in landscape soils accounted for more N losses in temperate watersheds (37%), compared to riverine loss (20%), and similar proportions were calculated by Korhonen et al. (2013) for soil denitrification and drainage losses. However, the latter study, which focused on an even-aged Scots pine forest in southern Finland showed that in a non-saturated low $N_{dep}$ site the N outputs were one order of magnitude lower than the input. About 90% of the N leaching from drainage flow was in the form of ON (0.12 kg $ha^{-1}$ $y^{-1}$) and N emissions as NO were negligible (0.01 kg $ha^{-1}$ $y^{-1}$) compared to the $N_2O$-N emission estimated at 0.2±0.1 kg $ha^{-1}$ $y^{-1}$.

Measuring $N_2O$ emissions at the ecosystem scale is challenging due to the high spatial (hotspots) and temporal (hot moments) variability in the N gas flux activity (Groffman 2012), as well as the difficulty of detecting the ultimate product of denitrification, $N_2$, due to its high atmospheric concentration. Consequently, and also taking into consideration that the $N_2O/N_2$ emissions ratio is highly variable, $N_2O$ measurements may be regarded as providing a minimum estimate of N loss through denitrification.

In summary, research in the past decade has made clearer that ON in forest soils represents the main N supply for plants and that the uptake of ON does not necessarily need prior mineralisation of N. Stable isotopes have been used as a tool

in a number of studies to follow the fate of N from soil to the plants, consisting predominantly of $^{15}N$ enriched mineral fertilisers (Nair et al. 2016). Few studies have used labelled litter to follow the fate of ON from soil to plants, and many of these have focused on broadleaves. Examples of these studies include that by van Huysen et al. (2013) who buried litterbags containing $^{15}N$-labelled $NH_4NO_3$ (99 atom %) broadleaf and conifer litter at 10 cm depth in a NW USA forest and collected them at intervals from 3 months to 2.5 years after burial. Key findings from their study were that initial litter chemistry may be an important control on N mineralisation and also gross mineralisation (estimated from the $\delta^{15}N$ signal) was up to 20% higher than net mineralisation (determined as the change from the litter initial N content). Zeller et al. (2001) monitored the decomposition of $^{15}N$-labelled beech litter over 3 years finding that whilst $^{15}N$ enrichment of microbial biomass occurred initially, leaves and fine roots were the dominant N sinks.

Building upon Chapters 3 and 4 which addressed N processing by the canopy and its transfer to the forest floor in aqueous form and litter, Chapter 5 focuses on the fate of litter in forest soil and the N loss from soil nitrification to help complete an overall estimation of the N cycle in a Sitka spruce plantation. The Chapter aims to answer the following questions:

1) How much ON was reallocated from litter to the soil and plant over 4 years?
2) Does the magnitude of $N_2O$ fluxes make a significant contribution to the forest N balance?
3) Do the specific soil features of a forest plantation (furrows, ridges and undisturbed soil) influence soil N cycling?

The first part of Chapter 5 will investigate how much organic N reallocated from the litter is stored in the soil and plant pools as a consequence of substantial decomposition. To do so, it will use a 4-year $^{15}N$-labelled litter experiment to derive estimates of the $^{15}N$ remaining in litter and soil and $^{15}N$ taken up by roots. In the second part of the chapter the other main pathway of N loss from the soil, i.e. N lost through denitrification, will be quantified through $N_2O$ fluxes measured over a 3-year period using static chambers. The chapter concludes by discussing the role of the plantation soil features on the reallocation of organic N and denitrification.

## 5.2 Methods

In this section the fieldwork, laboratory procedures and analysis, and data analysis will be described separately for two experiments which address the questions identified at the end of the Introduction above. The first experiment addressed question 1 by using $^{15}$N-labelled Sitka spruce litter plots established in 2013. Four years after the plots were established, soil cores and root samples were taken for analysis from the three different soil features typical of forest plantations (furrows, ridges and undisturbed soil) to estimate the ON still recovered in litter and soil, and the fraction of ON taken up in the roots.

The second experiment, addressing question 2, used the manual static chamber method to measure fluxes of greenhouse gases (including $N_2O$) from the three different features of forest plantation soil throughout a 3-year time span. Selected environmental parameters were measured, including soil extractable N, at the same time as gas samplings to try to understand the controls on $N_2O$ fluxes. Sampling in both experiments targeted the three different soil features typical of forest plantations (furrows, ridges and undisturbed soil) in order to answer question 3.

### 5.2.1 $^{15}$N-labelled litter plots experiment

#### 5.2.1.1 Field soil sampling

Four plots of $^{15}$N-labelled Sitka spruce litter were established by Richard Nair as part of his PhD project (Nair 2014) in each of the T and C locations at Griffin Forest – 8 plots in total (see Figure 5.2). Due to budget constraints for sample analyses, three labelled plots (indicated by the red text in Figure 5.2) were sampled in this research, T10, T11T12 and C11. Among the available labelled plots T10 and C11 were selected for sampling due to their proximity to the static chambers (see section 5.2.2) installed beside these plots, whilst T11T12 was selected as it was part of the 2015 sampling (conducted by D. Ferraretto and not reported here) to investigate possible variation of results from different starting $\delta^{15}$N signal and labelled litter mass.

Figure 5-2. Location of the plots, subplots and static gas chambers in Griffin Forest [PNG map]. Default downloaded scale 1:40000, Aerial Imagery, Ordnance Survey, GB. Using: EDINA Digimap Service <http://edina.ac.uk/digimap>. Sampled labelled litter plots are indicated in red text.

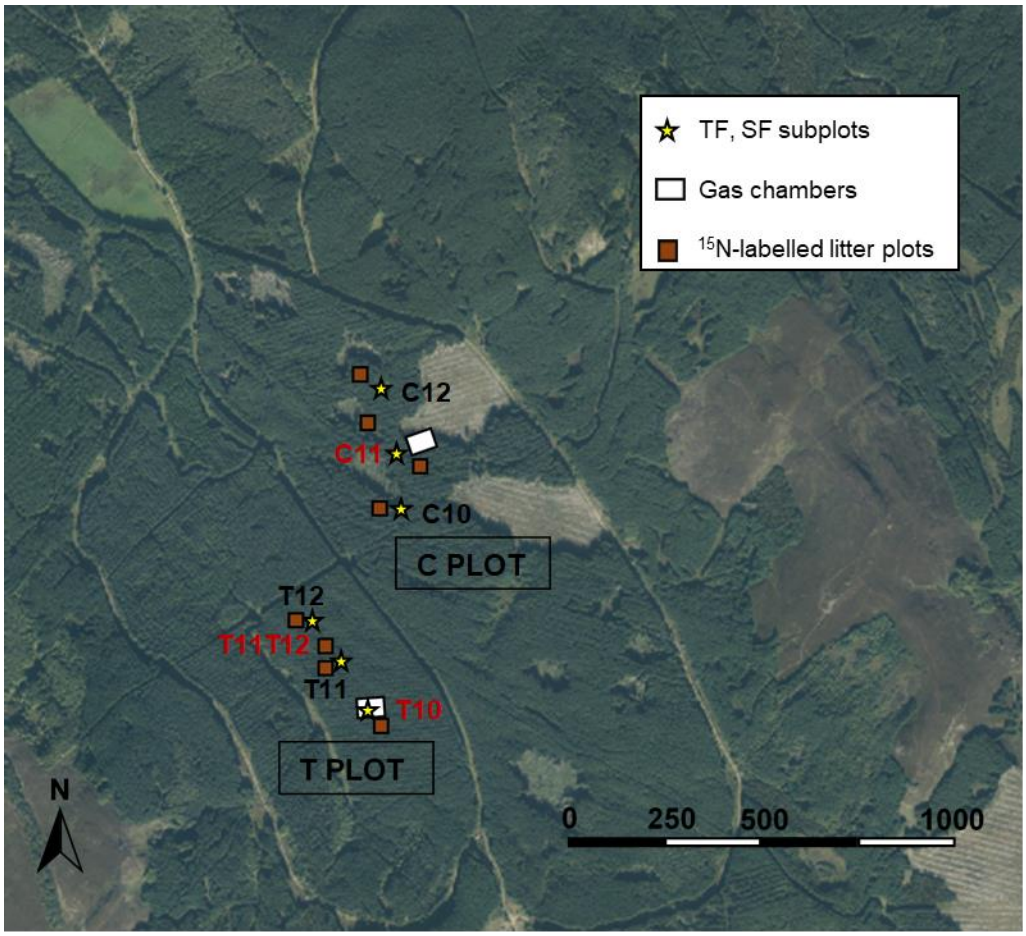


Each labelled litter plot is approximately square-shaped with dimensions of c.4 m x 4 m. The exact dimensions of each plot were determined by the linear distances between a central tree and the 8 surrounding trees (or stumps, wherever one or more trees were removed during the plantation thinning), as shown in Figure 5.3. Each plot contained the three different surface features typical of an upland forest plantation in the UK in which the ground was prepared by ploughing: (1) undisturbed soil, (2) ploughed furrows for drainage, and (3) elevated ridges on which trees are planted (Figure 5.4). In Griffin Forest these features represent 50%, 25%, and 25%, respectively, of the total plantation area (Conen et al. 2005).

Figure 5-3. Schematic showing the layout of a typical labelled litter plot established at Griffin Forest. Central target tree (red circle) with 8 surrounding trees/stumps (grey circles). $^{15}N$ labelled litter was deployed in the shaded area.

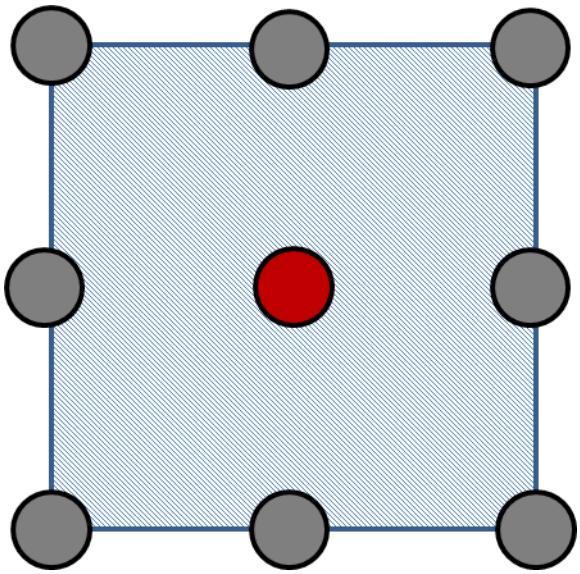

Figure 5-4. Typical schematic soil horizons under the three different surface features at Griffin Forest. The depths of each layer vary from core to core and cannot be related to the separation of the soil cores extracted into 0-5 and 5-15 cm depths.

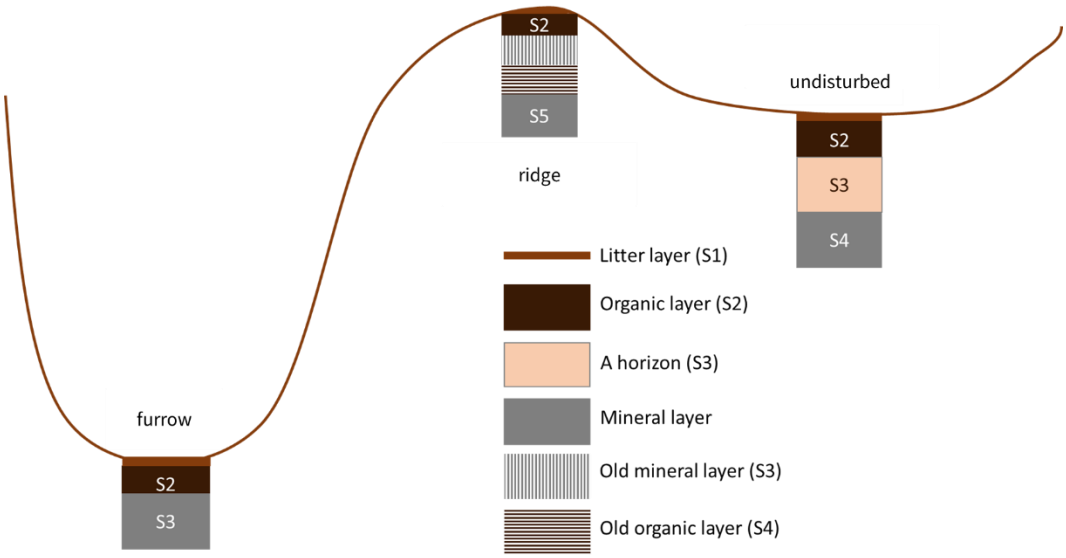


The labelled litter was produced by Nair et al. (2014) by injecting a double labelled $^{15}N$-$NH_4NO_3$ solution into the stem of 21 Sitka spruce trees on the edge of Cardrona Forest in the Scottish Borders (55°61′50″N, 3°12′87″E) in July-August 2011. After 4.5 months, to allow the labelled N to disperse throughout the foliage, the entire needle biomass from the injected trees (in total, 173 kg of litter) was harvested in December 2011 keeping it separated by tree and vertical/radial section. The harvested material was oven-dried for 2 weeks at 70°C, then carefully mixed and analysed for total N concentration and $\delta^{15}N$ on a SerCon Callisto CF-IRMS Isotope Ratio Mass

Spectrometer (School of Biological Sciences, University of Aberdeen, Aberdeen, UK). The separated litter from different trees and vertical/radial sections was mixed together and then divided into four portions, each of which was deployed at the four plots in Griffin Forest by Richard Nair in July 2013. The existing entire litter layer was removed from the plots with a spade and replaced with a known mass of Sitka spruce labelled litter with a distinct $^{15}N$ signature (see Table 5.1). There was no significant understory vegetation in any of the labelled litter plots so nearly all of the litter accumulating after the application derives from the Sitka spruce canopy.

Table 5-1. Mass of litter applied and its $\delta^{15}N$ signal for three of the four labelled litter plots established at Griffin Forest in July 2013 which were sampled in July 2017. Source: Richard Nair (pers. comm.)

| Plots in location "T" | Plots in location "C" | Mass litter applied per plot (kg dry weight) | Mean $^{15}N$ atom % at application | $\delta^{15}N$ |
|---|---|---|---|---|
| T10 | | 24.6 | 1.63818 | +4547 |
| T11T12 | | 19.3 | 1.50631 | +4175 |
| | C11 | 22.1 | 1.67651 | +4655 |

Soil samples from the three labelled litter plots shown in Table 5.1 were collected in July 2017, using excavated cores rather than an auger to minimise contamination between samples. The cores were extracted using a 15 cm wide spade to obtain square soil blocks with sides of ~15-20 cm, to depths of 20 cm or more in the ridges and undisturbed soil, and 15 cm or less in the furrows, where the soil depth was less due to erosion by water. The spade was cleaned between extraction of each soil core using a spatula and tissue. A control unlabelled plot to determine the background $\delta^{15}N$ signal of soil, litter and roots was chosen 3 tree lines upslope of the T10 labelled plot. In each plot 6 soil cores were excavated, comprising 2 replicate cores of each surface feature (undisturbed, furrow, ridge). After removal, the soil cores were wrapped in cling film, and transported back to the laboratory in a cool box for processing. The dry soil conditions at the time of soil core collection made it difficult to maintain the original soil density due to soil crumbling after core excavation. Therefore, dry bulk density of the soil layers was estimated using the values obtained from a previous similar soil collection in July 2015 at T11 and T11T12, when soil conditions were wetter. The dry bulk density values of the 2015 soil layers were calculated by dividing the oven-dry

mass of each soil layer by its volume (obtained by multiplying the length, height and width of the square cross-section cores). Other similar studies where labelled litter was deployed have estimated litter decomposition rates by using litter bags (Zeller et al. 2000, van Huysen et al. 2013, Nair 2014). In the absence of a similar tool, it was assumed in this study that litter did not accumulate and that the amount of new litter deposited on the labelled litter layer compensated for the decomposed litter in the 4 year period considered.

#### 5.2.1.2 Laboratory soil preparation and analysis

On return to the laboratories, the edges and upper and lower parts of each soil core were removed to minimise any $^{15}N$ contamination of the lower layers by the more enriched surface layers due to the action of the spade in the field. The core was then weighed and separated into litter and soil depths of 0-5 cm and 5-15 cm. Due to variability between cores, these two soil depths could contain one or more of the layers shown in Figure 5.4. All of the soil sub-samples were passed through a 2 mm mesh sieve. Roots (including all fine roots) were separated into 2 sub-samples (roots in 0-5 cm and in 5-15 cm depth soil), washed and rinsed 3 times with deionised water. The separate roots, litter and <2 mm soil fractions were oven dried at 80°C to constant weight and then ground to a fine powder using stainless steel balls in a ball mill (MM 400, Retsch Ltd., UK).

Due to resource limitations, analysis of $\delta^{15}N$ was conducted on 112 samples in total from 17 cores separated into litter, soil, root samples and extractable $NH_4$-N and $NO_3$-N as detailed in Table 5.2. Soil samples for extractable N were taken from 0-5 cm soil depth only. Litter, soil and root samples were ground to a fine powder using a ball mill, then transported by courier along with the freeze-dried filters of extractable N, to the Max Planck Institute for Biogeochemistry, Jena, Germany, for $\delta^{15}N$ and N% analysis. All samples were run on a DeltaPlus isotope ratio mass spectrometer (Thermo Fisher, Bremen, Germany) coupled via a ConFlow III open split to an elemental analyser (Carlo Erba 1100 CE analyser; Thermo Fisher Scientific, Rodano, Italy). Standard deviation of the measured standards was 0.2‰ or better.

Table 5-2. Table summarising the number of soil core samples analysed for $\delta^{15}N$ from different locations and plots. F = furrow, U = undisturbed, R = ridge. 5-15 cm soil samples could not be collected from some furrows due to local erosion by water. Roots were not present in some soil layers. *additional replicate root samples were analysed from some T11T12 and C11 cores to verify the homogeneity of the $\delta^{15}N$ signal through the milled samples.

| Location code | Labelled/ unlabelled | Feature | Litter | Soil | | Roots | | Total number of samples |
|---|---|---|---|---|---|---|---|---|
| | | | | 0-5 cm | 5-15 cm | 0-5 cm | 5-15 cm | |
| T10 | Labelled | F | 2 | 2 | 1 | 2 | 1 | 8 |
| T10 | Labelled | U | 2 | 2 | 2 | 1 | 2 | 9 |
| T10 | Labelled | R | 2 | 2 | 2 | 2 | 1 | 9 |
| T11T12 | Labelled | F | 1 | 2 | 1 | 3* | 2 | 9 |
| T11T12 | Labelled | U | 2 | 2 | 2 | 2 | 1 | 9 |
| T11T12 | Labelled | R | 2 | 2 | 2 | 2 | 3 | 11 |
| C11 | Labelled | F | 2 | 2 | 1 | 3* | 2 | 10 |
| C11 | Labelled | U | 2 | 2 | 2 | 3* | 1 | 10 |
| C11 | Labelled | R | 2 | 2 | 2 | 2 | 2 | 10 |
| T10 ctrl | Unlabelled | F | 2 | 2 | 2 | 1 | 1 | 8 |
| T10 ctrl | Unlabelled | U | 2 | 2 | 2 | 2 | 1 | 9 |
| T10 ctrl | Unlabelled | R | 2 | 2 | 2 | 2 | 2 | 10 |

#### 5.2.1.3 Calculations and statistical analysis

Three assumptions were made in the calculations of $^{15}N$ content and recovery in the 2017 samples. Firstly, leaching, gaseous loss or major disturbances to the labelled $^{15}N$ litter layer and soil have been small compared to other sources of uncertainty between the dates of application of the labelled litter in 2013 and the sampling in 2017. Secondly, the calculations of $^{15}N$ recovery for roots used data for root dry weight per surface feature (undisturbed, furrow, ridge) and depth per soil volume measured in 2001 in the same area of Griffin Forest (Conen, unpublished data). Thirdly, the dry bulk densities of the 2017 cores were assumed to be the same as determined for similar soil cores taken in 2015 as explained above.

The N mass (g $m^{-2}$) of each soil layer was calculated by multiplying the dry soil density (from 2015 data, expressed as g $cm^{-3}$) by the depth of each layer (cm) and the N%:

$$Soil\ layer\ N\ mass = \text{dry soil density} \times \text{soil N\%} \times \text{soil depth} \times 10000 \qquad \text{(Eq. 5.1)}$$

The $^{15}N$ recovery was calculated for each sample from its measured $\delta^{15}N$ following the calculations shown below.

$\delta^{15}N$ (‰) measured in each sample was converted to atom percent (atom%) as:

$$atom\% = \frac{100 \times \mathrm{RA} \times \left(\frac{\delta^{15}\mathrm{N}}{1000} + 1\right) )}{1 + \mathrm{RA} \times \left(\frac{\delta^{15}\mathrm{N}}{1000} + 1\right)} \quad \text{(Eq. 5.2)}$$

where RA = absolute ratio of $^{15}N/^{14}N$ in the air (RA= 0.036764).

Then $^{15}N$ atom excess, which reflects the enrichment of $^{15}N$ of the $i^{th}$ sample layer compared to an unlabelled sample, was calculated as:

$$atom\%_{i\ excess} = atom\%_{i\ labelled} - atom\%_{unlabelled} \quad \text{(Eq. 5.3)}$$

The values used for $atom\%_{unlabelled}$ were calculated using the natural abundance $\delta^{15}N$ signal from the relevant equivalent layer in soil cores from the unlabelled T10 unlabelled plot, averaged by soil feature (furrow, undisturbed, ridge).

Next, the N concentration [N] (%) was converted to N content (g) in each sample and then the $^{15}N$ excess in each sample was calculated as:

$$^{15}N_{i\ excess\ content}(g) = \frac{N_{content} \times atom\%_{i\ excess}}{100} \quad \text{(Eq. 5.4)}$$

The values of $atom\%_i$ and $N_i$ used in Eq. 5.3 and 5.4 are specific to the treatment plot considered (see Table 5.1).

The total $^{15}N$ input for each labelled plot was calculated as the sum of the $^{15}N$ content in the labelled litter applied and the total background $^{15}N$ deposited in litterfall to the plot from the date of the labelled litter application in 2013 to the soil core sampling date in 2017. The mass of N in litterfall to each plot was estimated by using the litter values of the closest subplot and calculated as the sum of the different yearly values per hectare (similarly to the whole forest, as shown in Chapter 3.5), from the month of the application until the month of the soil core collection (July 2017). The value used for the background $\delta^{15}N$ of litterfall was the mean $\delta^{15}N$ value of the litter samples collected from the unlabelled control plot in July 2017.

Finally, the $^{15}N$ recovery ($N\%_{rec}$) in samples was calculated as

$$N\%_{rec} = \frac{^{15}N_{excess\ content}}{^{15}N_{total\ input}} \times 100 \quad \text{(Eq. 5.5)}$$

The factors determining %N content, $\delta^{15}N$ and $^{15}N$ recovery in litter, soil and roots were tested separately for each compartment and depth. Datasets were tested for

normality before statistical analysis was conducted. Table 5.3 summarises, for the tests that were significant for the different datasets, the best fitting data transformation if required for normality (tested using the Shapiro-Wilk test) and the type of test conducted. When ANOVA was used a Levene's test was run to assess the homogeneity of variances of multiple datasets. The significance level for all the tests presented in this chapter was $p < 0.05$. More details of the statistical analysis approaches are given in the text following Table 5.3 (a complete list of statistics that were run including non significant results is shown in Appendix G).

Table 5-3. Summary of statistical tests conducted on litter, soil, and roots samples results that were significant ($p<0.05$). U and L represent unlabelled and $^{15}N$ labelled plots, respectively. "Soil type" indicates surface feature (undisturbed, furrow, ridge).

| Tested differences | Applied transformations for normality | Test | Test p-value | notes |
|---|---|---|---|---|
| *litter $\delta^{15}N$ U/L* | *none* | *Welch two-sample t-test* | *<0.001* | |
| *soil 0-5 cm $\delta^{15}N$ U/L* | *sqrt* | *Welch two-sample t-test* | *<0.001* | |
| *soil 5-15 cm $\delta^{15}N$ U/L* | *none* | *Welch two-sample t-test* | *<0.01* | |
| *$\delta^{15}N$ by soil depth* | *sqrt* | *Welch two-sample t-test* | *<0.05* | |
| *roots* 0-5 cm *$\delta^{15}N$ U/L* | *none* | *Welch two-sample t-test* | *<0.001* | |
| *roots* 5-15 cm *$\delta^{15}N$ U/L* | *sqrt* | *Welch two-sample t-test* | *<0.001* | *shifted (+1.05)** |
| *roots $\delta^{15}N$ by* labelled plots(a)+*depth(b)* | *sqrt* | *Two-way ANOVA* | (a)0.1 *(b)0.01* | *shifted (+1.82)** |
| *roots $\delta^{15}N$ labelled soil type(a)+depth(b)* | *sqrt* | *Two-way ANOVA* | *(a)0.05 (b)0.01* | *shifted* (+1.82)* |

* some of the $\delta^{15}N$ values from root samples were <0. As a square root transformation needs values ≥0, the minimum value of $\delta^{15}N$ was added to all values to transform them.

Differences in %N and the $\delta^{15}N$ signal between labelled litter addition plots and the unlabelled plot were tested separately for litter, roots, and different soil depths using the Welch two-sample t-test.

To build explanatory models of $\delta^{15}N$ distribution in each of litter, soil and roots, four potential predictors were considered: soil depth, plot, surface feature and N% of the sample. Sample N% was discarded at an early stage after a Variance Inflation Factor test (VIF, package *car*).

Before proceeding with the ANOVA tests shown in Table 5-3, soil $\delta^{15}N$ data were analysed through one generalised linear models (glm) having $\delta^{15}N$ and with soil depth

as the dependent variable. The model significantly explained the variation of δN among soil samples by soil depth ($p<0.01$).

In order to determine whether surface features (undisturbed, furrow, ridge – referred to as "soil type" in Table 5.3) or soil depth had any significant effect on $\delta^{15}N$ in soil and roots, ANOVA tests were conducted separately on litter, root and soil data. Mixed effects models were not explored due to the low number of levels of the predictors to address the random effects, as widely recommended (e.g. Harrison et al. 2018).

The datasets were first visually inspected (ggboxplot, package *ggpubr*) by using consecutively 2 or 3 variables combined. Following the results of this first step the best fitting type of ANOVA test for each dataset was chosen. A one-way ANOVA was used to test the effect of surface feature on soil and litter, whilst a two-way ANOVA was used to test two combinations of variables on root $\delta^{15}N$: 1) surface feature + soil depth and 2) labelled plot + soil depth.

Data from 16 soil cores collected in Griffin Forest in 2001 (Conen, unpublished data) are presented alongside those collected during the present research project to help explain the variability of N in soil pools over time and space. The 2001 dataset was sampled on undisturbed soil and ridges. Cores were divided into 2 cm depth increments between the litter layer and the parent material. Each depth increment was divided into soil < 2 mm, stones and roots. The dataset includes litter and soil depth for each core and soil and root N%, soil and root C%, and soil bulk density for each 2 cm depth increment.

The overall N input to soil was calculated using the litter deposition data presented in Chapter 3, making the assumption that the soil N pool is constant over the study period and that leaching and gaseous loss is small compared to other sources of uncertainty. The latter assumption will be verified through the static chamber study introduced in the next section of this chapter, as $N_2O$ emissions vary under different conditions and can represent a significant percentage of the total $NO_3^-$ losses.

### 5.2.2 $N_2O$ flux measurement using chambers

Surface $N_2O$ fluxes were measured monthly from September 2013 to November 2016 using the manual static chamber method, with opaque PVC chambers (0.4 m × 0.4 m × 0.25 m height) placed on permanently installed frames, following the technique of Ryden and Rolston (1983). Under the supervision of Forest Research, 18 closed

chambers were installed in Griffin Forest (see examples in Figure 5.5), 9 in the T plot and 9 in the C plot. They were located respectively in the proximity of the T10 and C11 throughfall and stemflow subplots (see Figure 5.2) and comprised 3 replicates of each surface feature (undisturbed, furrow, ridge, see Figure 5.4). The top of each frame had a water channel to ensure a gas-tight seal.

Figure 5-5. Left: Chamber 1 (furrow), centre: Chamber 3 (undisturbed soil) and right: Chamber 8 (ridge) in the T plot, July 2017.

Each chamber was left beside its respective frame in between the measurements so as not to alter the soil within the frames. Initially the chamber body was left with the opening towards the ground, but, after damage to the valve pipes by rodents starting in October 2015, they were kept upside down, as shown in Figure 5.5 (left), in order to protect the chamber valve. However, this could cause water pooling and freezing in chambers during the coldest months. Gas samples from the air-tight samplers were taken monthly from October 2013 to November 2016, except in the winter months when snow or ice in the valve tubes and in the water channels meant that sampling was not feasible.

Before the chamber body was placed on each frame, air temperature at ~2 m above the ground surface and soil temperature at 10 cm depth were measured with a digital temperature probe (HI-98509 Checktemp 1, Hanna Instruments Ltd.) and soil moisture ($m^3\ m^{-3}$) was measured inside each frame at 10 cm depth using a moisture sensor (SM 200 attached to a handheld HH2 moisture meter, Delta-T Devices Ltd., Cambridge, UK). Next, the chamber body was placed on the frame, and duplicate samples of the chamber headspace were taken at 20-minute intervals (0, 20, 40, 60 min) by connecting a polypropylene 60 mL syringe to the chamber sampling port fitted

with a three-way stopcock. The syringe was emptied immediately into pre-evacuated 20 mL glass vials fitted with chlorobutyl rubber septa. The vials were kept in a cool box and sent to Forest Research's laboratory (Alice Holt Lodge, Surrey, UK) for $N_2O$ analysis.

Concentrations of $N_2O$ were determined in the samples using a headspace-sampler (TurboMatrix 110) and gas chromatograph (Clarus 500, PerkinElmer) fitted with two identical 30 mm × 30 mm internal diameter megabore capillary porous Layer Open Tubular columns (Elite PLOT Q) maintained at 35°C. The chromatograph was equipped with an electron capture detector (ECD) operated at 350°C for $N_2O$ analysis (Yamulki et al. 2013). The calculated $N_2O$ flux was estimated taking into account the rate of change in $N_2O$ concentration over time during the hour of chamber headspace sampling, the measured soil temperature and the chamber dimensions as follows:

$$N_2O\ flux\ (g\ ha^{-1}\ d^{-1}) = \frac{\partial N_2O}{\partial t} \times \frac{28}{22.4} \times \frac{chamber_{vol}}{chamber_{area}} \times \frac{273}{273 + soil\ temp\ ℃} * \frac{10000}{1000} \quad \text{(Eq. 5.6)}$$

Where $\frac{\partial N_2O}{\partial t}$ = slope of the concentration increase with time (ppb $N_2O$ $d^{-1}$), $chamber_{vol}$ = the volume of the chamber ($m^3$), $chamber_{area}$ = surface covered by the chamber ($m^2$), 28 = molar mass of $N_2$ and 22.4 = ideal molar gas volume at standard temperature and pressure (STP).

For statistical analysis of the flux data, all negative values were excluded (as advised by S. Yamulki *pers. comm.*) as well as one high flux outlier (8 g $N_2O$-N $ha^{-1}$ $d^{-1}$).

On each gas sampling occasion from September 2015 to September 2016 a soil core was taken with a Dutch soil auger to ~12 cm depth beside each frame, close enough to be representative of the soil conditions within the frame but not to disturb conditions inside the frames. Each core was sealed separately in a plastic bag and extracted with KCl for determination of available soil N within 24 hours, following the procedure described in section 4.2.1.3. The results were compared with the chamber fluxes to determine if there was any correlation between the $N_2O$ fluxes and the extractable IN concentration.

Plot (T vs C plots) was used as a potential predictor in some of the statistical analyses described in section 5.3.5. In the project design, T and C represented two plots with similar features (forest vegetation and structure, elevation, slope, mean temperature, precipitation). However, due to wind throw in 2014 that affected areas close to the C

subplots there could have been local changes in temperature and throughfall conditions (and, consequently, different soil moisture conditions). Therefore samples from the T and C plots were considered separately for some of the statistical analyses.

Lastly, mean monthly $NH_4$-N and $NO_3$-N mass flux in bulk deposition were investigated as potential predictors of soil $N_2O$ fluxes using a general linear model. Both general linear models (package *stats*, package *rsq*) and mixed linear models were used to structure the data, but the best fit models provided a poor representation of the raw data, with high noise across the time series and outliers at the higher flux values.

## 5.3 Results

### 5.3.1 Nitrogen content in litter, soil and roots

The mean N% of the labelled litter applied to the plots in Griffin was 1.5%. In the 4 years following the application, litterfall from the canopy onto the labelled plots (N content values measured in 2013 are reported in Chapter 3 and ranged from 0.09±0.02% to 0.56±0.01%) is expected to have diluted the relatively high N content of the labelled litter applied. This was confirmed by a one-way t-test which showed that the mean N content of Sitka spruce forest floor litter sampled in the labelled plots at Griffin in July 2017 was significantly lower ($p<0.01$) than the mean N content of the applied labelled litter.

Figure 5.6 shows that the mean N content of Sitka spruce forest floor litter in the control plot at Griffin was lower than in the labelled litter plots for both undisturbed soil and ridge features, but this difference is not significant ($p=0.167$). The opposite pattern was present in the furrows, but the litter cover there is sparse and subject to great disturbance from runoff. Apparently inconsistent patterns in N% values in the litter and 0-5 cm soil depths between the different soil features of 2001 compared to 2017 could be due to different soil moisture conditions between the two sampling dates which affected the separation of the litter and the surface soil layer.

This study sampled soil below each of the three different soil profiles under the canopy as shown in Figure 5.4, whilst sampling in 2001 (white diamonds) was conducted on ridges and undisturbed soil, which together account for 75% of the plantation surface, but did not consider furrows. The N content in both the surface soil layer (0-5 cm), and the deeper (5-15 cm) layer for the undisturbed soil of 2017 samples appeared to

be lower, compared to the 2001 samples, whilst samples from the ridges shows an opposite results. Mean soil N content in the 0-5 cm layer of the labelled plots was slightly lower than in the T10 unlabelled plot for all soil features, but no significant differences in soil N% were found between samples from unlabelled and labelled plots.

There were also no significant differences in root N% in samples from unlabelled and labelled plots for both soil depths.

Figure 5-6. Mean N (% dry mass) of forest floor litter, soil pools and roots at different depths for the different surface features ± standard error (SE, n is shown for each sample group). Data shown by the open diamonds were collected in Griffin Forest in 2001 for ridges and undisturbed features (Conen, unpublished data). The open and the filled circles represent control and the labelled litter additional plots (treatment), respectively, sampled in July 2017.

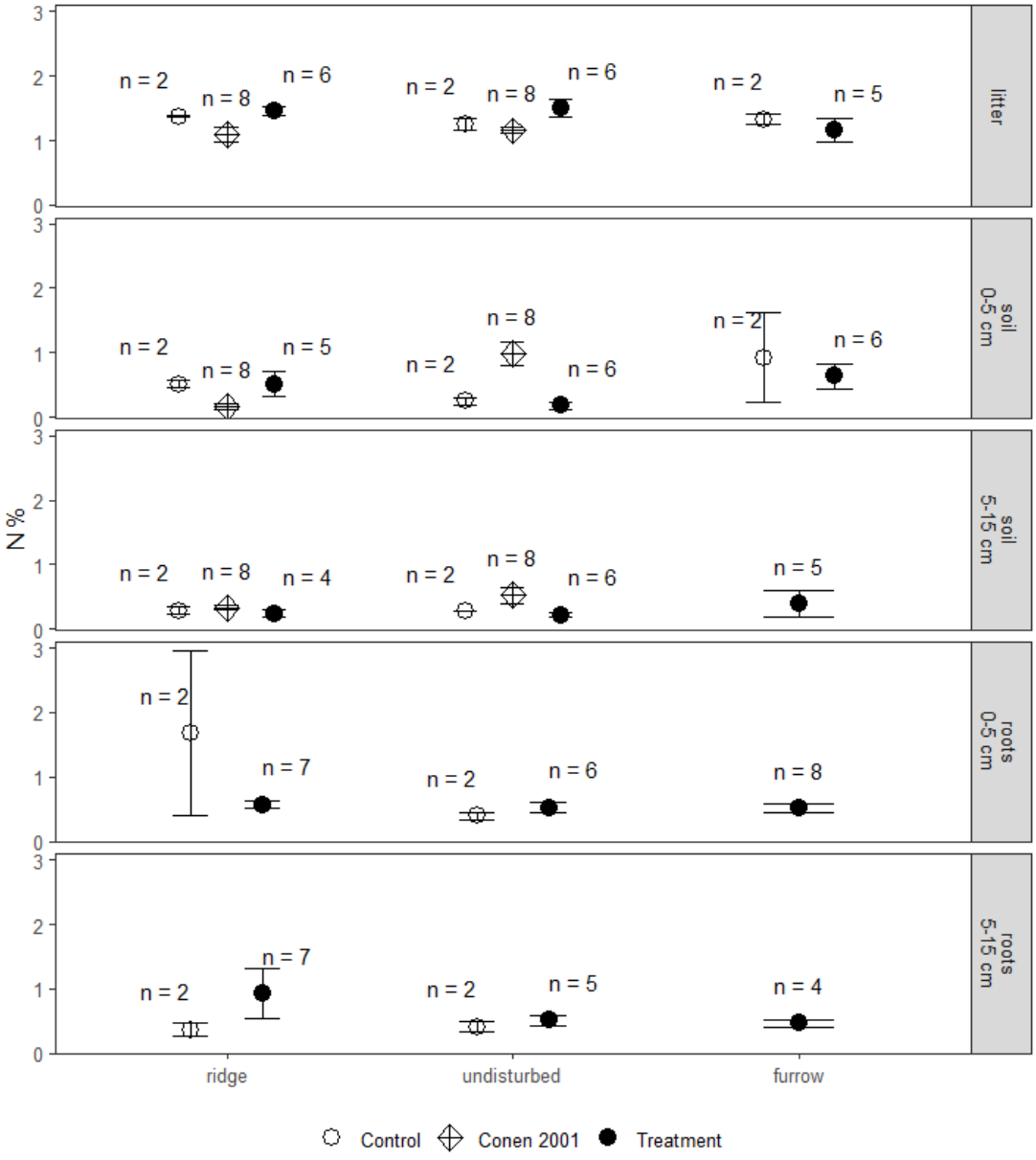


## 5.3.2 $\delta^{15}N$ changes over time in litter, soil and roots

Differences in the $\delta^{15}N$ signal between labelled litter addition plots and unlabelled plots were clearly detectable and significant in all layers and soil profiles (refer to Table 5.3 for p-values; Figure 5.7 for mean values ± SE). Within the labelled samples significant variations of the mean $\delta^{15}N$ signal were tested among different depths,

surface features and plot. Litter $\delta^{15}N$ content in samples from the labelled plots did not show any significant difference for any of these predictors. Soil $\delta^{15}N$ in samples from the labelled plots differed significantly with soil depth only. As expected, mean $\delta^{15}N$ value at 0-5 cm depth was significantly higher (26.3±3.8‰ (n = 17) than at 5-15 cm soil depth (11.3±1.7‰, n = 15). Soil $\delta^{15}N$ did not differ significantly between the three different surface features. Assessment of variation in $\delta^{15}N$ in roots using two-way ANOVA showed significant changes with soil depth ($p<0.001$) and surface features ($p<0.05$): the highest values of root $\delta^{15}N$ occurred in the shallower soil, where roots were mostly lignified (diameter ≥ 1 mm). Roots in furrows had slightly higher $\delta^{15}N$ than the other soil features at both soil depths, whilst ridges had the highest mean $\delta^{15}N$ values in the surface soil layer. The effect of initial treatment (plot) was least significant ($p<0.1$).

Surprisingly, the different $\delta^{15}N$ signatures of the litter applied to the plots is not reflected in statistically significant differences in litter $\delta^{15}N$ measured between plots in 2017. Plot was tested as a potential variable in the model, on the assumption that, due to the different $\delta^{15}N$ value at the time of application in 2013, samples from the same surface feature and depth might have different $\delta^{15}N$ values due to the initial difference in $\delta^{15}N$. However, plot has not shown to be a significant predictor for $\delta^{15}N$ values among soil layers.

Figure 5-7. Mean $\delta^{15}N$ in litter, soil and roots at different depths and for the different surface features ± SE (n is shown for each sample group) for unlabelled and labelled litter addition treatment plots sampled in July 2017. For clarity, the y axis scales are $log_{10}$.

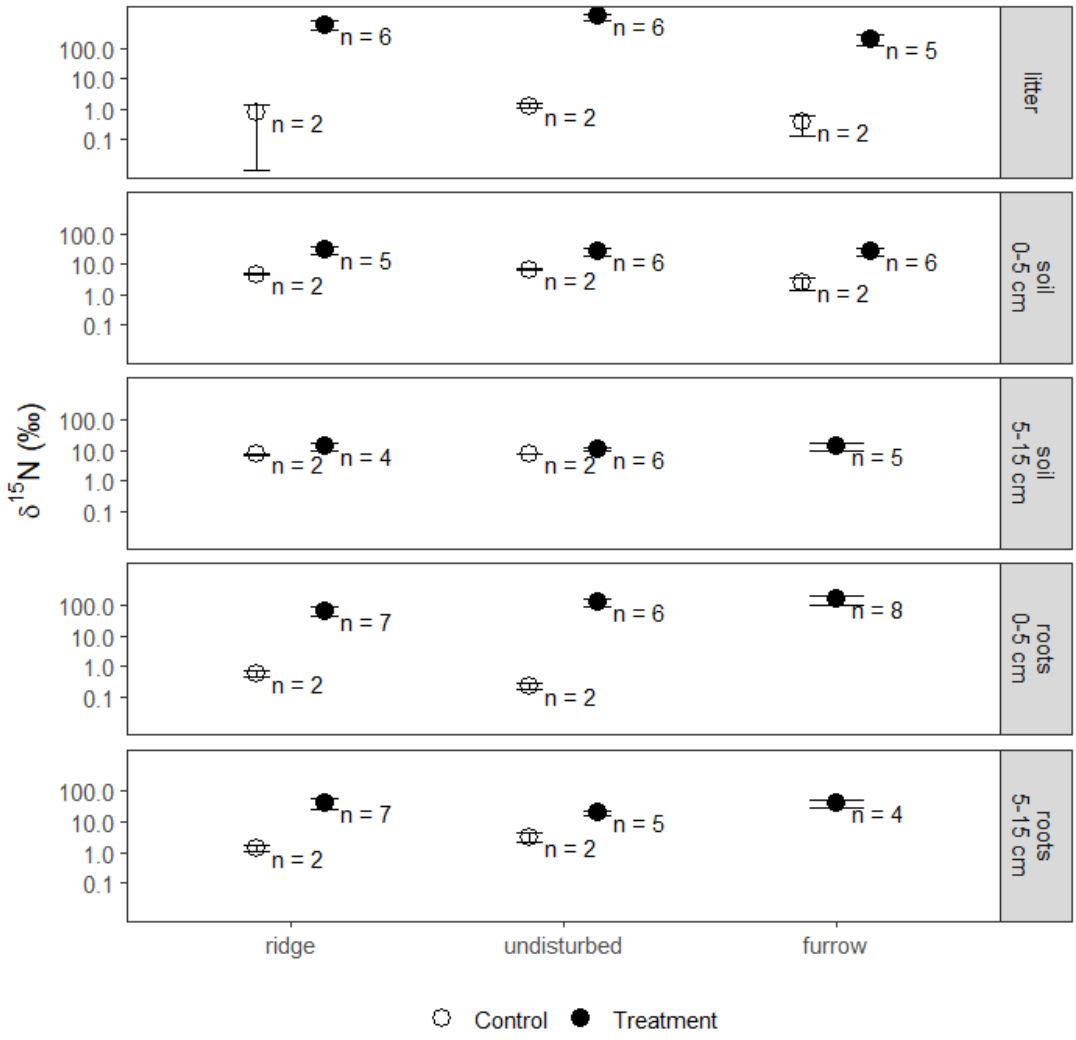


### 5.3.3 $^{15}N$ recovery in litter, soil and roots

The litter, soil and root $^{15}N$ recoveries in the labelled litter plots detailed by each soil feature are reported in Table 5-4. Four years after the labelled litter application a substantial percentage of the $^{15}N$ applied in litter was still recovered in the litter layer, whilst a minimal fraction was found in the soil down to 15 cm. Another important result is that recovery in the roots is greater than in the soil. A difference in recovery was found among surface soil features, with the higher $^{15}N$ recovery in litter occurring in the undisturbed soil. Furrows were the surface feature with the lowest overall $^{15}N$ recovery, mainly due to the low recovery in the litter layer. This is expected, as furrows

act as drainages in the plantation and runoff has removed most of the litter leaving a shallow soil layer on top of the parent material.

Table 5-4. Mean [SE] $^{15}N$ recovery (%) in the main soil pools in the labelled plots as percentage of the total $^{15}N$ input from labelled litter. Root $^{15}N$ recovery in furrows was not calculated as root mass was negligible in soil cores in the furrows.

| **Soil feature** | **litter** | **0-5 cm soil** | | **5-15 cm soil** | |
|---|---|---|---|---|---|
| | | roots | soil | roots | soil |
| **undisturbed** | 34.8[8.6] | 11.3[5.4] | 0.3[0.1] | 4.9[1.1] | 0.4[0.2] |
| **ridge** | 19.2[6.8] | 4.0[1.3] | 0.5[0.1] | 8.2[3.2] | 0.4[0.2] |
| **furrow** | 5.6[2.5] | - | 0.5[0.2] | - | 0.9[0.9] |
| **Weighted mean (50/25/25)** | 23.6[11.2] | 6.7[5.6] | 0.4[0.2] | 4.5[3.4] | 0.5[0.9] |

The $^{15}N$ recovered varied widely between the different surface features. The maximum total $^{15}N$ recovery was in the undisturbed soil (51.7±10.2(SE) %), followed by the ridges (34.1±5.1%) and furrows (7.0±2.7%).

The results of soil N recovery were visualised with three-way (soil feature, soil depth and plot) and two-way (soil feature and soil depth) boxplots (see Appendix H). Following this, plot as a potential predictor was discarded and a linear model with soil feature and soil depth only was constructed after testing datasets for normality. The data were cube root transformed to meet the normality conditions. A two-way ANOVA showed that only soil depth had a significant effect on $^{15}N$ recovery ($p<0.001$). Soil layer was introduced in a simple linear model to estimate the coefficients for each layer. Litter layer (0.723, $p <0.001$) and the 0-5 cm depth layer (0.764, $p <0.001$) explained most of the variability, whilst the deeper soil layer (estimate -0.046) was not significant ($p = 0.792$).

The mean $^{15}N$ recovery values among the 3 plots weighted by the relative surface of each soil profile type (undisturbed soil covers about 50% of the plantation and of each plot, whilst ridges and furrows each cover about 25% of the surface area) was as follows (given application +$^{15}N$ from natural litter input = 100%). The mean recovery for litter was 23.6±4.6%, whilst 0.4±0.1% was recovered from the surface soil (0-5 cm) and 0.5±0.3% from 5-15 cm depth soil. Since negligible root mass was found in the soil cores below the furrows, it was assumed that the mass of roots in the furrows

was zero. Thus the mean recovery in roots across all soil features was 4.6±1.9% in the upper soil layer and 3.1±0.7% in the deeper soil layer.

### 5.3.4 Soil $N_2O$ emissions

Figure 5-8 shows the time series of $N_2O$ fluxes by chamber and soil feature (furrow, undisturbed, ridge). The linear regression used to show the temporal trend in the plot (flux~date) indicates that fluxes have significantly increased over time for all chambers ($p<0.001$).

Figure 5-8. Time series of $N_2O$-N fluxes for each chamber at Griffin Forest measured approximately monthly from September 2013 to November 2016, displayed by soil feature (F = furrow, U = undisturbed, R = ridge). Chambers 1-9 were located in the T plot, chambers 10-18 were located in the C plot. The calculated $N_2O$ fluxes (expressed as g $N_2O$ $ha^{-1}$ $d^{-1}$) are courtesy of Forest Research. The trend line was built with a linear *geom_smooth* model.

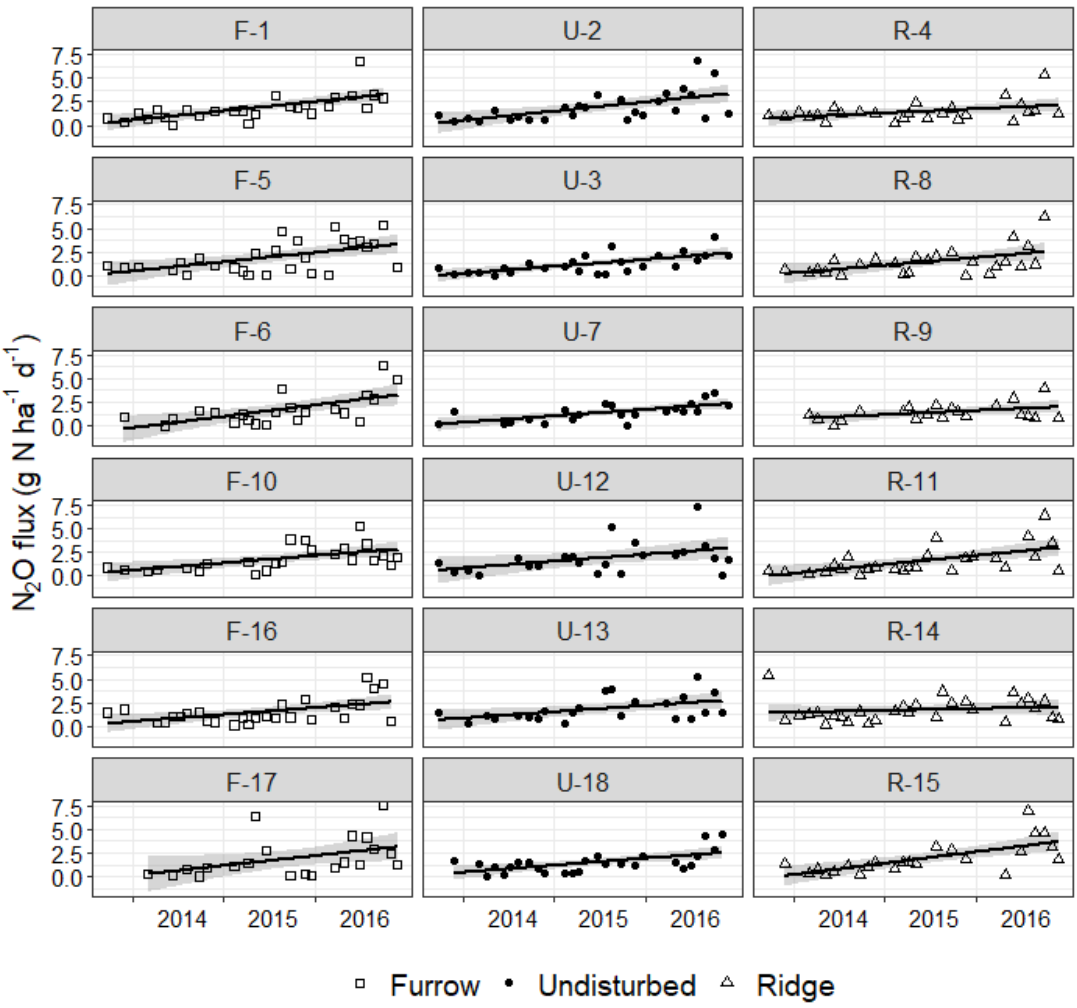

The main variables that control $N_2O$ emissions from soil are soil temperature, nitrate content and soil moisture (Hénault and Germon 2000; Linn and Doran 1984). In particular, soil moisture is influenced by the surface features of the forest plantation; for example, soil was often saturated in the furrows during wet periods, as they act like a drain, and yielded the lowest moisture values during dry periods. The following paragraphs examine potential controls on soil $N_2O$ emissions from Griffin Forest.

Figure 5-9 presents the $N_2O$ fluxes by soil features with and without plot differentiation. It was expected that soil feature would have a significant effect on $N_2O$ fluxes. Examination of the time series differentiated by the C plot and the T plot plots suggests a slightly different trend in the C plot, where $N_2O$ fluxes decrease or are stable in 2014 before increasing later in the time series, compared to the T plot in fluxes which display a more consistent increase throughout the time series. The effect of the interaction between soil feature and plot on the square root transformed $N_2O$ flux was analysed with a 2-way ANOVA, but no significance was found for plot ($p=0.334$), soil feature ($p=0.709$) and their interaction ($p=0.544$).

Figure 5-9. Time series of $N_2O$-N fluxes by surface feature (furrow, undisturbed, ridge) and plot location of chambers (C plot and T plot), followed by data from both plots shown together (total Griffin). The calculated $N_2O$ fluxes (expressed as g $N_2O$ $ha^{-1}$ $d^{-1}$) are courtesy of Forest Research. The trend line was built with a degree 2 polynomial *geom_smooth* model.

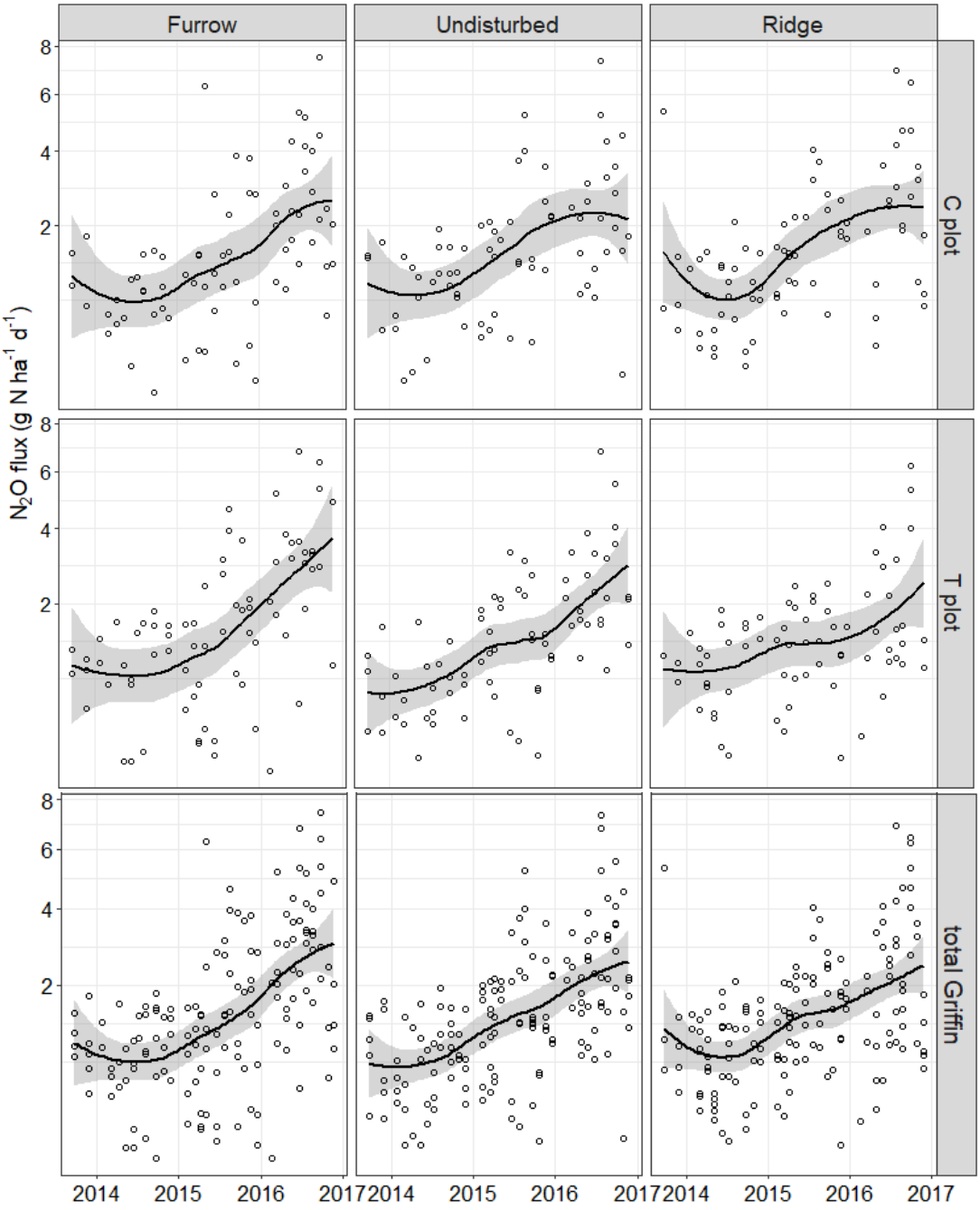


Figure 5-10 summarises soil moisture and soil temperature measured by the chambers on each gas sampling date. Soil moisture varied more between chambers than soil temperature on each sampling occasion as shown by the higher SE values in Figure 5-10. Mean monthly TF depth for each plot is also shown in the figure as a

solid line. TF monthly depth ($p<0.001$) was significantly and positively correlated with soil moisture content. Soil moisture content was also significantly different between plots ($p<0.05$).

In the period 2014-2016 the highest mean monthly soil temperature values occurred in 2016 in both plots (T plot: 11.6±0.3SE; C plot: 12.5±0.2SE). Soil temperature was significantly positively correlated with $N_2O$ fluxes ($p<0.001$). The correlation coefficient calculated between soil moisture and $N_2O$ emissions for all chamber samples was not significant ($p = 0.336$, Spearman's correlation coefficient = 0.041).

Figure 5-10. Mean (n=9) soil moisture ±SE and temperature ±SE measured at 10 cm depth at each static chamber in Griffin Forest in the period January 2014 – November 2016, shown by C plot (Chambers 10-18) and T plot (Chambers 1-9) and year. Data gaps, mainly in winter, occurred when chamber sampling was not conducted due to snow or frozen soil. Mean monthly TF depth (solid line) in each plot is also shown for comparison with soil moisture content.

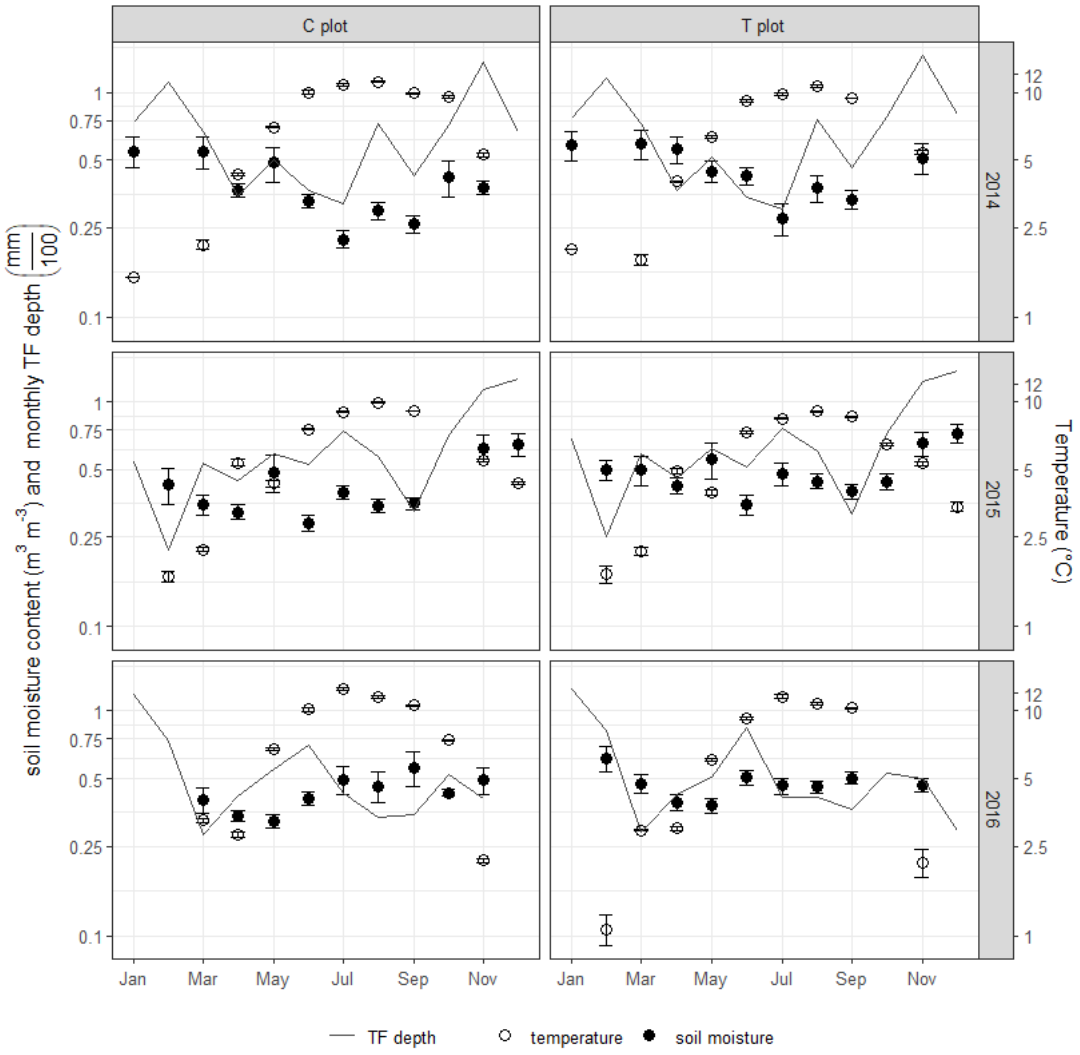

On eight gas sampling occasions between September 2015 and September 2016 soil cores were taken in the proximity of the static chambers and analysed for extractable soil $NH_4$-N and $NO_3$-N (see Figure 5-11). Extractable soil N was not significantly correlated with $N_2O$ fluxes for either N form (Pearson's correlation: p = 0.687 for $NH_4$-N, p = 0.341 for $NO_3$-N).

Figure 5-11. KCl soil IN extractions from soil cores taken from adjacent to the static chambers during the final year of the gas sampling campaign. Results are shown by N form and are expressed per soil dry weight. Missing data in October 2015 for the C plot are due to damage by animals to the valve pipes of chambers which meant completion of sampling and measurements was not possible on that date.

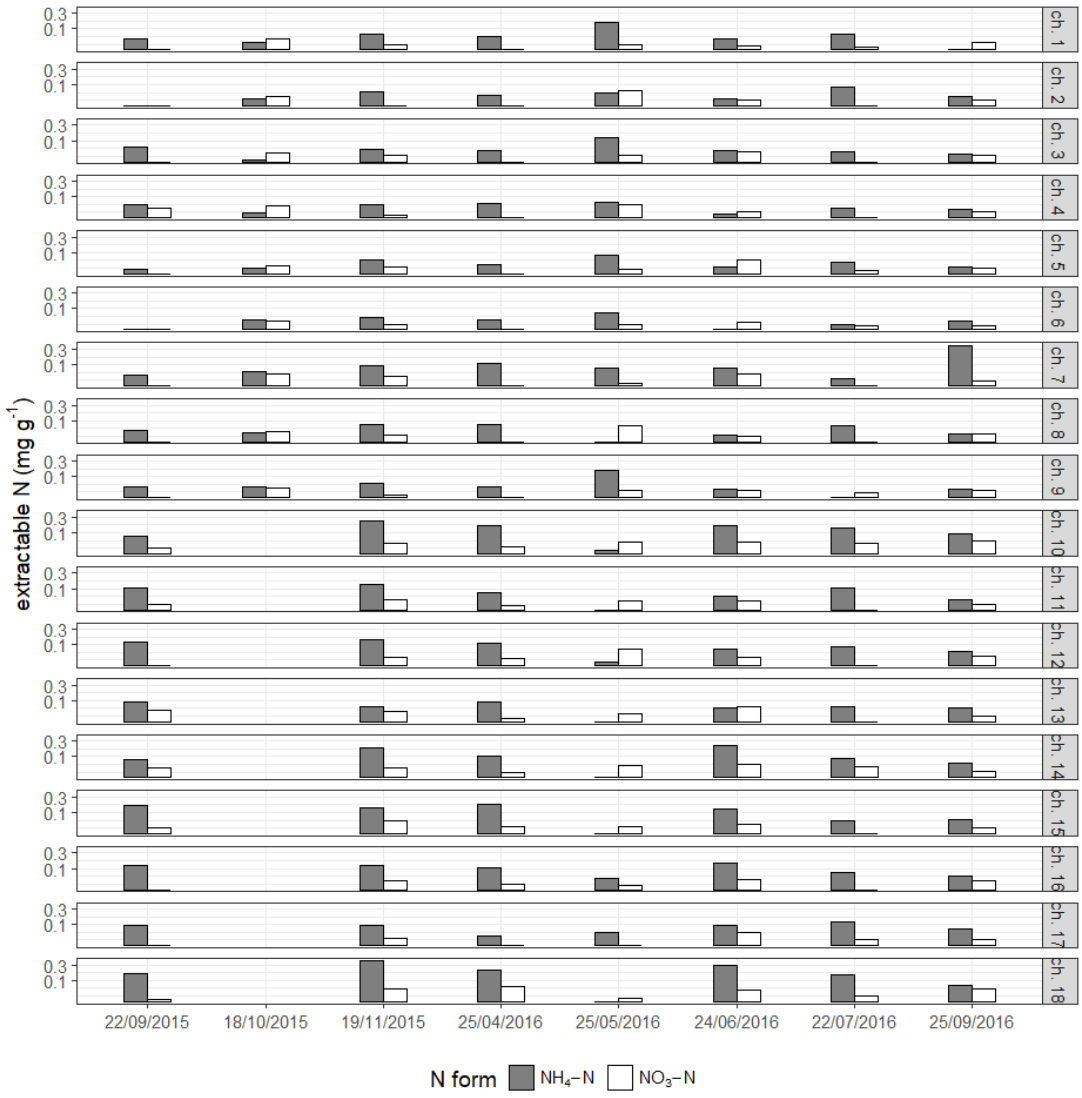


Based on all of the potential predictors of $N_2O$ fluxes described above, a general linear model was built as follows:

$$N_2O_{flux} \sim ℃_{soil} + \text{plot} * \text{soil feature} + \text{soil moisture} + NH_4 - N_{input} + NO_3 - N_{input} \quad \text{(Eq. 5-7)}$$

In the general linear model shown in Eq. 5.7 only soil temperature and $NH_4$-N showed a significant effect on $N_2O$ flux across features and plots ($p<0.001$). The interaction of plot and soil feature was significant only for ridges in the T plot ($p<0.05$).

Table 5-8 summarises the total $N_2O$-N fluxes (kg $ha^{-1}$ $y^{-1}$) as mean values of both the T and C plots by sampling year and weighted by the relative surface area coverage of each soil feature. There was a strong annual variability in mean $N_2O$ fluxes across all soil features, with a maximum across the whole area in 2016 which was over 5 times greater than the flux in 2014. Nitrous oxide flux did not have a significant seasonal pattern (seasonal Mann-Kendall test, package *trend*) although it did show a significant increase with time (Mann-Kendall test, $p<0.05$). The increase of the $N_2O$ fluxes in the period 2014-2016 can be especially related to the increase in soil temperature and $NH_4$-$N_{dep}$, whilst soil moisture did not appear to be a significant predictor.

Table 5-8. Mean $N_2O$-N fluxes across plots (in kg $ha^{-1}$ $y^{-1}$) by soil feature and year. Data courtesy of Dr. Sirwan Yamulki, Forest Research.

| | **2014** | **2015** | **2016** |
|---|---|---|---|
| Furrow (25%) | 0.17 | 0.44 | 0.82 |
| Ridge (25%) | 0.12 | 0.32 | 0.54 |
| Undisturbed (50%) | 0.09 | 0.34 | 0.71 |
| **Mean by % area coverage** | **0.12** | **0.36** | **0.70** |

Comparison with the main cumulative N fluxes in Griffin Forest (as reported in Chapter 3) shows that soil $N_2O$ fluxes and N losses through streamwater are of comparable order of magnitude and represent a small portion of the atmospheric inputs as well as of the IN fluxes to the soil (Figure 5-12).

Despite the relative increase in flux over time it is clear that $N_2O$-N, and generally soil denitrification, only account for a tiny proportion of the N removal from the forest.

Figure 5-12. Main cumulative N fluxes in Griffin compared to the loss as $N_2O$ (red line), September 2013-November 2016. The upper solid line represents the inputs as bulk deposition, the dashed line shows the throughfall, the dotted line shows the streamwater. Ribbons represent the cumulative SE of each cumulative N flux.

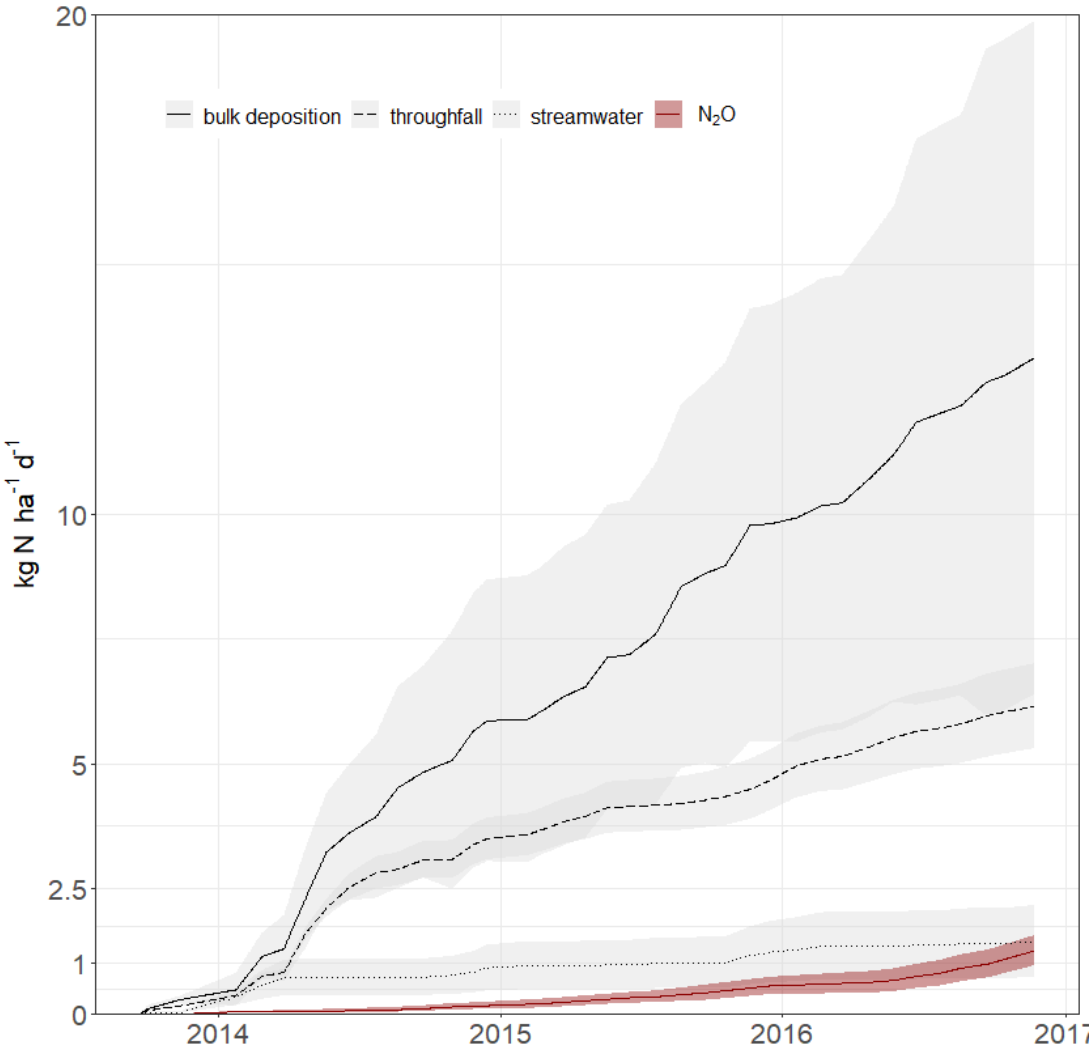

## 5.4 Discussion

As noted previously, the 2017 labelled litter plot sampling at Griffin Forest was preceded by a pilot study in 2015 where a smaller number of cores were examined. The results are not presented in this thesis as the low number of samples does not ensure adequate significance. However some outcomes from the 2015 study will be briefly mentioned in this section.

In previous N-labelled litter experiments involving Sitka spruce, Nair et al. (2017) reported that ~50% of litter mass was lost in 15 months, while van Huysen et al. (2013) found that only 35-45% of litter remained after 2 years, depending on the site.

The results of this experiment show that after 4 years the mean $^{15}N$ recovery in the litter is less than 25% of the applied N (35% in the undisturbed soil). This result is aligned with experiments at comparable time scales (e.g. van Huysen et al. (2013) recovered about 35% of $^{15}N$ labelled Sitka spruce litter; 36% in Zeller (2001) recovery after 876 days in a beech forest), but higher than the recovery of $^{15}N$ labelled beech litter reported by Bimuller et al. (2013) after 30 months (16% of the initial $^{15}N$ atom% excess enrichment). However, in this last study bioturbation was suggested as a cause of a rapid flush of $^{15}N$ from the litter layer within the first 140 days following the application.

Significant differences in $^{15}N$ litter recovery among the three soil profiles may be due to disturbances caused by runoff, especially for furrows, but also for the ridges due to its sloping surface. In estimating total recovery, the three different soil profile types were weighted by their relative surface area, but a likely underestimation of N recovery in furrows and ridges should be considered when comparing the results to other studies.

In contrast to the litter results, a minimal amount of labelled N was found in the soil profiles. This is consistent with studies such as by Inselsbacher and Näsholm (2012) or Oyewole et al. (2016). The first study used for the first time the microdialysis technique, a disturbance-free technique to monitor IN/ON applied in 15 boreal sites in situ. In some of the sites N was applied at 6 and 50 kg N $ha^{-1}$ in the form of $NH_4NO_3$. Unexpectedly, the addition led to an increase in ON diffusion. In all sites over 80% of diffusion on average was dominated by amino-N (74-89%) whilst ammonium and nitrate contributed only 5-15% and 5-11%, respectively. Oyewole et al. (2016) studied

the relationship of soil N diffusive fluxes and root uptake capacity of N-fertilised and N-limited Scots pine stands. They found that amino-N dominated N supply to the plants at the onset and the end of the growing season, and that IN fertilisation decreased root uptake rates leading to potential losses of $NO_3^-$ from the soil by leaching. In both these studies the diffusive flux of amino-N to roots and mycorrhizal hyphae provided around 80% of the total N supply to the plants, whilst IN played a minor role, in contrast to what studies based on traditional ways to estimate soil diffusion via cumulate N uptake and N delivered through mass flow, both of which suffer from uncertainties (Oyewole et al. 2016).

After 4 years, roots retained a relevant amount of $^{15}N$ (up to 11% in the undisturbed soil), particularly in the shallower roots. This recovery should be taken into account when accounting for the potential reallocation of N. Although some studies (e.g. Guo 2013) have reported extremely low $^{15}N$ recovery in plant biomass it should be expected that N has been transferred to other organs. Furthermore, it is known that fine roots have rapid turnover. For example, Park et al. (2008) calculated that the fine root production for conifer stands ranged between 900 and 2,300 kg $ha^{-1}$ $y^{-1}$ and Kitajima (2010) calculated fine root turnover in a mixed conifer ecosystem under Mediterranean climate of about 1000 kg $ha^{-1}$ $y^{-1}$. Santos et al. (2016) studied fine roots C and N mineralisation in a boreal-temperate hardwood forest in North America and reported only ~36% recovery of $^{15}N$ from applied labelled fine roots litter after 2 years. A combination of rapid fine root turnover, translocation to other parts of the tree and a decreasing $^{15}N$ concentration in soil could explain the low figures of $^{15}N$ recovery in roots in the Griffin Forest experiment. The content of $^{15}N$ in roots have all shown to be lower than the roots samples tested in 2015 (~20% recovery) and not shown in this work due to the small number of samples that do not guarantee statistical significance and comparability of the results between the two sampling dates.

Two more factors could have led to underestimation in $^{15}N$ recovery calculations. First, in contrast to the samples from the 2015 pilot study, almost no mycorrhizal tips were present in the 2017 root samples. This was due to the different soil moisture between the two sampling dates. In 2015 most of the soil cores were water-saturated and this allowed a thorough separation of fine roots saving most of the mycorrhizal tips. In 2017 the low soil moisture content made the fine root extraction from the cores more difficult and mycorrhizal tips were lost in the separation. Mycorrhizal tips have been shown to accumulate $^{15}N$ efficiently (Näsholm et al. 2013), with an average annual

increase in the signal of the same order of magnitude as the surface soil (Zeller et al. 2000, Zeller et al. 2001) and higher recoveries than from microbial biomass and fine roots (Pena et al. 2013; Schulze 2013). Secondly, recovery of bacterial biomass was not attempted in the Griffin Forest study due to the low percent of recovery shown in previous studies: Nair et al. (2017) suggest 2-3% as a reasonable figure. All of this leads to the conclusion that, unless there has been major leaching, the N recovered in roots represent a conservative minimum of the N absorbed by the trees at Griffin Forest in the 4-year time period as we would expect similar amounts of N to be translocated elsewhere in the trees.

Korhonen et al. (2013) showed that in a N-saturated spruce forest in Southern Germany, over 80 % of the N deposition was lost in the form of $NO_3$ leaching and $N_2O$ and NO emissions. In other studies, DON was the dominant N species in the percolation water of 16 pine and spruce forests in Finland (Mustajarvi et al. 2008). Whilst in the present study DON in streamwater was not measured, the total IN leaching and soil $N_2O$ fluxes have been shown to account for a very small fraction of the inputs as bulk N deposition and its transfer to the forest soil (see Figure 5-11). Nitrate leaching from forests to streams have shown to be only moderately increased by increased $N_{dep}$ alone, i.e. in the absence of other biotic or climatic perturbations (Aber et al. 2002), although Oyewole et al. (2016) warned of potential risks of nitrate leaching from fertilised stands. Griffin Forest receives a moderate amount of $N_{dep}$, well under the thresholds described by Dise and Wright (1995) of 8-10 kg N $ha^{-1}$ $y^{-1}$ TF $N_{dep}$ under which no leaching from forest soils were measured.

Although a robust model could not be fitted to the $N_2O$ flux data collected at Griffin Forest based on potential predictor variables, the estimated flux did not exceed N losses by leaching throughout the period of $N_2O$ flux monitoring. The mean value of emission from soil denitrification (0.4 kg N $ha^{-1}$ $y^{-1}$) is in line with those reported in Eickenscheidt et al. (2011), where the $N_2O$ flux from a spruce stand was estimated at 0.3±0.1 kg N $ha^{-1}$ $y^{-1}$ based on a $^{15}N$ simulated $N_{dep}$ experiment. In contrast, a study by Ball et al. (2007) on a Sitka spruce chronosequence showed $N_2O$ fluxes of up to one order of magnitude higher for a 30-year-old stand in northern England (4.7±1.2 kg N $ha^{-1}$ $y^{-1}$ in 2001; 1.9±0.5 kg N $ha^{-1}$ $y^{-1}$ in 2002). However, the highest $N_2O$ fluxes were measured when the soil volumetric water content was 0.40-0.43 $m^3$ $m^{-3}$, which rarely occurred. At Griffin Forests, soil moisture content was extremely variable both

in space and in time and this may mean that the ideal moisture content was met less often than in the Ball et al. (2007) study.

It should be remembered that $N_2O$ represents a variable and usually minor fraction of the N lost through denitrification in forests compared to $N_2$ (Kulkarni et al. 2015). However, the ratio of $N_2O$/ $N_2$, i.e. at what extent the oxidation of N is completed, is highly dependent on soil structure and wetness: if a $N_2O$ molecule can readily diffuse from the site of production into an oxygenated pore it has a good chance of being emitted to the atmosphere (Smith et al. 2003). The dry soil conditions described in Griffin Forest might have reasonably increased the ratio $N_2O$/ $N_2$ and the total loss of N might therefore not be directly proportional to the measured increase of $N_2O$ emissions during the 3-year monitoring period.

The soil features typical of Sitka spruce plantations were shown to influence the ON recycling. In particular litter deposited in furrows is easily washed away from runoff and can be considered a net loss of ON from about a quarter of the forest soil surface. Due to the drainage effect in furrows, the soil feature can also interact with the soil moisture content which is an important control on for soil denitrification. Furrows in particular had the most extreme variations in soil moisture which could lead to more mineralisation of ON and nitrification and denitrification processes, ultimately increasing the N losses in gaseous form.

Whilst the two experiments reported in this chapter helped to close the N cycle in a Sitka spruce plantation, collection of additional data could have helped to better refine the estimation of N reallocation. Sampling and analysis of branches, bark and stem wood from the central tree in each $^{15}N$-labelled litter subplot could have provided the missing information on the N reallocation from soil to the plant. Nevertheless, the studies have provided information on N cycling in a forest system representative of a forest type and ecological conditions that are widespread in the UK.

## 5.5 Conclusions

The first objective of this chapter was closing the N cycle for Griffin Forest as a typical temperate plantation forest. It was shown that in a forest plantation under low-middle $N_{dep}$ conditions N losses from the soil compartment are negligible and that most of the ON transferred from the canopy to the soil is rapidly reallocated to the plants, representing the most important N flux to the forest floor from the canopy. It was also shown that $N_2O$ from soil denitrification represents a small fraction of the N input from the atmosphere and is the smallest of the fluxes measured in the plantation, together with the N leaching from streamwater.

The data presented in this chapter, alongside with those presented in the previous chapter, provide useful insights into the different approaches used to estimate the impact of $N_{dep}$ on the forest N cycle, and a comparison of results obtained by similar studies that used different techniques to calculate input and output N fluxes in forests.

# Chapter 6. General discussion and conclusions

Chapter 6 summarises the main results from Chapters 3, 4 and 5 and discusses them in the context of the latest understanding of canopy nitrogen uptake in forests worldwide. The important ecological and societal implications of $N_{dep}$ are highlighted, such as for potential additional carbon sequestration, and suggestions for future research are identified.

## 6.1 Summary of key findings

This research aimed to provide a comprehensive analysis of the interaction between atmospheric nitrogen deposition ($N_{dep}$) and a Sitka spruce plantation. In particular, it focussed on the direct effects of the forest canopy on the atmospheric inorganic nitrogen input and the indirect effects of the canopy uptake (CNU) on the soil N cycle. The key findings are summarised below, with reference to the research objectives and hypotheses outlined in Section 1.4.

1. **$N_{dep}$ uptake by the canopy (Objective 1, H1).** The plantation was shown to intercept and process a high proportion of $N_{dep}$ under low-medium $N_{dep}$ conditions. On average 70% of IN in $N_{dep}$ was taken up by the forest canopy. This result has significant repercussions for the whole forest N cycle as, under low-medium $N_{dep}$ conditions, the canopy acts like a buffer and reduces the effects of IN on soil ecology and N loading in soils, surface waters and aquifers.
2. **$N_{dep}$ uptake at tree scale and at higher $N_{dep}$ rates (Objective 2, H2).** Under the higher $N_{dep}$ conditions of the experimental $N_{dep}$ treatment, individual Sitka spruce trees in the field had similar or higher proportions of $N_{dep}$ uptake during the growing season as under background $N_{dep}$ conditions and at the plot scale. During the winter season the canopy N uptake at the tree scale was lower but did not differ substantially from the retention levels measured at the plot scale under background $N_{dep}$ conditions. Canopy N uptake in winter differed substantially between different N forms: it was much higher for $NH_4$-N (≃64%) than for $NO_3$-N (≃23%-38% depending on methodology). Experiments applying double-labelled $^{15}NH_4{}^{15}NO_3$ solution to branches in situ showed that part of the N uptake as direct foliar uptake/ uptake from the canopy surface occurs within 24 hours following the application.

3. **Consistency of different methodologies for investigating CNU (Objective 2, H2).** The two different methodologies used to assess CNU at the tree scale in the field - (a) N concentration and (b) $^{15}N$ recovery - led to similar estimates of CNU. Comparable CNU results for the summer growing season were also obtained at the tree scale and plot.
4. **$N_{dep}$ and belowground N cycling (Objective 3, H3)**. A small proportion of $N_{dep}$ reaches the ground. Evidence of the effect of the IN input on $N_2O$ fluxes from forest soil was identified, as $NH_4$-N mass flux in bulk deposition had a significant influence on $N_2O$ fluxes. No significant losses of IN through leaching to streamwater were apparent.
5. **Fate of litter ON inputs to the soil (Objective 3, H3)**. High variability in the recovery of $^{15}N$-labelled litter between the plantation soil features was found after 4 years, with a maximum of one third of the applied $^{15}N$ recovered in litter from undisturbed soil, whilst a very small fraction was recovered in soil below furrows, where runoff rapidly removes any deposited litter. Tree roots were the most important pool for $^{15}N$ after the litter layer, suggesting that most of the ON transferred from the canopy, which is also the most important N input to the soil, was to be found in tree above and belowground biomass.

## 6.2 Relevance of the results to forest nitrogen cycling understanding

This study confirmed the high canopy nitrogen uptake (CNU) in Griffin Forest and gave further insight into the seasonal dynamics of CNU and potential transformations between the reduced and oxidised forms of N. The results are more widely applicable since the plantation represents a regionally widespread forest type and is managed, as are the majority of European forests. Furthermore, the study site has relatively low $N_{dep}$ (5-10 kg N $ha^{-1}$ $y^{-1}$), typical of many forests in the UK, Scandinavia and other Baltic countries and in North America.

Since the 1990s most of the studies investigating relations between $N_{dep}$ and C sequestration in forests measured $N_{dep}$ under the canopy or applied extra inorganic N directly to the soil. The results of this PhD research show that this approach would not be adequate to investigate the actual N dynamics in forests, in particular the buffer effect that the canopy has on the IN input, reducing the flux to the forest soil and changing the stoichiometry of the atmospheric N input. Recent publications have

come to similar conclusions for temperate forests in Asia (e.g. Zhang et al. 2015; Liu et al. 2020).

The rates of CNU were shown in this research to be consistent across scales from individual trees to the plot scale, even under increased $N_{dep}$ rate and during the growing season, although some differences in CNU rates occurred in winter between different deposition rates. The general homogeneity of Sitka spruce plantations in the UK suggests that these results can be considered as a reference for the larger scale situation.

Some of the differences found between this study and other experiments can be attributed to the complexity and variability of the forest N cycle, where variations in the quantity and ratios of different N forms in $N_{dep}$ and spatial and ecological differences, including species and climatic constraints, can lead to quite different results in terms of CNU rates and seasonal variability. This complexity and variability partly accounts for the debate surrounding the variability in estimates of the ΔC:ΔN ratio (the ratio of forest C sequestration to $N_{dep}$) that was generated by the paper by Magnani et al. (2007) and which inspired this project.

The significant seasonal variability and the different response of the two inorganic N forms in the interactions with the canopy can be used to indicate how CNU may vary with climate, levels of $N_{dep}$, tree species and other variables. CNU data might contribute to building regional carbon sequestration models or be implemented in wider models which take into account different responses by different forest types at different latitudes and under different $N_{dep}$ rates.

Canopy N uptake mechanisms were investigated in this research by tracking double-labelled $^{15}NH_4{}^{15}NO_3$ solution applied to branches in situ. The results from this experiment indicated that foliar uptake on bark and twig surfaces accounts for part of CNU processes. Due to the particularly dry conditions in which the experiment was conducted, it is possible that the magnitude of the foliar N uptake was underestimated. Also, the experiment did not attempt to quantify the rate of nitrification in the canopy, which other studies suggest is another important process in CNU.

The results from the labelled litter experiment highlighted how organic N is quickly reallocated to the plant. This can be linked with CNU through the assumption that part of the CNU is ultimately fluxed to the soil through the litter and recycled to the trees.

This transfer is better optimised by mycorrhizae than bacteria and efficiently reallocated to the roots (Bukovská et al. 2018). The substantial $^{15}N$ recovery measured in the roots of the deeper soil layer in the labelled litter experiment suggest significant N reallocation to other tree compartments. Even though aboveground tree compartments were not sampled in the labelled litter experiment, there are no indications that the N reallocation detected in the roots should not occur to the aboveground tree biomass. Based on findings from previous studies on broadleaves, it should be possible to detect the total $^{15}N$ deployed in the labelled litter plots at Griffin Forest in bolewood and branches from the central tree in the experimental plots. Such measurements could be included in future work, in order to estimate $^{15}N$ recovery in the tree through direct measurements.

The results from labelled litter experiment and $N_2O$ emissions monitoring reported in Chapter 5 also suggest that the furrows and the other soil features in the plantation (ridges and undisturbed soil) influence the N cycle differently, both in terms N reallocation from litter and $N_2O$ emissions. Although not statistically significant, these apparent effects are likely due to the hydraulic function of the furrows, as conduits for runoff which removes deposited litter and results in a higher soil moisture content compared to ridges and undisturbed soil. Such differences could be investigated in further research with a higher number of samples. This variability in N cycling in different soil features should be taken into account in future labelled litter experiments and in forest models.

Although this study provided a strong quantitative and qualitative description of the interaction of $N_{dep}$ with the forest canopy in a Sitka spruce plantation, the following areas of uncertainty have been identified.

1) Only IN was measured under the canopy. Since it is likely that part of the $IN_{dep}$ was transformed into organic N passing through the canopy, not measuring organic N in throughfall and stemflow below the canopy could have led to overestimation of the canopy N retention.
2) In addition to denitrification in soils, canopy nitrification could be a second process leading to loss of N from forests. Not considering canopy nitrification adds uncertainty both to the N balance and fluxes in forest ecosystems and the magnitude of GHG emissions from forests.

3) Similarly, measurement of $N_2O$ fluxes from soil are not a reliable predictor of total loss of N from forest ecosystems through soil nitrification and denitrification. A significant amount of N could be lost as $N_2$ and lead to an overestimation of N input retained in the forest ecosystem.
4) Recovery of ON in roots in the labelled litter experiment suggests that much of the ON in litter is take up by the trees and reallocated in other parts of the plant in addition to the roots. However, the lack of direct measurements on bolewood, bark, branches and needles means that the magnitude of the reallocation remains uncertain.

## 6.3 Suggestions for further research

Although the PhD research identified some of the main features of canopy N fluxes, further process investigation could represent an important step towards explaining the mechanisms of forest CNU. Bacterial activity in the phyllosphere is an expanding new research direction, since it was proven that nitrification occurs in the canopy. Their activity could potentially account for a substantial part of the CNU which is not absorbed via foliar uptake, explaining how this “hidden CNU” participates in the N cycle and enabling quantification of its contribution to the fixation of extra C. The potential release of further $N_2O$ by nitrification in the canopy, not accounted for by measurements at soil level, could also counteract the beneficial effects of $CO_2$ sequestration.

The investigation in this PhD of forest soil N dynamics indicated the importance of organic matter as a source of N in a Sitka spruce plantation. However, uncertainties due to possible loss or translocation of part of the added labelled litter due to runoff and the use of the litter by multiple trees would require further investigation in order to quantify more accurately the organic N uptake by trees. Comprehensive sampling of the branches, bolewood and roots of the central tree in the labelled litter subplots would allow estimation of the amount of organic N absorbed by the trees.

The research focused on the N cycle in order to inform more accurate estimates of the response of forests to $N_{dep}$ in terms of $\Delta C{:}\Delta N$. Quantifying the tree C storage response to $N_{dep}$ is the next step to complete the picture. The results from this research can be incorporated into parameterisation of process-based models to predict forest response to $N_{dep}$, management and climate changes. Relevant models used to assess the impact of N-deposition, elevated $CO_2$ and climate change on C

sequestration in temperate forests with different degrees of complexity are BASFOR, Century and BGC (Levy et al. 2004, Van Oljien et al. 2005).

## 6.4 Implications of the research results at the national level

At around 13%, the forest cover in the UK is among the lowest of any country in Europe (The UK Forestry Standard, 2017). Sitka spruce still plays a major role in UK forestry, due to its high adaptability and high productivity on marginal land. According to the suitability scenarios presented by Broadmeadow et al. (2003), Sitka spruce is expected to be the most suitable forest species for commercial activity in Northern England, Wales and Scotland by 2050. However, conifer plantations have been identified as a cause of freshwater acidification at acidic and acid sensitive sites (Reynolds 2004). In contrast, this study showed that in areas of low-medium $N_{dep}$, plantations may act as a N sink by consistently reducing and/or not increasing the N concentrations and fluxes in streamwater. The use of Sitka spruce in combination with other species could contribute to reducing the impact of N in moderate $N_{dep}$ areas counterbalancing the negative effects on freshwater pH.

The recently published Scotland's Forestry Strategy 2019-2029 (The Scottish Government 2019) includes the target of increasing forest cover to 21% of the total area of Scotland by 2032. Meeting this target will help to achieve the following related objectives to: 1) increase the contribution of forests and woodlands to Scotland's sustainable and inclusive economic growth; 2) improve the resilience of Scotland's forests and woodlands and increase their contribution to a healthy and high quality environment; and 3) increase the use of Scotland's forest and woodland resources to enable more people to improve their health, well-being and life chances.

In relation to objective 1), Sitka spruce will surely remain a key species for forestry, considering that the import of wood and wood products into the UK is predicted to increase to 78% by 2050 and that the main wood fibre produced in Scotland for downstream processing and manufacture is predominantly softwood from Sitka spruce. However, climate change is likely to lead to a differentiation in terms of species to increase the resilience of Scottish forests. The expected warmer climate will improve the tree growth particularly in Southern and Eastern Scotland, but at the same time, drought, especially in Eastern Scotland may create unfavourable conditions for Sitka spruce (Ray 2008). Petr el al. (2015) point out that the expected

drier future scenarios could reduce the traditional ecosystem services more in the lowlands than in the uplands, with a reduction of total carbon uptake by Sitka spruce up to 31% in the lowlands and 41% in the uplands by 2080. However, climate change will bring opportunities for other ecosystem services. The vision of the Forestry Strategy goes well beyond mere economic growth, and takes into account the need to increase environmental quality and biodiversity, as well as the potential positive added aesthetic value of forests for tourism, which is an important component of the economy in rural Scotland.

The positive interactions of Sitka spruce plantations in N cycling described in this research, and also consideration of forest N interception and carbon sequestration, should be taken into account in landscape planning as they are positive externalities which add to the productive function of commercial plantations.

## 6.5 Relevance of the work to nitrogen and carbon cycling in a regional/global perspective

In Chapter 4 the findings of this study on the function of forest canopy to retain atmospheric IN deposition were compared with figures from other studies reported in the literature. This section aims to expand on the global consequences of the changes in N cycle induced by anthropogenic activity and the role of forests in C and N fluxes and stores.

In their 2009 paper Rockström et al. introduced the concept of “planetary boundaries”. They argued that since the Industrial Revolution the relative stability reached by the planet’s environment during the Holocene has been challenged by human pressure. Planetary boundaries define the safe operating space for humanity and are associated with Earth’s biophysical processes. Among the nine planetary boundaries identified by Rockström et al. interference with the N cycle was one of the three identified to have already widely surpassed the safety threshold. In the Introduction chapter of this thesis, the link was noted between the development of inorganic N fertilisers essential for increasing agricultural production to feed the growing global human population and the increased reactive N in the biosphere. Concurrently, pollution from reactive N poses a threat to health, water and air quality, ecosystems and climate through emission of the powerful GHG $N_2O$ (Sutton et al. 2011). The results of this PhD research contribute in a small way in lowering these risks through

demonstrating the positive effect of Sitka spruce forest in removing a high proportion of IN in atmospheric deposition under low-medium deposition conditions. This removal is an especially important effect in the current time, as it is known that nitric oxide and ammonia emissions fuel fine particles and tropospheric $O_3$ formation, which exacerbate pulmonary disease (Galloway 2019), and Conticini et al. (2020) considered air pollution as an additional co-factor of the particularly high mortality rate in Northern Italy from Severe Acute Respiratory Syndrome CoronaVirus 2 (SARS-CoV-2). The scrubbing effect of the forest canopy on atmospheric $N_r$ actively removes reactive nitrogen from the biosphere, and as a direct consequence less IN reaches the soil and surface and groundwaters. In addition to the removal of reactive N by the biosphere, it should be noted that under elevated N deposition conditions, $N_2O$ emissions could be increased by the presence of N fixing trees at a rate that could eventually exacerbate climate change despite $CO_2$ sequestration by plant biomass (Kou-Giesbrecht & Menge, 2019).

There is considerable ongoing scientific, political and societal interest and discussion concerning the role of tree planting and restoration in mitigating climate change by drawing down atmospheric $CO_2$. The paper by Bastin et al. (2019) sparked debate around the extent of tree restoration and its potential carbon storage. They stated that worldwide there is space for 0.9 billion ha of tree restoration which could store 205 gigatonnes of carbon, comprising one of the most effective climate change solutions to date. Their estimates of tree restoration area and its C storage potential are much higher than reported in previous studies (Lewis et al. 2019). A number of their assumptions have also been questioned, including: underestimation of the carbon already present; overestimation of how much extra carbon a forest might store when replacing an existing biome; and the countereffects of increased tree cover from reduced albedo and higher evapotranspiration that could further reduce the positive effects of carbon sequestration on climate change (Friedlingstein et al. 2019; Veldman et al. 2019). Ultimately, even assuming that forest restoration can absorb a relevant fraction of the atmospheric $CO_2$ emissions to date, it will not affect future emissions and hence cannot be seen as an “ultimate solution” to global warming (Friedlingstein et al. 2019).

Even if the figures in Bastin et al. (2019) require revision, they should not be neglected. The importance of forests as a carbon sink is recognised beyond the scientific community and is part of International (see Article 5.1 of the Paris

Agreement, 2015) and national (e.g. The UK Forestry Standard, 2017) policy, as well as social debate (e.g. Project Drawdown, which includes action plans to reduce GHG emissions from agricultural and forestry activities that currently account for 24% of global emissions). Furthermore, increasing tree cover, especially in temperate areas, would potentially lead to other social and environmental benefits (Grainger et al. 2019), including biodiversity conservation, local livelihoods, economic gains, food security, well-being (Chazdon and Brancalion, 2019).

A better understanding of forest N cycling is important for understanding the potential impacts such an expansion of tree cover might have on ecosystem N and C stores and fluxes, with implications for carbon sequestration, ecosystems and downstream water quality. The present study indicates that Sitka spruce plantations have the potential to buffer atmospheric reactive N in low to medium $N_{dep}$ conditions. As a result, several beneficial effects can be expected, including: 1) less atmospheric IN enters into water bodies; 2) $N_2O$ emissions are reduced due to the combined action of less $IN_{dep}$ reaching the soil and the indirect effect of tree roots on soil moisture conditions and uptake of IN reducing its availability to soil bacteria; and 3) C storage is potentially increased, depending on other ecological conditions. Nevertheless, it is important to recognise that the interaction between forests and C and N biogeochemical cycles varies spatially, and thus each solution, including the choice of species, should reflect the specific regional ecological features following the “think globally, act locally” principle.

# References


Aber, J. D., S. V. Ollinger, C. T. Driscoll, G. E. Likens, R. T. Holmes, R. J. Freuder, and C. L. Goodale. 2002. Inorganic Nitrogen Losses from a Forested Ecosystem in Response to Physical, Chemical, Biotic and Climatic Perturbations. Ecosystems. **5**:648-658.

Aber, J., W. McDowell, K. Nadelhoffer, A. Magill, G. Berntson, M. Kamakea, S. McNulty, W. Currie, L. Rustad, and I. Fernandez. 1998. Nitrogen saturation in temperate forest ecosystems - Hypotheses revisited. Bioscience **48**:921-934.

Ackerman, D., D. B. Millet, and X. Chen. 2019. Global Estimates of Inorganic Nitrogen Deposition Across Four Decades. Global Biogeochemical Cycles **33**:100-107.

Adriaenssens, S., J. Staelens, K. Wuyts, R. Samson, K. Verheyen, and P. Boeckx. 2012. Retention of Dissolved Inorganic Nitrogen by Foliage and Twigs of Four Temperate Tree Species. Ecosystems **15**:1093-1107.

Ambus, P. and S. Zechmeister-Boltenstern. 2007. Denitrification and N-Cycling in forest ecosystems. Pages 343-358 *in* S.J. Ferguson, W.E. Newton, editors, Biology of the Nitrogen Cycle, Elsevier, Amsterdam

Arnold, G., and A. van Diest. 1991. Nitrogen supply, tree growth and soil acidification. Fertilizer Research **27**:29-38.

Averill C., B. Turner, and A. Finzi. 2014. Mycorrhiza-mediated competition between plants and decomposers drives soil carbon storage. Nature **505**:543-545.

Avila, A., L. Aguillaume, S. Izquieta-Rojano, H. Garcia-Gomez, D. Elustondo, J. M. Santamaria, and R. Alonso. 2017. Quantitative study on nitrogen deposition and canopy retention in Mediterranean evergreen forests. Environmental Science and Pollution Research **24**:26213-26226.

Balestrini, R., S. Arisci, M. C. Brizzio, R. Mosello, M. Rogora, and A. Tagliaferri. 2007. Dry deposition of particles and canopy exchange: Comparison of wet, bulk and throughfall deposition at five forest sites in Italy. Atmospheric Environment **41**:745-756.

Barnes, R. T., P. A. Raymond, and K. L. Casciotti. 2008. Dual isotope analyses indicate efficient processing of atmospheric nitrate by forested watersheds in the northeastern US. Biogeochemistry **90**:15-27.

Bastin, J.-F., Y. Finegold, C. Garcia, D. Mollicone, M. Rezende, D. Routh, C. M. Zohner, and T. W. Crowther. 2019. The global tree restoration potential. Science **365**:76-79.

Beeckman, F., H. Motte, and T. Beeckman. 2018. Nitrification in agricultural soils: impact, actors and mitigation. Current Opinion in Biotechnology **50**:166-173.

Berry, Z. C., J. C. White, and W. K. Smith. 2014. Foliar uptake, carbon fluxes and water status are affected by the timing of daily fog in saplings from a threatened cloud forest. Tree Physiology **34**:459-470.

Bimuller, C., P. S. Naumann, F. Buegger, M. Dannenmann, B. Zeller, M. von Lutzow, and I. Kogel-Knabner. 2013. Rapid transfer of $^{15}N$ from labeled beech leaf litter to functional soil organic matter fractions in a Rendzic Leptosol. Soil Biology & Biochemistry **58**:323-331.

Bourgeois, I., J. C. Clement, N. Caillon, and J. Savarino. 2019. Foliar uptake of atmospheric nitrate by two dominant subalpine plants: insights from in situ triple-isotope analysis. New Phytologist **223**:1784-1794.

Bouwman, A. F. 1998. Environmental science - Nitrogen oxides and tropical agriculture. Nature **392**:866-867.

Bouwman, A. F., D. S. Lee, W. A. H. Asman, F. J. Dentener, K. W. VanderHoek, and J. G. J. Olivier. 1997. A global high-resolution emission inventory for ammonia. Global Biogeochemical Cycles **11**:561-587.

Bowatte, S., P. C. D. Newton, P. Theobald, S. Brock, C. Hunt, M. Lieffering, S. Sevier, S. Gebbie, and D. W. Luo. 2014. Emissions of nitrous oxide from the leaves of grasses. Plant and Soil **374**:275-283.

Bowatte, S., P. C. D. Newton, S. Brock, P. Theobald, and D. Luo. 2015. Bacteria on leaves: a previously unrecognised source of $N_2O$ in grazed pastures. Isme Journal **9**:265-267.

Boyce, R. L., A. J. Friedland, C. P. Chamberlain, and S. R. Poulson. 1996. Direct canopy nitrogen uptake from $^{15}N$-labeled wet deposition by mature red spruce. Canadian Journal of Forest Research-Revue Canadienne De Recherche Forestiere **26**:1539-1547.

British Standard. 1981. Methods of measurement of liquid flow in open channels. In Method using thin-plate weirs **39**.

Broadmeadow, M., D. Ray, L. Sing, and L. Poulson. 2003. Climate change and British woodland: what does the future hold?, Forest Research, Edinburgh.

Buckley, S., R. Brackin, T. Näsholm, S. Schmidt, and S. Jamtgard. 2017. Improving in situ recovery of soil nitrogen using the microdialysis technique. Soil Biology & Biochemistry **114**:93-103.

Bukovská, P., M. Bonkowski, T. Konvalinková, O. Beskid, M. Hujslová, D. Püschel, V. Řezáčová, M. S. Gutiérrez-Núñez, M. Gryndler, and J. Jansa. 2018. Utilization of organic nitrogen by arbuscular mycorrhizal fungi-is there a specific role for protists and ammonia oxidizers? Mycorrhiza **28**:465-465.

Burkhardt, J., and M. Hunsche. 2013. "Breath figures" on leaf surfaces-formation and effects of microscopic leaf wetness. Frontiers in Plant Science **4**:9.

Butterbach-Bahl K., and R. Kiese. 2005. Significance of Forests as Sources for $N_2O$ and NO *in* D. Binkley, and O. Menyailo, editors. Tree Species Effects on Soils: Implications for Global Change. NATO Science Series IV: Earth and Environmental Sciences, vol 55. Springer, Dordrecht

Butterbach-Bahl, K., Gundersen, P., Ambus, P., Augustin, J., Beier, C., Boeckx, P., Dannenmann, M., Sanchez Gimeno, B., Ibrom, A., Kiese, R., Kitzler, B., Rees, R. M., Smith, K. A., Stevens, C., Vesala, T. and S. Zechmeister-Boltenstern. 2011. Nitrogen processes in terrestrial ecosystems. Pages 99–125 *in* M. A. Sutton, C. M. Howard, J. W. Erisman, G. Billen, A. Bleeker, P. Grennfelt, H. van Grisven and B. Grizzetti, editors. The European Nitrogen Assessment : Sources, Effects and Policy Perspectives. Cambridge, UK: Cambridge University Press.

Butterbach-Bahl, K., Willibald G., and H. Papen. 2002. Soil core method for direct simultaneous determination of $N_2$ and $N_2O$ emissions from forest soils. Plant and Soil **240**:105-116.

Cape, J. N., A. Dunster, A. Crossley, L. J. Sheppard, and F. J. Harvey. 2001. Throughfall chemistry in a Sitka spruce plantation in response to six different simulated polluted mist treatments. Water Air and Soil Pollution **130**:619-624.

Cape, J. N., L. J. Sheppard, A. Crossley, N. van Dijk, and Y. S. Tang. 2010. Experimental field estimation of organic nitrogen formation in tree canopies. Environmental Pollution **158**:2926-2933.

Castaldi, S., A. Carfora, A. Fiorentino, A. Natale, A. Messere, F. Miglietta, and M. F. Cotrufo. 2009. Inhibition of net nitrification activity in a Mediterranean woodland: possible role of chemicals produced by *Arbutus unedo*. Plant and Soil **315**:273-283.

Centre for Hidrology & Ecology. 2012. Review of Transboundary Air Pollution (RoTAP). Contract Report to the Department for Centre for Hidrology&Ecology. 2017. EMEP4UK.

Chazdon, R., and P. Brancalion. 2019. Restoring forests as a means to many ends. Science **365**:24-25.

Chen, T., O. Oenema, J. Z. Li, T. Misselbrook, W. X. Dong, S. P. Qin, H. J. Yuan, X. X. Li, and C. S. Hu. 2019. Seasonal variations in $N_2$ and $N_2O$ emissions from a wheat-maize cropping system. Biology and Fertility of Soils **55**:539-551.

Chiwa, M., A. Crossley, L. J. Sheppard, H. Sakugawa, and J. N. Cape. 2004. Throughfall chemistry and canopy interactions in a Sitka spruce plantation sprayed with six different simulated polluted mist treatments. Environmental Pollution **127**:57-64.

Choularton, T. W., M. J. Gay, A. Jones, D. Fowler, J. N. Cape, and I. D. Leith. 1988. The Influence of Altitude on Wet Deposition Comparison between Field-Measurements at Great Dun Fell and the Predictions of a Seeder Feeder Model. Atmospheric Environment **22**:1363-1371.

Ciais, P., Sabine, C., Bala, G., Bopp, L., Brovkin, V., Canadell, J., Chhabra, A., DeFries, R., Galloway, J., Heimann, M., Jones, C., Le Quéré, C., Myneni, R. B., Piao, S., and Thornton, P. 2013. Carbon and Other Biogeochemical Cycles *in*: Climate Change 2013: The Physical Science Basis. Contribution of Working Group I to the Fifth Assessment Report of the Intergovernmental Panel on Climate Change. Stocker, T. F., Qin, D., Plattner, G.-K., Tignor, M., Allen, S. K., Boschung, J., Nauels, A., Xia, Y., Bex, V., and Midgley, P. M., editors. Cambridge, UK: Cambridge University Press.

Clement, R. J., P. G. Jarvis, and J. B. Moncrieff. 2012. Carbon dioxide exchange of a Sitka spruce plantation in Scotland over five years. Agricultural and Forest Meteorology **153**:106-123.

Cloutier, M. L., A. Bhowmik, T. H. Bell, and M. A. Bruns. 2019. Innovative technologies can improve understanding of microbial nitrogen dynamics in agricultural soils. Agricultural & Environmental Letters **4**:6.

Cole, D. W. 1981. Nitrogen uptake and translocation by forest ecosystems. Ecological Bulletins **33**:219-232.

Conen, F., A. Zerva, D. Arrouays, C. Jolivet, P. G. Jarvis, J. Grace, and M. Mencuccini. 2005. The carbon balance of forest soils: detectability of changes in soil carbon stocks in temperate and Boreal forests. SEB Exp Biol Ser:235-249.

Conticini, E., B. Frediani, and D. Caro. 2020. Can atmospheric pollution be considered a co-factor in extremely high level of SARS-CoV-2 lethality in Northern Italy? Environmental Pollution **261**:3.

Corbeels, M., A. M. O'Connell, T. S. Grove, D. S. Mendham, and S. J. Rance. 2003. Nitrogen release from eucalypt leaves and legume residues as influenced by their biochemical quality and degree of contact with soil. Plant and Soil **250**:15-28.

Craig, G. Y. Geology of Scotland. 1925, Edinburgh: Scottish Academics.

Dail, D. B., D. Y. Hollinger, E. A. Davidson, I. Fernandez, H. C. Sievering, N. A. Scott, and E. Gaige. 2009. Distribution of $^{15}N$ tracers applied to the canopy of a mature spruce-hemlock stand, Howland, Maine, USA. Oecologia **160**:589-599.

Dail, D. B., D. Y. Hollinger, E. A. Davidson, I. Fernandez, H. C. Sievering, N. A. Scott, and E. Gaige. 2009. Distribution of $^{15}N$ tracers applied to the canopy of a mature spruce-hemlock stand, Howland, Maine, USA. Oecologia **160**:589-599.

Dammgen, U., J. W. Erisman, J. N. Cape, L. Grunhage, and D. Fowler. 2005. Practical considerations for addressing uncertainties in monitoring bulk deposition. Environmental Pollution **134**:535-548.

Dawson, T. E., and G. R. Goldsmith. 2018. The value of wet leaves. New Phytologist **219**:1156-1169.

De Schrijver, A., K. Verheyen, J. Mertens, J. Staelens, K. Wuyts, and B. Muys. 2008. Nitrogen saturation and net ecosystem production. Nature **451**:E1.

de Vries, W., S. Solberg, M. Dobbertin, H. Sterba, D. Laubhahn, G. J. Reinds, G.-J. Nabuurs, P. Gundersen, and M. A. Sutton. 2008. Ecologically implausible carbon response? Nature **451**:E1-E3.

Dentener, F., J. Drevet, J. F. Lamarque, I. Bey, B. Eickhout, A. M. Fiore, D. Hauglustaine, L. W. Horowitz, M. Krol, U. C. Kulshrestha, M. Lawrence, C. Galy-Lacaux, S. Rast, D. Shindell, D. Stevenson, T. Van Noije, C. Atherton, N. Bell, D. Bergman, T. Butler, J. Cofala, B. Collins, R. Doherty, K. Ellingsen, J. Galloway, M. Gauss, V. Montanaro, J. F. Muller, G. Pitari, J. Rodriguez, M. Sanderson, F. Solmon, S. Strahan, M. Schultz, K. Sudo, S. Szopa, and O. Wild. 2006. Nitrogen and sulfur deposition on regional and global scales: A multimodel evaluation. Global Biogeochemical Cycles **20**: GB4003

Dirnböck, T., G. Pröll, K. Austnes, J. Beloica, B. Beudert, R. Canullo, A. De Marco, M. F. Fornasier, M. Futter, K. Goergen, U. Grandin, M. Holmberg, A. J. Lindroos, M. Mirtl, J. Neirynck, T. Pecka, T. M. Nieminen, J. F. Nordbakken, M. Posch, G. J. Reinds, E. C. Rowe, M. Salemaa, T. Scheuschner, F. Starlinger, A. K. Uzieblo, S. Valinia, J. Weldon, W. G. W. Wamelink, and M. Forsius. 2018. Currently legislated decreases in nitrogen deposition will yield only limited plant species recovery in European forests. Environmental Research Letters **13**: 12.

Dise, N. B., and R. F. Wright. 1995. Nitrogen Leaching from European Forests in Relation to Nitrogen Deposition. Forest Ecology and Management **71**:153-161.

Dodds, W. K., A. J. Burgin, A. M. Marcarelli, and E. A. Strauss. 2017. Chapter 32 - Nitrogen Transformations. Pages 173-196 *in* G. A. Lamberti and F. R. Hauer, editors. Methods in Stream Ecology (Third Edition). Academic Press.

Dore, A. J., M. R. Theobald, M. Kryza, M. Vieno, S. Y. Tang, and M. A. Sutton. 2008. Modelling the deposition of reduced nitrogen at different scales in the United Kingdom. Air Pollution Modeling and Its Application **XIX**:127-135.

Duckstein, L., M. M. Fogel, and J. L. Thames. 1973. Elevation effects on rainfall: A stochastic model. Journal of Hydrology **18**:21-35.

Edmonds, R. L., T. B. Thomas, and R. D. Blew. 1995. Biogeochemistry of an old-growth forested watershed, Olympic National-Park, Washington. Water Resources Bulletin **31**:409-419.

Eickenscheidt, N., R. Brumme, and E. Veldkamp. 2011. Direct contribution of nitrogen deposition to nitrous oxide emissions in a temperate beech and spruce forest - a $^{15}N$ tracer study. Biogeosciences **8**:621-635.

Engardt, M., D. Simpson, M. Schwikowski, and L. Granat. 2017. Deposition of sulfur and nitrogen in Europe 1900–2050. Model calculations and comparison to historical observations. Tellus B: Chemical and Physical Meteorology **69**:1328945.

Entwistle, E. M., D. R. Zak, and W. A. Argiroff. 2018. Anthropogenic N deposition increases soil C storage by reducing the relative abundance of lignolytic fungi. Ecological Monographs **88**:225-244.

Erisman, J. W., M. A. Sutton, J. Galloway, Z. Klimont, and W. Winiwarter. 2008. How a century of ammonia synthesis changed the world. Nature Geoscience **1**:636-639.

Etzold, S., M. Ferretti, G. J. Reinds, S. Solberg, A. Gessler, P. Waldner, M. Schaub, D. Simpson, S. Benham, K. Hansen, M. Ingerslev, M. Jonard, P. E. Karlsson, A. J. Lindroos, A. Marchetto, M. Manninger, H. Meesenburg, P. Merila, P. Nojd, P. Rautio, T. G. M. Sanders, W. Seidling, M. Skudnik, A. Thimonier, A. Verstraeten, L. Vesterdal, M. Vejpustkova, and W. de Vries. 2020. Nitrogen deposition is the most important environmental driver of growth of pure, even-aged and managed European forests. Forest Ecology and Management **458**:117762

Fang, Y., K. Koba, A. Makabe, C. Takahashi, W. Zhu, T. Hayashi, A. A. Hokari, R. Urakawa, E. Bai, B. Z. Houlton, D. Xi, S. Zhang, K. Matsushita, Y. Tu, D. Liu, F. Zhu, Z. Wang, G. Zhou, D. Chen, T. Makita, H. Toda, X. Liu, Q. Chen, D. Zhang, Y. Li, and M. Yoh. 2015. Microbial denitrification dominates nitrate losses from forest ecosystems. Proceedings of the National Academy of Sciences of the United States of America **112**:1470-1474.

Fassbinder, J. J., N. M. Schultz, J. M. Baker, and T. J. Griffis. 2013. Automated, Low-Power Chamber System for Measuring Nitrous Oxide Emissions. Journal of Environmental Quality **42**:606-614.

Fenn, M. E., C. S. Ross, S. L. Schilling, W. D. Baccus, M. A. Larrabee, and R. A. Lofgren. 2013. Atmospheric deposition of nitrogen and sulfur and preferential canopy consumption of nitrate in forests of the Pacific Northwest, USA. Forest Ecology and Management **302**:240-253.

Fernandez, V., and T. Eichert. 2009. Uptake of hydrophilic solutes through plant leaves: current state of knowledge and perspectives of foliar fertilization. Critical Reviews in Plant Sciences **28**:36-68.

Finzi, A. C., D. J. P. Moore, E. H. DeLucia, J. Lichter, K. S. Hofmockel, R. B. Jackson, H. S. Kim, R. Matamala, H. R. McCarthy, R. Oren, J. S. Pippen, and W. H.

Schlesinger. 2006. Progressive nitrogen limitation of ecosystem processes under elevated $CO_2$ in a warm-temperate forest. Ecology **87**:15-25.

Flechard, C. R., M. van Oijen, D. R. Cameron, W. de Vries, A. Ibrom, N. Buchmann, N. B. Dise, I. A. Janssens, J. Neirynck, L. Montagnani, A. Varlagin, D. Loustau, A. Legout, K. Ziemblinska, M. Aubinet, M. Aurela, B. H. Chojnicki, J. Drewer, W. Eugster, A. J. Francez, R. Juszczak, B. Kitzler, W. L. Kutsch, A. Lohila, B. Longdoz, G. Matteucci, V. Moreaux, A. Nefte, J. Olejnik, M. J. Sanz, J. Siemens, T. Vesala, C. Vincke, E. Nemitz, S. Zechmeister-Boltenstern, K. Butterbach-Bahl, U. M. Skiba, and M. A. Sutton. 2020. Carbon-nitrogen interactions in European forests and semi-natural vegetation - Part 2: Untangling climatic, edaphic, management and nitrogen deposition effects on carbon sequestration potentials. Biogeosciences **17**:1621-1654.

Focht D.D. 1981. Soil Denitrification. Pages 499-516 *in* Lyons J.M., Valentine R.C., Phillips D.A., Rains D.W., Huffaker R.C., editors. Genetic Engineering of Symbiotic Nitrogen Fixation and Conservation of Fixed Nitrogen. Springer, Boston, MA

Forestry Commission. 2011. National Forest Inventory Woodland Area Statistics: Scotland 17. www.forestry.gov.uk (11/10/2017).

Forestry Commission. 2017. Forestry statistics and Forestry in facts and figures. 2017. https://www.forestry.gov.uk/forestry/infd-7aqdgc (accessed 30/05/2020).

Forestry Commission. 2017. The UK Forestry Standard, Edinburgh.

Forestry Commission. 2017. The UK Forestry Standard. Edinburgh

Fowler, Z. K., M. B. Adams, and W. T. Peterjohn. 2015. Will more nitrogen enhance carbon storage in young forest stands in central Appalachia? Forest Ecology and Management **337**:144-152.

Friedlingstein, P., M. Allen, J. G. Canadell, G. P. Peters, and S. I. Seneviratne. 2019. Comment on “The global tree restoration potential”. Science **366**:eaay8060.

Gagkas, Z., K. V. Heal, M. Vieno, T. R. Nisbet, and N. Stuart. 2011. Assessing the effect of broadleaf woodland expansion on acidic dry deposition and streamwater acidification. Forest Ecology and Management **262**:1434-1442.

Gaige, E., D. B. Dail, D. Y. Hollinger, E. A. Davidson, I. J. Fernandez, H. Sievering, A. White, and W. Halteman. 2007. Changes in canopy processes following whole-

forest canopy nitrogen fertilization of a mature spruce-hemlock forest. Ecosystems **10**:1133-1147.

Gallagher, M. W., K. Beswick, T. W. Choularton, H. Coe, D. Fowler, and K. Hargreaves. 1992. Measurements and modelling of cloudwater deposition to moorland and forests. Environmental Pollution **75**:97-107.

Galloway, J. N., F. J. Dentener, D. G. Capone, E. W. Boyer, R. W. Howarth, S. P. Seitzinger, G. P. Asner, C. C. Cleveland, P. A. Green, E. A. Holland, D. M. Karl, A. F. Michaels, J. H. Porter, A. R. Townsend, and C. J. Vörösmarty. 2004. Nitrogen cycles: past, present, and future. Biogeochemistry **70**:153-226.

Garten, C. T., A. B. Schwab, and T. L. Shirshac. 1998. Foliar retention of $^{15}N$ tracers: implications for net canopy exchange in low- and high-elevation forest ecosystems. Forest Ecology and Management **103**:211-216.

Gentilesca, T., M. Vieno, M. P. Perks, M. Borghetti, and M. Mencuccini. 2013. Effects of Long-Term Nitrogen Addition and Atmospheric Nitrogen Deposition on Carbon Accumulation in Picea sitchensis Plantations. Ecosystems **16**:1310-1324.

Gilliam, F. S., and M. B. Adams. 2011. Effects of Nitrogen on Temporal and Spatial Patterns of Nitrate in Streams and Soil Solution of a Central Hardwood Forest. ISRN Ecology:1-9.

Gilliam, F. S., D. A. Burns, C. T. Driscoll, S. D. Frey, G. M. Lovett, and S. A. Watmough. 2019. Decreased atmospheric nitrogen deposition in eastern North America: Predicted responses of forest ecosystems. Environmental Pollution **244**:560-574.

Groffman, P. M. 2012. Terrestrial denitrification: challenges and opportunities. Ecological Processes **1**:11.

Groffman, P. M., K. Butterbach-Bahl, R. W. Fulweiler, A. J. Gold, J. L. Morse, E. K. Stander, C. Tague, C. Tonitto, and P. Vidon. 2009. Challenges to incorporating spatially and temporally explicit phenomena (hotspots and hot moments) in denitrification models. Biogeochemistry **93**:49-77.

Guerrieri, R., L. Lecha, S. Mattana, J. Caliz, E. O. Casamayor, A. Barcelo, G. Michalski, J. Penuelas, A. Avila, and M. Mencuccini. 2020. Partitioning between atmospheric deposition and canopy microbial nitrification into throughfall nitrate fluxes in a Mediterranean forest. Journal of Ecology **108**:626-640.

Guerrieri, R., M. Mencuccini, L. J. Sheppard, M. Saurer, M. P. Perks, P. Levy, M. A. Sutton, M. Borghetti, and J. Grace. 2011. The legacy of enhanced N and S deposition as revealed by the combined analysis of $\delta^{13}C$, $\delta^{18}O$ and $\delta^{15}N$ in tree rings. Global Change Biology **17**:1946-1962.

Guo, C. J., J. Simon, R. Gasche, P. S. Naumann, C. Bimuller, R. Pena, A. Polle, I. Kogel-Knabner, B. Zeller, H. Rennenberg, and M. Dannenmann. 2013b. Minor contribution of leaf litter to N nutrition of beech (*Fagus sylvatica*) seedlings in a mountainous beech forest of Southern Germany. Plant and Soil **369**:657-668.

Guo, C. J., M. Dannenmann, R. Gasche, B. Zeller, H. Papen, A. Polle, H. Rennenberg, and J. Simon. 2013a. Preferential use of root litter compared to leaf litter by beech seedlings and soil microorganisms. Plant and Soil **368**:519-534.

Hambuckers, A., and J. Remacle. 1993. Relative importance of factors controlling the leaching and uptake of inorganic-ions in the canopy of a spruce forest. Biogeochemistry **23**:99-117.

Harrison, X. A., L. Donaldson, M. E. Correa-Cano, J. Evans, D. N. Fisher, C. E. Goodwin, B. S. Robinson, D. J. Hodgson, and R. Inger. 2018. A brief introduction to mixed effects modelling and multi-model inference in ecology. Peerj **6**:e4794

Hawkes, C. V., K. M. DeAngelis, and M. K. Firestone. 2007. Root Interactions with Soil Microbial Communities and Processes. Pages 1-29 *in* Z. G. Cardon and J. L. Whitbeck, editors. The Rhizosphere. Academic Press, Burlington.

Haynes, R. J. 1986. Uptake and Assimilation of Mineral Nitrogen by Plants. Pages 303-378 *in* Mineral Nitrogen in the Plant-soil System. R J Haynes, editor. Academic Press, San Diego.

Heal, K. V., R. T. Stidson, C. A. Dickey, J. N. Cape, and M. R. Heal. 2004. New data for water losses from mature Sitka spruce plantations in temperate upland catchments. Hydrological Sciences Journal-Journal Des Sciences Hydrologiques **49**:477-493.

Hedwall, P., L. Gruffman, T. Ishida, F. From, T. Lundmark, T. Näsholm, and A. Nordin. 2018. Interplay between N-form and N-dose influences ecosystem effects of N addition to boreal forest. Plant and Soil **423**:385-395.

Hénault, C., and J. C. Germon. 2000. NEMIS, a predictive model of denitrification on the field scale. European Journal of Soil Science **51**:257-270.

Herckes, P., P. Mirabel, and H. Wortham. 2002. Cloud water deposition at a high-elevation site in the Vosges Mountains (France). Science of the Total Environment **296**:59-75.

Hertel, O., S. Reis, C. A. Skjøth, A. Bleeker, R. Harrison, J. N. Cape, D. Fowler, U. Skiba, D. Simpson, T. Jickells, A. Baker, M. Kulmala, S. Gyldenkærne, L. L. Sørensen, and J. W. Erisman. 2011. Nitrogen processes in the atmosphere. Pages 177-208 *in* A. Bleeker, B. Grizzetti, C. M. Howard, G. Billen, H. van Grinsven, J. W. Erisman, M. A. Sutton, and P. Grennfelt, editors. The European Nitrogen Assessment: Sources, Effects and Policy Perspectives. Cambridge University Press, Cambridge.

Hill, E. J., D. L. Jones, E. Paterson, and P. W. Hill. 2019. Hotspots and hot moments of amino acid N in soil: Real-time insights using continuous microdialysis sampling. Soil Biology & Biochemistry **131**:40-43.

Hill, K. A., P. B. Shepson, E. S. Galbavy, and C. Anastasio. 2005. Measurement of wet deposition of inorganic and organic nitrogen in a forest environment. Journal of Geophysical Research-Biogeosciences **110**:14.

Högberg, P., A. Nordgren, N. Buchmann, A. F. S. Taylor, A. Ekblad, M. N. Högberg, G. Nyberg, M. Ottosson-Löfvenius, and D. J. Read. 2001. Large-scale forest girdling shows that current photosynthesis drives soil respiration. Nature **411**:789-792.

Holland, E. A., B. H. Braswell, J. Sulzman, and J. F. Lamarque. 2005. Nitrogen deposition onto the United States and western Europe: Synthesis of observations and models. Ecological Applications **15**:38-57.

Holtmeier, F.-K., and G. Broll. 2010. Wind as an Ecological Agent at Treelines in North America, the Alps, and the European Subarctic. Physical Geography 31:203-233.

Houle, D., C. Marty, and L. Duchesne. 2015. Response of canopy nitrogen uptake to a rapid decrease in bulk nitrate deposition in two eastern Canadian boreal forests. Oecologia **177**:29-37.

Inselsbacher, E., and T. Näsholm. 2012. The below-ground perspective of forest plants: soil provides mainly organic nitrogen for plants and mycorrhizal fungi. New Phytologist **195**:329-334.

Inselsbacher, E., J. Öhlund, S. Jämtgård, K. Huss-Danell, and T. Näsholm. 2011. The potential of microdialysis to monitor organic and inorganic nitrogen compounds in soil. Soil Biology & Biochemistry **43**:1321-1332.

Izquieta-Rojano, S., H. Garcia-Gomez, L. Aguillaume, J. M. Santamaria, Y. S. Tang, C. Santamaria, F. Valino, E. Lasheras, R. Alonso, A. Avila, J. N. Cape, and D. Elustondo. 2016. Throughfall and bulk deposition of dissolved organic nitrogen to holm oak forests in the Iberian Peninsula: Flux estimation and identification of potential sources. Environmental Pollution **210**:104-112.

Jalota, S. K., B. B. Vashisht, S. Sharma, and S. Kaur. 2018. Chapter 3 - Climate Change Impact on Crop Productivity and Field Water Balance. Pages 87-148 *in* S. K. Jalota, B. B. Vashisht, S. Sharma, and S. Kaur, editors. Understanding Climate Change Impacts on Crop Productivity and Water Balance. Academic Press.

Janssens, I. A., W. Dieleman, S. Luyssaert, J. A. Subke, M. Reichstein, R. Ceulemans, P. Ciais, A. J. Dolman, J. Grace, G. Matteucci, D. Papale, S. L. Piao, E. D. Schulze, J. Tang, and B. E. Law. 2010. Reduction of forest soil respiration in response to nitrogen deposition. Nature Geoscience **3**:315-322.

Jickells, T., A. R. Baker, J. N. Cape, S. E. Cornell, and E. Nemitz. 2013. The cycling of organic nitrogen through the atmosphere. Philosophical Transactions of the Royal Society B-Biological Sciences **368** : 20130115

Johnson, D. W., and S. E. Lindberg, 1992. Atmospheric Deposition and Forest Nutrient Cycling. Springer, New York.

Kalina, M. F., S. Stopper, E. Zambo, and H. Puxbaum. 2002. Altitude-dependent wet, dry and occult nitrogen deposition in an Alpine Region. Environmental Science and Pollution Research **9**:16-22.

Kang, H. Z., T. J. Fahey, K. Bae, M. Fisk, R. E. Sherman, R. D. Yanai, and C. R. See. 2016. Response of forest soil respiration to nutrient addition depends on site fertility. Biogeochemistry **127**:113-124.

Klinka, K., J. Worrall, L. Skoda, P. Varga, and C. Chourmouzis. 2000. The Distribution and Synopsis of Ecological and Silvical Characteristics of Tree Species of British Columbia's Forests. Forest Sciences Department, University of British Columbia. Retrieved May 30, 2020, from https://open.library.ubc.ca/collections/facultyresearchandpublications/52383/items/1.0107280

Klopatek, J. M., M. J. Barry, and D. W. Johnson. 2006. Potential canopy interception of nitrogen in the Pacific Northwest, USA. Forest Ecology and Management **234**:344-354.

Koopmans, C. J., A. Tietema, and A. W. Boxman. 1996. The fate of $^{15}N$ enriched throughfall in two coniferous forest stands at different nitrogen deposition levels. Biogeochemistry **34**:19-44.

Kopacek, J., J. Hejzlar, and M. Posch. 2013. Quantifying nitrogen leaching from diffuse agricultural and forest sources in a large heterogeneous catchment. Biogeochemistry **115**:149-165.

Korhonen, J. F. J., M. Pihlatie, J. Pumpanen, H. Aaltonen, P. Hari, J. Levula, A. J. Kieloaho, E. Nikinmaa, T. Vesala, and H. Ilvesniemi. 2013. Nitrogen balance of a boreal Scots pine forest. Biogeosciences **10**:1083-1095.

Kortelainen, P., T. Mattsson, L. Finér, M. Ahtiainen, S. Saukkonen, and T. Sallantaus. 2006. Controls on the export of C, N, P and Fe from undisturbed boreal catchments, Finland. Aquatic Sciences **68**:453-468.

Kulkarni, M. V., P. M. Groffman, J. B. Yavitt, and C. L. Goodale. 2015. Complex controls of denitrification at ecosystem, landscape and regional scales in northern hardwood forests. Ecological Modelling **298**:39-52.

Lewis, S. L., E. T. A. Mitchard, C. Prentice, M. Maslin, and B. Poulter. 2019. Comment on “The global tree restoration potential”. Science **366**:eaaz0388.

Liang, J. Y., X. Qi, L. Souza, and Y. Q. Luo. 2016. Processes regulating progressive nitrogen limitation under elevated carbon dioxide: a meta-analysis. Biogeosciences **13**:2689-2699.

Linn, D. M., and J. W. Doran. 1984. Effect of Water-Filled Pore Space on Carbon Dioxide and Nitrous Oxide Production in Tilled and Nontilled Soils. Soil Science Society of America Journal **48**:1267-1272.

Liu, L. L., and T. L. Greaver. 2010. A global perspective on belowground carbon dynamics under nitrogen enrichment. Ecology Letters **13**:819-828.

Liu, T., F. Wang, G. Michalski, X. H. Xia, and S. D. Liu. 2013. Using $^{15}N$, $^{17}O$, and $^{18}O$ to determine nitrate sources in the Yellow River, China. Environmental Science & Technology **47**:13412-13421.

Liu, T., P. Mao, L. L. Shi, N. Eisenhauer, S. J. Liu, X. L. Wang, X. X. He, Z. Y. Wang, W. Zhang, Z. F. Liu, L. X. Zhou, Y. H. Shao, and S. L. Fu. 2020. Forest canopy maintains the soil community composition under elevated nitrogen deposition. Soil Biology & Biochemistry **143**: 107733.

Llorens, P., R. Poch, J. Latron, and G. F. 1997. Rainfall interception by a *Pinus sylvestris* forest patch overgrown in a Mediterranean mountainous abandoned area I. Monitoring design and results down to the event scale. Journal of Hydrology **199**:331-345.

Lovett, G. M., M. A. Arthur, K. C. Weathers, R. D. Fitzhugh, and P. H. Templer. 2013. Nitrogen addition increases carbon storage in soils, but not in trees, in an Eastern US deciduous forest. Ecosystems **16**:980-1001.

Luo, Y., B. Su, W. S. Currie, J. S. Dukes, A. C. Finzi, U. Hartwig, B. Hungate, R. E. McMurtrie, R. Oren, W. J. Parton, D. E. Pataki, M. R. Shaw, D. R. Zak, and C. B. Field. 2004. Progressive nitrogen limitation of ecosystem responses to rising atmospheric carbon dioxide. Bioscience **54**:731-739.

Maaroufi, N. I., A. Nordin, N. J. Hasselquist, L. H. Bach, K. Palmqvist, and M. J. Gundale. 2015. Anthropogenic nitrogen deposition enhances carbon sequestration in boreal soils. Global Change Biology **21**:3169-3180.

Machacova, K., J. Bäck, A. Vanhatalo, E. Halmeenmäki, P. Kolari, I. Mammarella, J. Pumpanen, M. Acosta, O. Urban, and M. Pihlatie. 2016. *Pinus sylvestris* as a missing source of nitrous oxide and methane in boreal forest. Scientific Reports **6**: 23410.

Magnani, F., J. Grace, and M. Borghetti. 2002. Adjustment of tree structure in response to the environment under hydraulic constraints. Functional Ecology **16**:385-393.

Magnani, F., M. Mencuccini, M. Borghetti, F. Berninger, S. Delzon, A. Grelle, P. Hari, P. G. Jarvis, P. Kolari, A. S. Kowalski, H. Lankreijer, B. E. Law, A. Lindroth, D. Loustau, G. Manca, J. B. Moncrieff, V. Tedeschi, R. Valentini, and J. Grace. 2008. Magnani et al. reply. Nature **451**:E3-E4.

Magnani, F., M. Mencuccini, M. Borghetti, P. Berbigier, F. Berninger, S. Delzon, A. Grelle, P. Hari, P. G. Jarvis, P. Kolari, A. S. Kowalski, H. Lankreijer, B. E. Law, A. Lindroth, D. Loustau, G. Manca, J. B. Moncrieff, M. Rayment, V. Tedeschi, R.

Valentini, and J. Grace. 2007. The human footprint in the carbon cycle of temperate and boreal forests. Nature **447**:849-851.

Maier, R. M. 2009. Chapter 14 - Biogeochemical Cycling. Pages 287-318 *in* R. M. Maier, I. L. Pepper, and C. P. Gerba, editors. Environmental Microbiology (Second Edition). Academic Press, San Diego.

Mariotti, A. 1983. Atmospheric nitrogen is a reliable standard for natural $^{15}N$ abundance measurements. Nature. **303**:685--687.

McFadyen, G. G., and J. N. Cape. 2005. Peroxyacetyl nitrate in eastern Scotland. Science of the Total Environment **337**:213-222.

Meunier, C. L., M. J. Gundale, I. S. Sanchez, and A. Liess. 2016. Impact of nitrogen deposition on forest and lake food webs in nitrogen-limited environments. Global Change Biology **22**:164-179.

Misselbrook, T. H., T. J. Van Der Weerden, B. F. Pain, S. C. Jarvis, B. J. Chambers, K. A. Smith, V. R. Phillips, and T. G. M. Demmers. 2000. Ammonia emission factors for UK agriculture. Atmospheric Environment **34**:871-880.

Mitchell, J. 2013. Above ground nitrogen dynamics of a Scottish Sitka spruce plantation. Honours disssertation. University of Edinburgh, Edinburgh.

Morse, J. L., and E. S. Bernhardt. 2013. Using $^{15}N$ tracers to estimate $N_2O$ and $N_2$ emissions from nitrification and denitrification in coastal plain wetlands under contrasting land-uses. Soil Biology and Biochemistry **57**:635-643.

Mulholland, P. J., and W. R. Hill. 1997. Seasonal patterns in streamwater nutrient and dissolved organic carbon concentrations: Separating catchment flow path and in-stream effects. Water Resources Research **33**:1297-1306.

Mustajarvi, K., P. Merila, J. Derome, A. J. Lindroos, H. S. Helmisaari, P. Nojd, and L. Ukonmaanaho. 2008. Fluxes of dissolved organic and inorganic nitrogen in relation to stand characteristics and latitude in Scots pine and Norway spruce stands in Finland. Boreal Environment Research **13**:3-21.

Myhre, G., D. Hindell, and J. Pongratz. 2014. Anthropogenic and Natural Radiative Forcing *in* T. Stocker, editor. Climate change 2013 : the physical science basis; Working Group I contribution to the fifth assessment report of the Intergovernmental Panel on Climate Change. Cambridge University Press, Cambridge.

Nadelhoffer, K. J. 2000. The potential effects of nitrogen deposition on fine-root production in forest ecosystems. New Phytologist **147**:131-139.

Nadelhoffer, K. J., M. R. Downs, and B. Fry. 1999. Sinks for $^{15}N$ -enriched additions to an oak forest and a red pine plantation. Ecological Applications **9**:72-86.

Nagy, J., L. Nagy, C. J. Legg, and J. Grace. 2013. The stability of the Pinus sylvestris treeline in the Cairngorms, Scotland over the last millennium. Plant Ecology & Diversity 6:7-19.

Nair R. 2014. Using Stable Isotopes to Investigate Interactions between the Forest Carbon and Nitrogen Cycles. PhD thesis, School of GeoSciences, University of Edinburgh, Edinburgh, UK. URI: http://hdl.handle.net/1842/10573

Nair, R. K. F., M. P. Perks, A. Weatherall, E. M. Baggs, and M. Mencuccini. 2016. Does canopy nitrogen uptake enhance carbon sequestration by trees? Global Change Biology **22**:875-888.

Nair, R. K. F., M. P. Perks, and M. Mencuccini. 2017. Decomposition nitrogen is better retained than simulated deposition from mineral amendments in a temperate forest. Global Change Biology **23**:1711-1724.

Nair, R., A. Weatherall, M. Perks, and M. Mencuccini. 2014. Stem injection of $^{15}NH_4{}^{15}NO_3$ into mature Sitka spruce (*Picea sitchensis*). Tree Physiology **34**:1130-1140.

Näsholm, T., A. Ekblad, A. Nordin, R. Giesler, M. Högberg, and P. Högberg. 1998. Boreal forest plants take up organic nitrogen. Nature **392**:914-916.

Näsholm, T., K. Kielland, and U. Ganeteg. 2009. Uptake of organic nitrogen by plants. New Phytologist **182**:31-48.

Näsholm, T., P. Högberg, O. Franklin, D. Metcalfe, S. G. Keel, C. Campbell, V. Hurry, S. Linder, and M. N. Högberg. 2013. Are ectomycorrhizal fungi alleviating or aggravating nitrogen limitation of tree growth in boreal forests? New Phytologist **198**:214-221.

Neff, J. C., E. A. Holland, F. J. Dentener, W. H. McDowell, and K. M. Russell. 2002. The origin, composition and rates of organic nitrogen deposition: A missing piece of the nitrogen cycle? Biogeochemistry **57**:99-136.

Öhlund, J., and T. Näsholm. 2001. Growth of conifer seedlings on organic and inorganic nitrogen sources. Tree Physiology **21**:1319-1326.

Oosthoek, K. J. 2013. Conquering the Highlands A history of the afforestation of the Scottish uplands. Australian National University E Press.

Oyewole, O. A., S. Jämtgård, L. Gruffman, E. Inselsbacher, and T. Näsholm. 2016. Soil diffusive fluxes constitute the bottleneck to tree nitrogen nutrition in a Scots pine forest. Plant and Soil **399**:109-120.

Paerl, H. W. 1993. Emerging role of atmospheric nitrogen deposition in coastal eutrophication - biogeochemical and trophic perspectives. Canadian Journal of Fisheries and Aquatic Sciences **50**:2254-2269.

Papen, H., A. Gessler, E. Zumbusch, and H. Rennenberg. 2002. Chemolithoautotrophic nitrifiers in the phyllosphere of a spruce ecosystem receiving high atmospheric nitrogen input. Current Microbiology **44**:56-60.

Paungfoo-Lonhienne, C., T. G. A. Lonhienne, D. Rentsch, N. Robinson, M. Christie, R. I. Webb, H. K. Gamage, B. J. Carroll, P. M. Schenk, and S. Schmidt. 2008. Plants can use protein as a nitrogen source without assistance from other organisms. Proceedings of the National Academy of Sciences of the United States of America **105**:4524-4529.

Pena, R., J. Tejedor, B. Zeller, M. Dannenmann, and A. Polle. 2013. Interspecific temporal and spatial differences in the acquisition of litter-derived nitrogen by ectomycorrhizal fungal assemblages. New Phytologist **199**:520-528.

Peterjohn, W. T., M. B. Adams, and F. S. Gilliam. 1996. Symptoms of nitrogen saturation in two central Appalachian hardwood forest ecosystems. Biogeochemistry **35**:507-522.

Peterson, B. J., W. M. Wollheim, P. J. Mulholland, J. R. Webster, J. L. Meyer, J. L. Tank, E. Martí, W. B. Bowden, H. M. Valett, A. E. Hershey, W. H. McDowell, W. K. Dodds, S. K. Hamilton, S. Gregory, and D. D. Morrall. 2001. Control of Nitrogen Export from Watersheds by Headwater Streams. Science **292**:86-90.

Petr, M., L. G. J. Boerboom, D. Ray, and A. van der Veen. 2015. Adapting Scotland's forests to climate change using an action expiration chart. Environmental Research Letters 10:105005.

Pfautsch S., Bell T.L., and Gessler A. 2015. Uptake, Transport and Redistribution of Amino Nitrogen in Woody Plants. Pages 315-339 *in* J. P. F. D'mello, editor. Amino Acids in Higher Plants.

Polert, T. 2018. trend: Non-Parametric Trend Tests and Change-Point Detection. R package version 1.1.1. Pages https://CRAN.R-project.org/package=trend.

Prosser, J. I. 2005. Nitrogen in Soils | Nitrification. Pages 31-39 *in* D. Hillel, editor. Encyclopedia of Soils in the Environment. Elsevier, Oxford.

Rapson, T. D., and H. Dacres. 2014. Analytical techniques for measuring nitrous oxide. Trac-Trends in Analytical Chemistry **54**:65-74.

Ray, D. 2008. Impacts of climate change on forests and forestry in Scotland. Forestry Commission Scotland, Edinburgh.

Reay, D. S., F. Dentener, P. Smith, J. Grace, and R. A. Feely. 2008. Global nitrogen deposition and carbon sinks. Nature Geoscience **1**:430-437.

Reynolds, B. 2004. Continuous cover forestry: possible implications for surface water acidification in the UK uplands. Hydrology and Earth System Sciences 8:306-313.

Rockstrom, J., W. Steffen, K. Noone, A. Persson, F. S. Chapin, E. F. Lambin, T. M. Lenton, M. Scheffer, C. Folke, H. J. Schellnhuber, B. Nykvist, C. A. de Wit, T. Hughes, S. van der Leeuw, H. Rodhe, S. Sorlin, P. K. Snyder, R. Costanza, U. Svedin, M. Falkenmark, L. Karlberg, R. W. Corell, V. J. Fabry, J. Hansen, B. Walker, D. Liverman, K. Richardson, P. Crutzen, and J. A. Foley. 2009. A safe operating space for humanity. Nature **461**:472-475.

Rotter, P., M. Loreau, and C. de Mazancourt. 2020. Why do forests respond differently to nitrogen deposition? A modelling approach. Ecological Modelling **425**.

Rusjan, S., and A. Vidmar. 2017. The role of seasonal and hydrological conditions in regulating dissolved inorganic nitrogen budgets in a forested catchment in SW Slovenia. Science of the Total Environment **575**:1109-1118.

Sachs, J. D., G. Schmidt-Traub, M. Mazzucato, D. Messner, N. Nakicenovic, and J. Rockström. 2019. Six Transformations to achieve the Sustainable Development Goals. Nature Sustainability **2**:805-814.

Sala, O. E., F. S. Chapin, J. J. Armesto, E. Berlow, J. Bloomfield, R. Dirzo, E. Huber-Sanwald, L. F. Huenneke, R. B. Jackson, A. Kinzig, R. Leemans, D. M. Lodge, H. A. Mooney, M. Oesterheld, N. L. Poff, M. T. Sykes, B. H. Walker, M. Walker, and D. H. Wall. 2000. Biodiversity - Global biodiversity scenarios for the year 2100. Science **287**:1770-1774.

Salemaa, M., A. J. Lindroos, P. Merilä, R. Makipaa, and A. Smolander. 2019. $N_2$ fixation associated with the bryophyte layer is suppressed by low levels of nitrogen deposition in boreal forests. Science of the Total Environment **653**:995-1004.

Santos, F., K. Nadelhoffer, and J. A. Bird. 2016. Rapid fine root C and N mineralization in a northern temperate forest soil. Biogeochemistry **128**:187-200.

Schönherr, J., and M. J. Bukovac. 1972. Penetration of Stomata by Liquids. Dependence on Surface Tension, Wettability, and Stomatal Morphology **49**:813-819.

Schulte-Uebbing, L., and W. de Vries. 2018. Global-scale impacts of nitrogen deposition on tree carbon sequestration in tropical, temperate, and boreal forests: A meta-analysis. Global Change Biology **24**:E416-E431.

Schulze, E. D. 2013. Carbon and Nitrogen Cycling in European Forest Ecosystems. Springer-Verlag, Berlin, Heidelberg, New York.

Schwarz, M. T., S. Bischoff, S. Blaser, S. Boch, B. Schmitt, L. Thieme, M. Fischer, B. Michalzik, E. D. Schulze, J. Siemens, and W. Wilcke. 2014. More efficient aboveground nitrogen use in more diverse Central European forest canopies. Forest Ecology and Management **313**:274-282.

Sebilo, M., B. Mayer, M. Grably, D. Billiou, and A. Mariotti. 2004. The Use of the 'Ammonium Diffusion' Method for $\delta^{15}N\text{-}NH_4^+$ and $\delta^{15}N\text{-}NO_3^-$ Measurements: Comparison with Other Techniques. Environmental Chemistry **1**:99-103.

Shi, X. Z., H. W. Hu, J. Q. Wang, J. Z. He, C. Y. Zheng, X. H. Wan, and Z. Q. Huang. 2018. Niche separation of comammox *Nitrospira* and canonical ammonia oxidizers in an acidic subtropical forest soil under long-term nitrogen deposition. Soil Biology & Biochemistry **126**:114-122.

Sicard, C., L. Saint-Andre, D. Gelhaye, and J. Ranger. 2006. Effect of initial fertilisation on biomass and nutrient contentof Norway spruce and Douglas-fir plantations at the same site. Trees **20**:229-246.

Sievering, H., T. Tomaszewski, and J. Torizzo. 2007. Canopy uptake of atmospheric N deposition at a conifer forest: part I - canopy N budget, photosynthetic efficiency and net ecosystem exchange. Tellus Series B-Chemical and Physical Meteorology **59**:483-492.

Simpson, D., A. Benedictow, H. Berge, R. Bergstrom, L. D. Emberson, H. Fagerli, C. R. Flechard, G. D. Hayman, M. Gauss, J. E. Jonson, M. E. Jenkin, A. Nyiri, C. Richter, V. S. Semeena, S. Tsyro, J. P. Tuovinen, A. Valdebenito, and P. Wind. 2012. The EMEP MSC-W chemical transport model - technical description. Atmospheric Chemistry and Physics **12**:7825-7865.

Skiba, U. 2008. Denitrification. Pages 866-871 *in* S. E. Jørgensen and B. D. Fath, editors. Encyclopedia of Ecology. Academic Press, Oxford.

Smith, K. A., T. Ball, F. Conen, K. E. Dobbie, J. Massheder, and A. Rey. 2003. Exchange of greenhouse gases between soil and atmosphere: interactions of soil physical factors and biological processes. European Journal of Soil Science **54**:779-791.

Sparks, J. P., J. Walker, A. Turnipseed, and A. Guenther. 2008. Dry nitrogen deposition estimates over a forest experiencing free air $CO_2$ enrichment. Global Change Biology **14**:768-781.

Sponseller, R. A., M. J. Gundale, M. Futter, E. Ring, A. Nordin, T. Näsholm, and H. Laudon. 2016. Nitrogen dynamics in managed boreal forests: Recent advances and future research directions. Ambio **45**:S175-S187.

Stark, J. M. and Firestone, M. K. 1995. Mechanisms for soil moisture effects on activity of nitrifying bacteria. Applied and Environmental Microbiology, **61**: 218–221.

Steffen, W., K. Richardson, J. Rockstrom, S. E. Cornell, I. Fetzer, E. M. Bennett, R. Biggs, S. R. Carpenter, W. de Vries, C. A. de Wit, C. Folke, D. Gerten, J. Heinke, G. M. Mace, L. M. Persson, V. Ramanathan, B. Reyers, and S. Sorlin. 2015. Planetary boundaries: Guiding human development on a changing planet. Science **347**(6223): 1259855

Sterck, F. J., R. Zweifel, U. Sass-Klaassen, and Q. Chowdhury. 2008. Persisting soil drought reduces leaf specific conductivity in Scots pine (Pinus sylvestris) and pubescent oak (Quercus pubescens). Tree Physiology **28**:529-536.

Stevens, C. J., C. Dupre, E. Dorland, C. Gaudnik, D. J. G. Gowing, A. Bleeker, M. Diekmann, D. Alard, R. Bobbink, D. Fowler, E. Corcket, J. O. Mountford, V. Vandvik, P. A. Aarrestad, S. Muller, and N. B. Dise. 2010. Nitrogen deposition threatens species richness of grasslands across Europe. Environmental Pollution **158**:2940-2945.

Stevens, C. J., T. I. David, and J. Storkey. 2018. Atmospheric nitrogen deposition in terrestrial ecosystems: Its impact on plant communities and consequences across trophic levels. Functional Ecology **32**:1757-1769.

Sun, S. Q., Y. H. Wu, J. Zhang, G. X. Wang, T. H. DeLuca, W. Z. Zhu, A. D. Li, M. Duan, and L. He. 2019. Soil warming and nitrogen deposition alter soil respiration, microbial community structure and organic carbon composition in a coniferous forest on eastern Tibetan Plateau. Geoderma **353**:283-292.

Sutton, M. A., D. Simpson, P. E. Levy, R. I. Smith, S. Reis, M. van Oijen, and W. de Vries. 2008. Uncertainties in the relationship between atmospheric nitrogen deposition and forest carbon sequestration. Global Change Biology **14**:2057-2063.

Talhelm, A. F., A. J. Burton, K. S. Pregitzer, and M. A. Campione. 2013. Chronic nitrogen deposition reduces the abundance of dominant forest understory and groundcover species. Forest Ecology and Management **293**:39-48.

Templer, P. H., M. C. Mack, F. S. Chapin, L. M. Christenson, J. E. Compton, H. D. Crook, W. S. Currie, C. J. Curtis, D. B. Dail, C. M. D'Antonio, B. A. Emmett, H. E. Epstein, C. L. Goodale, P. Gundersen, S. E. Hobbie, K. Holland, D. U. Hooper, B. A. Hungate, S. Lamontagne, K. J. Nadelhoffer, C. W. Osenberg, S. S. Perakis, P. Schleppi, J. Schimel, I. K. Schmidt, M. Sommerkorn, J. Spoelstra, A. Tietema, W. W. Wessel, and D. R. Zak. 2012. Sinks for nitrogen inputs in terrestrial ecosystems: a meta-analysis of $^{15}N$ tracer field studies. Ecology **93**:1816-1829.

Teuber, M., H. Papen, R. Gasche, T. H. Eßmüller, and A. Geßler. 2007. The Apoplast of Norway Spruce (Picea abies) Needles as Habitat and Reaction Compartment for Autotrophic Nitrifiers *in* B. Sattelmacher and W. J. Horst, editors. The Apoplast of Higher Plants: Compartment of Storage,Transport and Reactions. Springer.

The Scottish Government. 2019. Scotland's Forestry Stategy 2019-2029. The Scottish Government, Edinburgh.

Tietema, A., B. A. Emmett, P. Gundersen, O. J. Kjonaas, and C. J. Koopmans. 1998. The fate of $^{15}N$-labelled nitrogen deposition in coniferous ecosystems. Forest Ecology and Management **101**:19-27.

Tompkins, S. Forestry in crisis: the battle for the hills. 1989, Helm.

Tonitto, C., C. L. Goodale, M. S. Weiss, S. D. Frey, and S. V. Ollinger. 2014. The effect of nitrogen addition on soil organic matter dynamics: a model analysis of the

Harvard Forest Chronic Nitrogen Amendment Study and soil carbon response to anthropogenic N deposition. Biogeochemistry **117**:431-454.

Vadeboncoeur, M. A., A. P. Ouimette, and E. A. Hobbie. 2015. Mycorrhizal roots in a temperate forest take up organic nitrogen from $^{13}C$- and $^{15}N$-labeled organic matter. Plant and Soil **397**:303-315.

van Breemen, N., E. W. Boyer, C. Goodale, N. Jaworski, K. Paustian, S. Seitzinger, K. Lajtha, B. Mayer, D. Van Dam, and R. Howarth. 2002. Where did all the nitrogen go? Fate of nitrogen inputs to large watersheds in the northeastern USA. Biogeochemistry **57**:267-293.

van der Salm, C., W. de Vries, G. J. Reinds, and N. B. Dise. 2007. N leaching across European forests: Derivation and validation of empirical relationships using data from intensive monitoring plots. Forest Ecology and Management **238**:81-91.

van Huysen, T. L., M. E. Harmon, S. S. Perakis, and H. Chen. 2013. Decomposition and nitrogen dynamics of $^{15}N$-labelled leaf, root, and twig litter in temperate coniferous forests. Oecologia **173**:1563-1573.

Veldman, J. W., J. C. Aleman, S. T. Alvarado, T. M. Anderson, S. Archibald, W. J. Bond, T. W. Boutton, N. Buchmann, E. Buisson, J. G. Canadell, M. d. S. Dechoum, M. H. Diaz-Toribio, G. Durigan, J. J. Ewel, G. W. Fernandes, A. Fidelis, F. Fleischman, S. P. Good, D. M. Griffith, J.-M. Hermann, W. A. Hoffmann, S. Le Stradic, C. E. R. Lehmann, G. Mahy, A. N. Nerlekar, J. B. Nippert, R. F. Noss, C. P. Osborne, G. E. Overbeck, C. L. Parr, J. G. Pausas, R. T. Pennington, M. P. Perring, F. E. Putz, J. Ratnam, M. Sankaran, I. B. Schmidt, C. B. Schmitt, F. A. O. Silveira, A. C. Staver, N. Stevens, C. J. Still, C. A. E. Strömberg, V. M. Temperton, J. M. Varner, and N. P. Zaloumis. 2019. Comment on “The global tree restoration potential”. Science **366**:eaay7976.

Vestgarden, L. S. 2001. Carbon and nitrogen turnover in the early stage of Scots pine (*Pinus sylvestris L.*) needle litter decomposition: effects of internal and external nitrogen. Soil Biology & Biochemistry **33**:465-474.

Vieno, M., M. R. Heal, M. M. Twigg, I. A. MacKenzie, C. F. Braban, J. J. N. Lingard, S. Ritchie, R. C. Beck, A. Moring, R. Ots, C. F. Di Marco, E. Nemitz, M. A. Sutton, and S. Reis. 2016. The UK particulate matter air pollution episode of March-April 2014: more than Saharan dust (vol 11, 044004, 2016). Environmental Research Letters **11**.

Vorholt, J. A. 2012. Microbial life in the phyllosphere. Nature Reviews Microbiology **10**:828-840.

Ward, B. B. 2013. Nitrification. Pages 351-358 *in* B. Fath, editor. Encyclopedia of Ecology (Second Edition). Elsevier, Oxford.

Watanabe, K., A. Kohzu, W. Suda, S. Yamamura, T. Takamatsu, A. Takenaka, M. K. Koshikawa, S. Hayashi, and M. Watanabe. 2016. Microbial nitrification in throughfall of a Japanese cedar associated with archaea from the tree canopy. Springerplus **5.** 1596

Weathers, K. C., G. M. Lovett, G. E. Likens, and N. F. M. Caraco. 2000. Cloudwater inputs of nitrogen to forest ecosystems in Southern Chile: forms, fluxes, and sources. Ecosystems **3**:590-595.

Wexler, S. K., C. L. Goodale, K. J. McGuire, S. W. Bailey, and P. M. Groffman. 2014. Isotopic signals of summer denitrification in a northern hardwood forested catchment. Proceedings of the National Academy of Sciences of the United States of America **111**:16413-16418.

Wortman, E., T. Tomaszewski, P. Waldner, P. Schleppi, A. Thimonier, W. Eugster, N. Buchmann, and H. Sievering. 2012. Atmospheric nitrogen deposition and canopy retention influences on photosynthetic performance at two high nitrogen deposition Swiss forests. Tellus Series B-Chemical and Physical Meteorology **64**.

Wyers, G. P., and J. W. Erisman. 1998. Ammonia exchange over coniferous forest. Atmospheric Environment **32**:441-451.

Wyka, T. P., R. Żytkowiak, and J. Oleksyn. 2016. Seasonal dynamics of nitrogen level and gas exchange in different cohorts of Scots pine needles: a conflict between nitrogen mobilization and photosynthesis? European Journal of Forest Research **135**:483-493.

Xu, R., H. Tian, S. Pan, S. A. Prior, Y. Feng, W. D. Batchelor, J. Chen, and J. Yang. 2019. Global ammonia emissions from synthetic nitrogen fertilizer applications in agricultural systems: Empirical and process-based estimates and uncertainty. Global Change Biology **25**:314-326.

Yamulki, S., R. Anderson, A. Peace, and J. I. L. Morison. 2013. Soil $CO_2$ $CH_4$ and $N_2O$ fluxes from an afforested lowland raised peatbog in Scotland: implications for drainage and restoration. Biogeosciences 10:1051-1065.

Zak, D. R., K. S. Pregitzer, W. E. Holmes, A. J. Burton, and G. P. Zogg. 2004. Anthropogenic N deposition and the fate of $^{15}NO_3$-N in a northern hardwood ecosystem. Biogeochemistry **69**:143-157.

Zak, D. R., W. E. Holmes, A. J. Burton, K. S. Pregitzer, and A. F. Talhelm. 2008. Simulated atmospheric $NO_3^-$ deposition increases soil organic matter by slowing decomposition. Ecological Applications **18**:2016-2027.

Zeller, B., M. Colin-Belgrand, E. Dambrine, and F. Martin. 1998. $^{15}N$ partitioning and production of $^{15}N$ -labelled litter in beech trees following $^{15}N$ urea spray. Annales Des Sciences Forestieres **55**:375-383.

Zeller, B., M. Colin-Belgrand, E. Dambrine, and F. Martin. 2001. Fate of nitrogen released from $^{15}N$-labeled litter in European beech forests. Tree Physiology **21**:153-162.

Zeller, B., M. Colin-Belgrand, E. Dambrine, F. Martin, and P. Bottner. 2000. Decomposition of $^{15}N$-labelled beech litter and fate of nitrogen derived from litter in a beech forest. Oecologia **123**:550-559.

Zhang, W., W. Shen, S. Zhu, S. Wan, Y. Luo, J. Yan, K. Wang, L. Liu, H. Dai, P. Li, K. Dai, W. Zhang, Z. Liu, F. Wang, Y. Kuang, Z. Li, Y. Lin, X. Rao, J. Li, B. Zou, X. Cai, J. Mo, P. Zhao, Q. Ye, J. Huang, and S. Fu. 2015. CAN Canopy Addition of Nitrogen Better Illustrate the Effect of Atmospheric Nitrogen Deposition on Forest Ecosystem? Scientific Reports **5**:11245-11245.

Zhang, Y., J. Wang, S. Dai, J. Zhao, X. Huang, Y. Sun, J. Chen, Z. Cai, and J. Zhang. 2019. The effect of C:N ratio on heterotrophic nitrification in acidic soils. Soil Biology and Biochemistry **137**:107562.

Zhu, X., W. Zhang, H. Chen, and J. Mo. 2015. Impacts of nitrogen deposition on soil nitrogen cycle in forest ecosystems: A review. Acta Ecologica Sinica **35**:35-43.

# Appendix A. Air and soil temperature measurements in Griffin Forest

The data shown in Table A1 were measured in association with sampling from the gas chambers located in the T plot and in the C plot at Griffin Forest from October 2013 to November 2016 (see Chapter 5.2.2 for the Methodology). One air temperature measurement was made at breast height above the ground in each plot, whilst soil temperature was measured at 5 cm depth adjacent to each of the 9 gas sampling chambers in each plot. The time gap between making measurements in the T plot and the C plot was at least 2 hours, due to the time needed for collection of 4 gas samples from each chamber at 20 minutes intervals and the preparation of the chambers before the sampling. Some differences in air temperature and soil temperature reflects this time gap, as the T plot was usually sampled in the late morning and the C plot was always sampled afterwards, usually in the early mid-afternoon. Consequently, on sampling dates in spring and summer, air and soil temperatures are often higher in the C plot compared to the T plot.

Table A1. Air and soil temperatures measured adjacent to the gas sampling chambers in each of the T plot and C plot in Griffin Forest, October 2013 to November 2016. A single air temperature measurement was made at each plot. Minimum, maximum and arithmetical mean values of the soil temperature on each sampling occasion are shown for the 9 gas chambers in each plot. NA = not available.

| Date | T plot | | C plot | |
|---|---|---|---|---|
| | Temp air (°C) | Temp soil at 5 cm min-max(mean) | Temp air (°C) | Temp soil at 5 cm min-max(mean) |
| 18-10-2013 | 6.7 | 7.1-7.6(7.4) | NA | NA |
| 28-11-2013 | 3.0 | 4.3-4.8(4.6) | 2.6 | 4.2-4.9(4.6) |
| 04-03-2014 | 2.4 | 1.3-2.3(1.8) | 3.1 | 1.7-2.5(2.1) |
| 08-04-2014 | 3.9 | 3.8-4.2(4.0) | 5.8 | 4.1-4.6(4.3) |
| 09-05-2014 | 6.6 | 6.0-6.7(6.4) | 9.3 | 6.7-7.3(7.0) |
| 12-06-2014 | 11.1 | 8.3-9.7(9.2) | 14.4 | 9.4-10.7(10.0) |
| 10-07-2014 | 13.5 | 9.3-10.2(9.8) | 17.3 | 9.9-11.2(10.7) |
| 07-08-2014 | 12.4 | 10.2-11.1(10.6) | 12.1 | 10.7-11.3(11.1) |
| 23-09-2014 | 11.3 | 9.2-9.6(9.4) | 10.7 | 9.6-10.2(9.9) |
| 27-10-2014 | 11.6 | 8.8-9.2(8.9) | 11.8 | 9.1-10.1(9.6) |
| 25-11-2014 | 3.7 | 4.9-6.0(5.4) | 4.3 | 4.7-5.8(5.3) |
| 10-02-2015 | 1.1 | 1.1-2.4(1.7) | 3.5 | 1.3-23.3(1.7) |
| 16-03-2015 | 2.1 | 1.8-2.7(2.2) | 2.1 | 2.0-2.4(2.2) |
| 07-04-2015 | 7.9 | 4.3-5.3(4.9) | 7.6 | 4.6-6.2(5.3) |
| 04-05-2015 | 5.2 | 3.6-4.7(3.9) | NA | 3.9-4.8(4.3) |
| 18-06-2015 | 8.0 | 6.9-7.7(7.3) | 8.7 | 7.1-7.8(7.5) |
| 23-07-2015 | 10.6 | 8.1-8.6(8.4) | 11.9 | 8.8-9.3(9.0) |
| 18-08-2015 | 11.6 | 8.7-9.4(9.0) | 13.4 | 9.6-10.2(9.9) |
| 22-09-2015 | 8.4 | 8.4-8.8(8.6) | 11.8 | 8.9-9.2(9.1) |
| 18-10-2015 | 7.4 | 6.0-6.9(6.5) | 11.8 | NA |
| 19-11-2015 | 5.0 | 5.0-5.8(5.3) | 5.0 | 5.1-5.9(5.5) |
| 25-04-2016 | 6.6 | 2.6-3.2(3.0) | 2.3 | 2.4-3.1(2.8) |
| 25-05-2016 | 9.1 | 5.7-6.3(6.1) | 8.5 | 6.4-7.2(6.8) |
| 24-06-2016 | 11.8 | 8.5-9.9(9.3) | 12.5 | 9.5-10.9(10.1) |
| 22-07-2016 | 14.5 | 10.3-12.6(11.6) | 15.0 | 11.5-13.6(12.5) |
| 20-08-2016 | 11.9 | 10.3-11.3(10.8) | 12.5 | 11.1-12.1(11.5) |
| 25-09-2016 | 8.2 | 9.8-10.6(10.3) | 8.7 | 10.1-10.9(10.6) |
| 22-11-2016 | NA | 1.0-4.0(2.1) | 2.1 | 1.9-2.4(2.2) |

# Appendix B. Relationships between volume and water depth in the throughfall and stemflow collection barrels

Three different types of barrels were used to collect TF and SF below the forest canopy in Griffin Forest. Barrels were chosen to contain the expected TF and SF volumes based on mean monthly TF and SF measurements conducted at Griffin Forest in 2000 by Xiangqing Ma (2000, data not published). The small round-cross section barrels, with a capacity of 30 L, were used for most of the stemflow samplers in the long-term monitoring study (see section 2.3) and for the multiple throughfall collectors set up in the $^{15}N$ labelled $N_{dep}$ application to the forest canopy experiment (see section 4.2.1.1). Larger barrels with a volume of over 120 L and either square- or round-cross sections were used for the TF collectors in the long-term monitoring (see section 2.2.2). The use of different barrel shapes arose due to a change in supplier stock between orders.

To facilitate rapid assessment of TF and SF volumes in the field, the relationship between volume and water depth for each barrel type was established in the laboratory by repeatedly adding a litre of water and measuring the water depth in the centre of the barrel. The linear regression relationship obtained for each barrel type ($R^2 \geq 0.999$) (see Fig. B1) was used to convert the water depth measured in the centre of the barrel in the field to the nearest cm into a volume in L. The attribution to the nearest cm gives uncertainties in the volume estimations of about 0.4 L for the small barrels, 0.6 L for the large square barrels and 1 L for the large round barrels. These uncertainties in volumes represent ~ 1% of the maximum barrel volumes.

Figure B1. Relationship between volume and water depth for each barrel type used in Griffin Forest to collect throughfall and stemflow.

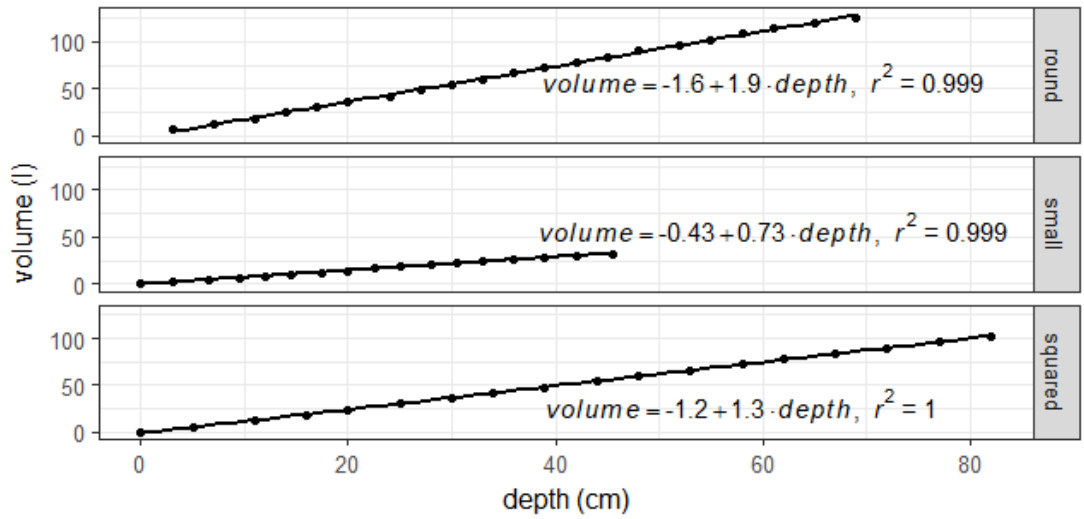

# Appendix C. Details of overflowing throughfall and stemflow collectors at Griffin Forest 2012-2016

Table C1. Numbers of overflowing throughfall (TF) and stemflow (SF) samplers on each sampling date during the long-term monitoring of Griffin Forest 2012-2016.

| Sampling date | TF collectors overflowing | SF collectors overflowing |
|---|---|---|
| 12-01-2012 | 1 | 16 |
| 16-02-2012 | 0 | 1 |
| 26-04-2012 | 0 | 9 |
| 25-05-2012 | 0 | 1 |
| 21-06-2012 | 0 | 1 |
| 20-07-2012 | 3 | 0 |
| 22-08-2012 | 0 | 11 |
| 18-10-2012 | 0 | 10 |
| 15-11-2012 | 0 | 4 |
| 17-01-2013 | 17 | 19 |
| 20-02-2013 | 4 | 17 |
| 28-03-2013 | 0 | 7 |
| 18-04-2013 | 0 | 6 |
| 23-05-2013 | 0 | 2 |
| 28-07-2013 | 0 | 1 |
| 13-11-2013 | 8 | 11 |
| 24-01-2014 | 18 | 18 |
| 27-02-2014 | 18 | 18 |
| 27-03-2014 | 0 | 3 |
| 24-04-2014 | 0 | 1 |
| 21-05-2014 | 0 | 1 |
| 20-06-2014 | 0 | 1 |
| 21-08-2014 | 0 | 5 |
| 31-10-2014 | 0 | 7 |
| 27-11-2014 | 11 | 11 |
| 15-12-2014 | 0 | 6 |
| 05-02-2015 | 3 | 13 |
| 25-03-2015 | 0 | 5 |
| 19-05-2015 | 0 | 4 |
| 17-06-2015 | 0 | 1 |
| 21-07-2015 | 0 | 4 |
| 23-08-2015 | 0 | 1 |

| | | |
|---|---|---|
| 24-09-2015 | 0 | 1 |
| 19-10-2015 | 0 | 1 |
| 20-11-2015 | 5 | 7 |
| 17-12-2015 | 4 | 11 |
| 19-01-2016 | 18 | 17 |
| 20-02-2016 | 0 | 10 |
| 24-04-2016 | 0 | 2 |
| 22-06-2016 | 0 | 6 |
| 20-09-2016 | 0 | 1 |
| 12-10-2016 | 0 | 1 |
| 22-11-2016 | 0 | 5 |
| **Total overflows 2012-2016** | **110** | **277** |

# Appendix D. Comparison between instantaneous stream discharge estimated from the V-notch weirs and the volumetric method

Before calculating N fluxes in streamwater and N leaching as the net balance of the streamwater N fluxes above and below the forest canopy in the T plot, the quality of the discharge values estimated via water height measurements from the V-notch weirs (see Section 2.2.6) were checked as follows. When bucket-gauged discharge measurements were available, a comparison was made with the instantaneous discharge calculated from the water height measured above the V-notch. The number of comparative measurements was limited by the fact bucket gauging requires at least two people in the field, one to deploy the bucket to catch flow over the V-notch weir and one to operate a stopwatch. However, comparative measurements were made on 24 occasions the two methods gave very similar values over a range of instantaneous discharge values. Figure D1 shows significant positive relationships between discharges estimated by the two methods for the two river flow measurement points for the T plot. The comparison was a useful tool to test the confidence in flow measurements from V-notch along the 5-year monitoring after local perturbations due to intense precipitation events (i.e. erosion, pools partially filled with debris).

Figure D1. Regression relationships between discharge estimated through the V-notch weir method and with the “bucket” volumetric gauging method for the T plot streamwater sampling points. For both regressions p-value<0.001.

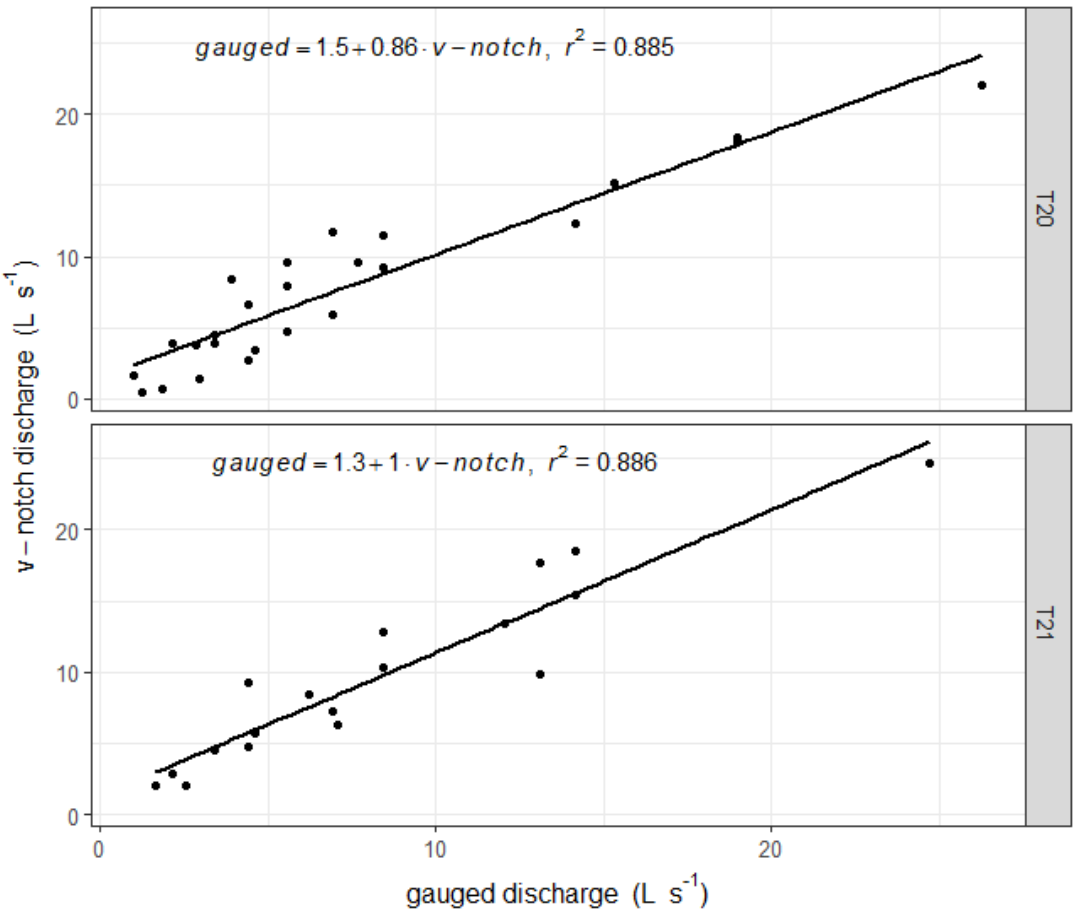

# Appendix E. Throughfall and stemflow depths and volumes

This Appendix shows all the throughfall (TF) and stemflow (SF) raw data by individual sampler and sampling date used to build the 5-year dataset. TF data (Table E1) are expressed as cumulative depths (mm) after correcting for the surface area of the gutters and the colander since the previous sampling date. The SF data (Table E2) are expressed as volumes (L), as calculated from the raw data measured in field and transformed as explained in Chapter 2.2.4 and Appendix B.

Table E1. TF depth (mm) for each sampler for every sampling date during the long-term monitoring at Griffin Forest. Values are the cumulative depth since the previous sampling date. The samplers are shown by plot and subplot. LOD refers to water depth in the barrel < 1 cm. NA = not available, mostly because barrels had fallen over or the gutters had become disconnected from the collection barrel.

| Date | C PLOT | | | | | | | | | T PLOT | | | | | | | | |
|---|---|---|---|---|---|---|---|---|---|---|---|---|---|---|---|---|---|---|
| | subplot C10 | | | subplot C11 | | | subplot C12 | | | subplot T10 | | | subplot T11 | | | subplot T12 | | |
| | T1 | T2 | T3 | T1 | T2 | T3 | T1 | T2 | T3 | T1 | T2 | T3 | T1 | T2 | T3 | T1 | T2 | T3 |
| 12/01/2012 | 108.0 | 110.0 | 106.6 | 80.1 | 87.8 | *NA* | 79.2 | 65.4 | 156.8 | 73.6 | 84.7 | 74.4 | 74.1 | 67.6 | 96.2 | 70.0 | 60.3 | 87.3 |
| 16/02/2012 | 26.7 | 29.2 | 18.8 | 16.4 | 19.0 | 23.0 | 33.0 | *<LOD* | 33.2 | 23.2 | 27.0 | 22.9 | *<LOD* | 18.6 | 29.8 | 20.7 | *<LOD* | 26.0 |
| 15/03/2012 | 9.0 | 7.5 | 6.4 | 3.2 | 6.4 | 8.1 | 12.9 | 4.4 | 10.7 | 8.1 | 8.1 | 6.4 | 5.4 | 6.4 | 11.7 | 4.3 | 4.3 | 8.7 |
| 26/04/2012 | 61.2 | 64.4 | 47.6 | 44.1 | 63.5 | 59.5 | 74.1 | 43.7 | 86.8 | 63.4 | 61.0 | 47.6 | 38.2 | 52.3 | 97.2 | 47.4 | 37.7 | 61.4 |
| 25/05/2012 | 51.1 | 48.9 | 34.9 | 48.2 | 48.7 | 44.6 | 57.6 | 47.8 | 61.0 | 49.1 | 51.7 | 45.6 | 33.0 | 45.2 | 69.7 | 42.3 | 31.6 | 47.8 |
| 21/06/2012 | 40.9 | 42.7 | 26.9 | 26.5 | 43.3 | 41.9 | *NA* | 29.2 | 47.6 | 36.9 | 41.4 | 34.2 | 24.8 | 32.9 | 57.4 | 32.0 | 20.6 | 38.2 |
| 20/07/2012 | 101.9 | 117.2 | 83.1 | 80.1 | 114.8 | 112.1 | 105.8 | 83.0 | 150.6 | 115.2 | 118.7 | 102.2 | 97.6 | 100.3 | 156.4 | 100.7 | 79.5 | 112.5 |
| 22/08/2012 | 73.4 | 56.1 | 49.7 | 48.9 | 51.4 | 71.6 | 82.3 | 56.1 | 97.1 | 77.7 | 84.7 | 66.2 | 70.0 | 68.6 | 95.2 | 65.9 | 54.8 | 60.0 |
| 26/09/2012 | 51.1 | 54.1 | 38.9 | 35.3 | 52.7 | 55.4 | 63.8 | 39.6 | 62.0 | 31.4 | 60.0 | 43.5 | 43.3 | 49.2 | 75.8 | 47.4 | 38.4 | 51.8 |
| 18/10/2012 | 81.6 | 81.0 | 64.4 | 61.1 | 79.7 | 77.0 | 94.6 | 66.5 | 97.1 | 83.2 | 88.8 | 74.4 | 57.6 | 75.8 | 114.6 | 78.2 | 61.7 | 81.8 |
| 15/11/2012 | 38.9 | 33.4 | 22.9 | 21.8 | 29.8 | 31.1 | 39.2 | 25.1 | 37.3 | 34.1 | 35.3 | 29.1 | 26.9 | 28.8 | 41.1 | 26.9 | 22.0 | 31.4 |
| 10/12/2012 | 69.4 | 70.6 | 49.7 | 47.5 | 54.1 | 51.4 | 61.7 | 47.8 | 82.6 | 70.9 | 76.5 | 60.0 | 55.6 | 41.1 | 98.2 | 55.6 | 49.4 | 70.9 |
| 17/01/2013 | 154.8 | 157.6 | 101.9 | 103.1 | 114.8 | 102.7 | 156.1 | 157.6 | 156.8 | 115.9 | 156.8 | 156.8 | 137.6 | 155.4 | 155.4 | 156.1 | 116.4 | 115.9 |
| 20/02/2013 | *NA* | 123.4 | 90.5 | 57.0 | 76.4 | 60.8 | *NA* | 69.6 | 136.2 | 115.9 | 108.4 | 109.4 | 108.9 | 104.4 | 155.4 | 72.0 | 76.7 | 117.2 |
| 28/03/2013 | 30.7 | 34.4 | 10.8 | 9.6 | 16.3 | 8.9 | 26.9 | 27.1 | 46.6 | 31.8 | 34.8 | 28.7 | 24.4 | 53.3 | 43.1 | 30.0 | 29.5 | 30.7 |
| 18/04/2013 | 55.1 | 62.3 | 45.6 | 46.2 | 56.8 | 58.1 | 67.9 | 49.9 | 80.6 | 65.5 | 72.3 | 55.9 | 55.6 | 57.4 | 86.0 | 59.7 | 45.3 | 60.0 |
| 23/05/2013 | 34.8 | 39.6 | 25.5 | *NA* | 36.5 | 40.6 | 51.5 | 25.1 | 51.7 | 35.5 | 41.4 | 33.2 | 31.0 | 32.9 | 51.3 | 31.0 | 24.7 | 36.9 |
| 20/06/2013 | 34.8 | 33.4 | 22.9 | 24.5 | 19.0 | 33.2 | 41.2 | 25.1 | 39.4 | 34.1 | 37.3 | 31.1 | 28.9 | 32.9 | 45.2 | 33.0 | 23.4 | 32.8 |
| 28/07/2013 | 44.0 | 43.7 | 31.6 | 28.6 | 46.0 | 48.0 | 57.6 | 30.3 | 49.7 | 43.7 | 45.6 | 62.0 | 33.0 | 39.0 | 40.0 | 39.2 | 28.8 | 28.7 |

| | | | | | | | | | | | | | | | | | | |
|---|---|---|---|---|---|---|---|---|---|---|---|---|---|---|---|---|---|---|
| 22/08/2013 | 34.8 | 14.7 | 17.5 | 13.6 | 27.1 | 25.7 | 26.9 | 25.1 | 22.9 | 21.9 | 22.9 | 16.7 | 14.6 | 18.6 | 34.9 | 14.6 | 11.0 | 21.9 |
| 03/10/2013 | 42.9 | 45.8 | 29.6 | 28.6 | 44.6 | 44.6 | 53.5 | 29.2 | 55.9 | 39.6 | 43.5 | 33.2 | 31.0 | 37.0 | 61.5 | 35.1 | 27.5 | 38.2 |
| 13/11/2013 | 133.4 | 141.0 | 98.6 | 88.2 | 114.8 | 117.5 | 156.1 | 97.5 | 160.9 | 117.9 | 158.9 | 123.8 | 119.2 | 128.9 | 157.4 | 121.2 | 100.0 | 118.6 |
| 24/01/2014 | 150.7 | 155.5 | 116.6 | 116.7 | 116.2 | 114.8 | 154.0 | 155.5 | 156.8 | 117.2 | 152.7 | 152.7 | 152.0 | 151.3 | 153.4 | 154.0 | 117.8 | 118.6 |
| 27/02/2014 | 148.7 | 151.4 | 116.6 | 116.7 | 116.2 | 116.2 | 154.0 | 155.5 | 158.9 | 118.6 | 156.8 | 152.7 | 152.0 | 151.3 | 153.4 | 154.0 | 117.8 | 118.6 |
| 27/03/2014 | 40.9 | 95.5 | 67.1 | 34.0 | 59.5 | 62.2 | 102.8 | 49.9 | 70.3 | 70.9 | 103.2 | 68.2 | 57.6 | 77.8 | 96.2 | 55.6 | 39.8 | 65.5 |
| 24/04/2014 | 30.7 | 29.2 | 25.5 | 17.7 | 28.4 | 29.8 | 39.2 | 18.9 | 39.4 | 31.4 | 37.3 | 27.0 | 31.0 | 30.9 | 47.2 | 24.8 | 17.9 | 28.7 |
| 21/05/2014 | 51.1 | 47.8 | 43.0 | 31.3 | 46.0 | 50.0 | 61.7 | 2.3 | 64.1 | 49.1 | 51.7 | 37.3 | 43.3 | 47.2 | 73.7 | 37.1 | 31.6 | 46.4 |
| 20/06/2014 | 51.1 | 41.6 | 40.3 | 28.6 | 52.7 | 54.1 | 61.7 | 37.5 | 57.9 | 50.5 | 51.7 | 39.4 | 41.2 | 43.1 | 73.7 | 39.2 | 27.5 | 43.7 |
| 24/07/2014 | 18.5 | 18.9 | 12.8 | 8.2 | 13.6 | 19.0 | 26.9 | 10.6 | 19.8 | 13.7 | 16.7 | 8.5 | 14.6 | 10.4 | 20.7 | 10.5 | 8.3 | 16.4 |
| 21/08/2014 | 79.5 | 83.0 | 63.1 | 55.7 | 79.7 | 81.1 | 106.9 | 70.6 | 111.5 | 85.9 | 86.8 | 70.3 | 84.3 | 75.8 | 124.8 | 74.1 | 63.0 | 85.9 |
| 23/09/2014 | 45.0 | 23.0 | 34.9 | 24.5 | 37.9 | 39.2 | 47.4 | 31.3 | 53.8 | 23.2 | 41.4 | 55.9 | 41.2 | 41.1 | 53.3 | 63.8 | 30.2 | 23.2 |
| 31/10/2014 | 97.8 | 99.6 | 88.5 | 57.0 | 78.4 | 87.8 | 104.8 | 70.6 | 109.4 | 99.5 | 105.3 | 82.6 | 94.6 | 88.0 | 139.1 | 84.3 | 71.3 | 92.7 |
| 27/11/2014 | 146.7 | 147.2 | 115.3 | 95.0 | 116.2 | 116.2 | 152.0 | 116.2 | 156.8 | *NA* | 156.8 | 138.3 | 133.5 | 139.1 | 159.5 | 127.4 | 117.1 | 118.6 |
| 15/12/2014 | 53.1 | 60.3 | 36.3 | 27.2 | 33.8 | 36.5 | 55.6 | 37.5 | 76.5 | 53.2 | 49.7 | 53.8 | 49.4 | 51.3 | 69.7 | 45.3 | 49.4 | 61.4 |
| 05/02/2015 | 91.7 | 116.2 | *NA* | 63.8 | 75.7 | 75.7 | 100.7 | 78.9 | 121.8 | 118.6 | 121.8 | 109.4 | 121.2 | 96.2 | 143.2 | 100.7 | 94.5 | 118.6 |
| 23/02/2015 | 4.3 | 4.4 | *NA* | 1.4 | 2.8 | 5.5 | 8.4 | 0.2 | 2.3 | 2.8 | 0.2 | 6.4 | *NA* | 2.3 | 8.4 | 2.3 | 2.8 | 4.2 |
| 25/03/2015 | 59.2 | 74.8 | 43.0 | 38.0 | 48.7 | 55.4 | 72.0 | 41.6 | 74.4 | 61.4 | 66.2 | 55.9 | 51.5 | 59.4 | 94.2 | 55.6 | 49.4 | 65.5 |
| 21/04/2015 | 28.7 | 29.2 | 26.9 | 16.4 | 25.7 | 41.9 | 45.3 | 23.0 | 31.1 | 30.1 | 31.1 | 25.0 | 24.8 | 26.8 | 47.2 | 28.9 | 20.6 | 30.1 |
| 19/05/2015 | 71.4 | 76.8 | 51.0 | 46.2 | 62.2 | 71.6 | 84.3 | 56.1 | 78.5 | 76.4 | 78.5 | 62.0 | 57.6 | 69.7 | 106.4 | 65.9 | 54.8 | 72.3 |
| 17/06/2015 | 32.8 | 39.6 | 48.3 | 21.8 | 28.4 | 33.8 | 33.0 | 25.1 | 35.3 | 34.1 | 35.3 | 29.1 | 24.8 | 32.9 | 45.2 | 31.0 | 23.4 | 31.4 |
| 21/07/2015 | 83.6 | 95.5 | 84.5 | 58.4 | 86.5 | 95.9 | 104.8 | 68.5 | 95.0 | 92.7 | 74.4 | 76.5 | 74.1 | 86.0 | 128.9 | 86.4 | 67.2 | 84.5 |
| 23/08/2015 | 79.5 | 56.1 | 38.9 | 46.2 | 73.0 | 81.1 | 74.1 | 74.8 | 105.3 | 45.0 | 76.5 | 107.4 | 49.4 | 69.7 | 114.6 | 121.2 | 54.8 | 40.9 |
| 24/09/2015 | 34.8 | 31.3 | 30.9 | 24.5 | 29.8 | 33.8 | 41.2 | 25.1 | 37.3 | 34.1 | 37.3 | 27.0 | 22.8 | 30.9 | 53.3 | 28.9 | 20.6 | 30.1 |
| 19/10/2015 | 34.8 | 37.5 | 32.2 | 36.7 | 55.4 | 29.8 | 35.1 | 25.1 | 37.3 | 34.1 | 39.4 | 29.1 | 24.8 | 34.9 | 43.1 | 33.0 | 26.1 | 31.4 |

| | | | | | | | | | | | | | | | | | | |
|---|---|---|---|---|---|---|---|---|---|---|---|---|---|---|---|---|---|---|
| 20/11/2015 | 116.1 | 130.7 | 115.3 | 76.0 | 105.4 | 114.8 | 149.9 | 95.5 | 140.3 | 80.4 | 148.6 | 177.4 | 98.7 | 118.7 | 155.4 | 119.2 | 102.7 | 117.2 |
| 17/12/2015 | 99.9 | 118.2 | 115.3 | 67.9 | 90.5 | 97.3 | 135.6 | 91.3 | 156.8 | 117.2 | 142.4 | 117.7 | 119.2 | 116.6 | 157.4 | 121.2 | 102.7 | 117.2 |
| 19/01/2016 | 144.6 | 153.4 | 116.6 | 115.3 | 114.8 | 114.8 | 154.0 | 155.5 | 152.7 | 115.9 | 152.7 | 154.7 | 149.9 | 153.4 | 151.3 | 152.0 | 101.4 | 113.1 |
| 20/02/2016 | 116.1 | 136.9 | 103.2 | 100.4 | 77.0 | 94.6 | 121.2 | 91.3 | 140.3 | 114.5 | 144.4 | 111.5 | *NA* | 114.6 | 153.4 | 121.2 | 106.8 | 114.5 |
| 18/03/2016 | 18.5 | 14.7 | 14.8 | 6.9 | 10.9 | 16.3 | 24.8 | 14.7 | 16.7 | 15.1 | 16.7 | 14.7 | 10.5 | 14.5 | 22.7 | 14.6 | 5.6 | 16.4 |
| 24/04/2016 | 55.1 | 54.1 | 49.7 | 35.3 | 47.3 | 52.7 | 65.9 | 47.8 | 51.7 | 62.7 | 64.1 | 51.7 | 39.2 | 47.2 | 67.6 | 72.0 | 38.4 | 51.8 |
| 24/05/2016 | 36.8 | 35.4 | 30.9 | 55.7 | 75.7 | 35.2 | 65.9 | 31.3 | 37.3 | 36.9 | 37.3 | 35.3 | 24.8 | 32.9 | 47.2 | 31.0 | 24.7 | 34.1 |
| 22/06/2016 | 79.5 | 87.2 | 71.1 | 62.5 | 78.4 | 78.4 | 72.0 | 72.7 | 99.1 | 106.3 | 107.4 | 99.1 | 80.2 | 92.1 | 112.5 | 100.7 | 80.8 | 92.7 |
| 25/07/2016 | 51.1 | 43.7 | 41.6 | 28.6 | 37.9 | 59.5 | 61.7 | 47.8 | 60.0 | 50.5 | 49.7 | 39.4 | 33.0 | 39.0 | 67.6 | 43.3 | 30.2 | 34.1 |
| 19/08/2016 | 47.0 | 33.4 | 18.8 | 13.6 | 17.6 | 29.8 | 24.8 | 25.1 | 41.4 | 20.5 | 33.2 | 45.6 | 28.9 | 39.0 | 59.4 | 47.4 | 23.4 | 27.3 |
| 20/09/2016 | 36.8 | 33.4 | 30.9 | 20.4 | 27.1 | 35.2 | 43.3 | 31.3 | 39.4 | 42.3 | 43.5 | 33.2 | 28.9 | 34.9 | 53.3 | 33.0 | 24.7 | 35.5 |
| 12/10/2016 | 30.7 | 33.4 | 40.3 | 16.4 | 21.7 | 32.5 | 35.1 | 29.2 | 31.1 | 34.1 | 37.3 | 29.1 | 22.8 | 26.8 | 41.1 | 26.9 | 19.3 | 31.4 |
| 22/11/2016 | 81.6 | 78.9 | 72.4 | 51.6 | 66.2 | 74.3 | 94.6 | 70.6 | 97.1 | 84.5 | 86.8 | 74.4 | 74.1 | 94.2 | 116.6 | 57.6 | 50.7 | 73.6 |

Table E2. SF volume (L) collected by each sampler for every sampling date during the long-term monitoring at Griffin Forest. Values the volume accumulated since the previous sampling date. The samplers are shown by plot and subplot. LOD refers to water depth in the barrel < 1 cm. NA = not available, mostly because the draining pipe had become disconnected from the collection barrel.

| Date | C PLOT | | | | | | | | | | | | | T PLOT | | | | | | | | |
|---|---|---|---|---|---|---|---|---|---|---|---|---|---|---|---|---|---|---|---|---|---|---|
| | subplot C10 | | | subplot C11 | | | | | | | subplot C12 | | | subplot T10 | | | subplot T11 | | | subplot T12 | | |
| | S1 | S2 | S3 | S1 | S2 | S3 | S4 | S5 | S6 | S7 | S1 | S2 | S3 | S1 | S2 | S3 | S1 | S2 | S3 | S1 | S2 | S3 |
| 12/01/2012 | 107.3 | 27.9 | 71.0 | 27.5 | 7.6 | 27.9 | 27.9 | 27.5 | 71.0 | 71.0 | 66.2 | 68.1 | 69.1 | 27.2 | *NA* | 23.9 | 26.5 | 27.2 | 28.6 | 26.1 | 14.1 | 22.5 |
| 16/02/2012 | 19.3 | 6.8 | 9.8 | 11.2 | *NA* | 9.0 | 8.6 | 10.5 | 70.0 | 27.0 | 36.5 | 27.9 | 28.9 | *NA* | *NA* | 17.7 | 26.5 | 21.4 | 10.5 | 25.0 | *NA* | *NA* |
| 15/03/2012 | 0.8 | 0.2 | *<LOD* | 0.8 | 0.2 | 0.4 | 0.4 | 0.8 | 11.3 | 0.8 | 4.0 | 1.5 | 2.5 | 0.3 | 0.2 | 1.3 | 2.1 | 1.2 | 0.8 | 1.7 | 0.2 | 0.3 |
| 26/04/2012 | 31.8 | 9.7 | 21.3 | 18.5 | 2.1 | 26.8 | 15.6 | 22.1 | 70.0 | 58.5 | 70.0 | *NA* | 66.2 | 27.2 | *NA* | 22.5 | 26.1 | 27.5 | 27.5 | 26.8 | 3.9 | 14.1 |
| 25/05/2012 | 29.9 | *NA* | 24.1 | 14.5 | 3.2 | 27.2 | 23.5 | 26.8 | 69.1 | 57.6 | *NA* | 58.5 | 67.1 | 26.5 | 14.1 | 16.3 | 22.5 | 27.2 | 27.5 | 26.1 | 23.2 | *NA* |
| 21/06/2012 | 12.6 | 2.1 | 10.7 | 8.3 | 1.7 | 16.6 | 7.6 | 12.3 | 49.9 | 31.2 | 65.2 | 33.7 | 50.9 | 13.4 | 2.5 | 18.5 | 27.5 | 18.5 | 13.4 | 26.5 | 1.7 | 0.6 |
| 20/07/2012 | 59.5 | 18.8 | 49.9 | 26.5 | 7.6 | 26.8 | 29.4 | 28.6 | 70.0 | 71.0 | 69.1 | 68.1 | 66.2 | 27.2 | 12.6 | 25.7 | 26.5 | 26.8 | 27.5 | 22.1 | 10.5 | 20.6 |
| 22/08/2012 | 49.9 | 15.6 | 27.0 | 17.0 | *NA* | 28.3 | 22.5 | 27.5 | 71.0 | *NA* | 67.1 | 71.0 | 69.1 | 27.2 | 22.1 | 24.6 | 27.9 | 27.5 | 27.9 | 26.5 | 13.7 | 19.2 |
| 26/09/2012 | 2.1 | 14.8 | 15.5 | 17.0 | 3.9 | 24.3 | 21.4 | 23.5 | 71.0 | 71.0 | 71.0 | 59.5 | 69.1 | 27.9 | 25.7 | 17.7 | 27.2 | 27.2 | 27.2 | 26.5 | 9.7 | 10.5 |
| 18/10/2012 | 65.2 | 25.0 | 23.2 | 27.9 | 7.6 | 27.9 | 21.4 | 9.0 | 72.9 | 69.1 | 71.0 | 69.1 | 67.1 | 27.9 | 9.7 | 24.3 | 27.9 | 27.9 | 29.4 | 27.2 | 14.8 | 14.1 |
| 15/11/2012 | 23.2 | 8.3 | 9.8 | 10.5 | 2.5 | 16.3 | 9.7 | 13.4 | 71.0 | 34.6 | 40.4 | 32.7 | 46.1 | 18.5 | 9.0 | 24.3 | 27.9 | 22.8 | 17.0 | 27.2 | 4.6 | 7.6 |
| 10/12/2012 | 59.5 | 22.8 | 23.2 | 20.6 | *NA* | 14.8 | 22.1 | 27.2 | 71.0 | 71.0 | 67.1 | 65.2 | 69.1 | 29.0 | *NA* | 26.1 | 29.4 | 29.4 | 29.4 | 27.9 | 13.4 | 11.9 |
| 17/01/2013 | 72.9 | 23.9 | 72.9 | 25.0 | 22.8 | 25.0 | 27.9 | 27.5 | 69.1 | 69.1 | 68.1 | 68.1 | 68.1 | 27.9 | 27.9 | 24.3 | 26.5 | 28.3 | 27.2 | 26.1 | 28.6 | 21.4 |
| 20/02/2013 | 69.1 | 23.9 | 69.1 | 25.0 | 5.4 | 25.0 | 27.9 | 27.5 | 69.1 | 69.1 | 68.1 | 68.1 | 68.1 | 24.3 | 9.0 | 24.3 | 26.5 | 28.3 | 27.2 | 26.1 | 28.6 | 26.5 |
| 28/03/2013 | 21.3 | 11.9 | 0.2 | 9.0 | 1.0 | 19.9 | 8.3 | 0.3 | 67.1 | 27.0 | 36.5 | 28.9 | 42.3 | 19.9 | *NA* | 23.5 | 25.7 | 27.9 | 14.8 | 25.7 | 3.9 | *NA* |
| 18/04/2013 | 65.2 | 23.9 | 28.9 | 19.2 | 3.9 | 27.2 | 28.6 | 27.2 | 71.0 | 71.0 | 65.2 | 69.1 | 71.0 | 44.6 | 0.6 | 24.3 | 26.5 | 28.3 | 27.2 | 26.1 | 12.6 | 13.4 |
| 23/05/2013 | 23.2 | 7.9 | 6.0 | 8.3 | 1.0 | 15.6 | 9.7 | 11.9 | 19.3 | 17.4 | 25.1 | 13.6 | 19.3 | 15.6 | 11.2 | 24.3 | 4.6 | 22.8 | 16.6 | 25.7 | 4.6 | 11.2 |
| 20/06/2013 | 17.4 | 3.6 | 6.9 | 9.0 | *<LOD* | 14.5 | *NA* | 11.9 | 33.7 | 12.6 | 23.2 | 8.8 | 15.5 | 11.2 | 18.8 | 6.8 | 26.8 | 15.2 | 14.5 | 26.8 | 2.5 | 9.7 |
| 28/07/2013 | 9.8 | 1.0 | 7.9 | 6.8 | 0.3 | 11.9 | 7.6 | 8.3 | 19.3 | 9.8 | 23.2 | 11.7 | 15.5 | 6.8 | 2.5 | 18.5 | 15.6 | 11.2 | 16.6 | 25.7 | *NA* | 6.1 |
| 22/08/2013 | 9.8 | 1.7 | 7.9 | 3.2 | *<LOD* | 5.4 | 2.5 | 1.7 | 6.0 | 4.0 | 2.1 | *NA* | *NA* | 3.9 | *NA* | 6.8 | 4.6 | 6.1 | 7.6 | 12.6 | *NA* | 3.2 |
| 03/10/2013 | 15.5 | 7.6 | 4.0 | 11.2 | 0.3 | 17.7 | 11.9 | 11.9 | 32.7 | 15.5 | 21.3 | 21.3 | 21.3 | 9.7 | 6.1 | 17.7 | 26.5 | 14.8 | 15.6 | 27.5 | 5.4 | 3.2 |
| 13/11/2013 | 125.5 | 22.5 | 36.5 | 27.2 | 6.8 | 28.6 | 29.7 | 17.7 | 114.9 | 45.2 | 76.7 | 84.3 | 86.3 | 27.5 | 18.8 | 26.8 | 27.2 | 29.0 | 29.7 | 27.5 | 30.5 | 11.6 |
| 24/01/2014 | 109.2 | 26.5 | 59.5 | 27.2 | 21.4 | 28.6 | 30.8 | 24.3 | 95.8 | 71.0 | 78.6 | 97.7 | 107.3 | 30.1 | 22.1 | 26.5 | 26.5 | 28.6 | 28.6 | 27.2 | 29.4 | 28.6 |
| 27/02/2014 | 114.9 | 25.7 | 43.2 | 26.5 | 14.5 | 30.1 | 29.4 | 27.2 | 95.8 | *NA* | 76.7 | 97.7 | 107.3 | 27.9 | 22.1 | 27.2 | 27.2 | 28.6 | 29.4 | 27.2 | 29.4 | *NA* |
| 27/03/2014 | 23.2 | 8.3 | 15.5 | 11.2 | 5.4 | 22.8 | 9.7 | 9.7 | 48.0 | 13.6 | 63.3 | 34.6 | 48.0 | 22.8 | 10.5 | 20.6 | 27.2 | 28.6 | *NA* | 27.2 | 6.8 | 19.9 |
| 24/04/2014 | 19.3 | 3.2 | *NA* | 4.6 | 0.3 | 9.0 | 3.2 | 4.6 | 13.6 | 4.0 | 17.4 | 11.7 | 15.5 | 0.3 | 4.6 | 7.6 | 27.2 | 11.9 | 9.7 | 22.1 | 1.0 | 1.7 |
| 21/05/2014 | 34.6 | 9.0 | 7.9 | 7.6 | *<LOD* | 16.3 | 7.6 | 9.7 | 23.2 | 9.8 | 30.8 | 21.3 | 28.9 | 20.6 | 6.8 | 17.7 | 25.0 | 28.6 | 15.6 | 27.2 | 6.1 | 9.7 |
| 20/06/2014 | 7.9 | 1.0 | 4.0 | 5.4 | 0.3 | 13.4 | 3.2 | 9.0 | 7.9 | 4.0 | 25.1 | 13.6 | 19.3 | 8.3 | 2.5 | 16.3 | 25.7 | 8.3 | 14.1 | 5.4 | 22.1 | 0.3 |
| 24/07/2014 | 0.2 | *<LOD* | *<LOD* | 0.3 | *<LOD* | 1.0 | 1.0 | 1.7 | *<LOD* | *<LOD* | 6.9 | 2.1 | 3.1 | *<LOD* | *<LOD* | 1.7 | 6.8 | 1.0 | 2.5 | 4.6 | *<LOD* | 0.6 |

| | | | | | | | | | | | | | | | | | | | | | |
|---|---|---|---|---|---|---|---|---|---|---|---|---|---|---|---|---|---|---|---|---|---|
| 21/08/2014 | 53.8 | 8.3 | 6.0 | 19.9 | 3.9 | 30.1 | 16.3 | 24.3 | 11.7 | 9.8 | 55.7 | 32.7 | 53.8 | 27.9 | 3.2 | 25.7 | 24.3 | 20.6 | 28.6 | 27.9 | 4.6 | 20.6 |
| 23/09/2014 | 21.3 | 3.9 | 4.0 | 9.7 | 1.0 | 16.3 | 6.8 | 10.5 | 13.6 | 4.0 | 0.2 | 9.8 | 15.5 | 27.2 | 3.2 | 3.9 | 28.6 | 11.2 | 13.4 | 12.6 | 2.5 | 14.1 |
| 31/10/2014 | 74.8 | 22.8 | 11.7 | 25.0 | 5.4 | 30.1 | 19.2 | 26.5 | 48.0 | 11.7 | 69.1 | 30.8 | 46.1 | 25.7 | 4.6 | 26.5 | 28.6 | 27.2 | 28.6 | 27.2 | 19.9 | 9.7 |
| 27/11/2014 | 107.3 | 25.0 | 7.9 | 25.7 | 6.1 | 35.2 | 27.9 | 27.5 | 94.9 | 19.3 | 76.7 | 55.7 | 44.2 | 27.2 | 11.9 | 27.2 | 28.6 | 27.9 | 29.0 | 27.2 | 22.8 | 17.0 |
| 15/12/2014 | 48.0 | 17.7 | 2.1 | 19.2 | 1.7 | 17.0 | 22.1 | 17.7 | 95.8 | 13.6 | 30.8 | 21.3 | 17.4 | 27.2 | 9.7 | 27.2 | 28.6 | 27.9 | 29.4 | 27.2 | 17.0 | 15.6 |
| 05/02/2015 | 72.9 | 26.5 | 11.7 | 25.7 | 5.4 | 28.6 | 28.6 | 27.2 | 74.8 | 21.3 | 59.5 | 51.8 | 21.3 | 28.6 | 0.3 | 28.6 | 29.4 | 28.6 | 29.4 | 27.9 | 27.2 | 27.2 |
| 23/02/2015 | *<LOD* | *<LOD* | *<LOD* | *<LOD* | *<LOD* | *<LOD* | *<LOD* | *<LOD* | *<LOD* | *<LOD* | *<LOD* | *<LOD* | *<LOD* | *<LOD* | *<LOD* | *<LOD* | 1.7 | *<LOD* | *<LOD* | 1.0 | *<LOD* | *<LOD* |
| 25/03/2015 | 30.8 | 13.4 | 6.0 | 17.7 | 1.0 | 27.9 | 16.3 | 14.8 | 38.5 | 11.7 | 38.5 | 21.3 | 23.2 | 24.3 | 11.9 | 27.2 | 17.7 | 27.9 | 21.4 | 27.2 | 11.2 | 20.6 |
| 21/04/2015 | 4.0 | 0.3 | *<LOD* | 3.9 | *<LOD* | 6.1 | 2.5 | 2.5 | 15.5 | 0.2 | 15.5 | 4.0 | 4.0 | *<LOD* | 6.1 | 9.0 | 21.4 | 5.4 | 6.1 | 22.8 | *<LOD* | 3.9 |
| 19/05/2015 | 42.3 | 14.8 | 6.0 | 18.5 | 2.5 | 28.6 | 22.8 | 15.6 | 38.5 | 19.3 | 46.1 | 27.0 | 21.3 | 17.0 | 3.2 | 25.0 | 27.9 | 22.1 | 23.5 | 27.2 | 8.3 | 23.2 |
| 17/06/2015 | 13.6 | 4.6 | 2.1 | 5.4 | 0.3 | 14.1 | 9.0 | 7.6 | 11.7 | 9.8 | 19.3 | 7.9 | 7.9 | 9.7 | 9.0 | 17.0 | 29.0 | 1.7 | 8.3 | 27.2 | 6.1 | 9.0 |
| 21/07/2015 | 36.5 | 5.4 | *<LOD* | 15.6 | 3.2 | 27.9 | 10.5 | 17.0 | 21.3 | 23.2 | 48.0 | 15.5 | 27.0 | 25.0 | 10.5 | 25.7 | 11.9 | 28.6 | *NA* | 27.2 | 11.2 | 13.4 |
| 23/08/2015 | 38.5 | 5.4 | 15.5 | 8.3 | 0.3 | 22.8 | 2.5 | 9.0 | 9.8 | 6.0 | 19.3 | 11.7 | 4.0 | 26.5 | 2.5 | 17.0 | 28.6 | 4.6 | 22.1 | 14.1 | 1.0 | 19.2 |
| 24/09/2015 | 11.7 | *<LOD* | *<LOD* | 6.8 | 0.6 | 13.4 | 3.9 | 9.0 | 4.0 | 6.0 | 19.3 | 7.9 | 7.9 | 5.4 | *<LOD* | 3.9 | 27.9 | *NA* | 9.7 | 25.0 | 1.7 | 6.8 |
| 19/10/2015 | 17.4 | 3.9 | 1.2 | 7.6 | 0.3 | 11.9 | 3.2 | 5.4 | 6.0 | *<LOD* | 17.4 | 6.0 | 7.9 | 8.3 | 9.0 | 15.6 | 28.6 | 13.4 | 9.7 | 19.2 | 3.2 | 8.3 |
| 20/11/2015 | 86.3 | 14.8 | 9.8 | 27.9 | 3.9 | 30.8 | 18.5 | 27.9 | 23.2 | 25.1 | 78.6 | 27.0 | 46.1 | 19.2 | 3.9 | 24.3 | 28.6 | 27.9 | 28.6 | 25.0 | 16.3 | 6.8 |
| 17/12/2015 | 84.3 | 26.5 | 27.0 | 25.7 | 3.9 | 25.0 | 27.9 | 28.6 | 30.8 | 53.8 | 74.8 | 27.0 | 30.8 | 26.5 | 18.5 | 25.0 | 28.6 | 11.9 | 29.4 | 26.5 | 20.6 | 26.5 |
| 19/01/2016 | 107.3 | 26.5 | 27.0 | 28.6 | 23.5 | 24.3 | 27.2 | 29.4 | 69.1 | 46.1 | 76.7 | 97.7 | 105.4 | 27.2 | 21.4 | 25.7 | 28.6 | 5.4 | 29.4 | 14.8 | 29.4 | 27.2 |
| 20/02/2016 | 95.8 | 26.5 | 19.3 | 26.5 | 3.9 | 6.1 | 26.5 | 29.4 | 30.8 | *NA* | 78.6 | 34.6 | 40.4 | 27.2 | *NA* | 27.2 | 30.1 | 28.6 | 29.4 | 25.0 | 27.9 | 27.2 |
| 18/03/2016 | 0.2 | 0.3 | 1.2 | 0.4 | *<LOD* | 2.5 | 1.0 | 1.7 | 0.4 | 0.2 | 4.0 | 1.6 | 0.4 | *NA* | 4.6 | 1.7 | 15.6 | 4.6 | 3.2 | 6.8 | 0.2 | 4.6 |
| 24/04/2016 | 19.3 | 4.6 | 7.9 | 4.6 | 0.3 | 17.0 | 5.4 | *NA* | 4.0 | 4.0 | 40.4 | *NA* | 6.0 | 4.6 | 0.1 | 19.2 | 27.9 | 18.5 | 12.6 | 26.5 | 4.6 | 19.2 |
| 24/05/2016 | 6.0 | *<LOD* | 2.1 | 4.6 | *<LOD* | 9.0 | 2.5 | 4.6 | 6.0 | *<LOD* | 15.5 | 7.9 | 4.0 | 3.9 | 2.5 | 6.1 | 25.7 | 4.6 | 5.4 | 15.6 | *NA* | 8.3 |
| 22/06/2016 | 36.5 | 9.7 | 19.3 | 17.0 | 5.4 | 25.0 | 15.6 | 14.1 | 44.2 | 7.9 | 46.1 | 21.3 | 15.5 | 25.0 | 11.9 | 25.7 | 29.0 | 17.0 | 29.4 | 26.5 | 15.6 | 26.5 |
| 25/07/2016 | 4.0 | *<LOD* | 4.0 | 4.6 | *<LOD* | 11.9 | 2.5 | 6.1 | 6.0 | 2.1 | 21.3 | 7.9 | 11.7 | *NA* | *<LOD* | 7.6 | 27.9 | 6.1 | 9.0 | 10.5 | 1.0 | 10.5 |
| 19/08/2016 | 4.0 | *<LOD* | 2.1 | 3.2 | *<LOD* | 6.8 | 1.7 | 3.9 | 0.2 | 11.7 | 6.0 | 6.0 | *NA* | 23.5 | *<LOD* | 3.9 | 19.2 | 3.2 | 6.8 | 9.7 | *NA* | 6.8 |
| 20/09/2016 | 7.9 | 3.2 | 4.0 | 6.8 | *<LOD* | 9.0 | 3.9 | 5.4 | 2.1 | 2.1 | 9.8 | 4.0 | 7.9 | 5.4 | *<LOD* | 6.1 | 27.9 | 12.6 | 9.7 | 17.0 | 0.3 | 7.6 |
| 12/10/2016 | 4.0 | *<LOD* | 2.1 | 4.6 | *<LOD* | 8.3 | 2.5 | 5.4 | 4.0 | *<LOD* | 13.6 | 4.0 | 2.1 | 3.9 | *<LOD* | 5.4 | 28.6 | 7.6 | *NA* | 15.6 | 1.7 | *NA* |
| 22/11/2016 | 36.5 | 11.9 | 4.0 | 18.5 | 1.7 | 30.1 | 13.4 | 9.0 | 19.3 | 6.0 | 40.4 | 28.9 | 28.9 | 18.5 | *<LOD* | 18.5 | 27.2 | 9.7 | 27.2 | 29.4 | 22.8 | 28.6 |

# Appendix F. Mean monthly streamwater N flux at plot C, years 2012-2016

Figure F1. Mean monthly streamwater N flux at plot C. The values are not a net flux (streamwater N output) but include any upstream N mass entering the plot. December 2016 data are not available due to high discharge not measureable by the V-notch. September 2015 $NO_3$-N is not available due to non-identified samples contamination.

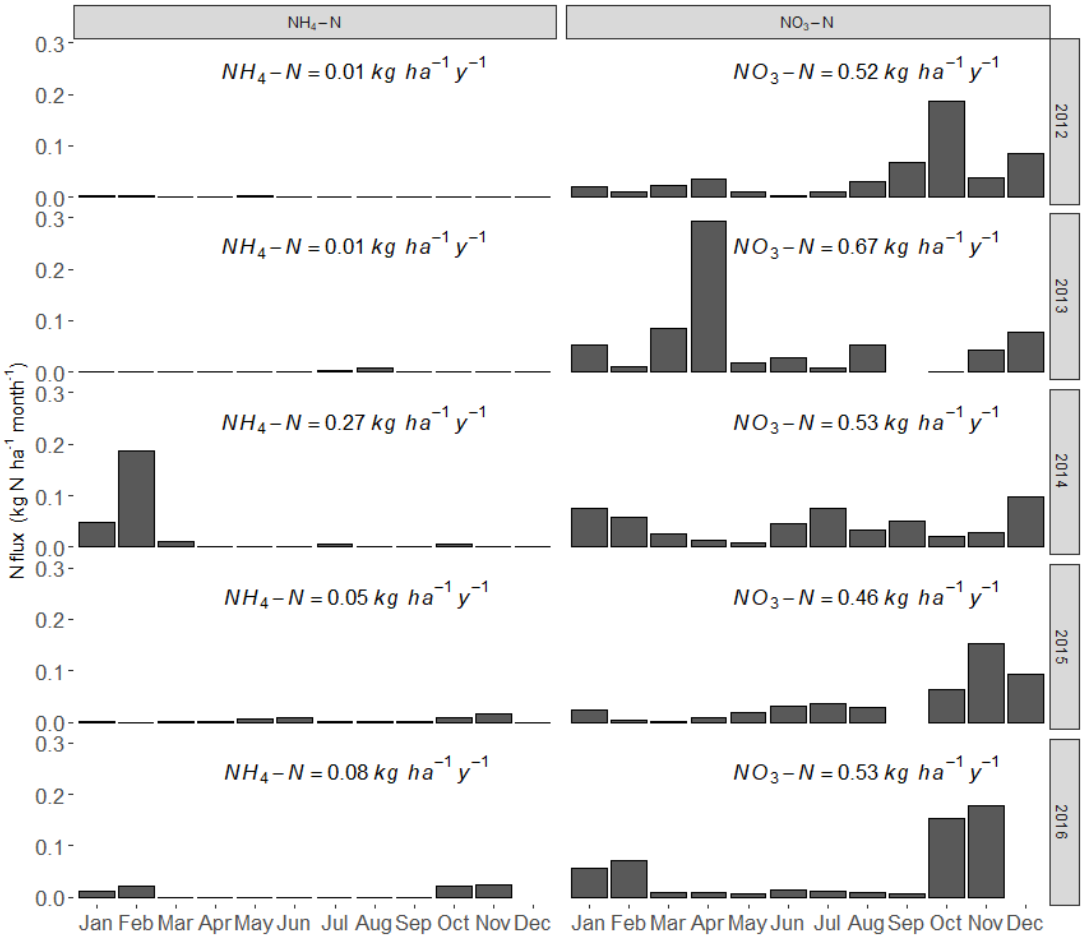

# Appendix G. Summary of all statistical tests conducted on the results from the labelled litter experiments

Table G1. Summary of statistical tests on litter, soil and roots samples from the labelled litter plots and significance. Significant ($p<0.05$) results are shown in italics. U and L represent unlabelled and $^{15}N$ labelled plots, respectively. "Soil type" indicates surface feature (undisturbed, furrow, ridge).

| **Tested differences** | **Applied transformations for normality** | **Test** | **Test p-value** | **notes** |
|---|---|---|---|---|
| litter N% U/L | Tukey's ladder of powers | Welch two-sample t-test | 0.167 | |
| soil 0-5 cm N% U/L | sqrt | Welch two-sample t-test | 0.547 | |
| soil 5-15 cm N% U/L | Tukey's ladder of powers | Welch two-sample t-test | 0.27 | |
| roots 0-5 cm N% U/L | sqrt | Welch two-sample t-test | 0.409 | |
| roots 5-15 cm N% U/L | Tukey's ladder of powers | Welch two-sample t-test | 0.181 | |
| *litter $\delta^{15}N$ U/L* | *none* | *Welch two-sample t-test* | *<0.001* | |
| litter $\delta^{15}N$ labelled plots | none | One-way ANOVA | 0.484 | |
| *soil 0-5 cm $\delta^{15}N$ U/L* | *sqrt* | *Welch two-sample t-test* | *<0.001* | |
| *soil 5-15 cm $\delta^{15}N$ U/L* | *none* | *Welch two-sample t-test* | *<0.01* | |
| soil 0-5 cm $\delta^{15}N$ by labelled plots | sqrt | One-way ANOVA | 0.522 | |
| *$\delta^{15}N$ by soil depth* | *sqrt* | *Welch two-sample t-test* | *<0.05* | |
| soil 0-5 cm $\delta^{15}N$ in labelled plots by soil type | sqrt | One-way ANOVA | 0.834 | |
| *roots* 0-5 cm *$\delta^{15}N$ U/L* | *none* | *Welch two-sample t-test* | *<0.001* | |
| *roots* 5-15 cm *$\delta^{15}N$ U/L* | *sqrt* | *Welch two-sample t-test* | *<0.001* | *shifted (+1.05)** |
| *roots $\delta^{15}N$ by* labelled plots(a)+*depth(b)* | *sqrt* | *Two-way ANOVA* | (a)0.1 *(b)0.01* | *shifted (+1.82)** |
| *roots $\delta^{15}N$ labelled soil type(a)+depth(b)* | *sqrt* | *Two-way ANOVA* | *(a)0.05 (b)0.01* | *shifted* (+1.82)* |

* some of the $\delta^{15}N$ values from root samples were <0. As a square root transformation needs values ≥0, the minimum value of $\delta^{15}N$ was added to all values to transform them.

# Appendix H. Data visualisation for labelled litter experiments

Figure H1. $^{15}N$ recovery in litter and soil (%) by surface feature (furrow, undisturbed, ridge), layer and subplot.

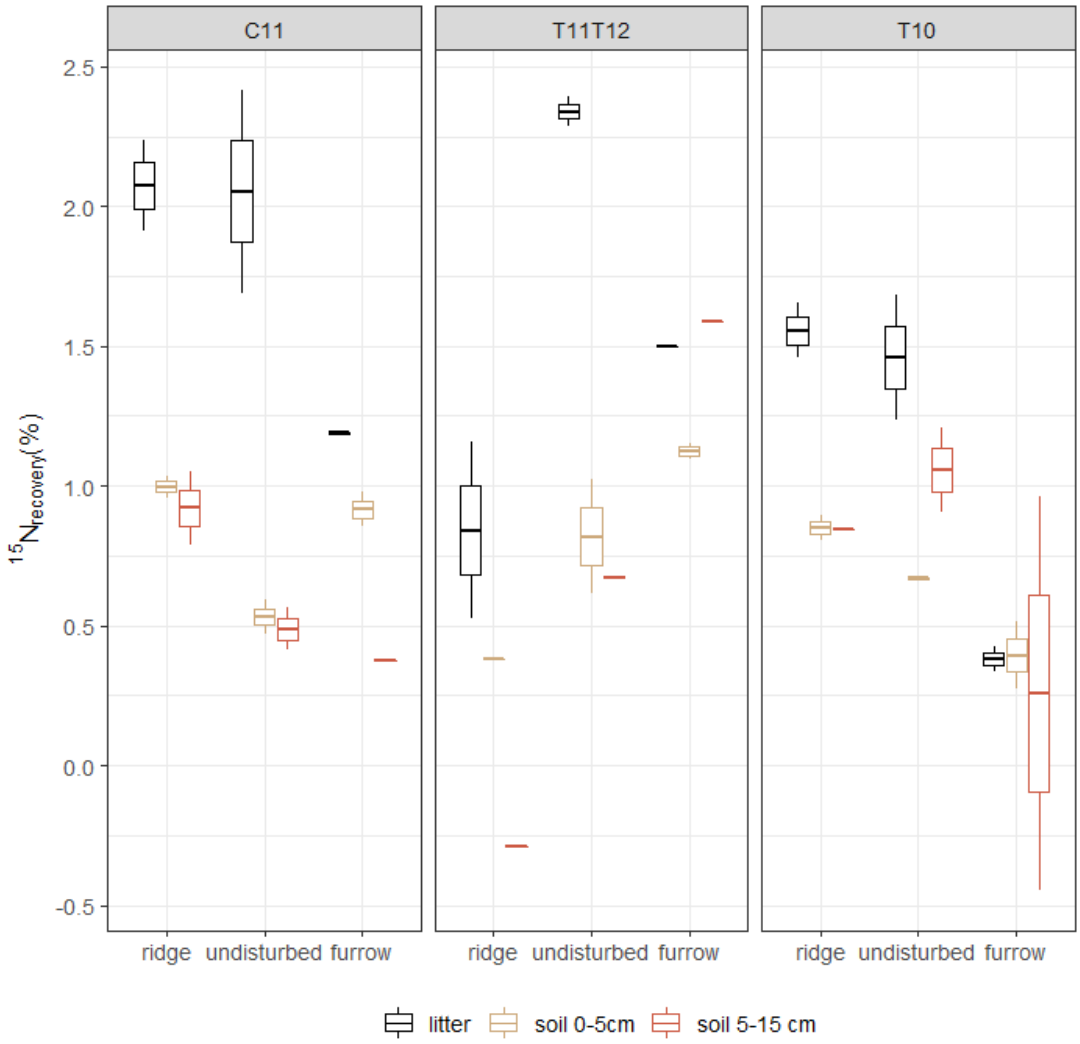

Figure H2. $^{15}N$ recovery in litter and soil (%) by surface feature (furrow, undisturbed, ridge) and layer.